TOPICS IN CURRENT CHEMISTRY 279

Volume Editor M. J. Krische

Metal Catalyzed Reductive C-C Bond Formation

A Departure from Preformed Organometallic Reagents

Springer

279
Topics in Current Chemistry

Topics in Current Chemistry

Recently Published and Forthcoming Volumes

Photochemistry and Photophysics of Coordination Compounds II
Volume Editors: Balzani, C., Campagna, S.
Vol. 281, 2007

Photochemistry and Photophysics of Coordination Compounds I
Volume Editors: Balzani, C., Campagna, S.
Vol. 280, 2007

Metal Catalyzed Reductive C–C Bond Formation
A Departure from Preformed Organometallic Reagents
Volume Editor: Krische, M. J.
Vol. 279, 2007

Combinatorial Chemistry on Solid Supports
Volume Editor: Bräse, S.
Vol. 278, 2007

Creative Chemical Sensor Systems
Volume Editor: Schrader, T.
Vol. 277, 2007

In situ NMR Methods in Catalysis
Volume Editors: Bargon, J., Kuhn, L. T.
Vol. 276, 2007

Sulfur-Mediated Rearrangements II
Volume Editor: Schaumann, E.
Vol. 275, 2007

Sulfur-Mediated Rearrangements I
Volume Editor: Schaumann, E.
Vol. 274, 2007

Bioactive Conformation II
Volume Editor: Peters, T.
Vol. 273, 2007

Bioactive Conformation I
Volume Editor: Peters, T.
Vol. 272, 2007

Biomineralization II
Mineralization Using Synthetic Polymers and Templates
Volume Editor: Naka, K.
Vol. 271, 2007

Biomineralization I
Crystallization and Self-Organization Process
Volume Editor: Naka, K.
Vol. 270, 2007

Novel Optical Resolution Technologies
Volume Editors:
Sakai, K., Hirayama, N., Tamura, R.
Vol. 269, 2007

Atomistic Approaches in Modern Biology
From Quantum Chemistry to Molecular Simulations
Volume Editor: Reiher, M.
Vol. 268, 2006

Glycopeptides and Glycoproteins
Synthesis, Structure, and Application
Volume Editor: Wittmann, V.
Vol. 267, 2006

Microwave Methods in Organic Synthesis
Volume Editors: Larhed, M., Olofsson, K.
Vol. 266, 2006

Supramolecular Chirality
Volume Editors: Crego-Calama, M., Reinhoudt, D. N.
Vol. 265, 2006

Metal Catalyzed Reductive C–C Bond Formation

A Departure from Preformed Organometallic Reagents

Volume Editor: Michael J. Krische

With contributions by

B. Breit · R. D. Broene · C.-A. Fan · A. Gansäuer · T. Hirao
H. Iida · J. Justicia · M. Kimura · M. J. Krische · J. Montgomery
H. Nishiyama · F. Piestert · T. Shiomi · G. J. Sormunen
Y. Tamaru · D. Worgull

Springer

The series *Topics in Current Chemistry* presents critical reviews of the present and future trends in modern chemical research. The scope of coverage includes all areas of chemical science including the interfaces with related disciplines such as biology, medicine and materials science. The goal of each thematic volume is to give the nonspecialist reader, whether at the university or in industry, a comprehensive overview of an area where new insights are emerging that are of interest to a larger scientific audience.

As a rule, contributions are specially commissioned. The editors and publishers will, however, always be pleased to receive suggestions and supplementary information. Papers are accepted for *Topics in Current Chemistry* in English.

In references *Topics in Current Chemistry* is abbreviated Top Curr Chem and is cited as a journal.

Visit the TCC content at springerlink.com

Library of Congress Control Number: 2007927651

ISSN 0340-1022
ISBN 978-3-540-72878-8 Springer Berlin Heidelberg New York
DOI 10.1007/978-3-540-72879-5

Springer is a part of Springer Science+Business Media

springer.com

Cover design: WMXDesign GmbH, Heidelberg
Typesetting and Production: LE-TEX Jelonek, Schmidt & Vöckler GbR, Leipzig

Printed on acid-free paper 02/3180 YL – 5 4 3 2 1 0

Volume Editor

Prof. Michael J. Krische

Department of Chemistry
& Biochemistry
University of Texas at Austin
1 University Station A5300
Austin, TX 78712-0165
USA
mkrische@mail.utexas.edu

Editorial Board

Topics in Current Chemistry
Also Available Electronically

For all customers who have a standing order to Topics in Current Chemistry, we offer the electronic version via SpringerLink free of charge. Please contact your librarian who can receive a password or free access to the full articles by registering at:

springerlink.com

If you do not have a subscription, you can still view the tables of contents of the volumes and the abstract of each article by going to the SpringerLink Homepage, clicking on "Browse by Online Libraries", then "Chemical Sciences", and finally choose Topics in Current Chemistry.

You will find information about the

- Editorial Board
- Aims and Scope
- Instructions for Authors
- Sample Contribution

at springer.com using the search function.

Preface

The prototypical catalytic reductive C–C bond formations, the Fischer-Tropsch reaction [1] and alkene hydroformylation [2], were discovered in 1922 and 1938, respectively [3,4]. These processes, which involve reductive coupling to carbon monoxide, have long been applied to the industrial manufacture of commodity chemicals [5]. Notably, alkene hydroformylation, also known as the oxo-synthesis, has emerged as the largest volume application of homogeneous metal catalysis, accounting for the production of over 7 million metric tons of aldehyde annually. Despite the impact of these prototypical reductive C–C bond formations, this field of research lay fallow for several decades. Eventually, the increased availability of mild terminal reductants, in particular silanes, led to a renaissance in the area of catalytic reductive C–C bond formation. For example, the first catalytic reductive C–C couplings beyond hydroformylation, which involve the hydrosilylative dimerization of conjugated dienes [6–12], appeared in 1969 – approximately 16 years after the first reported metal-catalyzed alkene hydrosilylation [13]. Following these seminal studies, the field of catalytic reductive C–C bond formation underwent explosive growth, culminating in the emergence of an ever growing body of research encompassing a powerful set of transformations.

To our knowledge, no thematic volumes devoted solely to metal-catalyzed reductive C–C bond formation have been assembled. For the first time, in this issue of *Topics in Current Chemistry*, we present a compilation of monographs from several leaders in this burgeoning area of research. This collection of reviews serves to capture the diversity of catalytic reductive C–C couplings presently available and, in turn, the remarkable range of reactivity embodied by such transformations. There is no indication that this field has reached its zenith and it is the hope of the present author that this volume will fuel further progress.

Of greatest significance, many of the reductive couplings described in this account involve the use of carbonyl compounds and imines as coupling partners. Hence, catalytic reductive additions to such conventional electrophiles herald a departure from the use of preformed organometallic reagents. For example, the catalytic reductive aldol couplings described in the volume employ metallo-enolates generated transiently in substoichiometric quantities under catalytic conditions, representing an alternative to stoichiometrically

preformed metallo-enolates and related enol derivates. Metal catalyzed reductive C–C bond formation promises to take organic chemistry beyond stoichiometric metallic reagents, thus fortifying a cornerstone of synthetic organic chemistry – the broad areas of carbonyl and imine addition.

University of Texas at Austin, April 2007 Michael J. Krische

References

1. (a) Fischer, F.; Tropsch, H. DRP 411416 (1922); DRP 484337 (1925). (b) Fischer, F.; Tropsch, H. *Ber.* **1923**, *56B*, 2428–2443. (c) Fischer, F.; Tropsch, H. *Brennst. Chem.* **1923**, *4*, 193–197. (d) Fischer, F.; Tropsch, H. *Brennst. Chem.* **1923**, *4*, 197. (e) Fischer, F.; Tropsch, H. *Brennst. Chem.* **1923**, *4*, 276–285.
2. Roelen, O. U.S. Patent 2,317,066, April 20, 1943.
3. For recent reviews on alkene hydroformylation and the Fischer-Tropsch reaction, see: (a) Breit, B. *Acc. Chem. Res.* **2003**, *36*, 264–275. (b) Breit, B.; Seiche, W. *Synthesis* **2001**, 1–36. (c) Herrmann, W. A. *Angew. Chem., Int. Ed.* **1982**, *21*, 117–130. (d) Rofer-Depoorter, C.-K. *Chem. Rev.* **1981**, *81*, 447–474.
4. For a brief historical perspective on the field of catalysis, see: Krische, M. J. *Tetrahedron* **2005**, *61*, 6169.
5. Weissermel, K.; Arpe, H.-J. *Industrial Organic Chemistry*, VCH: Weinheim, Germany, 1978; Chapter 6.1, pp. 111–123.

To our knowledge, the first examples of catalytic non-hydrogen-mediated reductive C–C bond formation involve the reductive dimerization (telomerization) of butadiene mediated by silane, see Ref. 6–12.

6. Takahashi, S.; Shibano, T.; Hagihara, N. *J. Chem. Soc., Chem. Comm.* **1969**, 161.
7. Takahashi, S.; Shibano, T.; Kojima, H.; Hagihara, N. *Organomet. Chem. Synth.* **1970**, *1*, 193–202.
8. Hara, M.; Ohno, K.; Tsuji, J. *J. Chem. Soc., Chem. Comm.* **1971**, 247.
9. Tsuji, J.; Hara, M.; Ohno, K. *Tetrahedron* **1974**, *30*, 2143–2146.
10. Lappert, M. F.; Nile, T. A.; Takahashi, S. *J. Organomet. Chem.* **1974**, *72*, 425–439.
11. Langova, J.; Hetflejs, J. *Coll. Czech. Chem. Comm.* **1975**, *40*, 420–431.
12. Kaneda, K.; Kurosaki, H.; Terasawa, M.; Imanake, T.; Teranishi, S. *J. Org. Chem.* **1981**, *46*, 2356–2362.
13. To our knowledge, the first example of metal-catalyzed alkene hydrosilylation, see: Wagner, G. H.; Strother, C. O. U.S. Patent 2,632,013, March 17, 1953. See also Speier, J. L.; Zimmerman, R.; Webster, J. *J. Am. Chem. Soc.* **1956**, *78*, 2278–2281.

Contents

Contents of Topics in Organometallic Chemistry Volume 18

Catalytic Carbonylation Reactions

Volume Editor: Beller, M.
ISBN: 978-3-540-33002-8

Top Curr Chem (2007) 279: 1–23
DOI 10.1007/128_2007_139

Published online: 14 June 2007

Nickel-Catalyzed Reductive Couplings of Aldehydes and Alkynes

John Montgomery (✉) · Grant J. Sormunen

Department of Chemistry, University of Michigan, 930 North University Avenue, Ann Arbor, Michigan 48109-1055, USA
jmontg@umich.edu

Abstract The nickel-catalyzed coupling of aldehydes and alkynes has evolved into a broadly useful procedure for the preparation of allylic alcohols. An overview of the many variants of the process, illustrations of complex synthetic applications, and a discussion of mechanism is provided. Additionally, a brief summary of mechanistically related nickel-catalyzed processes as well as a description of alternate strategies for the reductive coupling of aldehydes and alkynes using other metals is provided.

Keywords Allylic alcohol · Nickel · Reductive coupling · Reductive cyclization · Reductive cycloaddition

Abbreviations

COD	1,5-Cyclooctadiene
Cyp	Cyclopentyl

IMes	*N*,*N*′-Bis(2,4,6-trimethylphenyl)imidazol-2-ylidene
IPr	*N*,*N*′-Bis(2,6-diisopropylphenyl)imidazol-2-ylidene
MOM	Methoxy methyl
NHC	*N*-Heterocyclic carbene
TBS	*t*-Butyldimethylsilyl
TES	Triethylsilyl
TIPS	Triisopropylsilyl
TMEDA	Tetramethylethylene diamine

1 Introduction

Allylic alcohols are useful substructures as key subunits embedded within bioactive natural products as well as versatile precursors for a variety of synthetic transformations. The range of transformations that rely on allylic alcohol derivatives include diverse processes such as metal π-allyl chemistry [1], directed epoxidations [2] and cyclopropanations [3, 4], cationic cyclization processes [5], S_N2' allylic displacement processes [6], and various sigmatropic processes including Claisen rearrangements and related variants [7]. A number of classical procedures allow efficient synthesis of allylic alcohols, with the most widely used procedures involving 1,2-reduction of enones or addition of vinyl organometallics to aldehydes or ketones. In a more contemporary strategy, the Hiyama–Nozaki–Kishi coupling [8, 9], which involves the nickel-catalyzed addition of vinyl halides to aldehydes, has become a benchmark procedure that is widely used.

An alternative to these procedures is the direct union of aldehydes and alkynes in a reductive coupling process (Scheme 1). The primary advantage of the reductive coupling of aldehydes and alkynes is that the olefin stereochemistry, the configuration of the hydroxyl-bearing stereocenter, and the central carbon–carbon single bond of the product allylic alcohol are all established in a single operation. The widely used methods described in the previous paragraph, while very powerful in many applications, each require two or more steps to establish these key structural features. This review will focus specifically on the development of nickel-catalyzed reductive couplings of aldehydes

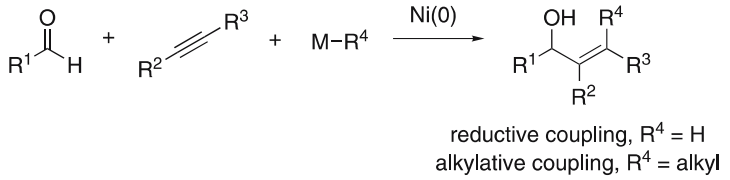

Scheme 1 Reductive coupling of aldehydes and alkynes

and alkynes [10–13]. Concluding sections will briefly describe mechanistically related nickel-catalyzed processes as well as summarize methods for alkyne/aldehyde reductive couplings involving other transition metals.

2
Aldehyde/Alkyne Couplings

The nickel-catalyzed coupling of aldehydes and alkynes was first described in 1997, and many variants of the process are now known (Scheme 1) [14]. The processes may proceed intermolecularly or intramolecularly to assemble rings ranging from five-membered up to macrocyclic ring systems. Both alkylative and reductive processes may be performed, with the distinction involving whether a carbon substituent (alkylative coupling) or hydrogen substituent (reductive coupling) is installed from the reducing agent. Catalyst systems involving low valent nickel species stabilized by COD, phosphines, or *N*-heterocyclic carbenes (NHCs) are known, with phosphines and NHCs typically being monodentate. Reducing agents (MR^4) typically employed include silanes, organozincs, organoboranes, or vinylzirconium reagents.

2.1
Reductive Cyclizations

The first examples of nickel-catalyzed reductive couplings of aldehydes and alkynes involved organozincs as reducing agents (Scheme 2) [14]. In five-membered ring cyclizations, reductive couplings are effective with a $Ni(COD)_2/PBu_3$ catalyst system, whereas phosphine-free catalyst formulations favored the alkylative variant. In the phosphine-free conditions, reactions are rapid and favor the alkylative manifold, even with organozincs that are sp^3-hybridized and possess β-hydrogens. Alternatively, with $Ni(COD)_2/PBu_3$ (1 : 4) as catalyst, reactions are slower and favor the reductive manifold with Et_2Zn as reducing agent. A metallacycle that may serve as a common intermediate for both alkylative and reductive manifolds is depicted, and mechanistic issues are described in more detail in Sect. 3.

Subsequent studies illustrated that Et_3SiH and Et_3B are more effective reducing agents than Et_2Zn in promoting the reductive cyclization pathway. A number of bicyclic heterocycles were prepared employing the Et_3SiH variant, and the approach proved general for a number of different quinolizidine, indolizidine, and pyrrolizidine skeletal frameworks (Scheme 3) [15, 16].

In addition to the methodological advances noted above, the Et_3SiH variant was utilized in the total synthesis of three members of the allopumiliotoxin family [15, 16]. In one of the more complex examples, ynal substrate **1** was converted to product **2** in 93% isolated yield as a single diastereomer (Scheme 4). Simple removal of the protecting groups allowed completion of

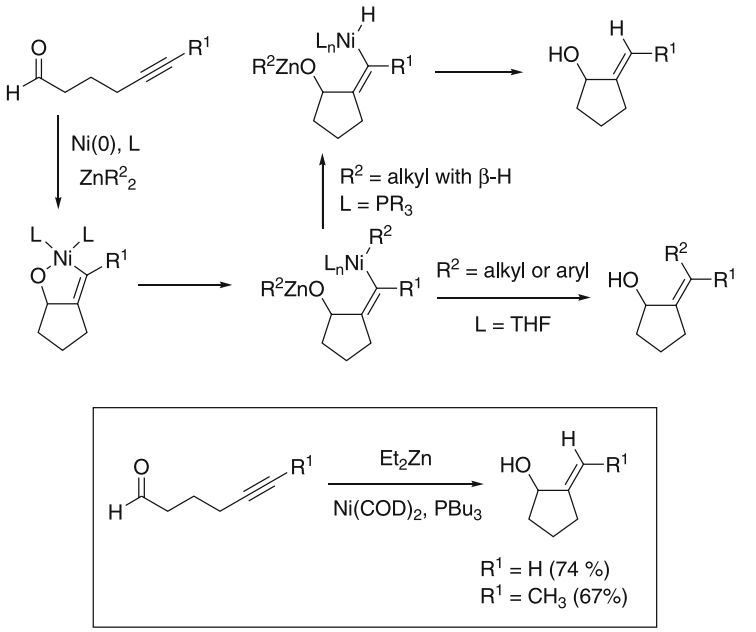

Scheme 2 Organozinc-mediated reductive cyclizations

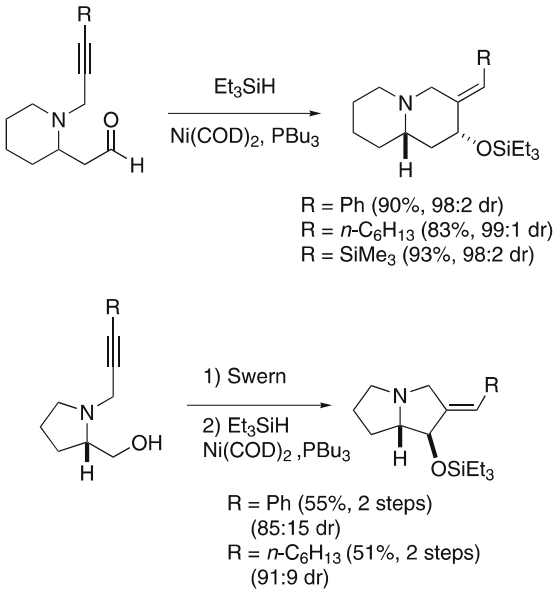

Scheme 3 Triethylsilane-mediated reductive cyclizations

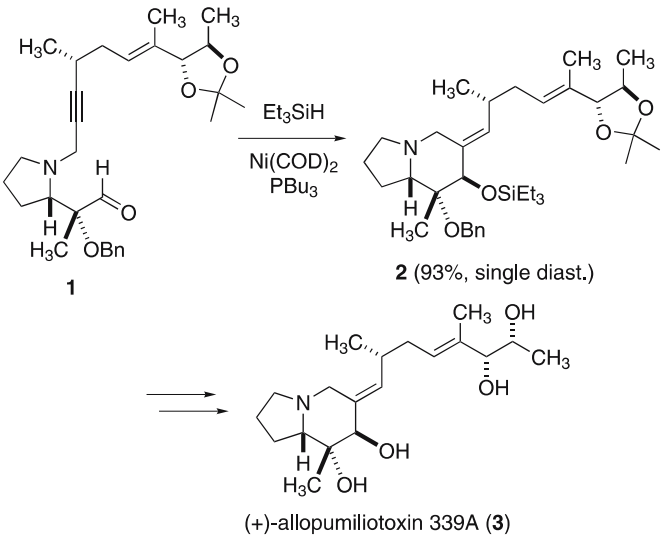

Scheme 4 Total synthesis of pumiliotoxin 339A

the synthesis of allopumiliotoxin 339A (**3**). This rapid approach to the pumiliotoxin framework provides an illustration of the complexity that can be installed in a single catalytic operation utilizing the ynal reductive cyclization method.

The Et_3B/PBu_3 and the NHC/Et_3SiH variants have largely been applied in intermolecular approaches, although both variants have been demonstrated to be useful in macrocyclizations. Elegant total syntheses of amphidinolides T1 and T4 were illustrated utilizing a complex macrocyclization involving the Et_3B variant (Scheme 5) [17, 18]. Cyclization of ynal **4** with $Ni(COD)_2/PBu_3$ with Et_3B as reducing agent allowed the efficient preparation of allylic alcohol **5**, which was converted to amphidinolide T1 (**6**). A key feature of the approach was the use of an aromatic alkyne, which directed the regiochemistry to favor the desired exocyclization process. An attempt to accomplish an endocyclic macrocyclization in the total synthesis of terpestacin was not successful since the exocyclic pathway predominated in that case as well. However, an intermolecular reductive coupling ultimately proved successful in that strategy (see Sect. 2.2.1).

The complementary regioselectivity of the NHC/Et_3SiH and PBu_3/Et_3B variants was demonstrated as a strategy for favoring either endocyclic or exocyclic macrocyclizations selectively in a ligand-controlled approach [19]. With ynal **7** for example, reductive macrocyclization with the very bulky IPr ligand and Et_3SiH as the reducing agent favored exocyclization product **8**, whereas cyclization with PMe_3 as the ligand and Et_3B as the reducing agent favored endocyclization product **9** (Scheme 6). A steric model was presented, suggesting that the bulky IPr ligand positions the alkyne in complex **10** such

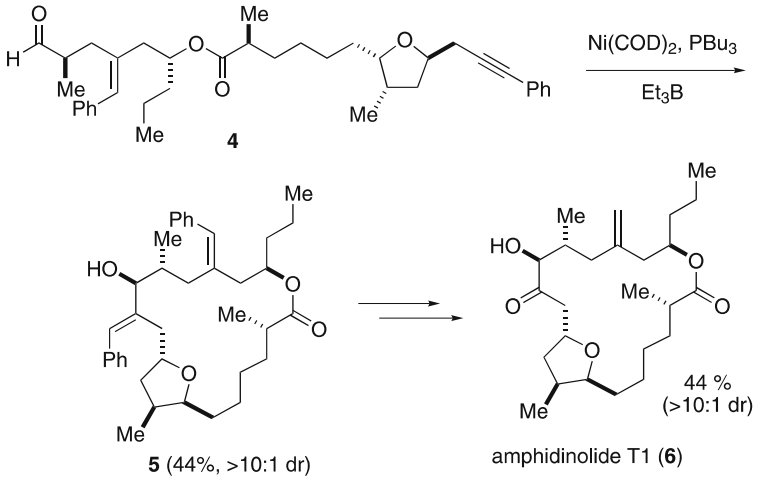

Scheme 5 Total synthesis of terpestacin

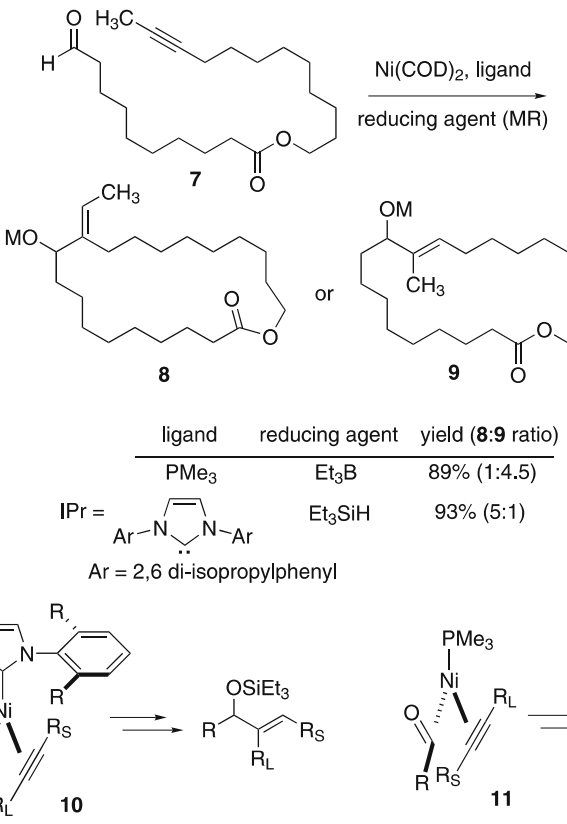

Scheme 6 Regiocontrol in macrocyclizations

that the more hindered alkyne terminus undergoes addition to the aldehyde, whereas the unhindered PMe_3 ligand positions the alkyne in complex **11** such that the least hindered alkyne terminus undergoes addition to the aldehyde. Five- and six-membered ring cyclizations have not been extensively investigated in the NHC/Et_3SiH or PBu_3/Et_3B variants; however, limited studies suggest that these processes are effective with a variety of ring sizes [20, 21].

2.2 Reductive Couplings

The intermolecular nickel-catalyzed reductive coupling of aldehydes and alkynes has largely been examined with the reaction variants involving either Et_3B with monodentate phosphines [22] or Et_3SiH with NHCs [21]. Substantial advances in simple couplings, large fragment couplings, diastereoselective variants, directed processes, and asymmetric variants have been made and are detailed below.

2.2.1 Basic Principles

Intermolecular aldehyde/alkyne reductive couplings involving PBu_3 and Et_3B have been explored on a variety of systems ranging from simple to quite complex [22]. Aromatic alkynes are generally the best substrates, whereas more substrate generality is observed on the aldehyde component (Scheme 7). In the course of examining asymmetric couplings (see Sect. 2.2.4), a variety of different monodentate phosphines were examined [23].

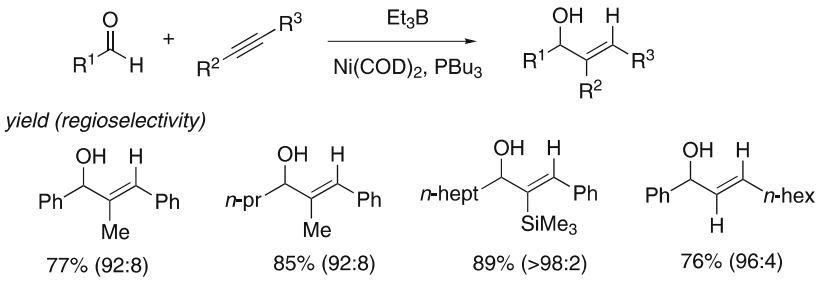

Scheme 7 Triethylborane-mediated reductive couplings

The participation of complex substrates was illustrated in an elegant total synthesis of (–)-terpestacin (Scheme 8) [24, 25]. Coupling of alkyne **12** and aldehyde **13** with $Ni(COD)_2$, phosphine **14**, and Et_3B afforded product **15** as a 2.6 : 1 mixture of regioisomers, and a 2 : 1 diastereoselectivity in a combined 85% yield. Whereas alkynes that possess two aliphatic substituents generally

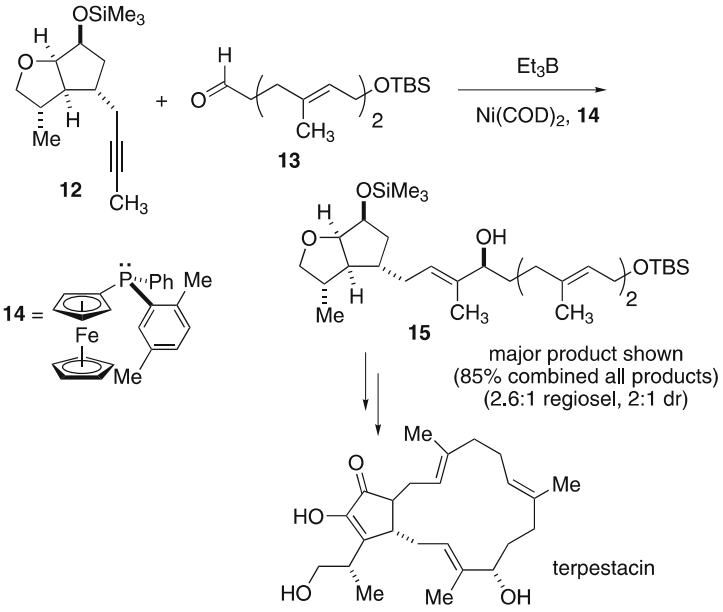

Scheme 8 Total synthesis of terpestacin

undergo coupling in lower yield than aromatic alkynes, the production of **15** illustrates that high yields are possible with non-aromatic alkynes.

The combination of $Ni(COD)_2$/NHC complexes with Et_3SiH as the reducing agent has also proved to be effective in intermolecular couplings of aldehydes and alkynes (Scheme 9) [21]. A broad range of substrates underwent couplings, including aromatic, non-aromatic, and terminal alkynes as well as branched, unbranched, and aromatic aldehydes. The regioselectivity with

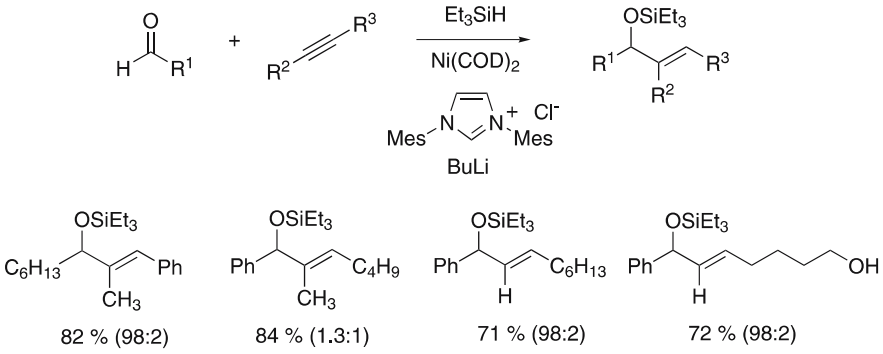

Scheme 9 Triethylsilane-mediated reductive couplings

internal alkynes is often complementary to that obtained with phosphine-promoted variants.

A limitation of the above methods is that terminal alkynes always display a strong bias towards formation of the 1,2-disubstituted alkene product derived from addition of the unsubstituted alkyne terminus to the aldehyde. An important complement to the above methods involves the catalytic reductive coupling of aldehydes and terminal alkynes employing $CrCl_2$ as the reducing agent with a $NiCl_2/PPh_3$ catalyst system in aqueous DMF as solvent (Scheme 10) [26, 27]. Under these conditions, the opposite regioisomer is obtained in comparison to the Et_3B and Et_3SiH methods described above. While the mechanistic details of this process are unclear, it appears that hydrometallation of the alkyne to generate a vinyl nickel species may be involved.

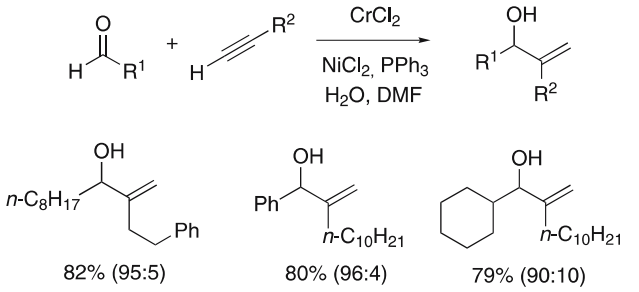

Scheme 10 Chromium(II)chloride-promoted reductive couplings

2.2.2 Diastereoselective Variants

Diastereoselective ynal cyclizations involving α-alkoxyaldehydes provided an exceptionally selective entry to the allopumiliotoxin framework as previously described (Sect. 2.1) [15, 16]. Diastereoselective intermolecular couplings of alkynes with α-alkoxy or α-silyloxy aldehydes have similarly proven to be effective in the production of *anti*-1,2-diols. Using Et_3B as the reducing agent, monoaryl-substituted internal alkynes underwent diastereoselective couplings with α-alkoxy aldehydes that possess a MOM protecting group (Scheme 11) [28]. Diastereoselectivities were excellent with β-branched aldehydes, whereas β-unbranched aldehydes participated with lower diastereselectivity. The best ligand for the process was a chiral ligand (+)-NMDPP (**16**). Little change in diastereoselectivity was observed when (–)-**16** was employed, illustrating that the steric and electronic properties of the ligand were important, not the absolute stereochemistry of the ligand.

Alternatively, silylalkynes underwent highly diastereoselective couplings with α-silyloxyaldehydes with $(i\text{-pr})_3SiH$ as the reducing agent and IMes as

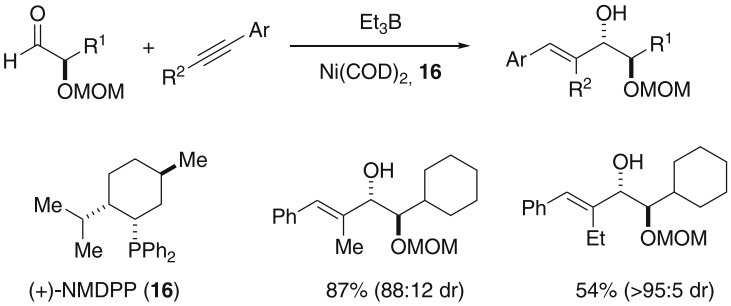

Scheme 11 Diastereoselective couplings of α-alkoxy aldehydes

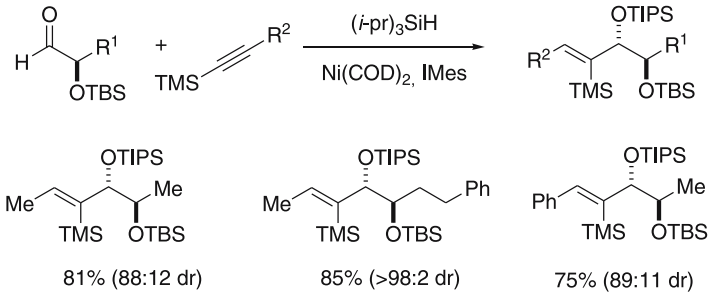

Scheme 12 Diastereoselective couplings of α-silyloxy aldehydes

ligand (Scheme 12) [29]. β-Unbranched aldehydes were the best substrates for this procedure, which rendered the method complementary to the Et_3B-based procedure. A broad range of aromatic and non-aromatic alkynes participate with excellent diastereoselectivities in this process.

2.2.3 Directed Processes

Examination of various enynes in intermolecular reductive couplings of aldehydes and alkynes illustrated that alkene direction is an effective strategy for controlling regioselectivity. Using conjugated enynes, both NHC/Et_3SiH [21] and PR_3/Et_3B [30] variants proceed with excellent diastereoselectivity favoring addition of the alkyne terminus that is distal to the alkene substituent (Scheme 13). This effect may be derived from predisposition of the alkyne in the orientation **17** that leads to the distal substitution, and increased stability of the η^3-stabilized metallacycle **18** may also be a factor.

1,6-Enynes are also especially effective in regioselective couplings, and the ligand structure and stoichiometry were both found to be important variables (Scheme 14) [31]. A model was proposed involving stereospecific ligand sub-

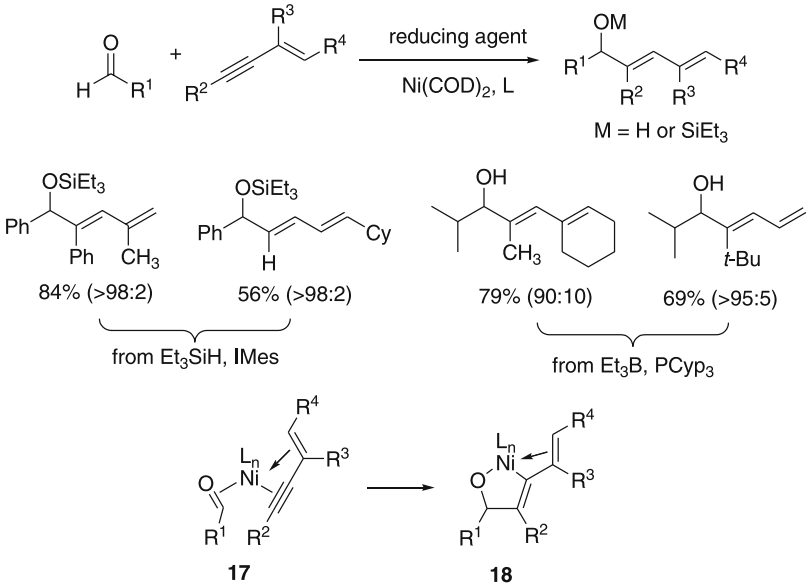

Scheme 13 Directed couplings of 1,3-enynes

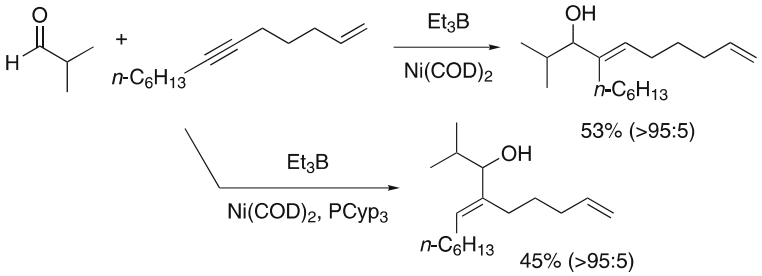

Scheme 14 Directed couplings of 1,6-enynes

stitution as a basis for regioselectivity [32]. The impact of chirality within the tether chain provided support for the model proposed.

2.2.4 Asymmetric Variants

A number of chiral monodentate phosphines have been examined in asymmetric nickel-catalyzed reductive couplings of aldehydes and alkynes. The best results to date have been obtained with (+)-NMDPP (**16**) [33]. Aromatic internal alkynes and branched aldehydes participate with excellent enantioselectivity (Scheme 15), although yields and enantioselectivities were somewhat lower with other combinations of aldehydes and alkynes. In a complemen-

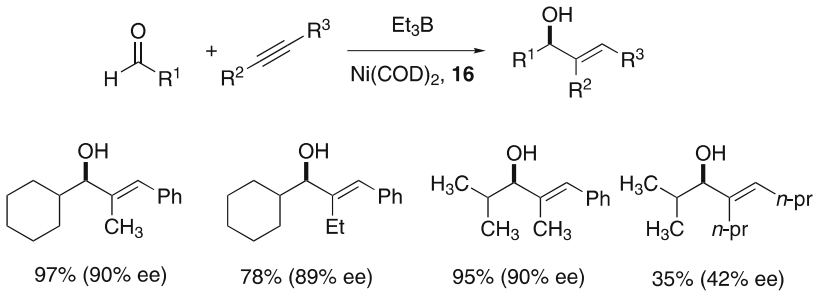

Scheme 15 Asymmetric couplings with (+)-NMDPP (**16**)

tary procedure, modest enantioselectivities were obtained with a variety of monodentate ferrocenyl phosphines [23].

2.3 Alkylative Cyclizations and Couplings

Whereas the majority of work in nickel-catalyzed aldehyde/alkyne couplings has focused on reductive coupling variants, as noted in Sect. 2.1, five-membered ring alkylative cyclizations of ynals are effective with $Ni(COD)_2$ under phosphine-free conditions [14]. Under these conditions, reactions are rapid and favor the alkylative manifold, even with organozincs that are sp^3-hybridized and possess β-hydrogens. Organozincs generated in situ from alkyl lithiums and anhydrous $ZnCl_2$ are effective participants in the process (Scheme 16). Although limited in scope, intermolecular alkylative couplings involving aldehydes, alkynes, and organozincs are also possible.

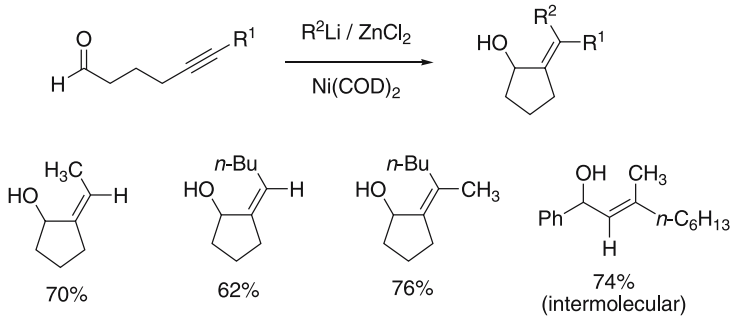

Scheme 16 Organozinc-promoted alkylative cyclizations

The above studies illustrated that sp^2-hybridized organozincs underwent direct addition to aldehydes rapidly, thus preventing the desired three-component couplings. However, alkenylzirconium reagents, derived from hy-

drozirconation of alkynes, do participate in intermolecular couplings of ynals and intramolecular couplings of aldehydes and alkynes (Scheme 17) [34]. This method provides a facile entry to functionalized 1,3-dienes, and a related process with unsaturated acyl oxazolidinones was developed as a key step in the total synthesis of isodomoic acid G [35]. Related intermolecular couplings of imines, alkynes, and organoboranes or boronic acids have been reported [36, 37].

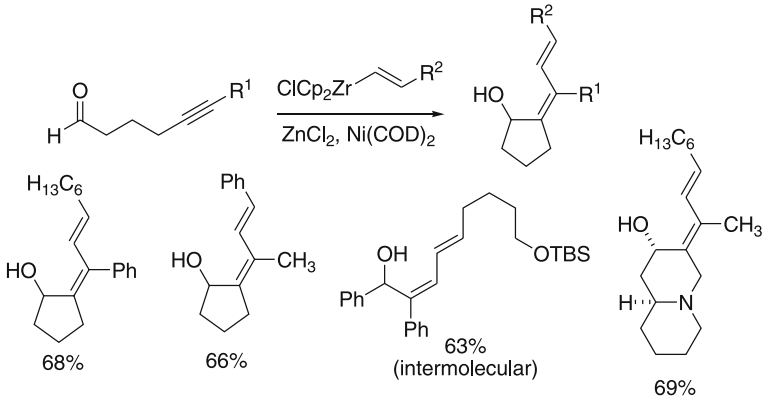

Scheme 17 Alkenylzirconium-promoted alkylative cyclizations

3 Mechanistic Considerations

A broad array of mechanistic pathways may be considered in the different variants of nickel-catalyzed reductive couplings of aldehydes and alkynes, and a generalized overview of possible mechanisms has been previously described [10]. Whereas a comprehensive mechanistic study has not been presented, a number of key observations have been illustrated that provide insight into how the nickel-catalyzed reductive couplings of aldehydes and alkynes proceed. It should be stressed at the outset that the different reaction variants may proceed by different mechanisms.

The initially proposed mechanism [14], and one that continues to be considered as the likely pathway for most variants, involves the oxidative cyclization of a Ni(0) complex of an aldehyde and alkyne to a metallacycle (Scheme 18). Metallacycle formation could proceed independently of the reducing agent via metallacycle **19**, or alternatively, metallacycle **20a** or **20b** could be formed via promotion of the oxidative cyclization transformation by the reducing agent. Cleavage of the nickel–oxygen bond in a σ-bond metathesis process generates an alkenyl nickel intermediate **21**. In the variants involv-

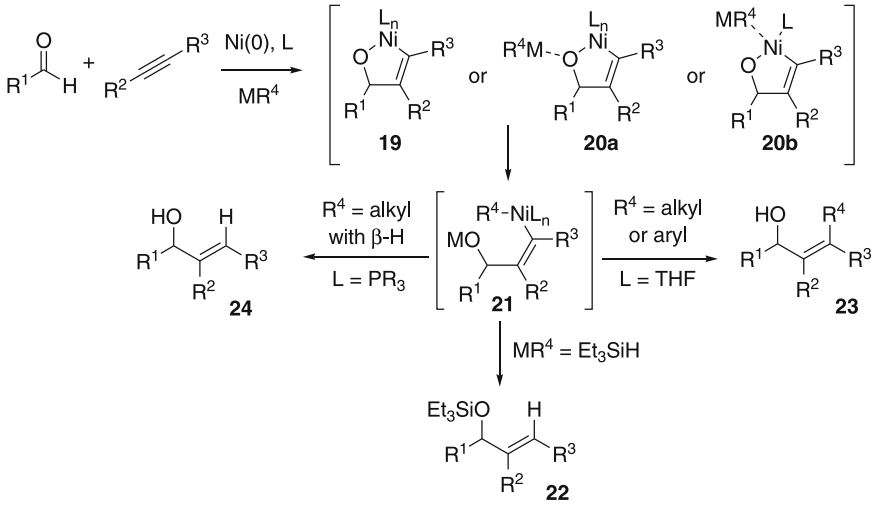

Scheme 18 Metallacycle-based mechanistic pathways

ing Et_3SiH, structure **21** is a nickel hydride (R = H), which would undergo reductive elimination to reductive coupling product **22**. In the variants involving organoboranes, organozincs, or alkenylzirconium reagents, structure **21** is an alkyl(alkenyl)nickel species (R = alkyl). Direct C – C bond reductive elimination would afford alkylative coupling product **23**, whereas β-hydride elimination of the R group would allow formation of a nickel hydride species, which leads to reductive coupling product **24**.

As noted above, it is likely in some cases that the reducing agent serves a promoter for the oxidative cyclization to produce **20a** or **20b**. Although not directly studied in nickel-catalyzed reductive couplings of aldehydes and alkynes, this effect has been proposed in closely related processes. For instance, in a study of enal/alkyne reductive couplings, the metallacycle formation in the absence of organozinc reducing agents was shown to be too slow to be involved in catalytic reactions, and an independently generated metallacycle was illustrated to not be kinetically competent [38]. In a computational evaluation of that reaction, a role of the organozinc involving a Lewis basic interaction with nickel and a Lewis acidic interaction with the carbonyl oxygen (essentially a hybrid of the interactions depicted in **20a** and **20b**) was described to explain the rate acceleration. In a separate study on the oxidative cyclization of nickel(0) with aldehydes and alkenes, direct evidence for the rate acceleration of metallacycle formation by trialkylsilyl triflates or organoaluminum reagents was documented [39, 40]. In nickel-catalyzed reductive couplings of aldehydes and alkynes, it is likely that similar accelerating roles of the reducing agent are often involved.

In addition to the metallacycle-based mechanism depicted above, stepwise insertion pathways such as alkyne hydrometallation followed by aldehyde

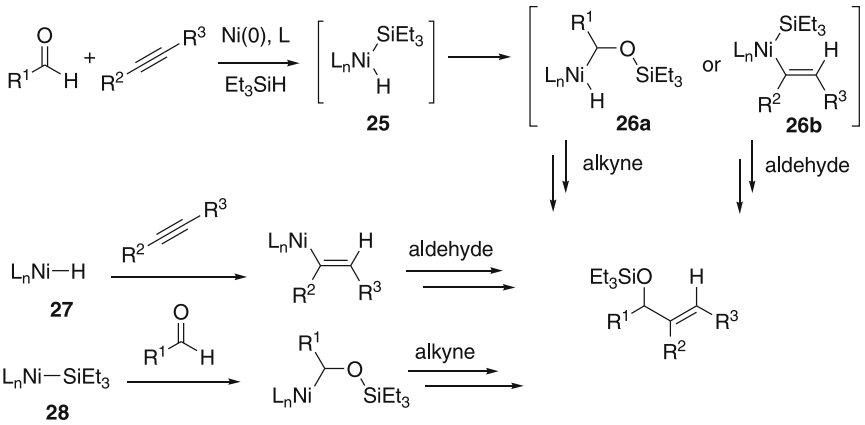

Scheme 19 Alternate mechanistic pathways

addition, or aldehyde silylmetallation followed by alkyne addition are also possible (Scheme 19) [41]. If the silane undergoes oxidative addition to Ni(0), species **25** would result. Species **25** could then be converted to product by aldehyde silylmetallation (via intermediate **26a**) or by alkyne hydrometallation (via intermediate **26b**). Alternatively, nickel hydride **27** or nickel silyl species **28** could be involved in similar sequences. Structures **27** and **28** may be formulated as neutral Ni(I) or cationic Ni(II) species. A recent study comparing NHC-catalyzed and phosphine-catalyzed reductive couplings involving trialkylsilanes lends support to the notion that multiple mechanisms may be operative according to the precise reaction conditions [21]. In that study, crossover experiments with Et_3SiD/nPr_3SiH illustrated that NHC-promoted processes proceed with only trace crossover, whereas significant crossover was observed in the PBu_3-promoted pathway (Scheme 20). Additionally, in the study of directed reactions of 1,6-enynes previously described (Sect. 2.2.3)

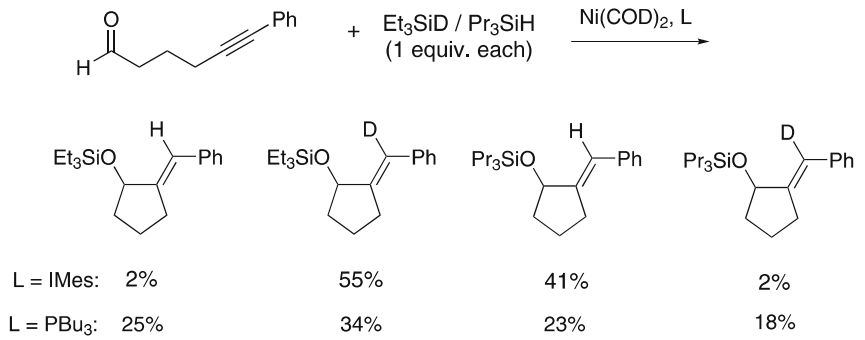

Scheme 20 Crossover studies that document multiple mechanistic pathways

a change in mechanism between a metallacycle-based pathway and a hydrometallation pathway was cited as a potential basis for the reversal of regioselection based on ligand structure [31].

4
Reductive Cycloadditions

The nickel-catalyzed reductive coupling of aldehydes and alkynes described in the previous sections provides a novel strategy for carbon–carbon bond formation. Recent advances have focused on applying this strategy in the context of cycloaddition processes rather than assembly of linear fragments. An advantage of the reductive cycloaddition strategy is that simple even-numbered π-systems can be converted to odd-numbered cycloaddition products, in contrast to traditional strategies ([4 + 2], [4 + 4], [6 + 2], etc.) that assemble even numbered rings from such precursors (Scheme 21) [42].

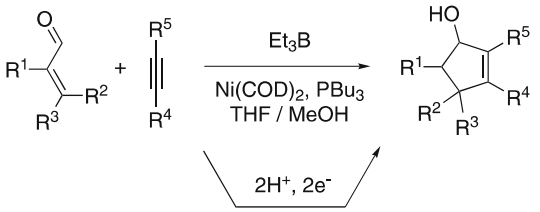

Scheme 21 Catalytic [3 + 2] reductive cycloadditions of enals and alkynes

Whereas stoichiometric versions of this strategy were initially reported [43, 44], a catalytic process involving a $Ni(COD)_2/PBu_3$ catalyst system, Et_3B as reducing agent, and a methanol/THF cosolvent system was recently developed. The process proceeds both inter- and intramolecularly to provide access to a variety of cyclopentenol derivatives (Scheme 22).

The mechanism of [3 + 2] reductive cycloadditions clearly is more complex than other aldehyde/alkyne couplings since additional bonds are formed in the process. The catalytic reductive [3 + 2] cycloaddition process likely proceeds via the intermediacy of metallacycle **29**, followed by enolate protonation to afford vinyl nickel species **30**, alkenyl addition to the aldehyde to afford nickel alkoxide **31**, and reduction of the Ni(II) alkoxide **31** back to the catalytically active Ni(0) species by Et_3B (Scheme 23). In an intramolecular case, metallacycle **29** was isolated, fully characterized, and illustrated to undergo [3 + 2] reductive cycloaddition upon exposure to methanol [45]. Related pathways have recently been described involving cobalt-catalyzed reductive cycloadditions of enones and allenes [46], suggesting that this novel mechanism may be general for a variety of metals and substrate combinations.

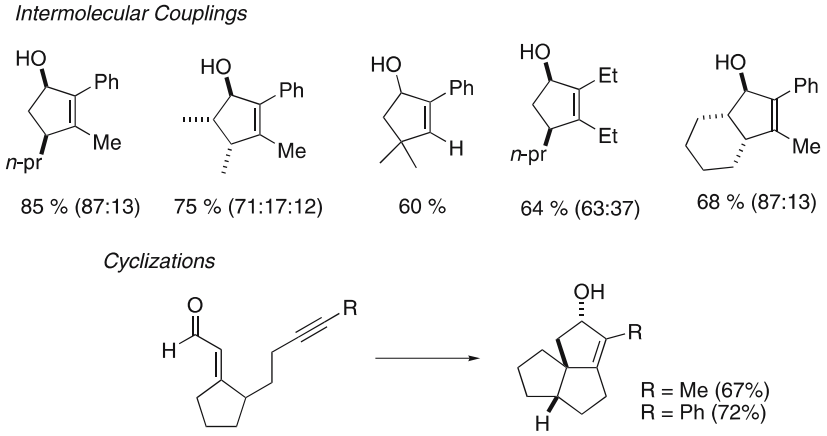

Scheme 22 Scope of catalytic [3 + 2] reductive cycloadditions

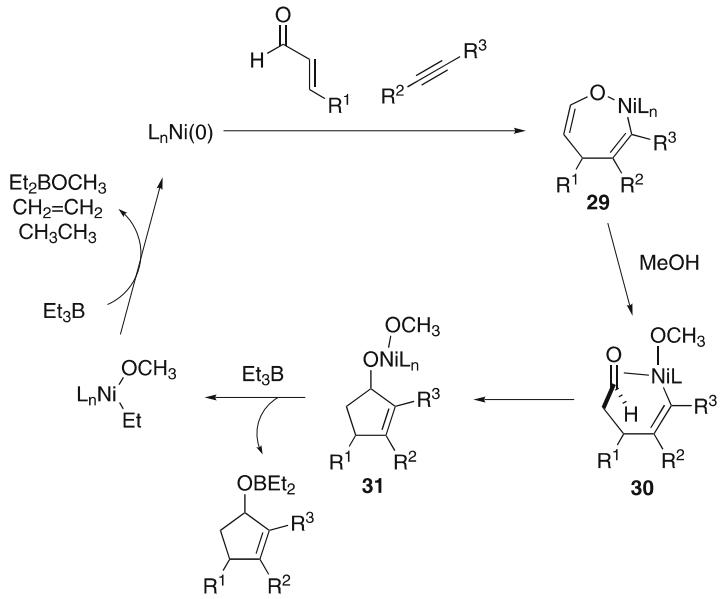

Scheme 23 Mechanism of catalytic [3 + 2] reductive cycloadditions

5
Mechanistically Related Processes

The nickel-catalyzed reductive coupling of aldehydes and alkynes is only one member of a growing class of processes that involve the three-component addition of two π-components and a reducing agent (Scheme 24). An

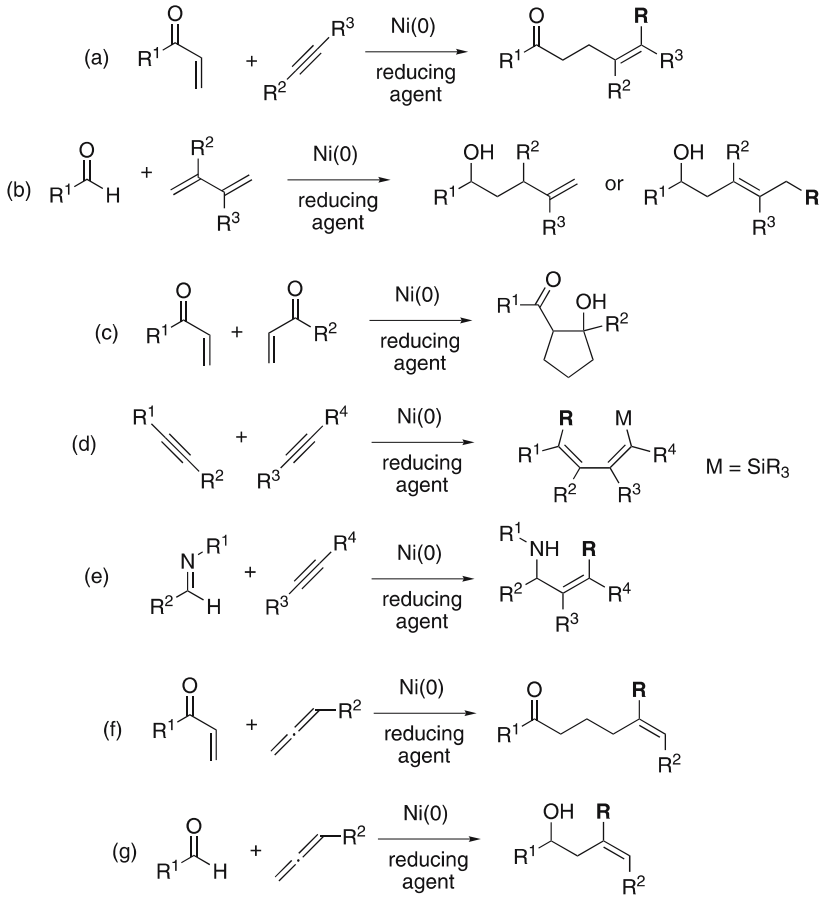

Scheme 24 Other classes of nickel-catalyzed reductive and alkylative couplings

overview of these methods was provided in a recent review [10]. Although the variants that involve aldehyde/alkyne coupling have been most extensively examined, significant advances have been made in the reductive and alkylative couplings of the following combinations of π systems: (a) alkynes and electron-deficient alkenes [47, 48], (b) aldehydes and dienes [49–52], (c) two electron-deficient alkenes [53, 54], (d) two alkynes [55, 56], (e) imines with alkynes [36, 37], (f) electron-deficient alkenes with allenes [57], and (g) aldehydes with allenes [58–62] (Scheme 24). Many of the mechanistic questions as well as the synthetic challenges (regio-, diastereo-, and enantioselection) described in this review for reductive couplings of aldehydes and alkynes pose similar challenges in these mechanistically related processes. Technical

or conceptual advances made in any one of these areas may potentially have impact on a number of related processes.

6
Summary of Alternative Methods

A variety of alternate methods for the reductive coupling of aldehydes and alkynes have been developed. A number of important hydrometallative strategies have been developed, although most of these methods require the stoichiometric formation of a vinyl metal species or metallacycle. A very attractive hydrogenative coupling method has recently been developed, and its scope is largely complementary to the nickel-catalyzed methods. A very brief overview of these methods is provided below.

6.1
Hydrometallation/Transmetallation Processes

Powerful methods for the reductive cyclization of aldehydes and alkynes have been developed that involve alkyne initial hydroboration [63, 64] or hydrozirconation [65, 66], followed by transmetalation with an organozinc reagent (Scheme 25). The resulting vinyl zinc species then undergoes addition to an aldehyde to afford the reductive coupling product. Both of these methods result in the formation of a *trans* alkene and are limited to terminal alkynes. The hydroboration was found to be selective for alkynes in the presence of aldehydes allowing for intramolecular reactions. Chiral amino alcohols or aminothiols promote the addition of the organozinc to the aldehyde and have been used to achieve enantioselectivities up to 98% in intermolecular couplings and up to 92% in macrocyclizations.

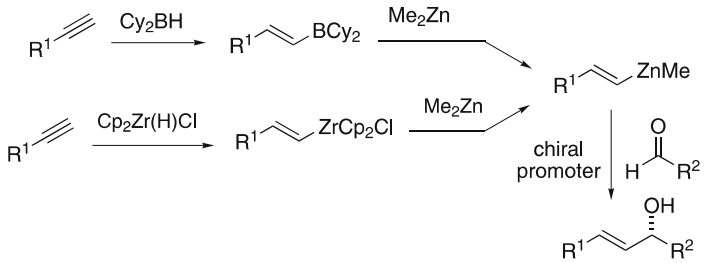

Scheme 25 Hydroboration and hydrozirconation strategies for aldehyde/alkyne reductive coupling

In earlier, conceptually related advances, an alkylative process was developed that involves a zirconium-catalyzed addition of trialkyl aluminum

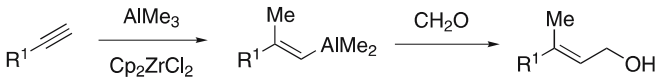

Scheme 26 Carboalumination strategy for aldehyde/alkyne alkylative coupling

reagents to the alkyne, which creates a vinyl aluminum species that undergoes addition to aldehydes (Scheme 26) [67]. The process was illustrated for terminal alkynes with a limited range of aldehydes, and the scope has not been extensively studied.

6.2 Zr and Ti Metallacycle-Based Approaches

A variety of aldehyde/alkyne reductive couplings involving the stoichiometric use of early transition metals (Ti and Zr) have been developed (Scheme 27) [68–70]. The low cost and ease of handling of titanium alkoxides render these stoichiometric processes very practical despite the lack of catalytic turnover. Recent variants of stoichiometric processes involving titanium alkoxides have demonstrated impressive scope in relatively complex applications [71–73].

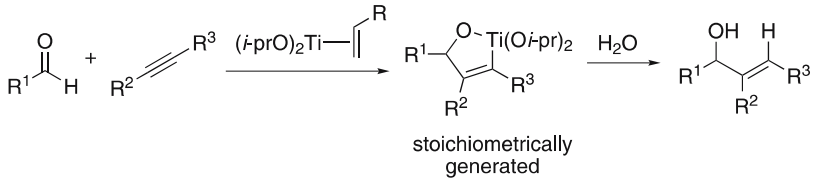

Scheme 27 Titanium alkoxide-based strategy for aldehyde/alkyne reductive coupling

Although the titanium-based methods are typically stoichiometric, catalytic turnover was achieved in one isolated example with trialkoxysilane reducing agents with titanocene catalysts (Scheme 28) [74]. This example (as part of a broader study of enal cyclizations [74, 75]) was indeed the first process to demonstrate catalysis in a silane-based aldehyde/alkyne reductive coupling and provided important guidance in the development of the nickel-catalyzed processes that are generally more tolerant of functionality and broader in scope.

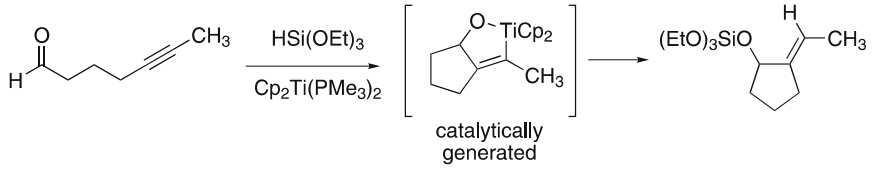

Scheme 28 Titanocene-based strategy for aldehyde/alkyne reductive coupling

6.3
Hydrogenative Couplings

The powerful rhodium-catalyzed coupling of aldehydes with alkynes under hydrogenation conditions have been described elsewhere in this volume. A variety of substrates participate in the process, and additions of polyunsaturated substrates such as enynes and diynes with α-ketoesters or α-ketoaldehydes have been most extensively studied (Scheme 29) [76, 77]. The use of hydrogen gas as the reducing agent is an especially attractive feature of this novel process. The levels of enantioselection obtained in several variants of the hydrogenative reductive coupling are now benchmarks for asymmetric processes of this general class [78, 79].

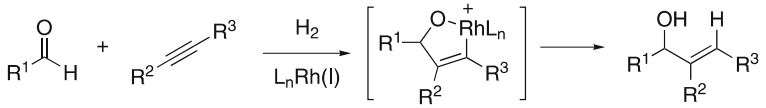

Scheme 29 Hydrogenative strategy for aldehyde/alkyne reductive coupling

7
Conclusion

In summary, a variety of nickel-catalyzed methods for the reductive or alkylative couplings of aldehydes and alkynes have been developed. The combination of variants available present a versatile series of reactions that allow allylic alcohols to be rapidly generated, often with excellent levels of regio-, diastereo-, and enantioselectivity. A number of complex illustrations in natural product synthetic applications demonstrate that the methods can be applied in a variety of challenging settings. Future developments that improve enantioselectivities with a larger variety of substrates, that increase regioselectivities with internal alkynes, and that facilitate large scale applications will continue to advance the utility of the process.

References

1. Godleski SA (1991) In: Trost BM, Fleming I (eds) Comprehensive organic synthesis. Pergamon, Oxford, p 585
2. Johnson RA, Sharpless KB (1991) In: Trost BM, Fleming I (eds) Comprehensive organic synthesis. Pergamon, Oxford, p 389
3. Denmark SE, O'Connor SP (1997) J Org Chem 62:584
4. Charette AB, Marcoux JF (1995) Synlett, p 1197
5. Overman LE (1992) Acc Chem Res 25:352

6. Lipshutz BH, Sengupta S (1992) In: Paquette LA (ed) Organic reactions. Wiley, New York, p 135
7. Wipf P (1991) In: Trost BM, Fleming I (eds) Comprehensive organic synthesis. Pergamon, Oxford, p 827
8. Jin H, Uenishi J, Christ WJ, Kishi Y (1986) J Am Chem Soc 108:5644
9. Takai K, Tagashira M, Kuroda T, Oshima K, Utimoto K, Nozaki H (1986) J Am Chem Soc 108:6048
10. Montgomery J (2004) Angew Chem Int Ed 43:3890
11. Montgomery J (2000) Acc Chem Res 33:467
12. Ikeda S (2003) Angew Chem Int Ed 42:5120
13. Miller KM, Molinaro C, Jamison TF (2003) Tetrahedron: Asymmetry 14:3619
14. Oblinger E, Montgomery J (1997) J Am Chem Soc 119:9065
15. Tang XQ, Montgomery J (1999) J Am Chem Soc 121:6098
16. Tang XQ, Montgomery J (2000) J Am Chem Soc 122:6950
17. Colby EA, O'Brien KC, Jamison TF (2004) J Am Chem Soc 126:998
18. Colby EA, O'Brien KC, Jamison TF (2005) J Am Chem Soc 127:4297
19. Knapp-Reed B, Mahandru GM, Montgomery J (2005) J Am Chem Soc 127:13156
20. Lozanov M, Montgomery J (2002) J Am Chem Soc 124:2106
21. Mahandru GM, Liu G, Montgomery J (2004) J Am Chem Soc 126:3698
22. Huang WS, Chan J, Jamison TF (2000) Org Lett 2:4221
23. Colby EA, Jamison TF (2003) J Org Chem 68:156
24. Chan J, Jamison TF (2003) J Am Chem Soc 125:11514
25. Chan J, Jamison TF (2004) J Am Chem Soc 126:10682
26. Takai K, Sakamoto S, Isshiki T (2003) Org Lett 5:653
27. Takai K, Sakamoto S, Isshiki T, Kokumai T (2006) Tetrahedron 62:7534
28. Luanphaisarnnont T, Ndubaku CO, Jamison TF (2005) Org Lett 7:2937
29. Sa-ei K, Montgomery J (2006) Org Lett 8:4441
30. Miller KM, Luanphaisarnnont T, Molinaro C, Jamison TF (2004) J Am Chem Soc 126:4130
31. Miller KM, Jamison TF (2004) J Am Chem Soc 126:15342
32. Moslin RM, Jamison TF (2006) Org Lett 8:455
33. Miller KM, Huang WS, Jamison TF (2003) J Am Chem Soc 125:3442
34. Ni Y, Amarasinghe KKD, Montgomery J (2002) Org Lett 4:1743
35. Ni Y, Amarasinghe KKD, Ksebati B, Montgomery J (2003) Org Lett 5:3771
36. Patel SJ, Jamison TF (2003) Angew Chem Int Ed 42:1364
37. Patel SJ, Jamison TF (2004) Angew Chem Int Ed 43:3941
38. Hratchian HP, Chowdhury SK, Gutiérrez-Garcia VM, Amarasinghe KKD, Heeg MJ, Schlegel HB, Montgomery J (2004) Organometallics 23:4636
39. Ogoshi S, Oka M, Kurosawa H (2004) J Am Chem Soc 126:11802
40. Ogoshi S, Ueta M, Arai T, Kurosawa H (2005) J Am Chem Soc 127:12810
41. Chaulagain MR, Mahandru GM, Montgomery J (2006) Tetrahedron 62:7560
42. Herath A, Montgomery J (2006) J Am Chem Soc 128:14030
43. Chowdhury SK, Amarasinghe KKD, Heeg MJ, Montgomery J (2000) J Am Chem Soc 122:6775
44. Mahandru GM, Skauge ARL, Chowdhury SK, Amarasinghe KKD, Heeg MJ, Montgomery J (2003) J Am Chem Soc 125:13481
45. Amarasinghe KKD, Chowdhury SK, Heeg MJ, Montgomery J (2001) Organometallics 20:370
46. Chang H-T, Jayanth TT, Cheng CH (2007) J Am Chem Soc 129:4166
47. Ikeda S, Sato Y (1994) J Am Chem Soc 116:5975

48. Montgomery J, Oblinger E, Savchenko AV (1997) J Am Chem Soc 119:4911
49. Sato Y, Takimoto M, Hayashi K, Katsuhara T, Takagi K, Mori M (1994) J Am Chem Soc 116:9771
50. Sato Y, Takimoto M, Mori M (2000) J Am Chem Soc 122:1624
51. Kimura M, Ezoe A, Shibata K, Tamaru Y (1998) J Am Chem Soc 120:4033
52. Kimura M, Matsuo S, Shibata K, Tamaru Y (1999) Angew Chem Int Ed 38:3386
53. Montgomery J, Savchenko AV (1996) J Am Chem Soc 118:2099
54. Seo J, Fain H, Blanc JB, Montgomery J (1999) J Org Chem 64:6060
55. Tamao K, Kobayashi K, Ito Y (1989) J Am Chem Soc 111:6478
56. Tamao K, Kobayashi K, Ito Y (1992) Synlett, p 539
57. Chevliakov MV, Montgomery J (1999) J Am Chem Soc 121:11139
58. Amarasinghe KKD, Montgomery J (2002) J Am Chem Soc 124:9366
59. Montgomery J, Song M (2002) Org Lett 4:4009
60. Kang S-K, Yoon S-K (2002) Chem Commun, p 2634
61. Ng S-S, Jamison TF (2005) J Am Chem Soc 127:7320
62. Ng S-S, Jamison TF (2005) Tetrahedron 61:11405
63. Oppolzer W, Radinov RN (1992) Helv Chim Acta 75:170
64. Oppolzer W, Radinov RN (1993) J Am Chem Soc 115:1593
65. Wipf P, Xu W (1994) Tetrahedron Lett 35:5197
66. Wipf P, Xu W (1998) Org Synth Coll Vol 9:143
67. Okukado N, Negishi E (1978) Tetrahedron Lett 19:2357
68. Van Wagenen BC, Livinghouse T (1989) Tetrahedron Lett 30:3495
69. Kataoka Y, Miyai J, Oshima K, Takai K, Utimoto K (1992) J Org Chem 57:1973
70. Harada K, Urabe H, Sato F (1995) Tetrahedron Lett 36:3203
71. Bahadoor AB, Flyer A, Micalizio GC (2005) J Am Chem Soc 127:3694
72. Shimp HL, Micalizio GC (2005) Org Lett 7:5111
73. Bahadoor AB, Micalizio GC (2006) Org Lett 8:1181
74. Crowe WE, Rachita MJ (1995) J Am Chem Soc 117:6787
75. Kablaoui NM, Buchwald SL (1996) J Am Chem Soc 118:3182
76. Ngai MY, Kong JR, Krische MJ (2007) J Org Chem 72:1063
77. Jang H-Y, Krische MJ (2004) Acc Chem Res 37:653
78. Komanduri V, Krische MJ (2006) J Am Chem Soc 128:16448
79. Rhee JU, Krische MJ (2006) J Am Chem Soc 128:10674

Top Curr Chem (2007) 279: 25–52
DOI 10.1007/128_2007_130

Published online: 9 May 2007

Reductive C–C Bond Formation after Epoxide Opening via Electron Transfer

Andreas Gansäuer (✉) · José Justicia · Chun-An Fan · Dennis Worgull · Frederik Piestert

Kekulé Institut für Organische Chemie und Biochemie, Universität Bonn, Gerhard-Domagk-Str. 1, 53121 Bonn, Germany
andreas.gansaeuer@uni-bonn.de

Abstract This review presents a description of the C – C bond-forming reactions that have emerged in the field of titanocene mediated or catalyzed epoxide opening over the last 5 years or so. The powerful tandem sequences for polycylization will be especially emphasized.

Keywords Catalysis · Cyclizations · Electron transfer · Radicals · Tandem reactions

Abbreviations

LDBB	lithium 4,4′-di-*tert*-butylbiphenylidene
THF	tetrahydrofuran
Tr	triphenylmethyl
TBS	*tert*-butyldimethyl silyl
PMB	*para*-methoxybenzyl
Coll	2,4,6-collidine (2,4,6-trimethylpyridine)
eq	equivalent(s)
ET	electron transfer
Ts	tosyl (p-$CH_3C_6H_4SO_2$)
dr	diastereomeric ratio
RT	room temperature
MCPBA	*meta*-chlorperoxybenzoic acid
Py	pyridine
DMAP	4-dimethylaminopyridine
AIBN	Azo-bis-isobutyronitrile

1 Introduction

Epoxides are amongst the most frequently employed substrates in organic synthesis. This is due to the ease of their preparation from readily available precursors, for example olefins and carbonyl compounds, and their high reactivity [1–4, 6]. The latter point arises from the strain inherent in the three-membered ring that is released during ring opening. Epoxides, especially when prepared in high enantiomeric excess, have been very useful in S_N2 reactions in this respect [7–9]. An alternative approach to exploiting the high reactivity of the strained epoxide is constituted by ring-opening reactions utilizing electron transfer reagents. In these reactions "Cp_2TiCl" has, to date, emerged as the most powerful reagent. Gratifyingly, the regioselectivity of ring opening is complementary to the S_N2-type reactions. After epoxide opening β-titanoxy radicals are obtained that can be used in many typical but also in quite unusual radical reactions. Moreover, many often highly functionalized products can be obtained in a straightforward manner. These developments will be reviewed in this article.

1.1 Epoxide Opening by Single Electron Transfer: Birch Conditions and Radical Anions

Before turning to epoxide opening with low valent metal complexes, the reduction of epoxides under Birch conditions [10–13] will be discussed very briefly for historical reasons. The initially formed radical is reduced further to give carbanionic species, that do not display the reactivity of radicals. No C – C bond-forming reactions have initially been reported.

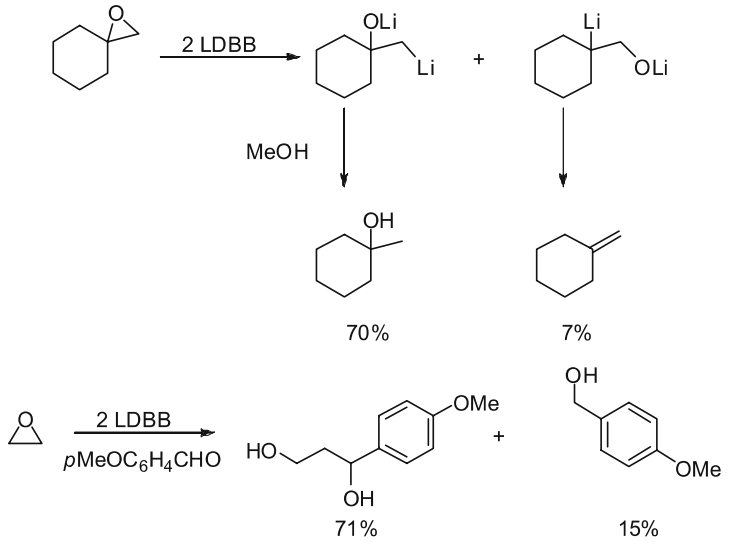

Scheme 1 Epoxide opening with arene radical anions under ET conditions

Bartmann [14], Cohen and Houk [15, 16] and Yus [17, 18] have employed aromatic radical anions as more convenient reducing agents to generate the same functionalized organolithium reagents. The typical electrophiles, such as aldehydes, and reactive alkylating agents were employed in C – C bond-forming reactions. Examples are shown in Scheme 1.

2
Epoxide Opening by Low Valent Metal Complexes: General Considerations and Mechanism of Epoxide Opening

2.1
General Considerations

With respect to the utilization of epoxide-derived radicals for organic synthesis the use of low valent metal complexes is highly promising. In principle, the advantages of Lewis-acid catalysis [19] and radical chemistry [20–23] can be combined by this approach. This is achieved by activating the epoxide towards ET by complexation with the metal and at the same time controlling the regioselectivity of epoxide opening through the metal and its ligands. The much stronger epoxide activation necessary for S_N-type reactions can be avoided by fine-tuning the acidity of the metal center [24]. Perhaps even more importantly, the ensuing radical reactions can be controlled by the metal complex and its ligands.

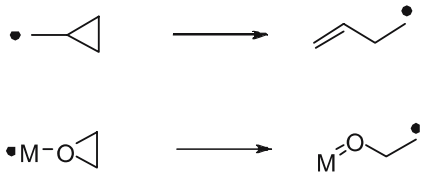

Scheme 2 Opening of the cyclopropylcarbinyl radical and epoxide opening by low valent metal complexes

To the best of our knowledge the first successful realization of this concept was achieved by Kochi in 1968, who described the deoxygenation of epoxides with Cr(II) reagents. However, no further attempts were undertaken to form C – C bonds with the pivotal β-metaloxy radicals [25].

Nugent and RajanBabu introduced titanocene (III) chloride "Cp_2TiCl" as an excellent reagent for the reductive opening of epoxides in 1988. They were also the first to outline the analogy of epoxide opening through ET with the well-established opening of a cyclopropylcarbinyl radical [26–29] (Scheme 2). As yet, "Cp_2TiCl" and substituted titanocenes have remained the most powerful reagent for this type of reaction and have recently attracted considerable interest [30–35].

The structure of the reagent, the mechanism of epoxide opening, deoxygenations, dimerizations and intermolecular additions will be discussed first before covering the preparatively much more important cyclization reactions [36].

2.2
Structure of the Reagent and Mechanism of Epoxide Opening

Before entering the discussion of the synthetic results, a brief description of the structure of "Cp_2TiCl" and the mechanism of epoxide opening is given. These results serve as a guide for choosing a suitable catalyst for a given application.

Usually zinc or manganese reduced solutions of the respective titanocene dichlorides are used in the practical reactions. Daasbjerg and his group have demonstrated that in the case of Cp_2TiCl_2 this reduced solution contains mainly the chlorine-bridged dimer $(Cp_2TiCl)_2$ and a small amount of the monomer Cp_2TiCl. No bimetallic complexes are involved [37–41]. For the sake of simplicity we denote this mixture of compounds as "Cp_2TiCl". Surprisingly the dimer, presumably in its half-open form, constitutes the more reactive species (Scheme 3) [42, 43].

Substitution of the Cp ligands reduces the tendency to dimerize. Introduction of a cyclohexyl group is sufficient for rendering the monomer the only detectable species by CV. The substituted titanocene chlorides open epoxides slower than "Cp_2TiCl". However, the resulting β-metaloxy radicals are more

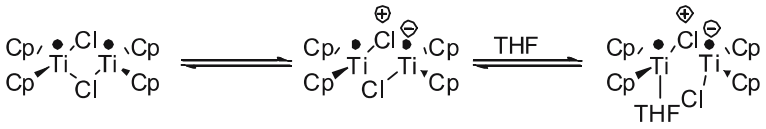

Scheme 3 Structure of "Cp_2TiCl" in solution

persistent. This can be advantageous for the use of substituted titanocenes in slow radical reactions [42, 43].

Epoxides are usually opened to give the higher substituted radicals, especially with substituted titanocenes. Chelation can be important when hydroxy groups are involved [26–29, 42, 43].

3
Formation of C–C Double Bonds by Epoxide Deoxygenation and Epoxide Dimerization

Olefins can be prepared by the deoxygenation of epoxides usually in good to excellent yields. However, the reaction is of synthetic use only if the epoxides employed as starting materials are prepared from other functional groups than olefins or if they can be isolated or readily accessed from natural sources. The issue of regioselectivity of deoxygenation is critical, however.

Nugent and RajanBabu described that with "Cp_2TiCl", that had been isolated and purified prior to use, an (*E*) to (*Z*) ratio of 3–4 : 1 of 5-decenes was observed from either *cis*- or *trans*-5-decene oxide [28, 29]. Therefore, it seems clear that a common long-lived β-titanoxy radical intermediate was formed from both epoxides. After further reduction and elimination the formation of the mixture of olefin diastereoisomers was observed.

Examples for straightforward epoxide preparation from natural sources can be found in carbohydrate chemistry [28, 29]. Deoxygenations of such compounds are shown in Scheme 4.

The first example amply demonstrates the exceptional chemoselectivity of the "Cp_2TiCl" reagent. The dihydrofuran product is already decomposed by traces of acid.

A limitation of epoxide deoxygenation with functionalized substrates became apparent in the second case where a mixture of olefins was isolated. Thus, the regioselectivity of epoxide opening and elimination of the titanium oxygen species was too low for practical use.

An effective deoxygenation using enantiomerically pure epoxides from primary allylic alcohols ("Sharpless epoxides") [44] to give enantiomerically pure secondary allylic alcohols was described by Yadav [45]. This approach circumvented a kinetic resolution of secondary allylic alcohols that implies a maximum yield of 50% (Scheme 5).

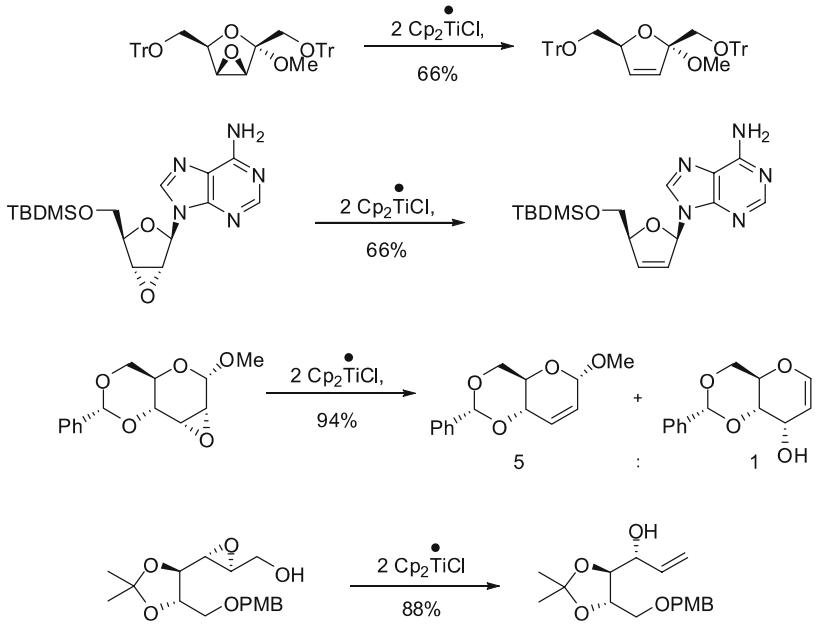

Scheme 4 Epoxide deoxygenation reactions

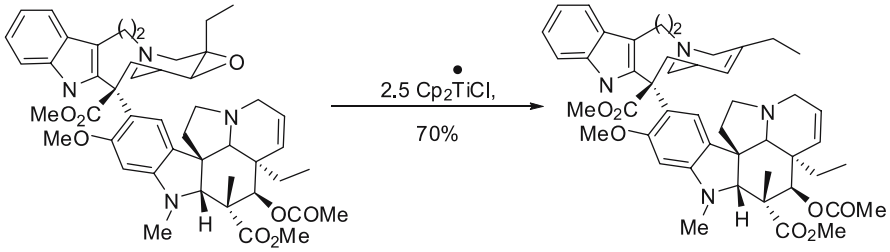

Scheme 5 Doris' deoxygenation en route to leurosine

Two deoxygenations of naturally occurring compounds have been reported. Anhydrovinblastine, an important intermediate for the anticancer drug navelbine, was prepared by Doris and coworkers from leurosine, an abundant alkaloid from the Madagascan periwinkle *Catharantus roseus*, in 70% yield by using Cp_2TiCl (Scheme 5) [46].

Stereospecific deoxygenations in the cryptophycin family of natural products from *Nostocaceae* were reported by Moore [47]. The products were important in the elucidation of the natural product's structure and for the preparation of novel cryptophycin derivatives.

Another interesting example of a reaction without additional organic radical trap has very recently been reported by Barrero and his group [48].

Vinylepoxides were used for the generation of β-titanoxy allylradicals. These species are too stable to be readily reduced by a second equivalent of "Cp_2TiCl" and can therefore dimerize to yield 1,5-dienes. While the diastereoselectivity is low in simple cases, the usefulness of the method is amply demonstrated by a very short and straightforward access to analogues of the natural onoceranes as shown in Scheme 6.

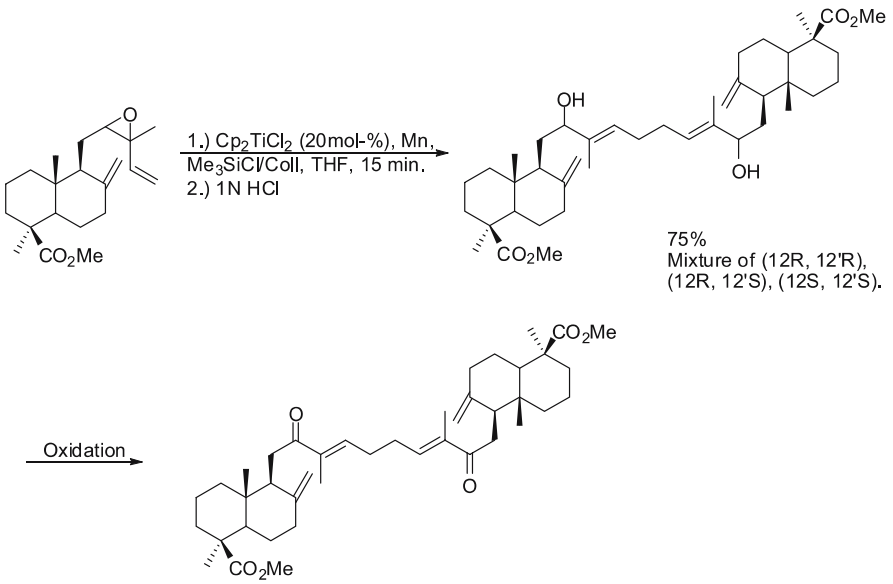

Scheme 6 Barrero's dimerization of vinylepoxides for the preparation of homoonecerans

4
Formation of C–C Bonds by Intermolecular Addition

4.1
Stoichiometric Reactions

Epoxide-derived radicals are generated under very mild reaction conditions and are therefore valuable for intermolecular C – C bond-forming reactions [27, 29]. The resulting products, δ-hydroxyketones, δ-hydroxyesters or δ-lactones constitute important synthetic intermediates. The first examples were reported by Nugent and RajanBabu who used a variety of epoxides, such as cyclohexene oxide and a "Sharpless" epoxide (Scheme 7).

Similar examples of the latter reactions were also reported by Chakraborty [49]. Analogous transformations cannot be achieved with organometallic

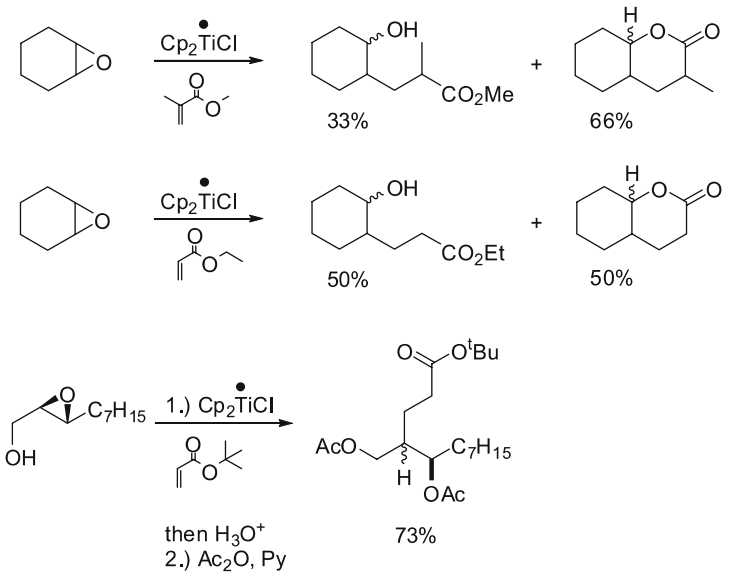

Scheme 7 Stoichiometric intermolecular addition reactions

reagents, for example cuprates, because of competing β-elimination pathways.

The outstanding chemoselectivity of "Cp_2TiCl" was amply demonstrated by Merlic [50, 51] and by Dötz [52] who employed α,β-unsaturated tungsten and chromium carbenes as radical traps for C – C bond formation. In the latter contribution the very acid sensitive glycal epoxides were used with good success. An example is shown in Scheme 8.

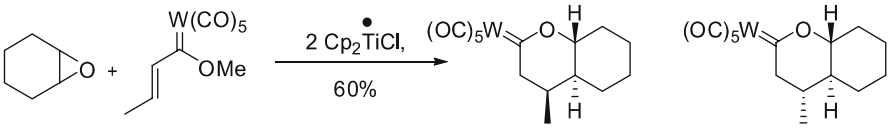

Scheme 8 Addition reactions with tungsten carbenes

Little used organic acceptors for these reactions, also [53, 54]. The use of a glycal as the radical source together with a functionalized enone as the radical acceptor is remarkable. Enones are swiftly reduced by "Cp_2TiCl" [55] and thus epoxide activation must be considered as even more efficient. The product of the addition constitutes a valuable intermediate en route to derivatives of thyrsiferiol.

Malacria has reported the use of epoxysilanes for intermolecular addition reactions to acrylates, acrylonitrile and vinylsulfones [56].

4.2 Catalytic Reactions

In stoichiometric applications of titanocene complexes, no attempt to use ligands other than unsubstituted cyclopentadienyl have been reported. The use of more complex titanocenes [57, 58] in catalytic reactions is, however, very promising for controlling the regio- and stereochemical course of the reaction.

Catalytic turn-over [59, 60] in McMurry couplings [61], Nozaki–Hiyama reactions [62, 63], and pinacol couplings [64, 65] has been reported by Fürstner and by Hirao by in situ silylation of titanium, chromium and vanadium oxo species with Me_3SiCl. In the epoxide-opening reactions, protonation can be employed for mediating catalytic turn-over instead of silylation because the intermediate radicals are stable toward protic conditions. The amount of "Cp_2TiCl" needed for achieving isolated yields similar to the stoichiometric process can be reduced to 1–10 mol % by using 2,4,6-collidine hydrochloride or 2,6-lutidine hydrochloride as the acid and Zn or Mn dust as the reductant (Scheme 9) [66, 67].

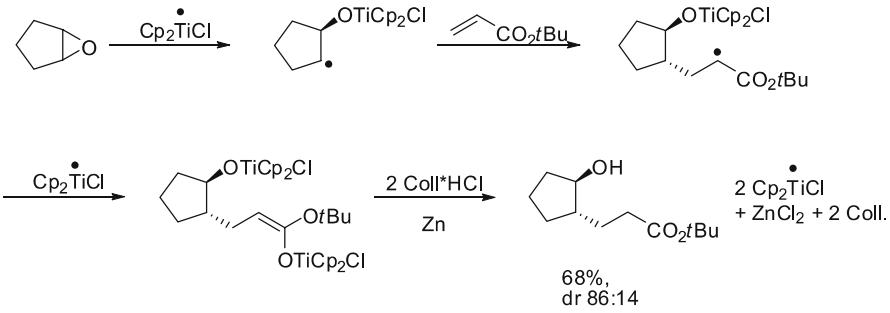

Scheme 9 Catalytic intermolecular addition (5 mol % [Ti])

These conditions were well suited for the preparation of δ-hydroxyesters, lactones, and δ-hydroxynitriles. Moreover, the usefulness of substituted titanocenes for enantio- and diastereoselective preparation of these products has been demonstrated as shown in Scheme 10 [68–72].

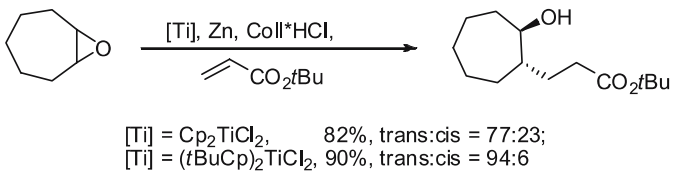

Scheme 10 Control of diastereoselectivity of the addition reaction

4.3
Polymerizations

Over the past decade there has been intense interest in living radical polymerizations. In these reactions molecular weight (*Mn*) and polydispersity (*Mw*/*Mn*) can be controlled by the reversible termination of the growing chains. Asandei and his group have demonstrated that the "Cp_2TiCl"-catalyzed epoxide opening can be successfully used in the initiation of a radical polymerization. The correlation between the epoxide and ligand structure in the initiation and catalysis of living radical polymerizations has been studied. Moreover, graft polymers can be readily accessed [73–76].

5
Cyclizations

The most frequently employed reactions in radical chemistry are cyclizations [36]. The preparation of 5-membered rings by 5-exo cyclizations has proven to be especially powerful. The kinetically disfavored 6-endo cyclizations and the significantly slower 6-exo cyclizations have attracted less attention, even though important applications have been reported.

5.1
5-exo, 6-exo and 6-endo Cyclizations

5.1.1
Evolution of the Reaction and Initial Examples

In the case of titanocene mediated or catalyzed epoxide opening 5-exo cyclizations were also investigated first. Nugent and RajanBabu reported

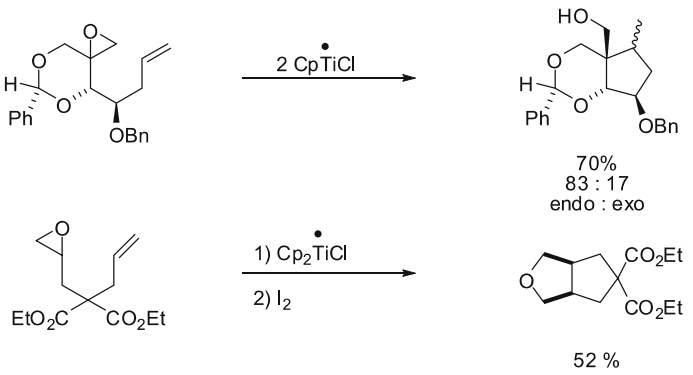

Scheme 11 Stoichiometric cyclizations

alkenes and alkynes as radical traps and demonstrated that alkyl radicals (originating from cyclizations with alkenes) were reduced by a second equivalent of "Cp_2TiCl" whereas vinyl radicals (obtained from alkynes) reacted by H-atom abstraction from THF. Moreover, THF derivatives could be obtained by oxidative trapping of the alkyltitanium species with iodine and ensuing nucleophilic substitution [26, 29].

As in the case of the intermolecular additions the cyclizations are tolerant to a wide range of functional groups. The mechanism of the cyclizations and two examples of the synthesis of more complex products are shown in Scheme 11.

5.1.2 Catalytic Conditions

To improve the utility of Nugent's and RajanBabu's conditions even further, catalytic conditions for cyclizations have been developed. They address the issue of reagent control of the cyclization and the mode of its termination. The formation of an alkyl titanocene species after reductive trapping allows two distinctive pathways for the regeneration of the catalyst.

Probably the most straightforward approach is constituted by protonation of the Ti – C bond. This was first realized by using collidine hydrochloride as the acid (Scheme 12). These conditions have proven especially useful in unusual cyclizations as discussed later [66, 67].

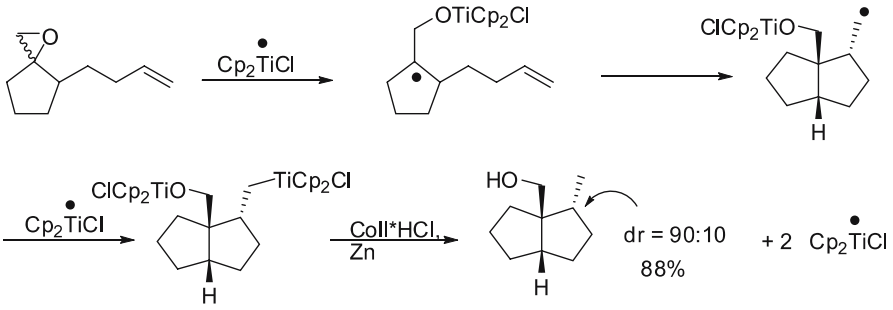

Scheme 12 Catalytic cyclizations employing Coll*HCl as mediator

In the organometallic literature it is well documented that alkyltitanium species can undergo β-hydride eliminations swiftly [77, 78]. This was exploited by the group of Oltra and Cuerva for the termination of the cyclization by employing Me_3SiCl and collidine for regenerating the redox-active catalyst by silylation of the Ti – O bond [79, 80]. Ti – C bonds are not affected and thus the alkyl titanocenes decompose via a β-hydride elimination with the most accessible hydrogen atoms to yield mainly exocyclic olefins (if applicable).

This regioselectivity of the termination of the cyclization is complementary to cationic reactions and therefore synthetically highly attractive. From "Cp_2TiClH", Cp_2TiCl_2 is regenerated with Me_3SiCl through an exchange of hydride for chloride. An example of a 6-endo cyclization using this methodology is shown in Scheme 13.

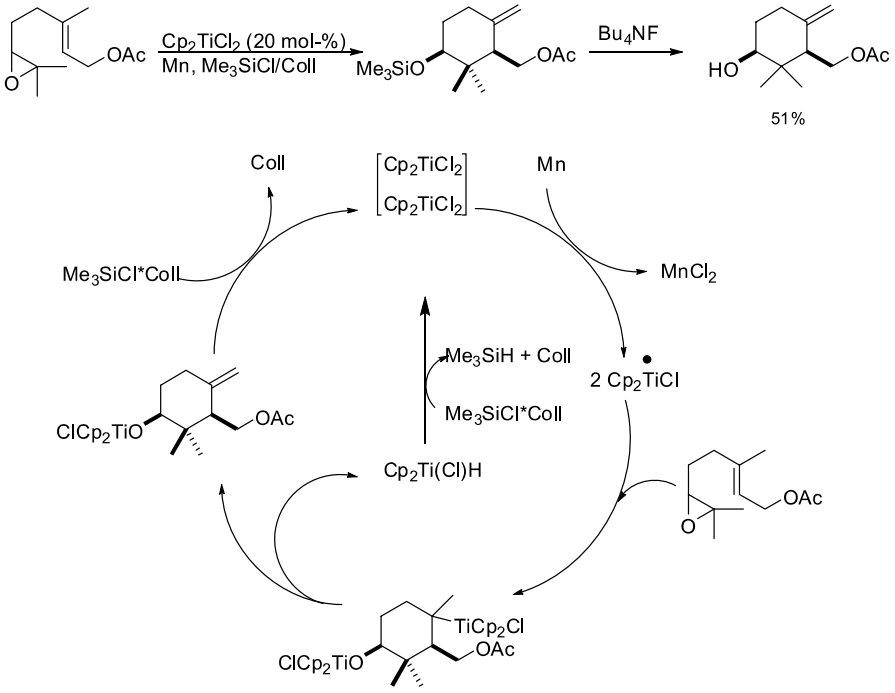

Scheme 13 Catalytic cyclization terminated by β-hydride elimination

Another method for conducting cyclizations catalytic in "Cp_2TiCl" is shown in Scheme 14. It relies on the thermodynamically favorable ring closure of THF from δ-titanoxy radicals [81, 82]. This step is mechanistically related to the "oxygen rebound" steps of oxidation reactions. While the scope of this transformation remains to be established, the presence of substituted THF-derivatives in many natural products renders the method potentially attractive.

A protocol relying on the use of BEt_3 together with lutidine hydrochloride has been described by Takahashi for the regeneration of "Cp_2TiCl" from cyclizations involving β-hydride elimination as the terminating step [83].

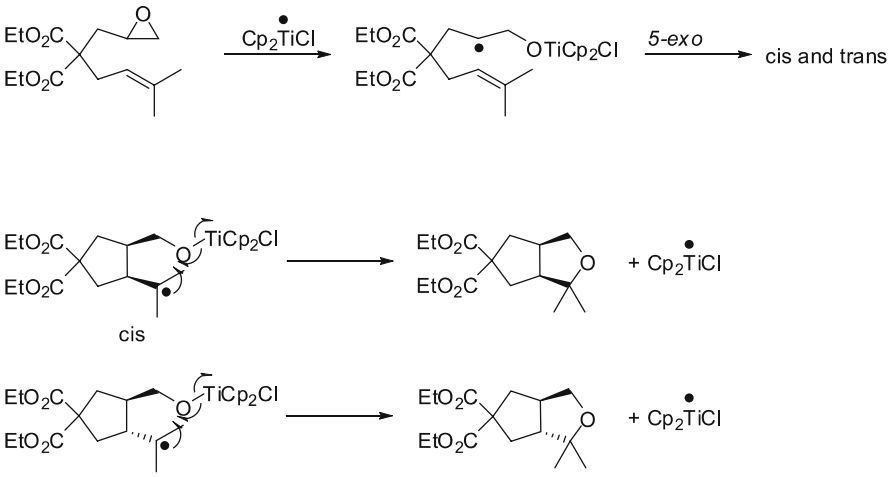

Scheme 14 Catalytic cyclization terminated by THF-formation

5.1.2.1 Synthetic Applications

The stoichiometric and catalytic protocols have been employed in a number of synthetic applications involving formations of one or more rings that will be discussed next. The functional group tolerance and short approaches to complex structure are especially relevant.

5.1.2.2 "Simple" Cyclizations

By simple cyclizations we imply reactions where only one ring is formed and for the sake of clarity these cases will be presented separately. The first example of such transformations in natural product synthesis was reported by Clive et al. in the synthesis of (±)-ceratopicanol as shown in Scheme 15 [84, 85].

Roy and his group have synthesized a number of THF derivatives from suitable ethers of "Sharpless epoxides" [86, 87]. The example shown

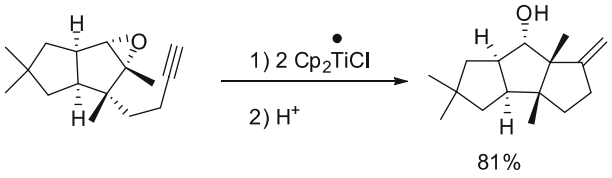

Scheme 15 Clive's cyclization en route to ceratopicanol

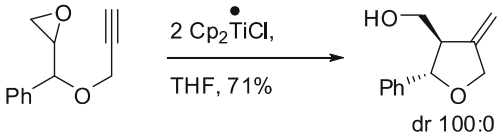

Scheme 16 Roy's diastereoconvergent cyclization

in Scheme 16 is in principle especially attractive as the cyclization is diastereoconvergent. However, it seems that the formation of the tetrahydropyrans from the regioisomer of epoxide opening in this reaction was overlooked (Gansäuer et al., unpublished results). Unfortunately, this reduces the usefulness of the method somewhat.

The same group has also reported the preparation of a number of furanolignans by the postulated mechanism shown in Scheme 17 [88–91]. After formation of a benzylic radical and reductive trapping by Cp_2TiCl a benzylic titanocene complex was assumed to be formed. This intermediate was then presumed to undergo a stereoselective oxidation with iodine and ensuing S_N2 reaction to deliver the desired second THF ring. It was later shown that THF formation occurred before addition of I_2 via the catalytic homolytic substitution tandem cyclization mentioned above. Addition of I_2 actually decreased the isolated yield of the furanolignans (Gansäuer et al., unpublished results) [81, 82].

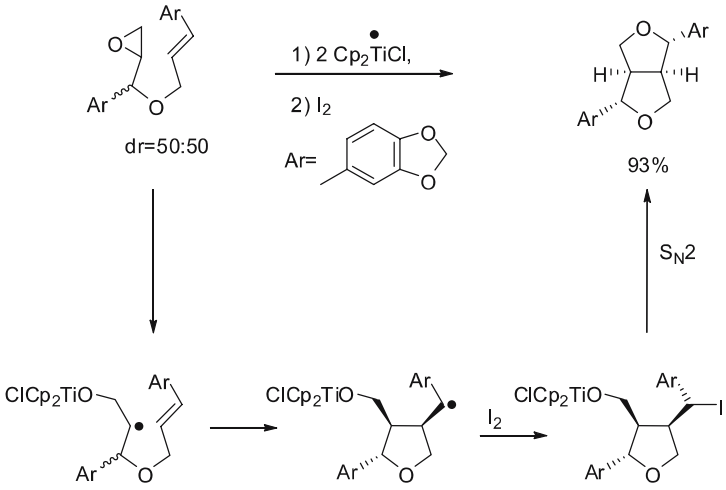

Scheme 17 Roy's mechanism of THF-formation

The catalytic preparation of substituted tetrahydrofurans and pyrrolidines with a number of N-protecting groups has been reported. The use of 1,2-

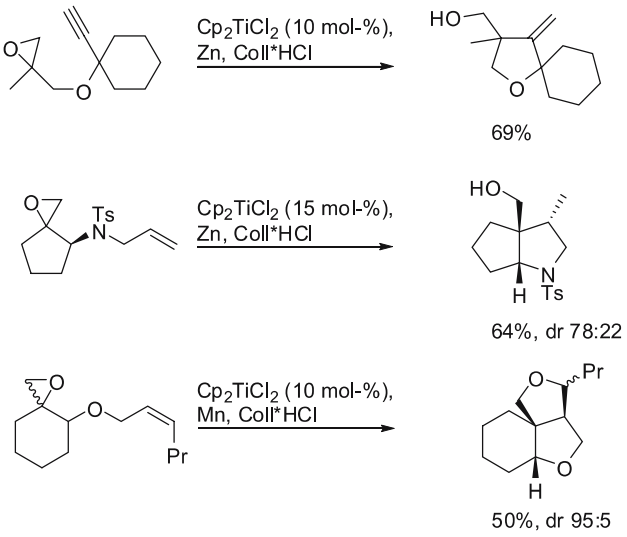

Scheme 18 Catalytic synthesis of heterocycles

disubstituted or trisubstituted olefins resulted in the formation of polycyclic THF derivatives (Scheme 18) [92, 93].

Barrero, Oltra and coworkers reported on the use of epoxygeranyl acetate in titanocene-mediated cyclizations and found that the termination of the reaction took place via a β-hydride elimination after trapping of the radical by the second equivalent of "Cp_2TiCl" [94, 95]. This finding together with Takahashi's tandem cyclization [96] (see below) marks the first example of extremely interesting developments in epoxypolyene cyclizations via radicals that are discussed separately in the following section.

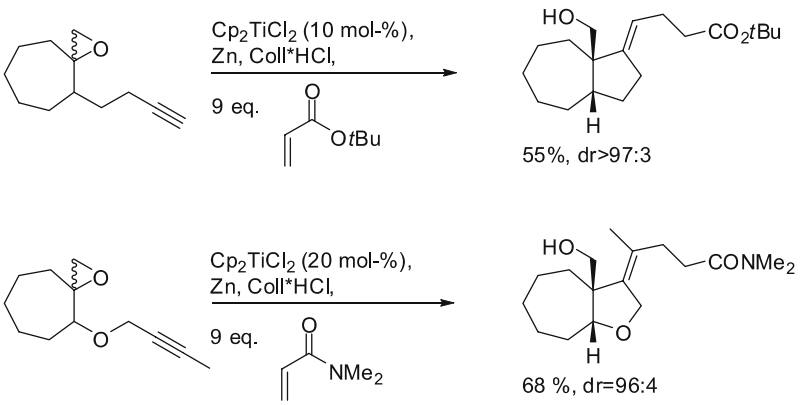

Scheme 19 Catalytic cyclization-addition sequence

The protic catalytic conditions are also compatible with trapping of the radicals formed after cyclization with acrylates or acrylonitriles prior to their reduction with "Cp_2TiCl". In this manner highly substituted alkenes for the potential preparation of modified steroids can be accessed (Scheme 19) [97].

Trost and his group reported a 6-endo cyclization en route to (–)-siccanin (Scheme 20). The minor diastereoisomer of the radical formed during cyclization yielded a THF derivative directly [98, 99].

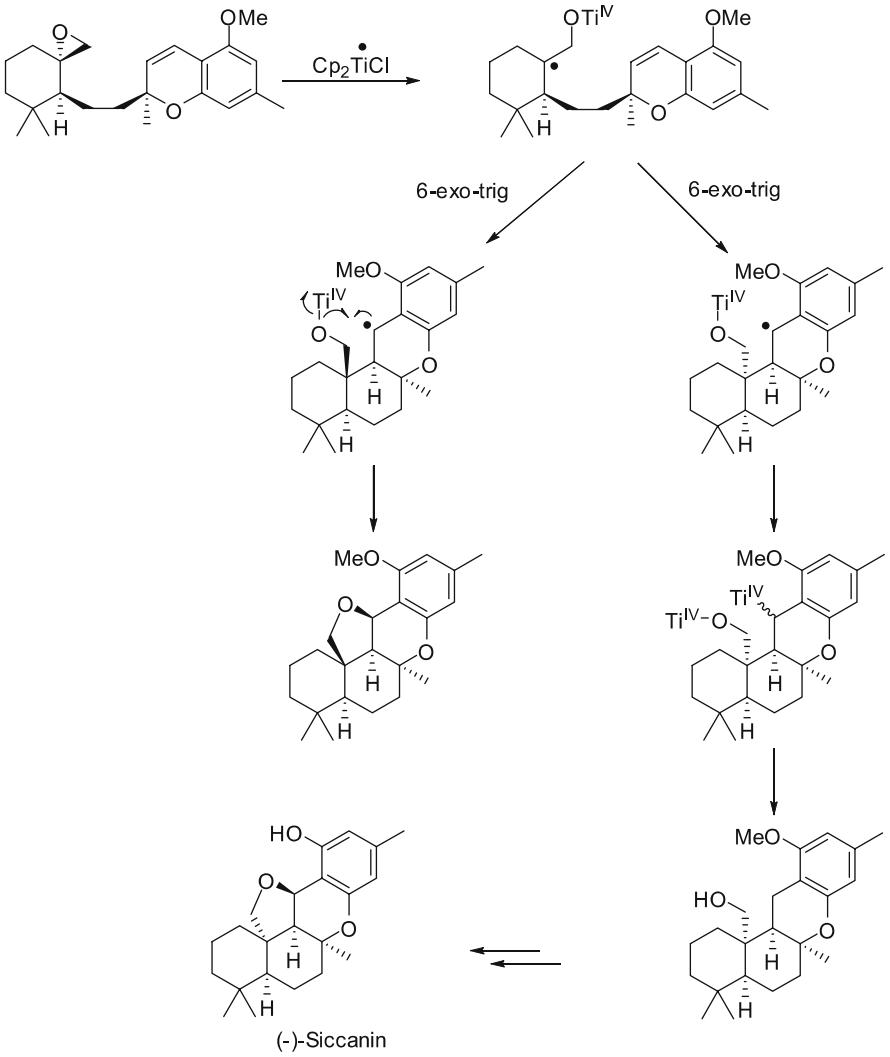

Scheme 20 Trost's approach to siccanin

The exceptional mildness of Nugent's and RajanBabu's system was demonstrated by Grande et al. in a synthesis of polyfunctionalized carbacephems as shown in Scheme 21. The sensitive β-lactam and the other functional groups are readily tolerated by "Cp_2TiCl" [100].

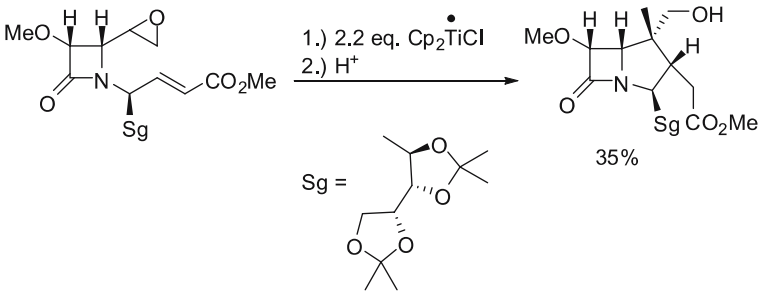

Scheme 21 Grande's synthesis of novel β-lactams

Ziegler and Saprong described a stoichiometric cyclization onto an alkyne for the synthesis of the carbocyclic core of "entecavir" from diacetone glucose. Inverse addition was required to minimize deoxygenation. The highly diastereoselective reaction is tolerant to silylethers [101].

Malacria and coworkers reported a vinylation sequence of epoxides by employing vinyl phosphine oxides as a radical trap. The overall sequence relies on the facile elimination of phosphinoyl radicals. With vinyl phosphonates the THF derivatives were obtained (Scheme 22). The reaction works equally well under stoichiometric or catalytic conditions [102, 103].

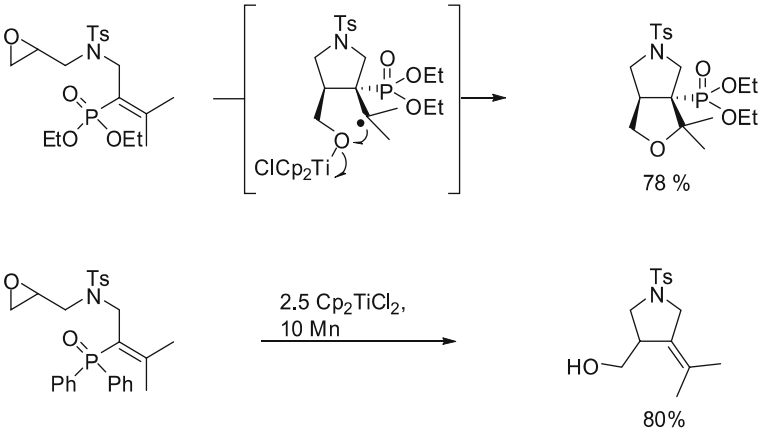

Scheme 22 Malacria's vinylation reaction and THF-synthesis

RajanBabu et al. have described an addition-elimination sequence employing vinyl stannanes for the preparation of homoallylic alcohols containing 5-membered rings [104].

Chakraborty has described the highly diastereoselective. Barrero and his group developed an approach to functionalized six-membered rings with exocyclic olefins from α-oxygenated derivatives of geraniol. The diastereoselectivity observed is reasonable and thus the method holds promise for natural product synthesis [105].

5.1.2.3 Tandem and Transannular Cyclizations

Tandem cyclizations are ideally suited for the efficient preparation of polycyclic compounds from simple starting materials, especially with radicals as reactive intermediates [106–108]. The first reports employing "Cp_2TiCl" as a reagent in epoxy polyene cyclizations appeared in 2001 from the group of Takahashi [96] for the synthesis of (±)-smenospondiol and from Barrero's group [94, 95]. While Takahasi employed alkynes for obtaining exocyclic olefins, Barrero used olefins as described above (Scheme 23). Both approaches yielded the desired compounds efficiently. However, it seems that the use of olefins is more general, as the "natural" substrates of the epoxypolyene cyclizations can be used.

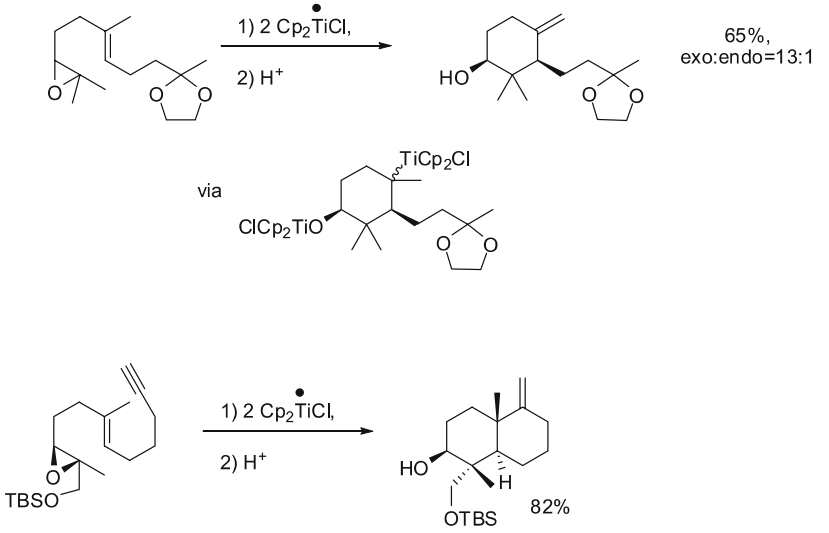

Scheme 23 Epoxy polyene cyclizations via radicals

Oltra and Cuerva have reported a unified strategy for the synthesis of the eudesmanolides that relies on the collidine-chlorotrimethylsilane reagent

combination for catalyst regeneration (Scheme 24) [77]. The desired products could be obtained by transannular cyclizations from either the alcohols or even the hydrocarbons. This amply demonstrates the flexibility of their catalytic protocol. It should be noted that by this elegant semisynthetic approach the side-products of biosynthesis can be efficiently obtained.

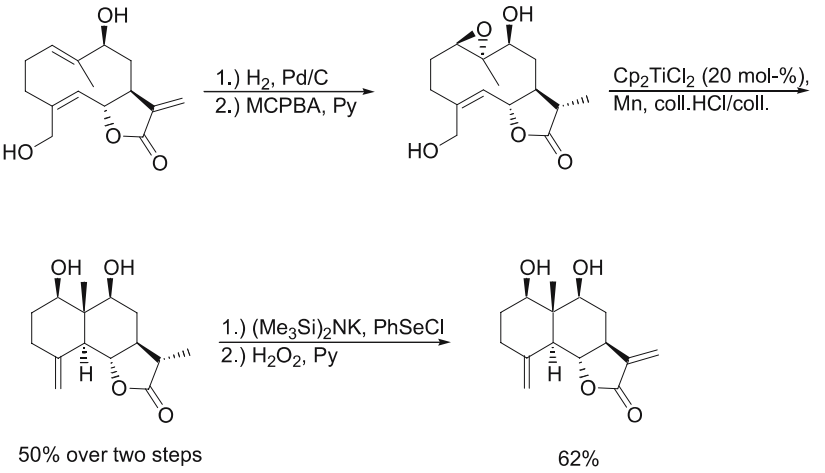

Scheme 24 Oltra's and Cuerva's transannular cyclizations

Later the same group reported the application of their method in the synthesis of a number of natural products from simple starting materials such as epoxygeranyl acetate, ketals of epoxygeranylacetone or the epoxy acetate of geranyl geraniol as shown in Scheme 25. Even oxidosqualene can serve as a useful substrate for this reaction. These findings raise the intriguing possibility of biological epoxypolyene cyclizations via radicals [78].

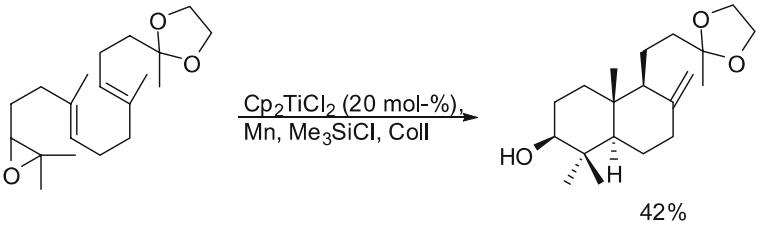

Scheme 25 Oltra's and Cuerva's catalytic epoxy polyene cyclizations

The method was later extended to the synthesis of a number of meroterpenoids from epoxygeranyl carbonates or acetates in a two-step approach combining titanocene catalysis with Stille reactions (carbonates) [108, 109] or copper-catalyzed allylic substitutions (acetates) [110–112]. The cyclizations

via radicals are superior to cationic reactions as no special groups are needed to control the termination of the sequence and functional group tolerance is much higher. Two examples are shown in Scheme 26.

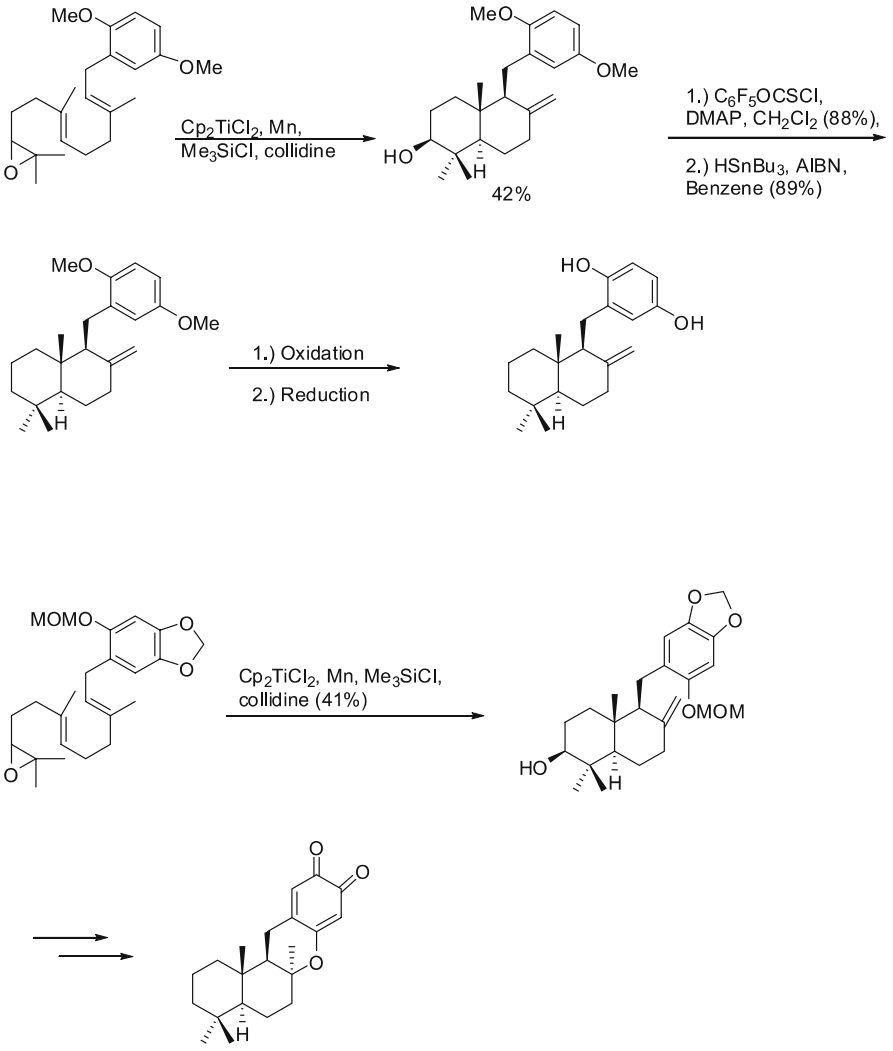

Scheme 26 Tandem cyclization approach to puupehedione

By combining the benefits of Pd(II) and Ti(III) chemistry, syntheses of γ-dioxygenated terpenoids, such as rostratone could be readily accessed (Scheme 27) [113].

A simple approach to sclareol oxide has also been reported [114].

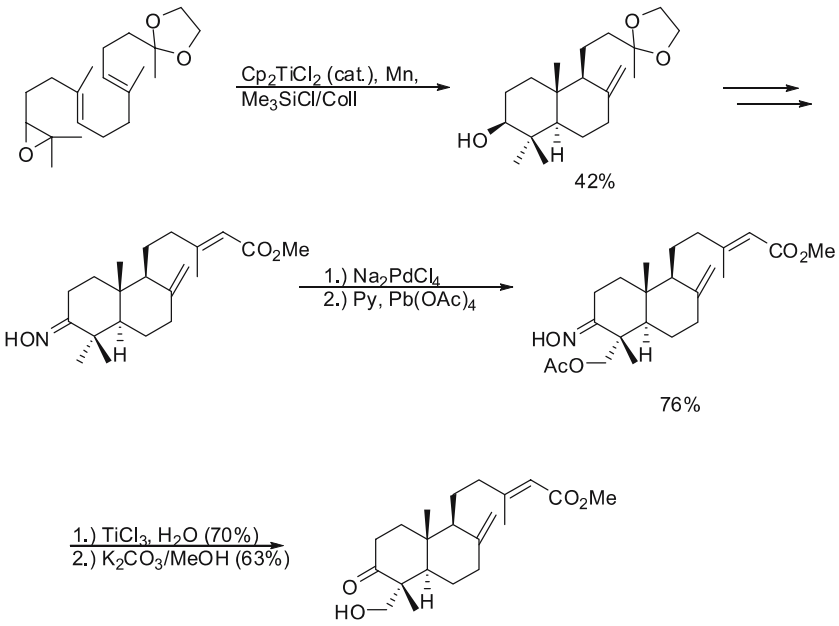

Scheme 27 Approach to dioxygenated terpenoids employing Ti and Pd chemistry

5.2
Unusual Radical Traps and Unusual Ring Sizes

The above-mentioned important and impressive applications of titanocene mediated and catalyzed epoxide opening have been achieved by using the already classical 5-exo, 6-exo and 6-endo cyclizations with alkenes or alkynes as radical acceptors. Besides these achievements, the high chemoselectivity of radical generation and slow reduction of the intermediate radicals by "Cp_2TiCl" has resulted in some remarkable novel methodology.

5.2.1
Unusual Radical Traps

The nucleophilic radicals generated after epoxide opening are slowly reduced by "Cp_2TiCl" and are therefore relatively persistent. Thus, many addition reactions to functional groups that are too slow for maintaining radical chain reactions can be realized. This is especially so when electrophilic radicals that are swiftly reduced by "Cp_2TiCl" are generated during the cyclization.

In this context Fernandez-Mateós and his group reported efficient cyclizations with aldehydes and ketones as radical traps [115]. The authors propose a reduction of the intermediate alkoxyl radicals by a second equivalent of

"Cp_2TiCl". Hydrogen atom abstraction from THF seems possible, also. Most remarkably, the reaction can be employed in the efficient synthesis of cyclopropanols and cyclobutanols as shown in Scheme 28.

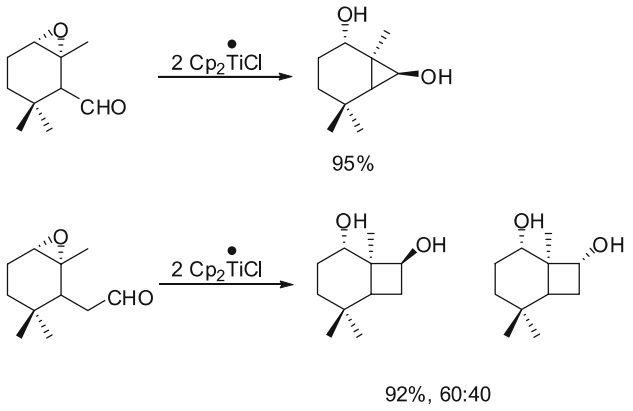

Scheme 28 Fernandez-Mateos cyclizations with aldehydes as radical traps

In general, aldehydes constitute the more efficient radical acceptors. Surprisingly, when enones were employed as radical acceptors 1,2-addition to the carbonyl group was in some cases preferred over the conjugate 1,4-addition [116].

The radical addition to a ketone has been used as a key step in the preparation of (*E*)-*endo*-begamoten-12-oic acids [115] and for the synthesis of carbacephams [118, 119].

Esters are commonly regarded as unreactive toward addition of alkyl radicals [120]. Recently, two studies have demonstrated that this may not be true. In the first, somewhat special, example, the addition of a benzylic radical to the carbonyl group of butenolides was observed during the preparation of potential novel β-lactam antibiotics (Scheme 29) [118].

In a more general study it has been reported that epoxy formates can be employed for the preparation of hydroxy lactols as shown in Scheme 30. Other esters failed to give the desired products, though [121].

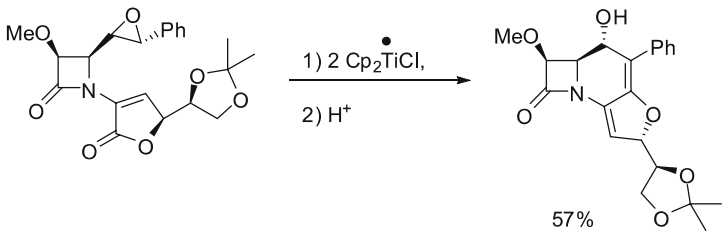

Scheme 29 Grande's cyclization onto the carbonyl group of a butenolide

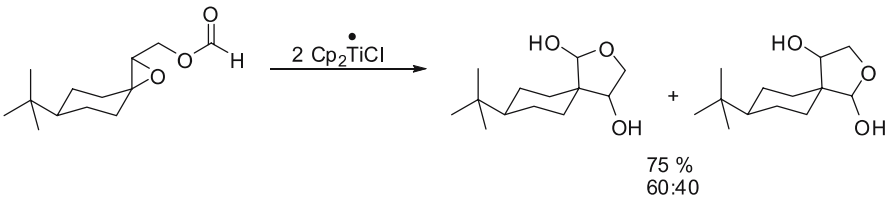

Scheme 30 Fernandez-Mateos' cyclizations with a formate

Fernandez–Matess recently demonstrated that nitriles constitute excellent radical traps in titanocene-mediated epoxide openings, even though these cyclizations are considered as being quite slow. As shown in Scheme 31 cyclobutanones, cyclopentanones, and cyclohexanones can be prepared in high yields [122].

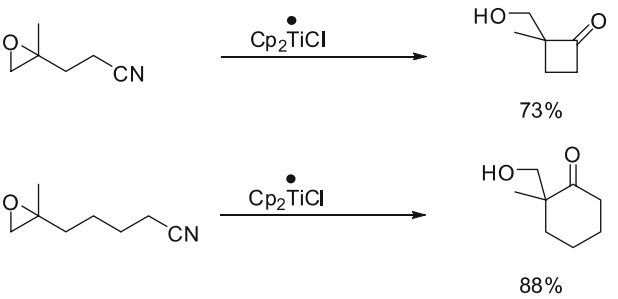

Scheme 31 Fernandez-Mateos' cyclizations with nitriles

5.2.2
Unusual Ring Sizes

Difficulties encountered in the preparation of three- and four-membered rings via radical cyclization are due to the strain of these compounds. Thus, ring opening usually proceeds much faster than ring closure.

The catalytic conditions are well suited for the preparation of cyclopropanes provided that α,β-unsaturated carbonyl compounds are employed as radical acceptors (formation of electrophilic radicals after cyclization) as shown in Scheme 32 [123].

It has been demonstrated that in these cases cyclopropane formation is reversible and thermodynamically favorable [124]. Recently, a single example of the stoichiometric version of this reaction has been independently reported by Fernandez-Mateós [116].

The preparation of cyclobutanes via the catalytic conditions can be extremely efficient provided that the radical formed after epoxide opening is sterically shielded and cyclization promoted by the Thorpe–Ingold effect. It

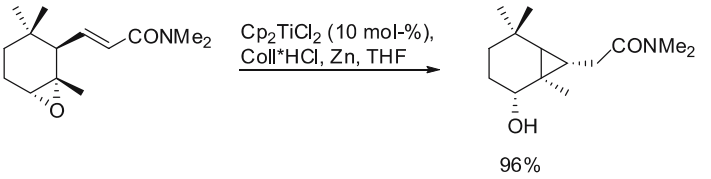

Scheme 32 Catalytic 3-exo cyclization

remains to be seen if the catalysts can be optimized to avoid these noticeable limitations.

Employing their catalytic system, the group of Oltra and Cuerva demonstrated that 7-endo cyclizations can be performed in surprisingly high yields. Moreover, 7-endo-cyclizations were used by the same group in elegant catalytic cyclization cascades for the preparation of a number of natural products as shown in Scheme 33 [125]. Barreo et al. reported similar methodology [105].

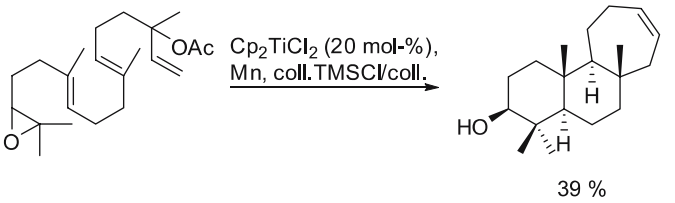

Scheme 33 Oltra's and Cuerva's tandem sequence featuring a 7-endo cyclization

Finally, Roy and his group reported the first examples of stoichiometric 8-endo cyclizations for the preparation of aromatic ethers [126].

6 Conclusion

Since the seminal contributions by Nugent and RajanBabu the field of reductive C – C bond formation after epoxide opening via electron transfer has developed at a rapid pace. Novel catalytic methodology, enantio- and stereoselective synthesis and numerous applications in the preparation of biologically active substances and natural products have evolved. In brief, a large repertoire of useful and original reactions is available. These reactions are waiting to be applied in a complex context!

Acknowledgements We are grateful for continued financial support by the Deutsche Forschungsgemeinschaft, the Alexander von Humboldt-Stiftung, the University of Granada and Spanish Ministerio de Educación y Ciencia for postdoctoral grants.

References

1. Johnson RA, Sharpless KB (2000) In: Ojima I (ed) Catalytic Asymmetric Synthesis. Wiley-VCH, New York, pp 231–280
2. Lane BS, Burgess K (2003) Chem Rev 103:2457
3. Shi Y (2004) In: Bäckvall J-E (ed) Modern Oxidation Methods. Wiley-VCH, Weinheim, pp 51–78
4. Yang D (2004) Acc Chem Res 37:497
5. Shi Y (2004) Acc Chem Res 37:488
6. McGarrigle EM, Gilheany DG (2005) Chem Rev 105:1564
7. Jacobsen EN (2000) Acc Chem Res 33:421
8. Nielsen LPC, Jacobsen EN (2006) In: Yudin AK (ed) Epoxides and Aziridines in Organic Synthesis. Wiley-VCH, Weinheim, pp 229–269
9. Schneider C (2006) Synthesis p 3919
10. Birch AJ (1949) J Proc Royal Soc New South Wales 83:245
11. Hallsworth AS, Henbest HB (1957) J Chem Soc :4604
12. Brown HC, Ikegami S, Kawakami JH (1970) J Org Chem 35:3243
13. Benkesser RA, Rappa A, Wolsieffer LA (1986) J Org Chem 51:3391
14. Bartmann E (1986) Angew Chem Int Ed Engl 25:653
15. Dorigo AE, Houk KN, Cohen T (1989) J Am Chem Soc 111:8976
16. Conrow RE (1993) Tetrahedron Lett 34:5533
17. Bachki A, Foubeto F, Yus M (1995) Tetrahedron: Asymmetr 6:1907
18. Bachki A, Foubeto F, Yus M (1996) Tetrahedron: Asymmetr 7:2997
19. Yamamoto H (2000) Lewis Acids in Organic Synthesis. Wiley-VCH, Weinheim
20. Curran DP, Porter NA, Giese B (1996) Stereochemistry of Radical Reactions. Wiley-VCH, Weinheim
21. Renaud P, Sibi MP (eds) (2001) Radicals in Organic Synthesis. Wiley-VCH, Weinheim
22. McCarroll AJ, Walton JC (2001) Angew Chem Int Ed 40:2225
23. Zard SZ (2003) Radical Reactions in Organic Synthesis. Oxford University, Oxford
24. Gansäuer A, Rinker B (2002) Tetrahedron 58:7017
25. Kochi JK, Singleton DM, Andrews LJ (1968) Tetrahedron 24:3503
26. Nugent WA, RajanBabu TV (1988) J Am Chem Soc 110:8561
27. RajanBabu TV, Nugent WA (1989) J Am Chem Soc 111:4525
28. RajanBabu TV, Nugent WA, Beattie MS (1990) J Am Chem Soc 112:6408
29. RajanBabu TV, Nugent WA (1994) J Am Chem Soc 116:986
30. Gansäuer A, Bluhm H (2000) Chem Rev 100:2771
31. Gansäuer A, Narayan S (2002) Adv Synth Catal 344:465
32. Gansäuer A, Lauterbach T, Narayan S (2003) Angew Chem Int Ed 42:5556
33. Cuerva CM, Justicia J, Oller-López JL, Bazdi B, Oltra JE (2006) Mini-Rev Org Chem 3:23
34. Barrero AF, Quílez del Moral JF, Sánchez E, Arteaga JF (2006) Eur J Org Chem :1627
35. Cuerva JM, Justicia J, Oller-López JL, Oltra JE (2006) Top Curr Chem 264:63
36. Giese B, Kopping B, Göbel T, Dickhaut J, Thoma G, Kulicke KJ, Trach F (1996) In: Paquette LA (ed) Organic Reactions. Wiley, New York, p 301
37. Enemærke RJ, Hjøllund GH, Daasbjerg K, Skrydstrup T (2001) CR Acad Sci 4:435
38. Enemærke RJ, Larsen J, Skrydstrup T, Daasbjerg K (2004) Organometallics 23:1866
39. Enemærke RJ, Larsen J, Skrydstrup T, Daasbjerg K (2004) J Am Chem Soc 126:7853
40. Enemærke RJ, Larsen J, Hjøllund GH, Skrydstrup T, Daasbjerg K (2005) Organometallics 24:1252

41. Larsen J, Enemærke RJ, Skrydstrup T, Daasbjerg K (2006) Organometallics 25:2031
42. Daasbjerg K, Svith H, Grimme S, Gerenkamp M, Mück-Lichtenfeld C, Gansäuer A, Barchuk A, Keller F (2006) Angew Chem Int Ed 45:2041
43. Gansäuer A, Barchuk A, Keller F, Schmitt M, Grimme S, Gerenkamp M, Mück-Lichtenfeld C, Daasbjerg K, Svith HJ (2007) J Am Chem Soc 129:1359
44. Katsuki T, Martin VS (1996) Organic Reactions 48:1
45. Yadav JS, Shekharam T, Gadgil VR (1990) Chem Commun p 843
46. Hardouin C, Doris E, Rousseau B, Mioskowski C (2002) Org Lett 4:1151
47. Golakoti T, Ogino J, Heltzel CE, Husebo TL, Jensen CM, Larsen LK, Petterson GML, Moore RE, Mooberry SL, Corbett TH, Valeriote FA (1995) J Am Chem Soc 117:12030
48. Barrero AF, Quílez del Moral JF, Sánchez EM, Arteaga JF (2006) Org Lett 8:669
49. Chakraborty TK, Samanta R, Das SJ (2006) Org Chem 71:3321
50. Merlic CA, Xu D (1991) J Am Chem Soc 113:9855
51. Merlic CA, Xu D, Nguyen MC, Truong V (1993) Tetrahedron Lett 34:227
52. Dötz KH, Gomes da Silva E (2000) Tetrahedron 56:8291
53. Parrish JD, Little RD (2002) Org Lett 4:1439
54. Nishiguchi GA, Little RD (2005) J Org Chem 70:5249
55. Moisan L, Hardouin C, Rousseau B, Doris E (2002) Tetrahedron Lett 43:2013
56. Puljic N, Albert M, Dhimane A-L, Fensterbank L, Lacôte E, Malacria M (2006) Helv Chim Acta 89:2297
57. Halterman RL (1992) Chem Rev 92:965
58. Halterman RL (1998) In: Togni A, Halterman RL (eds) Metallocenes, vol 1. Wiley-VCH, Weinheim, p 455
59. Fürstner A (1998) Pure Appl Chem 70:1071
60. Fürstner A (1998) Chem Eur J 4:567
61. Fürstner A, Hupperts A (1995) J Am Chem Soc 117:4468
62. Fürstner A, Shi N (1996) J Am Chem Soc 118:2533
63. Fürstner A, Shi N (1996) J Am Chem Soc 118:12349
64. Hirao T, Hasegawa T, Muguruma Y, Ikeda I (1996) J Org Chem 61:366
65. Hirao T (1999) Synlett p 175
66. Gansäuer A, Pierobon M, Bluhm H (1998) Angew Chem Int Ed Engl 37:101
67. Gansäuer A, Bluhm H, Pierobon M (1998) J Am Chem Soc 120:12849
68. Gansäuer A, Lauterbach T, Bluhm H, Noltemeyer M (1999) Angew Chem Int Ed 38:2909
69. Gansäuer A, Bluhm H, Pierobon M, Keller M (2001) Organometallics 20:914
70. Gansäuer A, Bluhm H, Lauterbach T (2001) Adv Synth Catal 343:785
71. Gansäuer A, Bluhm H, Rinker B, Narayan S, Schick M, Lauterbach T, Pierobon M (2003) Chem Eur J 9:531
72. Gansäuer A, Rinker B, Barchuk A, Nieger M (2004) Organometallics 23:1168
73. Asandei AD, Moran IW (2004) J Am Chem Soc 126:15932
74. Asandei AD, Moran IW (2006) J Polym Sci, Part A: Polym Chem 44:6028
75. Asandei AD, Moran IW (2005) J Polym Sci, Part A: Polym Chem 43:6039
76. Asandei AD, Moran IW (2006) J Polym Sci, Part A: Polym Chem 44:1060
77. Okamoto S, Livinghouse T (2000) J Am Chem Soc 122:1223
78. Sturla SJ, Kablaoui NM, Buchwald SL (1999) J Am Chem Soc 121:1976
79. Barrero AF, Rosales A, Cuerva JM, Oltra E (2003) Org Lett 5:935
80. Justicia J, Rosales A, Buñuel E, Oller-López JL, Valdivia M, Haïdour A, Oltra JE, Barrero AF, Cardenas DJ, Cuerva JM (2004) Chem Eur J 10:1778
81. Gansäuer A, Rinker B, Pierobon M, Grimme S, Gerenkamp M, Mück-Lichtenfeld C (2003) Angew Chem Int Ed 42:3687

82. Gansäuer A, Rinker B, Ndene-Schiffer N, Pierobon M, Grimme S, Gerenkamp M, Mück-Lichtenfeld C (2004) Eur J Org Chem :2337
83. Fuse S, Hanochi M, Doi T, Takahashi T (2004) Tetrahedron Lett 45:1961
84. Clive DLJ, Magnusson SR (1995) Tetrahedron Lett 36:15
85. Clive DLJ, Magnusson SR, Manning HW, Mayhew DL (1996) J Org Chem 61:2095
86. Maiti G, Roy SC (1996) J Chem Soc, Perkin Trans 1:403
87. Mandal PK, Maiti G, Roy SC (1998) J Org Chem 63:2829
88. Mandal PK, Roy SC (1999) Tetrahedron 55:11395
89. Rana KK, Guin C, Roy SC (2001) Tetrahedron Lett 41:9337
90. Rana KK, Guin C, Roy SC (2001) Synlett p 1249
91. Roy SC, Rana KK, Guin C (2002) J Org Chem 67:3242
92. Gansäuer A, Pierobon M (2000) Synlett p 1357
93. Gansäuer A, Pierobon M, Bluhm H (2001) Synthesis p 2500
94. Barrero AF, Cuerva JM, Herrador MM, Valdivia MV (2001) J Org Chem 66:4074
95. Barrero AF, Oltra JE, Cuerva JM, Rosales A (2002) J Org Chem 67:2566
96. Haruo Y, Hasegawa T, Tanaka H, Takahashi T (2001) Synlett p 1935
97. Gansäuer A, Pierobon M, Bluhm H (2002) Angew Chem Int Ed 41:3206
98. Trost BM, Shen HC, Surivet J-P (2003) Angew Chem Int Ed 42:3943
99. Trost BM, Shen HC, Surivet J-P (2004) J Am Chem Soc 126:12565
100. Anaya J, Fernández-Mateos A, Grande M, Matiánez J, Ruano G, Rubio González MR (2003) Tetrahedron 59:241
101. Ziegler FE, Sarpong MA (2003) Tetrahedron 59:9013
102. Leca D, Fensterbank L, Lacôte E, Malacria M (2004) Angew Chem Int Ed 43:4220
103. Leca D, Song K, Albert M, Goançalves MG, Fensterbank L, Lacôte E, Malacria M (2005) Synthesis p 405
104. Apte S, Radetich B, Shin S, RajanBabu TV (2004) Org Lett 6:4053
105. Barrero AF, Quílez del Moral JF, Mar Herrador M, Loayza I, Sánchez E, Arteaga JF (2006) Tetrahedron 62:5215
106. Malacria M (1996) Chem Rev 96:289
107. Albert M, Fensterbank L, Lacôte E, Malacria M (2006) Top Curr Chem 264:1
108. Justicia J, Oltra JE, Cuerva JM (2004) J Org Chem 69:5803
109. Justicia J, Oltra JE, Barrero AF, Guadaño A, González-Coloma A, Cuerva JM (2005) Eur J Org Chem :712
110. Gansäuer A, Justicia J, Rosales A, Rinker B (2005) Synlett p 1954
111. Gansäuer A, Rosales A, Justicia J (2006) Synlett p 927
112. Gansäuer A, Justicia J, Rosales A, Rinker B, Worgull D, Cuerva JM, Oltra JE (2006) Eur J Org Chem :4115
113. Justicia J, Oltra JE, Cuerva JM (2005) J Org Chem 70:8265
114. Gansäuer A, Worgull D, Justicia J (2006) Synthesis p 2151
115. Fernández-Mateos A, Martín de la Nava G, Pascual Coca A, Ramos Silvo A, Rubio González R (1999) Org Lett 1:607
116. Fernández-Mateos A, Mateos Burón L, Martin de la Nava E, Rabanedo Clemente R, Rubio González R, Sanz González F (2004) Synlett p 2553
117. Bermejo FA, Fernández Mateos A, Escribano AM, Lago RM, Mateos Burón L, Rodríguez López M, González RR (2006) Tetrahedron 62:8933
118. Ruano G, Grande M, Anaya JJ (2002) J Org Chem 67:8243
119. Ruano G, Matiánez J, Grande M (2003) J Org Chem 68:2024
120. Kim S (2004) Adv Synth Catal 346:19
121. Fernández-Mateos A, Herrero Teijón P, Rabanedo Clemente R, Rubio González R (2006) Tetrahedron Lett 47:7755

122. Fernández-Mateos A, Mateos Burón L, Rabanedo Clemente R, Ramos Silvo A, Rubio González R (2004) Synlett p 1011
123. Gansäuer A, Lauterbach T, Geich-Gimbel D (2004) Chem Eur J 10:4983
124. Friedrich J, Dolg M, Gansäuer A, Geich-Gimbel D, Lauterbach T (2005) J Am Chem Soc 127:7071
125. Justicia J, Oller-López JL, Campaña AG, Oltra JE, Cuerva JM, Buñuel E, Cárdenas DJ (2005) J Am Chem Soc 127:14911
126. Mandal SK, Roy SC (2006) Tetrahedron Lett 47:1599

Top Curr Chem (2007) 279: 53–75
DOI 10.1007/128_2007_120

Published online: 24 March 2007

Catalytic Reductive Coupling of Carbonyl Compounds – The Pinacol Coupling Reaction and Beyond

Toshikazu Hirao

Department of Applied Chemistry, Graduate School of Engineering, Osaka University, Yamada-oka, Suita, 565-0871 Osaka, Japan
hirao@chem.eng.osaka-u.ac.jp

Abstract Recent advances in the metal-catalyzed one-electron reduction reactions are described in this chapter. One-electron reduction induced by redox of early transition metals including titanium, vanadium, and lanthanide metals provides a variety of synthetic methods for carbon–carbon bond formation via radical species, as observed in the pinacol coupling, dehalogenation, and related radical-like reactions. The reversible catalytic cycle is achieved by a multi-component catalytic system in combination with a co-reductant and additives, which serve for the recycling, activation, and liberation of the real catalyst and the facilitation of the reaction steps. In the catalytic reductive transformations, the high stereoselectivity is attained by the design of the multi-component catalytic system. This article focuses mostly on the pinacol coupling reaction.

Keywords C – C bond formation · Co-reductant · One-electron reduction · Radical · Reversible redox cycle

Abbreviations
Cp Cyclopentadienyl
Cp* 1,2,3,4,5-Pentamethylcyclopentadienyl
DME 1,2-Dimethoxyethane
DMF *N*,*N*-Dimethylformamide
NMP *N*-Methyl-2-pyrrolidone
THF Tetrahydrofuran

1 Introduction

One-electron reduction or oxidation of organic compounds provides a useful method for the generation of anion radicals or cation radicals, respectively. These methods are used as key processes in radical reactions. Redox properties of transition metals can be utilized for the efficient one-electron reduction or oxidation (Scheme 1). In particular, the redox function of early transition metals including titanium, vanadium, and manganese has been of synthetic potential from this point of view [1–8]. The synthetic limitation exists in the use of a stoichiometric or excess amount of metallic reductants or oxidants to complete the reaction. Generally, the construction of a catalytic redox cycle for one-electron reduction is difficult to achieve. A catalytic system should be constructed to avoid the use of such amounts of expensive and/or toxic metallic reagents.

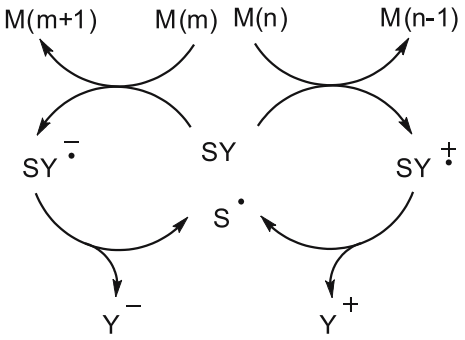

Scheme 1

The redox interaction with a co-reductant permits the formation of a reversible redox cycle for one-electron reduction as shown in Scheme 2. Furthermore, the function of transition metals is potentially and sterically controlled by ligands. A more efficient interaction between the orbitals of metals and substrates leads to facile electron transfer. Another interaction with an additive as a Lewis acid towards a substrate also contributes to such electron transfer.

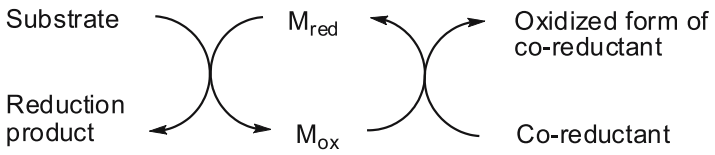

Scheme 2

It is important to select stoichiometric co-reductants or co-oxidants for the reversible cycle of a catalyst. A metallic co-reductant is ultimately converted to the corresponding metal salt in a higher oxidation state, which may work as a Lewis acid. Taking these interactions into account, the requisite catalytic system can be attained through multi-component interactions. Stereoselectivity should also be controlled, from synthetic points of view. The stereoselective and/or stereospecific transformations depend on the intermediary structure. The potential interaction and structural control permit efficient and selective methods in synthetic radical reactions. This chapter describes the construction of the catalytic system for one-electron reduction reactions represented by the pinacol coupling reaction.

2
Pinacol Coupling

The reductive dimerization of carbonyl compounds is a useful synthetic method for constructing vicinally functionalized carbon–carbon bonds. One-electron transfer from a metal to a carbonyl function generates the corresponding ketyl radical, which can dimerize to give either DL and/or *meso* isomers of 1,2-diols. A complementary route to 1,2-diols has been developed by the osmium-catalyzed dihydroxylation of olefins [9]. For stoichiometric reductive dimerization, low-valent metals such as aluminum amalgam, titanium, vanadium, zinc, and samarium compounds have been employed conveniently [10–13]. For example, the pinacol coupling reactions using $TiCl_3$/Zn-Cu and $[V_2Cl_3(THF)_6]_2[Zn_2Cl_6]$ have been employed successfully for the synthesis of paclitaxel and C_2-symmetrical HIV protease inhibitors, respectively [14–17]. To synthesize such complicated compounds, efficient control of the stereochemistry in the coupling reactions is of importance in addition to the construction of a catalytic cycle of low-valent metals. A catalytic process for the pinacol coupling has not been developed until recently. As described above, the multi-component redox systems are allowed to develop such processes.

2.1
Diastereoselective Coupling

The ternary system consisting of a metallic catalyst, a chlorosilane, and a stoichiometric co-reductant has been reported by us for the first time to achieve the catalytic pinacol coupling. The homocoupling of aliphatic aldehydes is catalyzed by $CpV(CO)_4$, Cp_2VCl_2, or Cp_2V in the presence of a chlorosilane and Zn in DME to give the 1,3-dioxolanes **1** via the coupling and acetalization (Scheme 3) [18, 19].

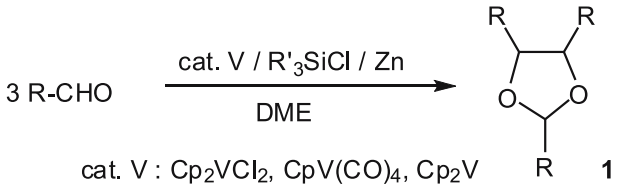

Scheme 3

A vanadium catalyst is essential although the combination of Zn and Me_3SiCl is capable of reductive dimerization of aldehydes [20]. A reversible redox cycle for the in situ generated low-valent vanadium species mediating the electron transfer is achieved in the presence of Zn as the stoichiometric co-reductant (Scheme 4).

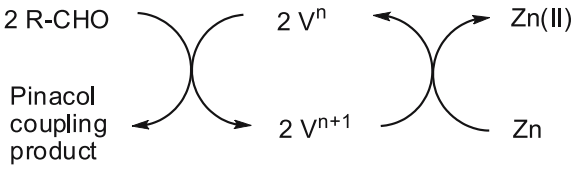

Scheme 4

Use of THF as a solvent leads to the highly diastereoselective formation of the DL-1,2-diols **2** from secondary aliphatic aldehydes without formation of any olefinic (McMurry coupling) products and 1,3-dioxolanes (Scheme 5) [21]. Elevated temperatures significantly decrease both yield and stereoselectivity. At a lower temperature, the product selectivity changes, giving the 1,3-dioxolane even in THF. The diastereoselectivity depends on chlorosilanes and is enhanced by using $PhMe_2SiCl$ in place of Me_3SiCl. Cp_2TiCl_2 can be also used as a catalyst in combination with a chlorosilane and Zn [22].

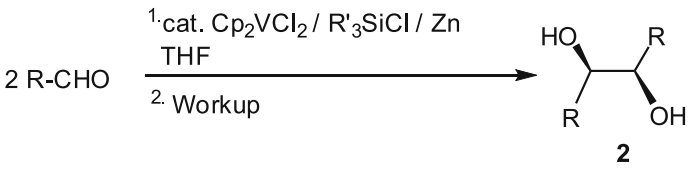

Scheme 5

In the absence of Me_3SiCl, the catalytic reaction does not proceed. Silylation is considered to liberate the catalyst through the formation of the silyl ether (Scheme 6). The Lewis-acidic interaction of chlorosilanes with the carbonyl oxygen is also suggested to facilitate the electron transfer from

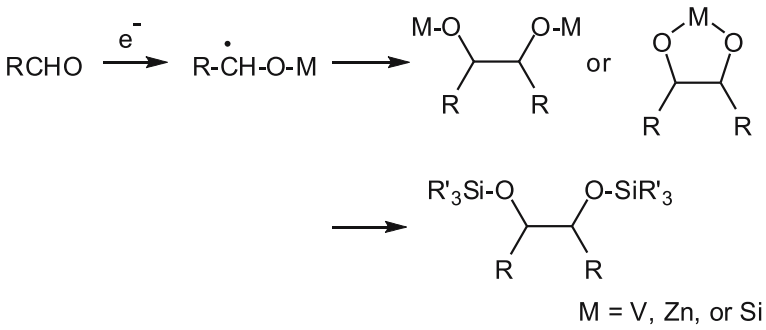

Scheme 6

a vanadium species to the carbonyl function, generating the stabilized silyloxyalkyl radical for dimerization. Another interaction with the catalyst may be possible since the UV-vis spectrum of Cp_2VCl_2 changes on the addition of Me_3SiCl. Furthermore, the diastereoselectivity partly depends on the substituent of chlorosilanes, which implies the steric contribution to the coupling step.

Fürstner has independently developed a catalytic method for the McMurry coupling by the assistance of a chlorosilane [23]. The oxoamide **3** undergoes reductive cyclization to indoles **4** using a catalytic amount of $TiCl_3$ and Zn in the presence of a chlorosilane (Scheme 7). A variety of chlorosilanes such as Me_3SiCl, $ClMe_2SiCH_2CH_2SiMe_2Cl$, or $ClMe_2Si(CH_2)_3CN$ are useful depending on the product structure. The reagent combination of Zn/Me_3SiCl without $TiCl_3$ also promotes the conversion under the conditions, but leads to a different product distribution.

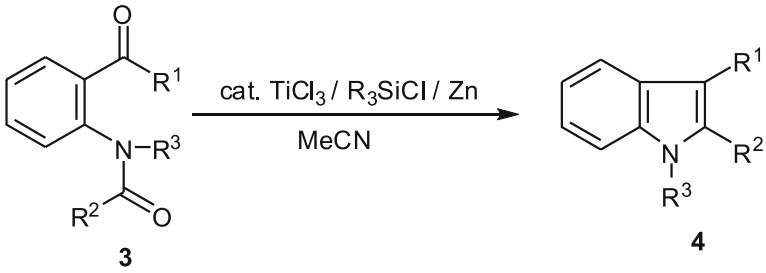

Scheme 7

Based on these observations [18, 19, 23], a variety of modified catalytic systems have been reported for the diastereoselective reductive carbon–carbon bond formation (Scheme 8). A complex **5** derived from Cp_2TiCl_2 and $MgBr_2$ is proposed to be an efficient catalyst for the DL-diastereoselective pinacol coupling of aromatic aldehydes [24]. Addition of a solution of benzalde-

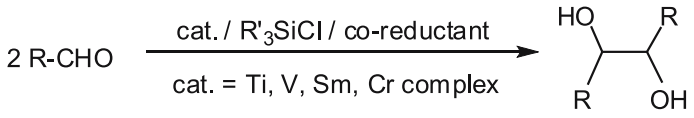

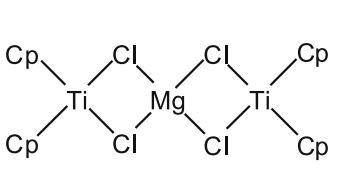

5

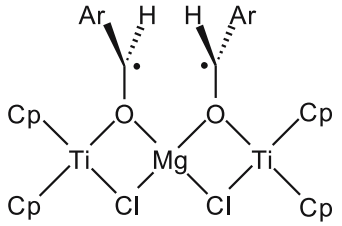

6

Scheme 8

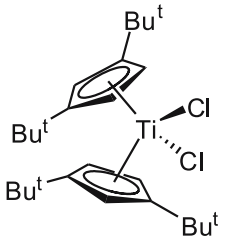

7

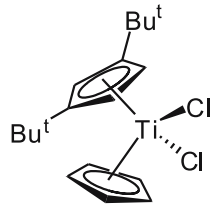

8

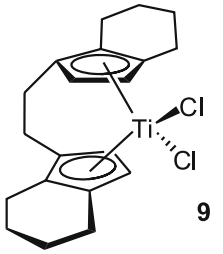

9

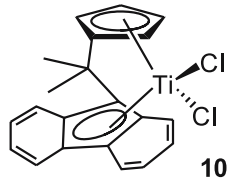

10

hyde and Me_3SiCl in THF to a mixture of Cp_2TiCl_2 and Zn in THF improves the diastereoselectivity. Further selectivity improvement is observed by the addition of one equivalent of $MgBr_2$. A tighter dimeric titanium catalyst **5** is formed by replacing Zn with Mg. The selectivity again depends on the substituent of the chlorosilanes, although no reaction is observed with Me_2Bu^tSiCl. Silylation seems to be the rate-determining step in the catalytic cycle. The observed DL selectivity is considered to be explained by minimization of steric interference through *anti*-orientation in the intermediate **6**. (1,3-$Bu^t{}_2C_5H_3)_2TiCl_2$ (**7**), (1,3-$Bu^t{}_2C_5H_3$)(Cp)$TiCl_2$ (**8**), *ansa*-[(η^5-tetrahydroindenyl)CH_2CH_2(η^5-tetrahydroindenyl)]$TiCl_2$ (**9**), and *ansa*-[(η^5-Cp)CH_2CH_2(η^5-fluorenyl)]$TiCl_2$ (**10**) depicted above have also been investi-

gated, showing that Cp_2TiCl_2 is the most active catalyst. Among them, the best DL/*meso* diastereoselectivity is observed with **9**. A dominant role of binuclear complexes is suggested in the catalytic reaction [25, 26].

The dependency of the Schiff base ligands **11–13** on the diastereoselectivity has been reported [27, 28].

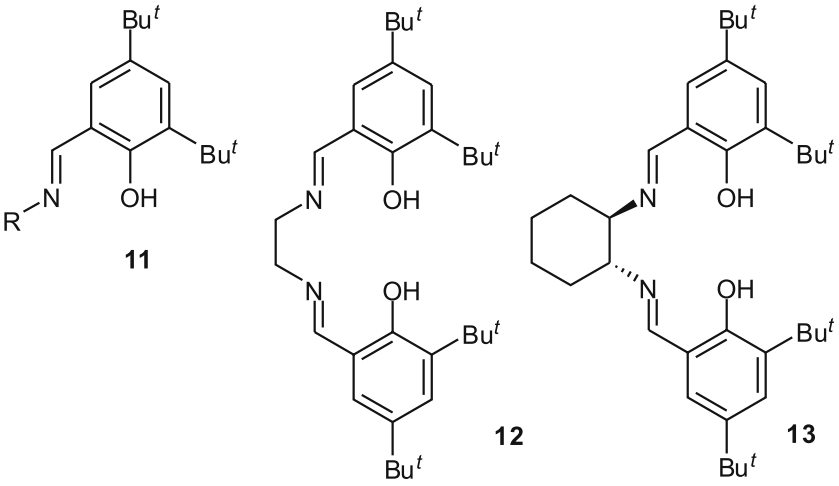

The diastereoselective titanium-catalyzed coupling of aromatic aldehydes is affected by the ligand or additive [29]. Higher selectivity is attained especially by use of $OC[N(Et)Ph]_2$ as a ligand. Use of substoichiometric quantities of a protic additive (Bu^tOH, catechol, and 2,2′-biphenol) or Lewis basic one (DMF and *N*,*N*-dimethylacetamide) results in five- to tenfold rate accelerations relative to the parent $TiCl_3(THF)_3$ catalyst. The catalyst consisting of cat. $TiCl_3(THF)_3$- Bu^tOH and 1,3-diethyl-1,3-diphenylurea proves to be useful in the diastereoselective coupling. π-Stacking interaction between the substrate and ligand is suggested to contribute to definition of the stereochemical course.

The above-mentioned results indicate the additive effect of protons. Actually, a catalytic process is formed by protonation of the metal–oxygen bond instead of silylation. 2,6-Lutidine hydrochloride or 2,4,6-collidine hydrochloride serves as a proton source in the Cp_2TiCl_2-catalyzed pinacol coupling of aromatic aldehydes in the presence of Mn as the stoichiometric reductant [30]. Considering the pKa values, pyridinium hydrochlorides are likely to be an appropriate proton source. Protonation of the titanium-bound oxygen atom permits regeneration of the active catalyst. High diastereoselectivity is attained by this fast protonation. Furthermore, pyridine derivatives can be recovered simply by acid–base extraction or distillation.

The coupling reaction of aromatic aldehydes proceeds well only in water by using VCl_3 as a catalyst in the presence of Al (Scheme 9). It should be noted that this method does not require a chlorosilane as an additive [31].

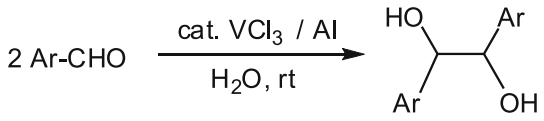

Scheme 9

Low-valent lanthanides represented by Sm(II) compounds induce one-electron reduction. Recycling of the Sm(II) species is first performed by electrochemical reduction of the Sm(III) species [32]. In one-component cell electrolysis, the use of sacrificial anodes of Mg or Al allows the samarium-catalyzed pinacol coupling. Samarium alkoxides are involved in the transmetallation reaction of Sm(III)/Mg(II), liberating the Sm(III) species followed by further electrochemical reduction to re-enter the catalytic cycle. The Mg(II) ion is formed in situ by anodic oxidation. $SmCl_3$ can be used in DMF or NMP as a catalyst precursor without the preparation of air- and water-sensitive Sm(II) derivatives such as SmI_2 or Cp_2Sm.

Redox interaction between Sm(II) and Mg has been reported to permit the catalytic pinacol coupling of aromatic and aliphatic aldehydes and ketones, in combination with Me_3SiCl as mentioned above [33]. No apparent difference in the diastereoselectivity is observed between the catalytic and stoichiometric reactions. Other lanthanide salts such as $CeCl_3$, $LaCl_3$, $NbCl_3$, $Yb(OTf)_3$, YbI_3, and $SmCl_3$ are not effective. Me_2SiCl_2 is utilized in the diastereoselective catalytic coupling of aldehydes and ketones [34]. $SmBr_2$ is generated and serves as a catalyst together with mischmetall in the absence of Me_3SiCl, as shown in Scheme 10 [35].

Cp_2ZnCl_2 similarly catalyzes the coupling reaction of aromatic aldehydes and ketones [36]. Another ternary-component system consists of a catalytic

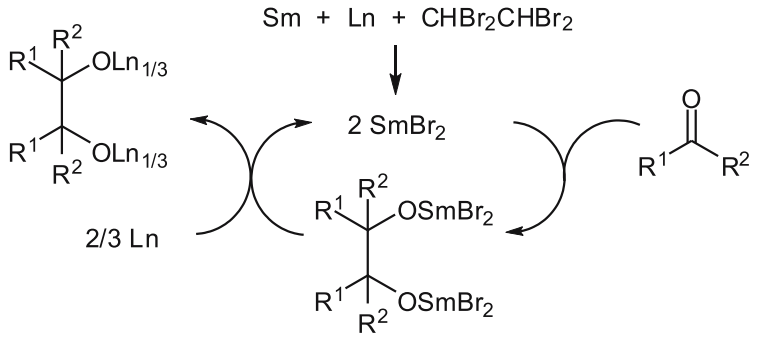

Scheme 10

amount of Cr(II) salt or chromocene, Mn powder, and a chlorosilane in THF/DMF. Reductive coupling of aromatic and heteroaromatic aldehydes and ketones is effectively catalyzed by this catalytic system [37]. Use of a sterically bulky chlorotrialkylsilane leads to excellent DL selectivity as observed in the vanadium-catalyzed reaction, albeit with lower yield. Besides the above-mentioned roles, chlorotrialkylsilane is suggested to serve as a source of chloride counter ions for dissolving Zn or Mn added as the co-reductant. The catalysis is not observed in the case of aliphatic aldehydes. $(BiPy)_3Cr(III)$ is not a catalyst for the coupling, but chromocene induces the pinacol coupling at comparable rates to $CrCl_3$.

Rieke Ni-promoted (Scheme 11) and cat. $NiCl_2/Mg/Me_3SiCl$-mediated pinacol coupling have been investigated [38]. The similar nickel-catalyzed reaction was also reported later [39].

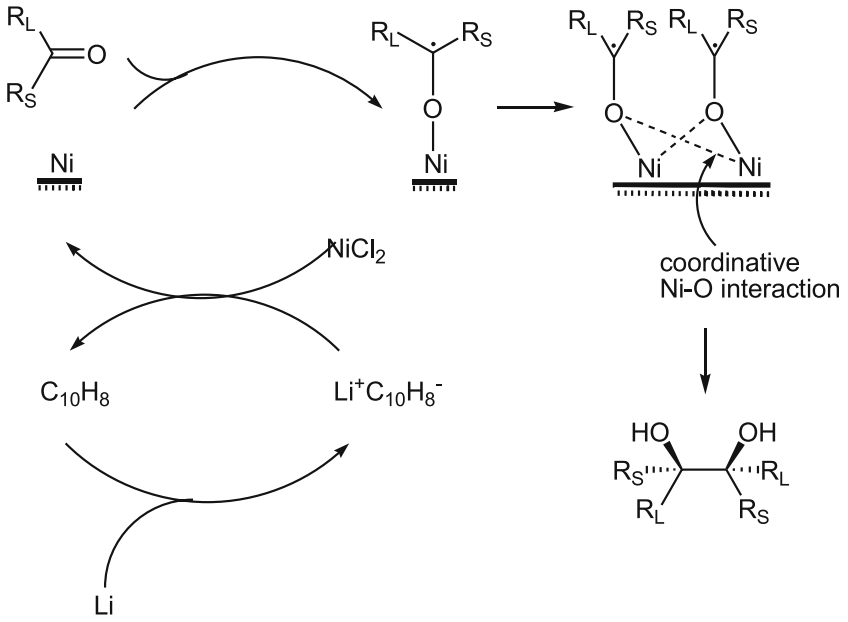

Scheme 11

Another method for reductive dimerization has been developed in hydrosilylation. $NiCl_2$-SEt_2 is an effective catalyst in silylative dimerization of aromatic aldehydes with a hydrosilane (Scheme 12) [40]. A catalytic thiolate-bridged diruthenium complex $[Cp^*RuCl(\mu_2\text{-}SPr^i)_2RuCp^*][OTf]$ also induces the conversion to 1,2-diaryl-1,2-disiloxyethane [41]. A dinuclear (siloxybenzyl)ruthenium complex is considered to be formed, and the homolytic Ru – C bond fission leads to the siloxybenzyl radicals, which couple to the coupling product **14**.

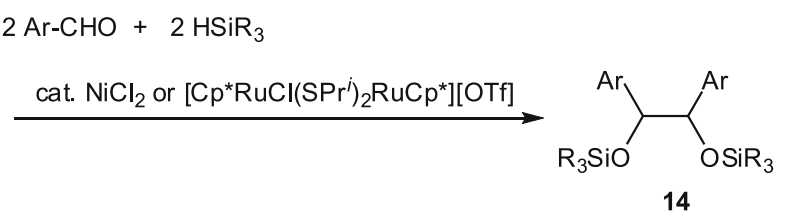

14

Scheme 12

2.2 Enantioselective Coupling

Catalytic enantioselective synthesis of *vic*-diols is a challenging issue. Chiral induction using chiral ligands is difficult to achieve. The moderately enantioselective pinacolization of benzaldehyde is demonstrated to be performed by the chiral titanocene catalysts **15** and **16** [42, 43].

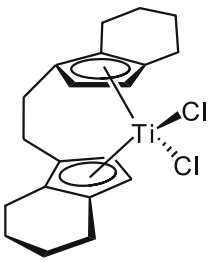

15

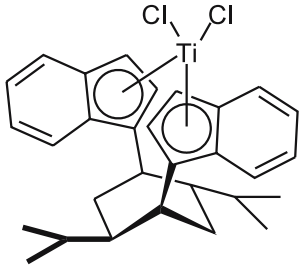

16 (*1R,2R,4R,5R*)

The chiral diol **17** derived from tartaric acid is exploited in the titanium-catalyzed asymmetric pinacol coupling in the presence of Zn and Me_3SiCl to give the corresponding diol in 11–71 ee % [44]. The chiral salen ligands **18–20** are used in the titanium-catalyzed enantioselective coupling reaction, which achieves the higher selectivity [45–47]. The chromium complex with TBOxH (**21**) efficiently catalyzes the asymmetric coupling reaction of both aromatic and aliphatic aldehydes [48].

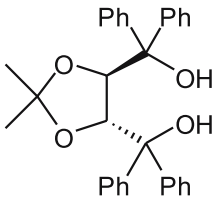

17

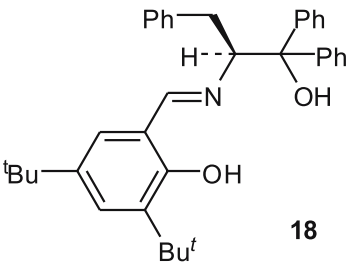

18

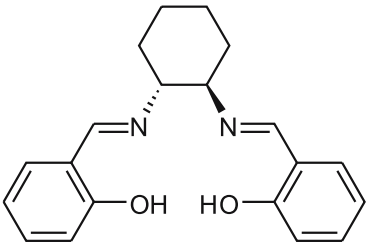

19

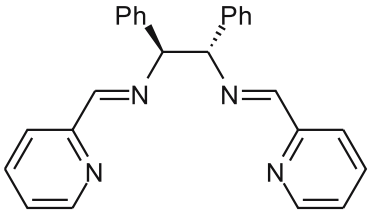

20

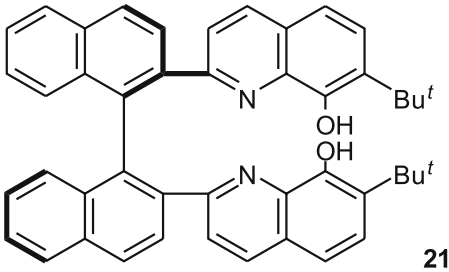

21

2.3 Intramolecular Coupling

The 1,5- and 1,6-dialdehydes **22** and **24** undergo the annulative pinacol coupling to give the cyclic *vic*-diols **23** and **25**, respectively (Scheme 13) [29]. The vanadium-catalyzed intramolecular coupling reaction of 1,5-diketone **26** also proceeds with excellent selectivity (Scheme 14) although the intermolecular coupling of ketones such as acetophenone results in low diastereoselectivity under these conditions [21].

Samarium-catalyzed pinacol coupling of **27** is used for *ansa*-bridge formation to give [n]paracyclophanediols **28** (Scheme 15) [49].

The Cp_2TiPh-catalyzed coupling reaction of the dials also gives the cyclic diols with excellent diastereoselectivity. The protocol is extended to the chiral synthesis as shown in Scheme 16 [50, 51].

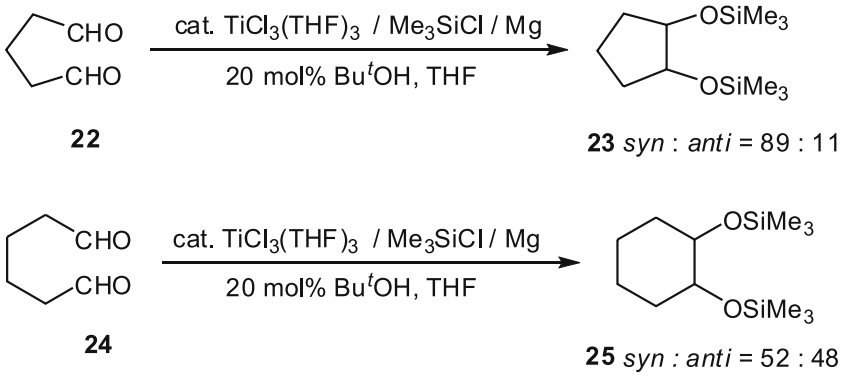

Scheme 13

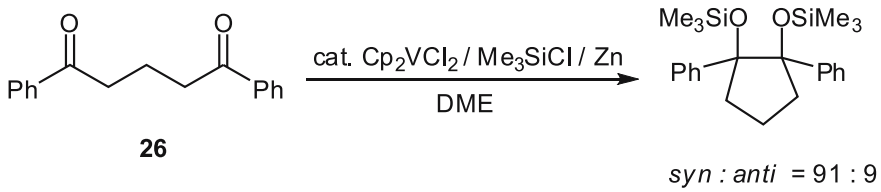

Scheme 14

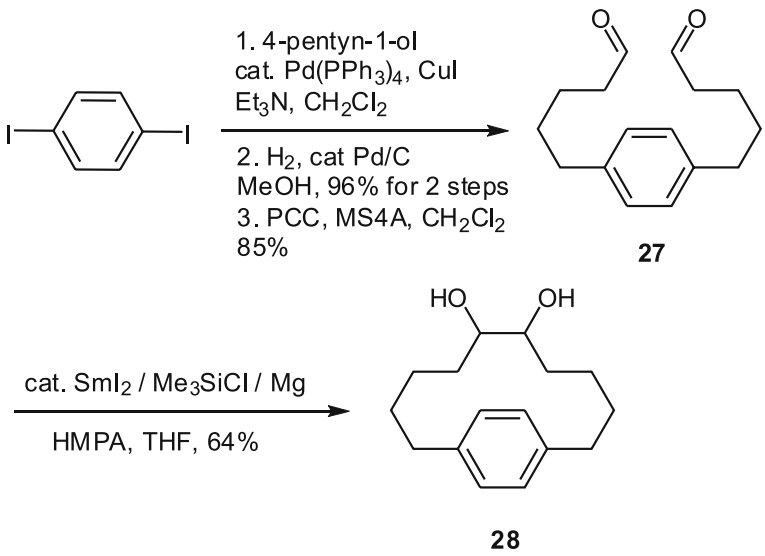

Scheme 15

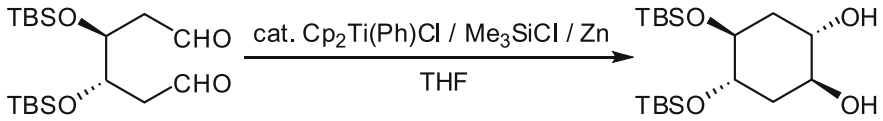

Scheme 16

2.4 Coupling to Diamines

The coupling reaction of imines has been less investigated despite the frequent occurrence of *vic*-diamine units in naturally occurring compounds. A cat. $PbBr_2$/Al system is effective for the coupling of aromatic imines in the presence of trifluoroacetic acid or $AlBr_3$ [52]. $PbCl_2$ or $SnCl_2$ salt is also used as a catalyst. No reductive coupling of aliphatic imines occurs with this catalytic system. The iminium ions, which are formed in the presence of trifluoroacetic acid or $AlBr_3$, are involved in facile one-electron reduction with the Pb(0) species, followed by the coupling. The thus-formed Pb(II) species is reduced to the Pb(0) species with Al. This recycling step is also performed using an undivided cell under constant current density [53]. Stereochemistry is not studied in these catalytic reactions. A cat. Cp_2TiCl_2/Sm system is effective at providing DL-diamines **30** from the imines **29** with moderate selectivity (Scheme 17) [54].

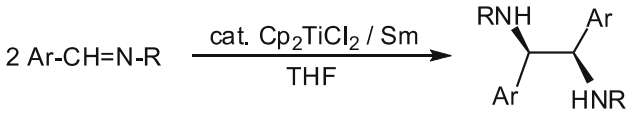

29 **30**

Scheme 17

The Cp_2VCl_2/R_3SiCl/Zn catalytic system can be used for the reductive coupling of the imines **29** (Scheme 18) [55]. These components of the ternary catalyst are essential and, interestingly, *meso*-diastereoselectivity is observed in contrast to the coupling with cat. Cp_2TiCl_2/Sm system. The selectivity de-

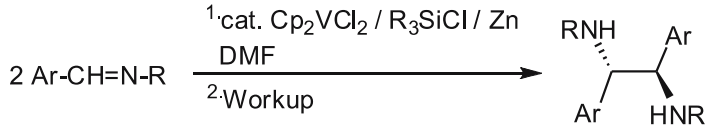

29 **31**

Scheme 18

pends on the substituents on both the nitrogen and silane atoms. The allyl or benzyl group on the nitrogen atom is advantageous for *meso* selection of **31**.

3 Related Radical-Like Coupling

The above-mentioned multi-component catalytic systems are of synthetic potential in radical reactions. The generated ketyl radicals are able to undergo the inter- and intra-molecular coupling with a variety of radical acceptors.

The reaction of the δ,ε-unsaturated aldehyde **32** with cat. $Cp_2VCl_2/Me_3SiCl/Zn$ is conducted in THF to afford the cyclic alcohol **33** with excellent diastereoselectivity (Scheme 19) [21]. The transformation may be explained by 5-*exo*-cyclization of the corresponding radical anion, followed by chlorination.

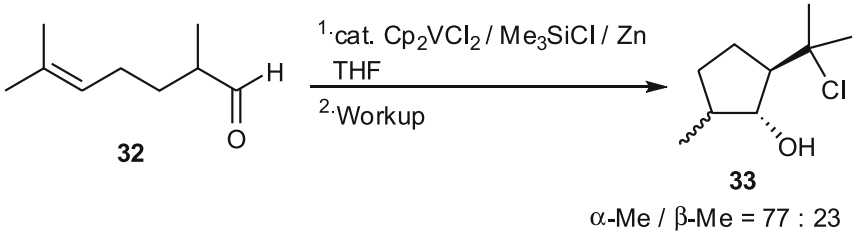

Scheme 19

A catalytic system consisting of cat. SmI_2, Zn/Hg, LiI, and Me_3SiOTf induces spirolactonization (Scheme 20) [56]. Me_3SiOTf plays a similar role in converting the intermediary alkoxides to the silyl ethers. The efficacy of LiI depends on the formation of SmI_3 from SmI_2OTf, which facilitates reduction by Zn/Hg. The Lewis acidity of Zn(II) is reduced by conversion to a non-Lewis-acidic species such as $Li_2ZnI_2(OTf)_2$.

Epoxides undergo deoxygenation with SmI_2 and Zn/Hg under these catalytic conditions to give the corresponding olefins. Use of Mn as the co-reductant prevents Lewis acid-initiated ring-opening of epoxides to chlorohydrins due to the less Lewis-acidic $MnCl_2$. The titanium-catalyzed intramolecular cyclization of the olefinic epoxide **34** occurs without deoxygenation (Scheme 21) [57]. The intermolecular radical addition of the epoxide **35** to methyl acrylate affords the lactone **36**. Zn as a co-reductant is used in methanol since the complexation of the generated $ZnCl_2$ with methanol reduces Lewis acidity.

The Cp_2TiCl_2-catalyzed reductive radical cyclization of the ketonitriles **37** results in the formation of the 2-amino-3-cyano-2-cyclopenten-1-ols **38**

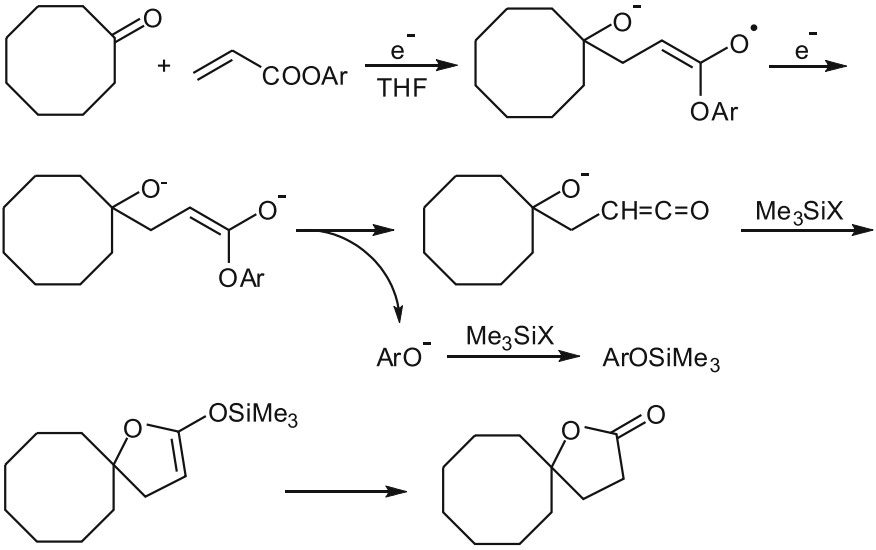

Scheme 20

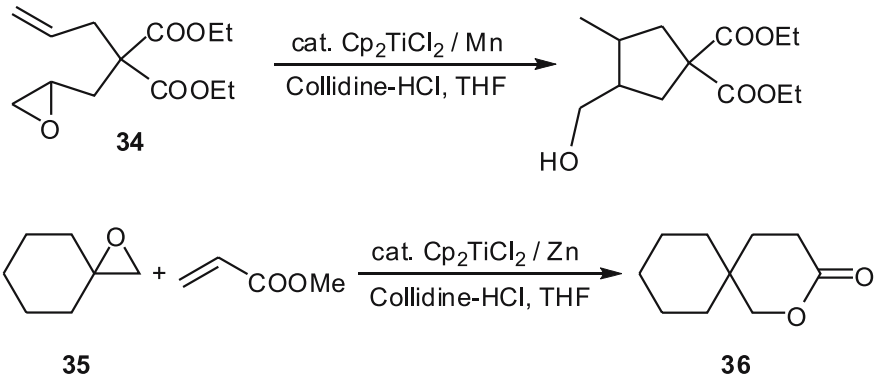

Scheme 21

in moderate to good yields with high *trans* selectivity (up to 94% *trans*, Scheme 22) [58].

Cyclodimerization is observed in the vanadium-catalyzed reaction of the arylidene malononitriles **39** in the presence of Me_3SiCl, giving **40** diastereoselectively as shown in Scheme 23 [59].

Acroleins and α,β-unsaturated ketones are coupled with aliphatic aldehydes in the Cr-catalyzed diastereoselective coupling in the presence of Mn and Me_3SiCl [60]. As shown in Scheme 24, the generated radical species undergoes the further one-electron reduction to afford the corresponding allylchromium **41**, which reacts with the aldehyde to give the corresponding

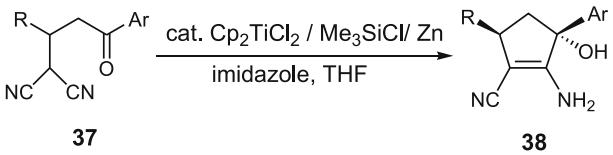

37 38

Scheme 22

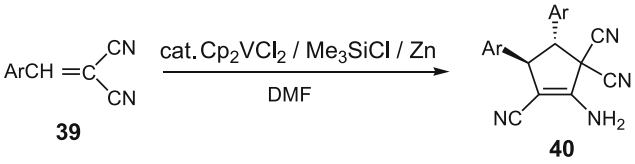

39 40

Scheme 23

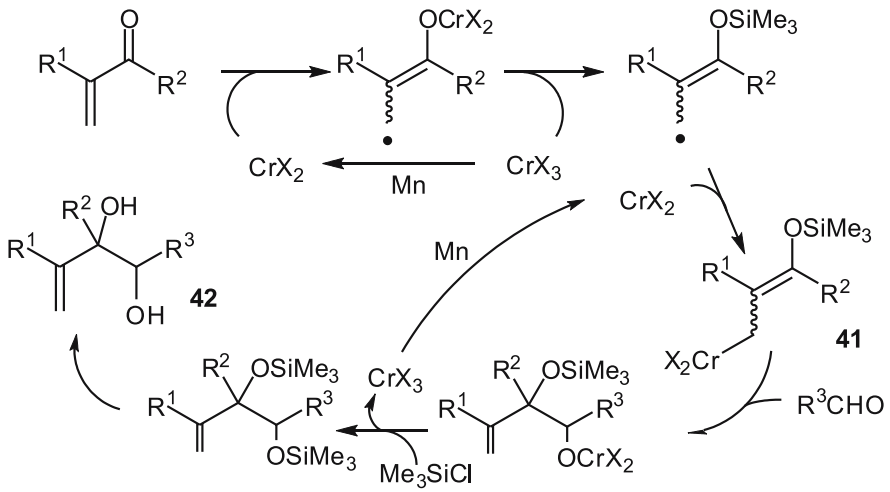

Scheme 24

diol **42**. The diastereoselectivity depends on the substituent on R^1. The reduction of Cr(III) to Cr(II) with Mn allows the formation of the catalytic cycle.

The chromium-catalyzed coupling is extended to the intramolecular cyclization to the dials **43**. The *O*-chelating silyl scavenger is used to control the stereoselectivity as shown in Scheme 25 [61, 62]. The ring size effect on the stereoselectivity is also investigated.

A novel chromium Brook rearrangement is suggested in the reductive olefination as shown in Scheme 26 [63].

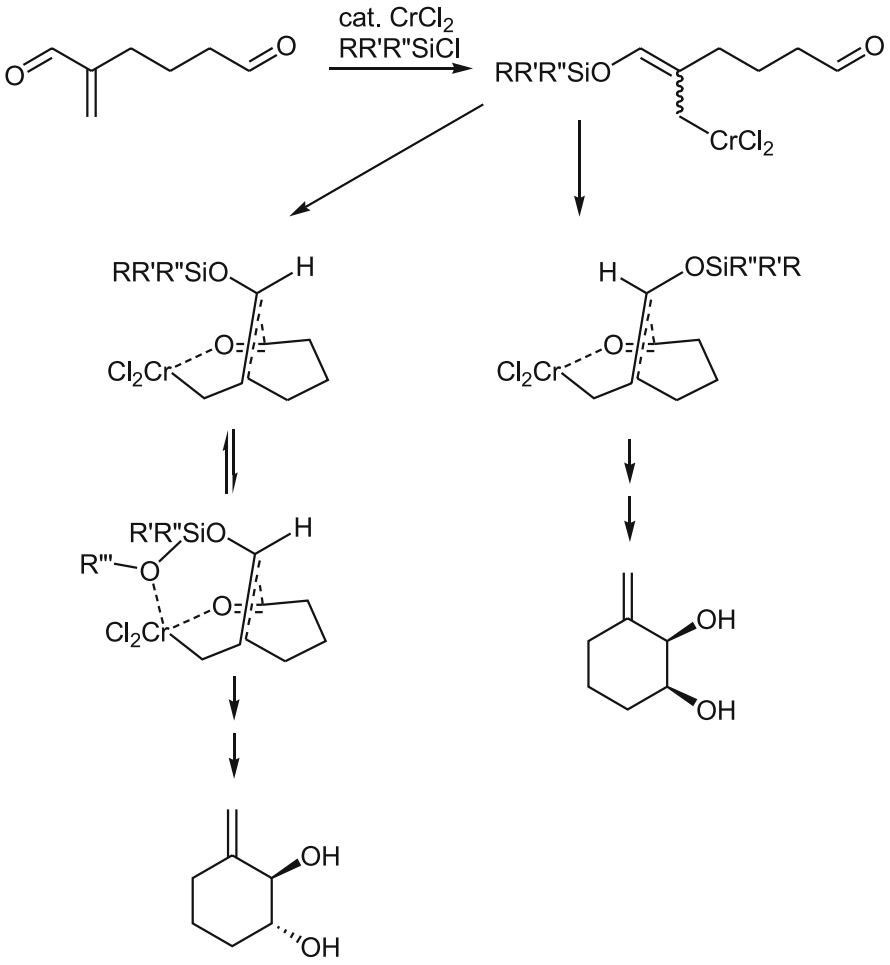

Scheme 25

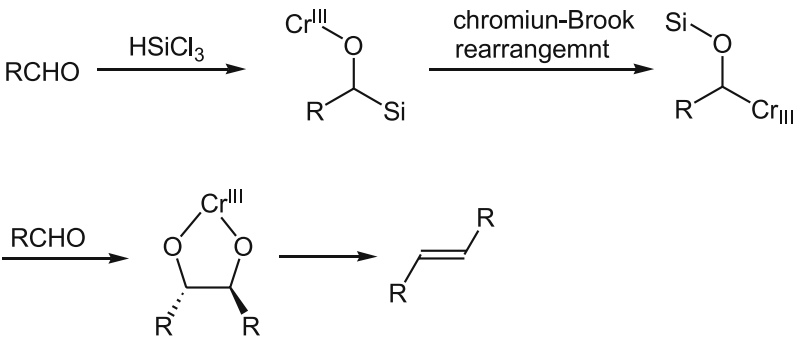

Scheme 26

$Cp_2Ti(PMe_3)_2$ catalyzes the reductive cyclization of the enones **44** to the cyclopentanols **46** via the metallacyclic intermediates **45** (Scheme 27) [64–66]. The cleavage of the titanium–oxygen bond in the metallacycles **45** by a hydrosilane provides a route to the generation of the active catalyst. The net transformation resembles the above-mentioned complementary radical pathway, which affords the opposite isomer.

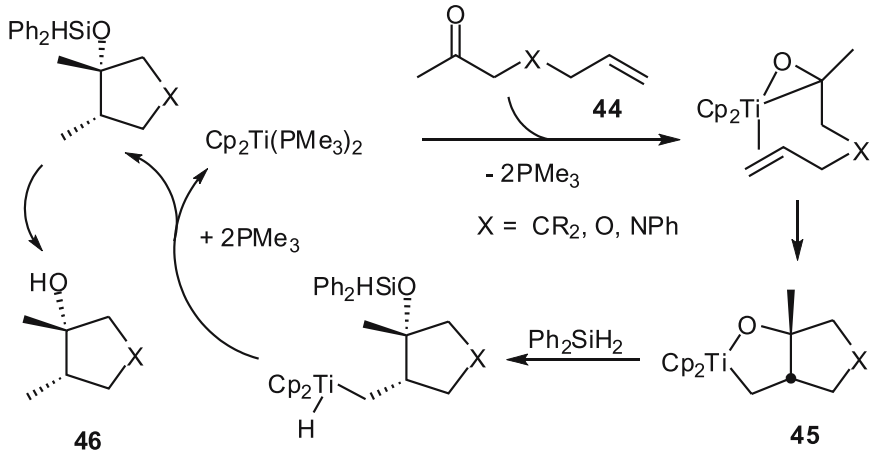

Scheme 27

4 Dehalogenative Coupling

One-electron reduction of organic halides is considered to afford the corresponding radical intermediates. A catalytic dehalogenation is developed by using a multi-component catalytic system. The highly stereoselective monodebromination of *gem*-dibromocyclopropanes **47** proceeds with a catalytic amount of a low-valent vanadium species generated from VCl_3 or $CpV(CO)_4$ and Zn as the stoichiometric reductant in DME, in cooperation with diethyl phosphonate or triethyl phosphite (Scheme 29) [67]. The phosphonate or phosphite is likely to play an important role in the debromination step. Coordination to the vanadium center affords the bulky and stronger reductant. The former effect may be related to the stereoselectivity, since the bulky reductant is liable to approach the bromide from the less hindered side. Furthermore, a hydrogen source seems to be available from the phosphonate or phosphite in the coordination sphere [68]. In this manner, the ternary reductant system contributes to the stereoselective catalytic debromination to the monobromide **48**.

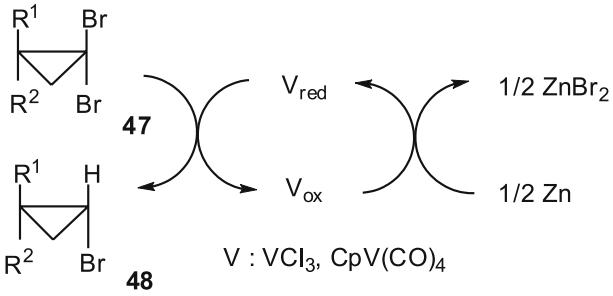

Scheme 29

A combination of cat. YbI_2 and Al is effective for the photo-induced catalytic hydrogenative debromination of alkyl bromide (Scheme 28) [69]. The ytterbium catalyst forms a reversible redox cycle in the presence of Al. In both vanadium- and ytterbium-catalyzed reactions, the multi-component redox systems are achieved by an appropriate combination of a catalyst and a co-reductant as described in the pinacol coupling, which is mostly dependent on their redox potentials.

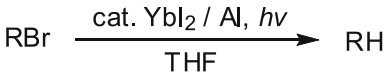

Scheme 28

A sequential 1,2-dechlorination/S – S bond fission of the 3,4-disubstituted 2-butenoate **49** is performed by cat. $PbBr_2$/Al in DMF, giving the 2-*exo*-methylenepenam **51** through the allene intermediate **50** (Scheme 30) [70].

The Barton–McCombie process is an important synthetic tool for the generation of radical species. Me_3SiO-$(SiHMeO)_n$-$SiMe_3$ works as a stoichiometric reductant in the tin-catalyzed reaction since $Bu_3Sn(OPh)$ is reduced to Bu_3SnH as shown in Scheme 31 [71].

Olefinic iodoethers **52** undergo the Cp_2TiCl_2-catalyzed reductive cyclization in the presence of Mn and Me_3SiCl (Scheme 32) [72]. This protocol provides a versatile method for the selective formation of multi-substituted tetrahydrofurans **53**.

The multi-component procedure is also effective for the chromium-catalyzed addition of organic halides to aldehydes (the Nozaki–Hiyama–Kishi reaction) [73]. The active Cr(II) species is recycled by redox interaction with Mn powder as the stoichiometric co-reductant in the presence of Me_3SiCl (Scheme 34), which mainly liberates the chromium catalyst from the alkoxide adduct. The chemo- and diastereo-selective addition reaction is performed with a variety of organic halides and alkenyl triflates. In the case of crotyl bromide, the addition is highly stereoconvergent, i.e., the respective *anti*-

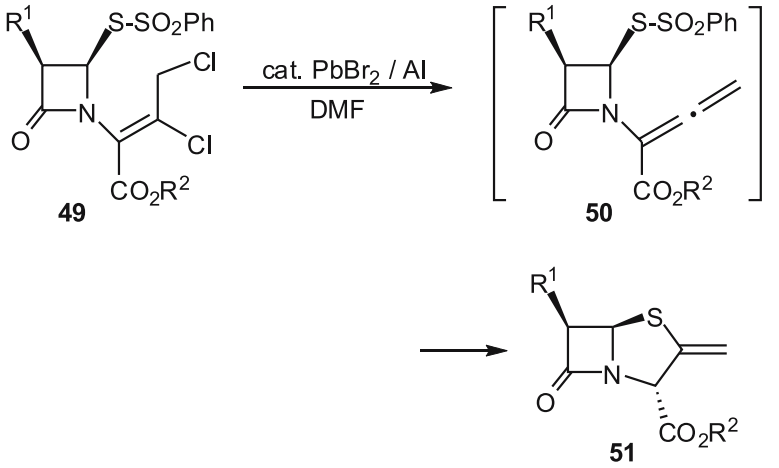

Scheme 30

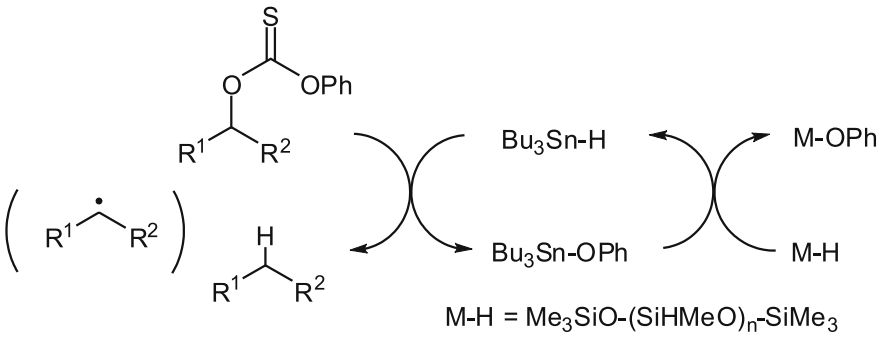

Scheme 31

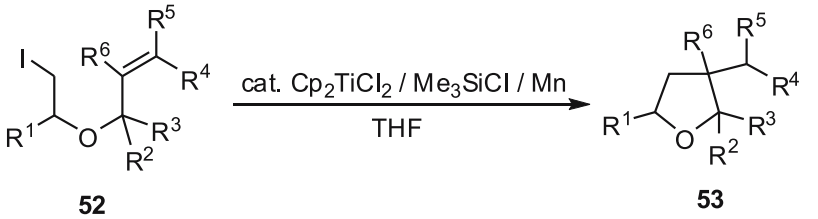

Scheme 32

configurated homoallyl alcohols are obtained with excellent diastereoselectivity independently of whether the starting halides are (*E*)- or (*Z*)-configurated. Cp-substituted chromium compounds are superior to $CrCl_2$ or $CrCl_3$ as a catalyst.

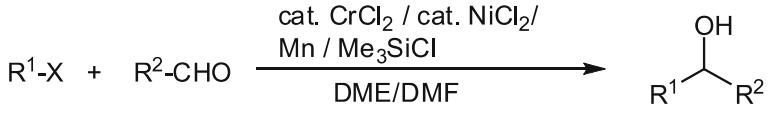

Scheme 34

The catalytic process is also achieved in the Pd(0)/Cr(II)-mediated coupling of organic halides with aldehydes (Scheme 33) [74]. Oxidative addition of a vinyl or aryl halide to a Pd(0) species, followed by transmetallation with a chromium salt and subsequent addition of the resulting organochromate to an aldehyde, leads to the alcohol **54**. The presence of an oxophile [Li(I) salts or Me_3SiCl] allows the cleavage of the Cr(III) – O bond to liberate Cr(III), which is reduced to active Cr(II) on the electrode surface.

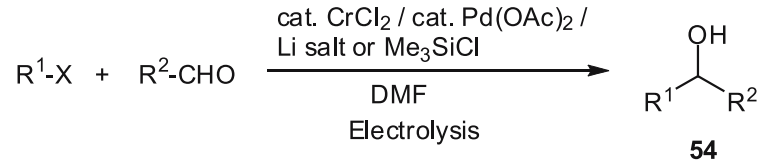

Scheme 33

5 Conclusion

The multi-component systems developed quite recently have allowed the efficient metal-catalyzed stereoselective reactions with synthetic potential [75–77]. Multi-components including a catalyst, a co-reductant, and additives cooperate with each other to construct the catalytic systems for efficient reduction. It is essential that the active catalyst is effectively regenerated by redox interaction with the co-reductant. The selection of the co-reductant is important. The oxidized form of the co-reductant should not interfere with, but assist the reduction reaction or at least, be tolerant under the conditions. Additives, which are considered to contribute to the redox cycle directly, possibly facilitate the electron transfer and liberate the catalyst from the reaction adduct. Co-reductants like Al, Zn, and Mg are used in the catalytic reactions, but from the viewpoint of green chemistry, an electron source should be environmentally harmonious, such as H_2.

This article mostly focuses on the catalytic pinacol coupling and related reductive transformations via one-electron transfer. On the other hand, the corresponding methods for catalytic oxidative transformations via one-electron oxidation have been scarcely investigated and remain to be developed. Both methods are complementary and useful for generating radical intermediates.

Attainment of higher chemoselectivity (cross-coupling) and stereoselectivity in both radical reactions is expected to be one of the coming goals in this field.

Acknowledgements The author is deeply indebted to the graduate coworkers, whose names are shown in the references.

References

1. Ho T-L (1979) Synthesis, p 1
2. Sheldon RA, Kochi JK (1981) Metal-catalyzed oxidations of organic compounds. Academic, New York
3. Freeman F (1986) Oxidation by oxochromium (VI) compounds. In: Mijs WJ, de Jonge CRHI (ed) Organic syntheses by oxidation with metal compounds. Plenum, New York, p 52
4. Pons J-M, Santelli M (1988) Tetrahedron 44:4295
5. Rehder D, Gailus H (1994) Trends Organomet Chem 1:397
6. Iqbal J, Bhatia B, Nayyar NK (1994) Chem Rev 94:519
7. Dalko PI (1995) Tetrahedron 51:7579
8. Hirao T (1997) Chem Rev 97:2707
9. Jacobsen EN, Marko I, Mungall WS, Schröder G, Sharpless KB (1988) J Am Chem Soc 110:1968
10. Nicolaou KC, Liu J-J, Yang Z, Ueno H, Guy RK, Sorensen EJ, Claiborne CF, Hwang C-K, Nakada M, Nantermet PG (1995) J Am Chem Soc 117:634
11. Shiina I, Nishimura T, Ohkawa N, Sakoh H, Nishimura K, Saitoh K, Mukaiyama T (1997) Chem Lett p 419
12. Kammermeier B, Beck G, Holla W, Jacobi D, Napierski B, Jendralla H (1996) Chem Eur J 2:307
13. Kammermeier B, Beck G, Jacobi D, Jendralla H (1994) Angew Chem Int Ed Engl 33:685
14. Freudenberger JH, Konradi AW, Pedersen SF (1989) J Am Chem Soc 111:8014
15. Park J, Pedersen SF (1990) J Org Chem 55:5924
16. Konradi AW, Pedersen SF (1992) J Org Chem 57:28
17. Konradi AW, Kemp SJ, Pedersen SF (1994) J Am Chem Soc 116:1316
18. Hirao T, Hasegawa T, Muguruma Y, Ykeda I (1996) J Org Chem 61:366
19. Hirao T, Hasegawa T, Muguruma Y, Ikeda I (1994) Abstracts for the 6th international Kyoto conference on new aspects of organic chemistry, Kyoto, 7–11 Nov 1994, p 175
20. Corey EJ, Pyne SG (1983) Tetrahedron Lett 24:2821
21. Hirao T, Asahara M, Muguruma Y, Ogawa A (1998) J Org Chem 62:4566
22. Hirao T, Hatano B, Asahara M, Muguruma Y, Ogawa A (1998) Tetrahedron Lett 39:5247
23. Fürstner A, Hupperts A (1995) J Am Chem Soc 117:4468
24. Gansäuer A (1997) Chem Commun, p 457
25. Gansäuer A (1997) Synlett, p 363
26. Dunlap MS, Nicholas KM (2001) J Organomet Chem 630:125
27. Bandini M, Cozzi PG, Morganti S, Umani-Ronchi A (1999) Tetrahedron Lett 40:1997
28. Tian Q, Jiang C, Li Y, Jiang C, You T (2004) J Mol Cat A Chem 219:315
29. Lipski TA, Hilfiker MA, Nelson SG (1997) J Org Chem 62:4566
30. Gansäuer A, Bauer D (1998) J Org Chem 63:2070
31. Xu X, Hirao T (2005) J Org Chem 70:8594

32. Léonard E, Duñach E, Périchon J (1989) J Chem Soc Chem Commun, p 276
33. Nomura R, Matsuno T, Endo T (1996) J Am Chem Soc 118:11666
34. Aspinall HC, Greeves N, Valla C (2005) Org Lett 7:1919
35. Helion F, Lannou M-L, Namy J-L (2003) Tetrahedron Lett 44:5507
36. Kantam ML, Aziz K, Likhar PR (2006) Synth Commun 36:1437
37. Svatos A, Boland W (1998) Synlett, p 549
38. Shi L, Fan C-A, Tu Y-Q, Wang M, Zhang F-M (2004) Tetrahedron 60:2851
39. Ogoshi S, Kamada H, Kurosawa H (2006) Tetrahedron 62:7583
40. Frainnet E, Bourhis R, Simonin F, Moulines F (1976) J Organomet Chem 105:17
41. Shimada H, Qü J-P, Matsuzaka M, Ishii Y, Hidai M (1995) Chem Lett, p 671
42. Dunlap MS, Nicholas KM (1999) Synth Commun 129:1097
43. Halterman RL, Zhu C, Chen Z, Dunlap MS, Khan MA, Nicholas KM (2000) Organometallics 19:3824
44. Wen J, Zhao J, You T (2006) J Mol Cat A Chem 245:278
45. Bensari A, Renaud J-L, Riant O (2001) Org Lett 3:3863
46. Chatterjee A, Bennur TH, Joshi NN (2003) J Org Chem 68:5668
47. Li Y-G, Tian Q-S, Zhao J, Feng Y, Li M-J, You T-P (2004) Tetrahedron Asymmetr 15:1707
48. Takenak N, Xia G, Yamamoto H (2004) J Am Chem Soc 126:13198
49. Ueda T, Kanomata N, Machida H (2005) Org Lett 7:2365
50. Yamamoto Y, Hattori R, Miwa T, Nakagai Y-I, Kubota T, Yamamoto C, Okamoto Y, Itoh K (2001) J Org Chem 66:3865
51. Yamamoto Y, Hattori R, Itoh K (1999) Chem Commun, p 825
52. Tanaka H, Dhimane H, Fujita H, Ikemoto Y, Torii S (1988) Tetrahedron Lett 29:3811
53. Tanaka H, Nakahara T, Dhimane H, Torii S (1989) Synlett, p 51
54. Liao P, Huang Y, Zhang Y (1997) Synth Commun 27:1483
55. Hatano B, Ogawa A, Hirao T (1998) J Org Chem 63:9421
56. Corey EJ, Zheng GZ (1997) Tetrahedron Lett 38:2045
57. Gansäuer A, Pierobon M, Bluhm H (1998) Angew Chem Int Ed 37:101
58. Zhou L, Hirao T (2001) Tetrahedron 57:6927
59. Zhou L, Hirao T (2000) Tetrahedron Lett 41:8517
60. Jung M, Groth U (2002) Synlett, p 2015
61. Groth U, Jung M, Vogel T (2004) Synlett, p 1054
62. Fischer S, Groth U, Jung M, Lindermaier M, Vogel T (2005) Tetrahedron Lett 46:6679
63. Baati R, Mioskowski C, Barma D, Kache R, Falck JR (2006) Org Lett 8:2949
64. Kablaoui NM, Buchwald SL (1995) J Am Chem Soc 117:6785
65. Kablaoui NM, Buchwald SL (1996) J Am Chem Soc 118:3182
66. Crowe WE, Rachita MJ (1995) J Am Chem Soc 117:6787
67. Hirao T, Hirano K, Hasegawa T, Ikeda I, Ohshiro Y (1993) J Org Chem 58:6529
68. Barton DHR, Jang DO, Jaszberenyi JC (1992) Tetrahedron Lett 33:2311
69. Ogawa A, Ohya S, Sumino Y, Sonoda N, Hirao T (1997) Tetrahedron Lett 38:9017
70. Tanaka H, Sumida S-I, Nishioka Y, Kobayashi N, Tokumaru Y, Kameyama Y, Torii S (1997) J Org Chem 62:3610
71. Lopez R, Hays DS, Fu GC (1997) J Am Chem Soc 119:6949
72. Zhou L, Hirao T (2003) J Org Chem 68:1633
73. Fürstner A, Shi N (1996) J Am Chem Soc 118:12349
74. Grigg R, Putnikovic B, Urch CJ (1997) Tetrahedron Lett 38:6307
75. Fürstner A (1998) Chem Eur J 4:567
76. Hirao T (2005) Pure Appl Chem 77:1539
77. Chatterjee A, Joshi NN (2006) Tetrahedron 62:12137

Top Curr Chem (2007) 279: 77–104
DOI 10.1007/128_2007_122

Published online: 21 April 2007

Catalytic Reductive Coupling of Alkenes and Alkynes to Carbonyl Compounds and Imines Mediated by Hydrogen

Hiroki Iida · Michael J. Krische (✉)

Department of Chemistry and Biochemistry, University of Texas at Austin,
1 University Station – A5300, Austin, TX 78712-1167, USA
mkrische@mail.utexas.edu

Abstract Catalytic transformations mediated by hydrogen or "hydrogenations" encompass a diverse range of environmentally benign processes, including large volume transformations of enormous socioeconomic impact, such as the Haber–Bosch process and the reduction of olefinic feedstocks. Despite considerable progress across diverse areas of catalytic hydrogenation, reductive C – C bond formations mediated by hydrogen have, until recently, been restricted to the incorporation of carbon monoxide, as illustrated by the Fischer–Tropsch reaction and alkene hydroformylation. In this account, the emerging family of hydrogen-mediated C – C bond formations beyond carbon monoxide coupling is reviewed. This new type of hydrogenation enables direct coupling of diverse π-unsaturated reactants to carbonyl compounds and imines under neutral condition with complete atom economy.

Keywords Atom economy · Cross-coupling · Green Chemistry · Hydrogenation · Iridium · Reductive coupling · Rhodium

1 Hydrogenation – The Proteus of Catalytic Transformations

Hydrogen is the most abundant element in the universe, constituting roughly 75% of the universe's normal mass and 90% of the atoms present in the universe. Elemental hydrogen was first described by the legendary Swiss alchemist Paracelsus (1493–1541), and later in 1671 by Robert Boyle, but was

not recognized as a discrete substance until 1766, when in a paper entitled "*On factitious airs*" Henry Cavendish recorded the density of "inflammable air" that is generated upon the mixing of acids with mercury and which produces water when burned. Cavendish characterized many important properties of hydrogen, but incorrectly believed that hydrogen emanated from mercury. Although Cavendish is usually credited with the discovery of hydrogen, it should be noted that his work is articulated in terms of the phlogiston theory. Indeed, Cavendish believed that his "inflammable air" was phlogiston in its pure form. Antoine Lavoisier reproduced the experiments of Cavendish involving the combustion of hydrogen to form water and, further, regenerated hydrogen and oxygen through the decomposition of water. These experiments demonstrated that water is not an element, but is a compound of hydrogen and oxygen, which led Lavoisier to designate hydrogen as an element. In 1783, the very year hydrogen first was used in balloon ascents, Lavoisier gave this new element its name from the ancient Greek words *hydro*: "water" and *genes*: "forming".

Catalytic transformations mediated by hydrogen, termed "hydrogenations", are among the earliest reported metal-catalyzed reactions [1]. The first catalytic hydrogenation appears to be the platinum-catalyzed reaction of hydrogen with atmospheric oxygen, described nearly two centuries ago. In 1823, at a time when fire was created using flint and tinder, Döbereiner devised a household lighter based on this process [2, 3]. The "Döbereiner lighter" instantly captured worldwide attention and served as a prototype for legion devices used for the self-ignition of coal-gas burners. The catalytic hydrogenation of atmospheric nitrogen to produce ammonia, reported by Haber in 1905 [4], continues to have massive socioeconomic impact [5]. Though developed in connection with the German military effort in WWI, the Haber–Bosch process provided cost-effective routes to nitrogenous fertilizer, increasing worldwide food production to unprecedented levels. At present, over 100 million metric tons of ammonia are produced annually through the Haber–Bosch process. The Fischer–Tropsch process, discovered in 1923 [6, 7] and broadly implemented in WWII, involves the production of liquid fuel via catalytic reductive polymerization of carbon monoxide mediated by hydrogen. In 1944, Germany produced over 6.5 million tons of synthetic petroleum using this process [8, 9]. The rising cost of crude oil has rekindled interest in Fischer–Tropsch chemistry, stimulating development of improved catalytic systems [10]. Finally, in 1938, further studies of the Fischer–Tropsch reaction led by Otto Roelen resulted in the discovery of alkene hydroformylation, also known as the "oxo-synthesis" [11]. Presently, over 7 million metric tons of aldehyde are produced annually via hydroformylation, making it the largest volume application of homogeneous metal catalysis [12, 13].

For the organic chemist, hydrogenation is typically associated with the reduction of C = X (X=C, N, O) π-bonds. The first heterogeneous catalysts for

Table 1 Twelve milestones in catalytic hydrogenation

1500s	Paracelsus (1493–1541) and Boyle (1671) describe gas generation upon mixing acid and metal filings	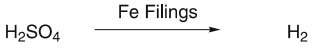
1766	Henry Cavendish (1731–1810) isolates and characterizes "inflammable air", which he believes to be phlogiston	
1783	Lavoisier coins the name "hydrogen" and recognizes hydrogen as an element	
1823	Döbereiner reports the first catalytic hydrogenation: the Pt-catalyzed combustion of hydrogen in air [2, 3]	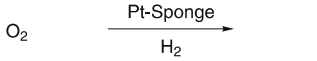
1897	Sabatier reports the first heterogeneous catalytic hydrogenation of an organic molecule [14–17]	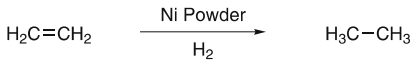
1905	The catalytic hydrogenation of atmospheric nitrogen to produce ammonia is reported by Haber [3]	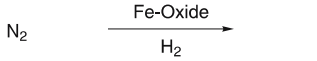
1923	The catalytic hydrogenation of carbon monoxide to produce petroleum is reported by Fischer and Tropsch [5, 6]	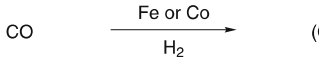
1938	Hydroformylation, the prototypical hydrogenative C – C coupling, is reported by Roelen [11]	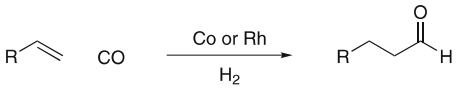
1938	Calvin reports the first homogeneous hydrogenation of an organic molecule [18, 19]	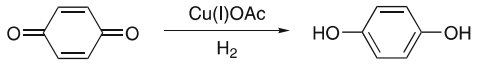
1961	Halpern reports the first homogeneous hydrogenation of an activated alkene [20, 21]	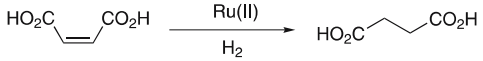
1964	Wilkinson reports the first homogeneous hydrogenation of an unactivated alkene [22–24]	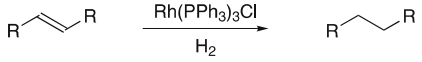
1968	Knowles reports the first enantioselective homogeneous hydrogenation of an alkene [25, 26]	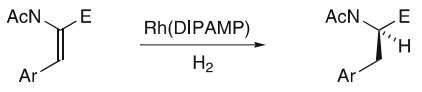

reactions of this type were developed by Paul Sabatier at the University of Toulouse in the late 1890s [14–17]. It was not until the 1960s that the first catalysts for the homogeneous alkene hydrogenation were developed [18, 19], largely owing to seminal contributions by Jack Halpern [20, 21] and Geoffrey Wilkinson [22–24]. Catalytic hydrogenation continued to evolve to encompass enantioselective variants, in large part due to the pioneering efforts of Knowles [25, 26], Kagan [27], and Noyori [28]. Clean, cost-effective and powerful, asymmetric hydrogenation is presently the most broadly utilized catalytic enantioselective process employed industrially, accounting for over half of the chiral compounds made by man not produced via physical or enzymatic resolution [29–31] (Table 1).

2
Hydrogenative C–C Bond Formations beyond Hydroformylation

The profound impact of hydrogenation portends an equally powerful approach to reductive C – C bond formations mediated by hydrogen: completely atom economical C – C couplings wherein two or more unsaturated molecules combine to furnish a single, more complex product simply through their exposure to gaseous hydrogen in the presence of a metal catalyst. However, since the discovery of the Fischer–Tropsch reaction and alkene hydroformylation, processes restricted to the incorporation of carbon monoxide, the field of hydrogen-mediated C – C bond formation has lain fallow. It is likely that the broad perception of hydrogenation as a method for the reduction of C = X π-bonds caused hydroformylation to be viewed as an anomalous reaction specific to carbon monoxide, impeding development of related hydrogenative couplings. Indeed, withstanding recent studies described in this account, systematic efforts toward the development of hydrogen-mediated C – C couplings beyond hydroformylation have been absent from the literature [32–35].

Among catalysts for alkene hydrogenation, those based upon rhodium have been studied in greatest detail. Through analysis of the mechanism of "conventional hydrogenation" catalyzed by *neutral* and *cationic* rhodium complexes, general strategies for intercepting the organometallic intermediates arising transiently in the course of catalytic hydrogenation may be formulated. For both the neutral and cationic rhodium catalysts, the dihydride based catalytic cycle involves three fundamental steps: (a) hydrogen oxidative addition, (b) substrate hydrometallation, and (c) C – H reductive elimination (Scheme 1).

The mechanism of alkene hydrogenation catalyzed by the neutral rhodium complex $RhCl(PPh_3)_3$ (Wilkinson's catalyst) has been characterized in detail by Halpern [36–38]. The hydrogen oxidative addition step involves initial dissociation of PPh_3, which enhances the rate of hydrogen activation by a factor

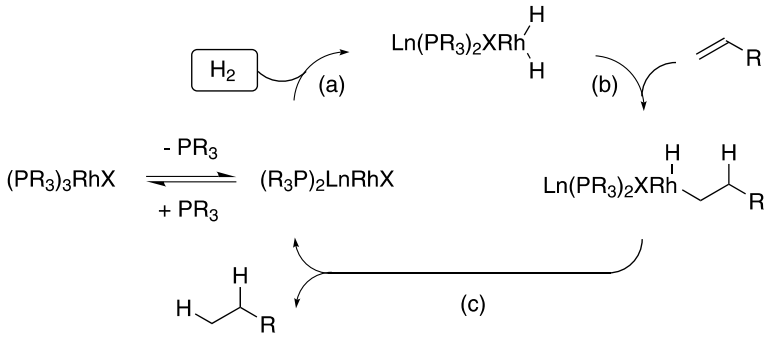

Scheme 1 Fundamental steps in Rh-catalyzed alkene hydrogenation involving a dihydride-based mechanism

of 1×10^4. The hydrogen oxidative addition step is reversible, as established by the equilibration of *para*-enriched hydrogen. Alkene hydrometallation is turnover-limiting, and the rapid nature of the subsequent C – H activation event renders the hydrometallation event irreversible. It should be emphasized that small changes in ligand or substrate are known to change the dominant reaction mechanism. Halpern elegantly demonstrates that none of the spectroscopically detectable species are actual participants in the catalytic cycle.

For cationic rhodium complexes, the mechanism for the hydrogenation of dehydroamino acid esters (i.e., α-amidocinnamates) has been characterized in detail [39–44]. For chirally modified catalysts, substrate coordination provides diastereomeric substrate complexes. The minor diastereomer activates hydrogen more quickly than the major diastereomer. Initially, it was presumed that substrate remains bound to rhodium during the hydrogen oxidative addition event. More recent studies suggest dissociation of substrate from the minor isomer occurs in advance of hydrogen oxidative addition [45]. Unlike the hydrogenations catalyzed by neutral rhodium complexes, the cationic systems irreversibly activate hydrogen in a turnover-limiting oxidative addition. At reduced temperatures (– 40 °C), the rate-determining step changes to C – H reductive elimination.

The hydrogenation of simple alkenes using cationic rhodium precatalysts has been studied by Osborn and Schrock [46–48]. Although kinetic analyses were not performed, their collective studies suggest that both monohydride- and dihydride-based catalytic cycles operate, and may be partitioned by virtue of an acid–base reaction involving deprotonation of a cationic rhodium(III) dihydride to furnish a neutral rhodium(I) monohydride (Eq. 1). This aspect of the mechanism finds precedent in the stoichiometric deprotonation of cationic rhodium(III) dihydrides to furnish neutral rhodium(I) monohydrides (Eq. 2). The net transformation ($H_2 + M – X \rightarrow M – H + HX$) is equivalent to a formal *heterolytic* activation of elemental

$$[RhH_2(PPhMe_2)_3S_x]^{\oplus} \rightleftharpoons [RhH(PPhMe_2)_3S_x] + H^{\oplus}$$

Cationic Dihydride — Neutral Monohydride

Equation 1

$$[Rh(NBD)(PPh_3)_2]^{\oplus} \xrightarrow[2)\ NEt_3]{1)\ 3\ PPh_3,\ H_2} RhH(PPh_3)_4 \qquad 80\%\ \text{Yield}$$

Equation 2

hydrogen [49, 50]. Cationic complexes are better at promoting heterolytic hydrogen activation, as the resulting dihydrides are more acidic than the neutral complexes [51].

Based upon the preceding data, the capture of reactive intermediate in catalytic hydrogenations catalyzed by cationic rhodium complexes appeared feasible. The cationic complexes are capable of promoting heterolytic hydrogen activation and entry into monohydride-based catalytic cycles. Substrate hydrometallation from the monohydride furnishes organometallic species that do not possess hydride ligands, thus disabling direct C – H reductive elimination manifolds, extending the lifetime of the resulting organometallic species to facilitate their capture. Further, because cationic rhodium complexes are slow to activate hydrogen, oxidative coupling of the reactants may precede hydrogen activation en route to products of C – C bond formation. The veracity of this analysis is supported by the transformations described herein, which uniformly require cationic rhodium precatalysts (Scheme 2).

In this account, the first systematic efforts toward hydrogen-mediated C – C couplings beyond alkene hydroformylation are described [52–54].

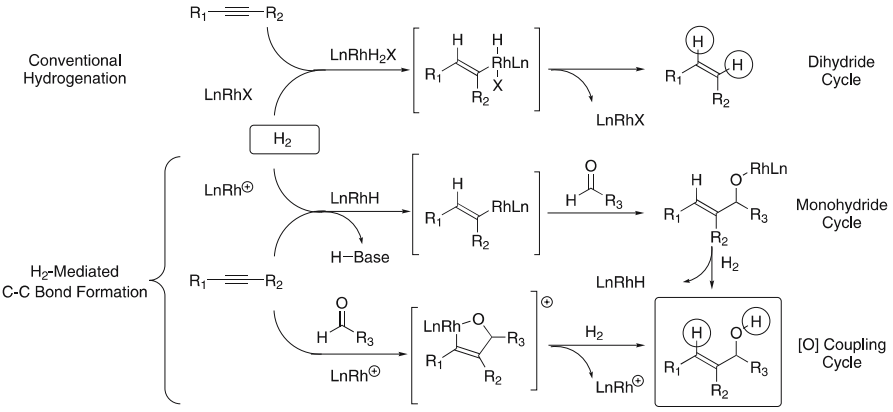

Scheme 2 General strategies for hydrogenative C – C coupling predicated on the mechanism of conventional Rh-catalyzed alkene hydrogenation

Whereas classical methods for the addition of *C*-nucleophiles to carbonyl compounds often require stoichiometric use of moisture-sensitive organometallic reagents, "C – C bond forming hydrogenation" enables direct C – C coupling of π-unsaturated reactants under neutral conditions with complete atom economy, thus taking catalytic hydrogenation in a powerful new direction. To date, we have only tapped into a fraction of the potential of catalytic hydrogenation to serve as a method of C – C bond formation. Just as the prototypical hydrogen-mediated C – C couplings, the Fischer–Tropsch reaction and alkene hydroformylation, are practiced on enormous scale. Hydrogenative couplings that extend beyond carbon monoxide coupling promise to add a new dimension to one of chemistry's oldest and most broadly utilized catalytic transformations.

2.1 Vinyl Ketone–C=X (X=O, NR) Coupling (Reductive Aldol and Mannich Additions)

Following seminal studies by Revis (1987) [55], the catalytic reductive coupling of α,β-unsaturated carbonyl compounds and aldehydes to form aldol products, termed the "reductive aldol reaction", has been the subject of intensive investigation. To date, catalysts for reductive aldol coupling based on rhodium [55–71], cobalt [72–75], iridium [76], palladium [73], copper [74–80], and indium have been described, which include highly diastereo- [57, 65, 66, 69–71, 73–75, 80–85] and enantioselective [58, 61, 62, 64, 76, 81–83] variants. Through studies of the rhodium-catalyzed reductive aldol reaction [65], it was found that organometallic intermediates arising transiently in catalytic hydrogenation may be diverted to products of C – C bond formation. Specifically, whereas catalytic hydrogenation of the indicated phenyl-substituted mono-enone mono-aldehyde using the neutral rhodium(I) catalyst $Rh(PPh_3)_3Cl$ furnishes the expected product of conventional hydrogenation, use of a rhodium salt that embodies increased cationic character, $Rh^I(COD)_2OTf/Ph_3P$, provides nearly equal proportions of the conventional hydrogenation and *syn*-aldol cyclization products. Finally, when $Rh^I(COD)_2OTf$ is used in conjunction with a more electron-deficient ligand and substoichiometric quantities of a mild basic additive, potassium acetate, formation of aldol product is increased to the point that conventional hydrogenation manifolds are virtually excluded. Reexposure of the conjugate reduction product to the reaction conditions does not produce the aldol product. Additionally, in the absence of hydrogen, Morita–Baylis–Hillman products are not observed, suggesting that tandem phosphine-catalyzed cyclization-conjugate reduction pathways en route to the aldol cyclization product are not operative. The observance of *syn*-aldol adducts suggests intermediacy of the *Z*-enolate and a closed Zimmerman–Traxler type of transition structure (Table 2) [86].

Table 2 Hydrogenative aldol cyclization is promoted through the use of cationic Rh pre-catalysts and substoichiometric quantities of mild basic additives [a]

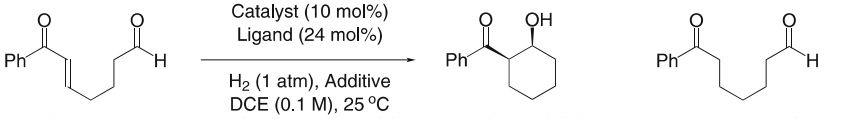

Catalyst	Ligand	Additive (mol%)	Aldol (*syn*:*anti*)	1,4%-Reduction
$Rh(PPh_3)Cl$	–	–	1 (99 : 1)	57
$Rh(COD)_2OTf$	PPh_3	–	21 (99 : 1)	25
$Rh(COD)_2OTf$	PPh_3	KOAc (30)	59 (58 : 1)	21
$Rh(COD)_2OTf$	$(p\text{-}CF_3Ph)_3P$	–	57 (14 : 1)	22
$Rh(COD)_2OTf$	**$(p\text{-}CF_3Ph)_3P$**	**KOAc (30)**	**89 (10 : 1)**	**0.1**

[a] As product ratios were found to vary with surface area to volume ratio of the reaction mixture, all transformations were conducted on 1.48 mmol scale in 50 mL round bottomed flasks

Under these conditions, the cycloreduction of aromatic, heteroaromatic and aliphatic enone substrates to form five- and six-membered ring products may be achieved (Table 3) [65]. Interestingly, the cycloreduction of substrates incorporating aryl-substituted enones yields aldol products with good levels of *syn*-diastereoselectivity, yet for substrates incorporating aliphatic enones, *anti*-diastereoselectivity is observed. These results are consistent with the generally accepted notion that *Z*-enolate formation is preferred for large

Table 3 Rh-catalyzed hydrogenative aldol cyclization of aldo-enones [a]

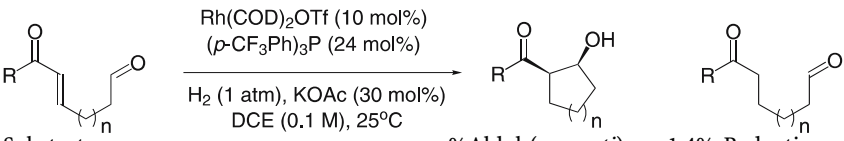

Substrate	%Aldol (*syn*:*anti*)	1,4%-Reduction
$n = 2$, R = Ph	89 (10 : 1)	0.1
$n = 2$, R = *p*-MeOPh	74 (5 : 1)	3
$n = 2$, R = 2-Naphthyl	90 (10 : 1)	1
$n = 2$, R = 2-Thiophenyl	76 (19 : 1)	2
$n = 2$, R = 2-Furyl	70 (6 : 1)	10
$n = 1$, R = Ph	71 (24 : 1)	1
$n = 2$, R = CH_3	65 (1 : 5)	–

[a] As product ratios were found to vary with surface area to volume ratio of the reaction mixture, all transformations were conducted on 1.48 mmol scale in 50 mL round bottomed flasks

acyl residues due to $A_{1,3}$-strain [87–90]. However, as demonstrated by the hydrogen-mediated cyclization of keto-enones [66], if the aldol addition event is rendered reversible, as is typically the case in enolate additions to ketones [87–90], the thermodynamically favored *syn*-aldol cyclization products are uniformly preferred (Tables 4 and 5).

Although a mechanism involving enone-aldehyde oxidative coupling cannot be excluded, the pronounced effect of basic additives on partitioning of the aldolization and 1,4-reduction manifolds suggests a monohydride catalytic cycle (Scheme 2). Basic additives may mediate deprotonation of the (hydrido)rhodium intermediates $LnRh^{III}(OTf)(H)_2$ or (enolato)Rh^{III}(OTf)(H)Ln, simultaneously disabling direct enolate-hydrogen reductive elimination and inducing entry into the monohydride catalytic cycle, which itself avoids regeneration of such intermediates. Consistent with this interpretation, hydrogenative aldol cyclization under an atmosphere of deuterium results in deuterium incorporation exclusively at the former enone β-position [66]. Deuterium incorporation at the α-position is not observed. Interestingly, the indicated distribution of deuterated products supports reversible enone hydrometallation in the case of ketone acceptors, where reversible aldol addition is anticipated (Scheme 3).

Table 4 Rh-catalyzed hydrogenative aldol cyclization of keto-enones[a]

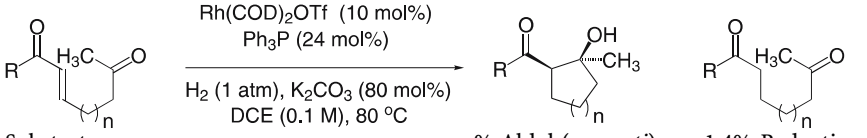

Substrate	% Aldol (*syn*:*anti*)	1,4%-Reduction
n = 1, R = Ph	75 (> 95 : 5)	8
n = 1, R = 2-Naphthyl	74 (> 95 : 5)	18
n = 1, R = 2-Thienyl	66 (> 95 : 5)	24
n = 1, R = 2-Furyl	70 (> 95 : 5)	24
n = 1, R = 2-(*N*-Methyl)pyrrolyl	75 (> 95 : 5)	11
n = 1, R = 3-Indolyl	74 (> 95 : 5)	8
n = 2, R = Ph	72 (> 95 : 5)	20
n = 2, R = 2-Naphthyl	78 (> 95 : 5)	18
n = 2, R = 2-Thienyl	78 (> 95 : 5)	8
n = 2, R = 2-Furyl	83 (> 95 : 5)	8
n = 2, R = 2-(*N*-Methyl)pyrrolyl	82 (> 95 : 5)	12
n = 2, R = 3-Indolyl	72 (> 95 : 5)	17

[a] As product ratios were found to vary with surface to volume ratio of the reaction mixture, all transformations were conducted on 0.46 mmol scale in 13 × 100 mm test tubes at 80 °C. Reactions performed at 25 °C gave similar results but with diminished reproducibility

Table 5 Rh-catalyzed hydrogenative aldol cyclization of 1,3-diketone-enones[a]

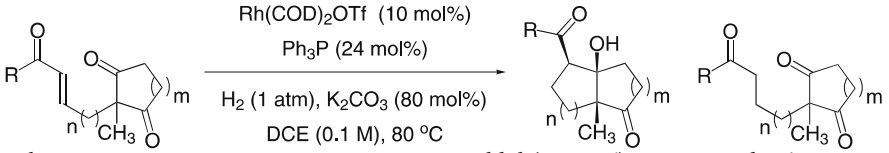

Substrate	% Aldol (*syn*:*anti*)	1,4%-Reduction
n = 1, m = 1, R = Ph	84 (> 95 : 5)	> 1
n = 1, m = 1, R = CH_3	88 (> 95 : 5)	> 1
n = 1, m = 2, R = Ph	86 (> 95 : 5)	> 1
n = 2, m = 1, R = Ph	81 (> 95 : 5)	> 1
n = 2, m = 1, R = CH_3	73 (> 95 : 5)	> 1
n = 2, m = 2, R = Ph	65 (> 95 : 5)	15

[a] As product ratios were found to vary with surface to volume ratio of the reaction mixture, all transformations were conducted on 0.46 mmol scale in 13 × 100 mm test tubes at 80 °C. Reactions performed at 25 °C gave similar results but with diminished reproducibility

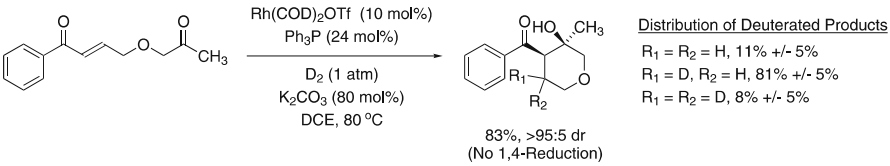

Scheme 3 Rh-catalyzed hydrogenative aldol cyclization of a keto-enone under an atmosphere of deuterium

Intermolecular hydrogenative aldol coupling using triphenylphosphine ligated rhodium catalysts provides aldol products in good yield, but with poor levels of diastereoselection [65]. A progressive increase in diastereoselectivity is achieved upon sequential replacement of the ligand phenyl residues for 2-furyl residues (Ph_3P, $FurPh_2P$, Fur_2PhP, Fur_3P) [69]. Indeed, for reactions employing tri-2-furylphosphine [91–93] ligated rhodium catalysts, the observed levels of *syn*-diastereoselectivity for reactions performed at ambient temperature exceed those observed in corresponding aldol additions of lithium enolates conducted at – 78 °C [69]. These high levels of *syn*-diastereoselectivity suggest kinetic control at the stages of both enolization and aldol addition. The *anti*-aldol diastereomers are thermodynamically preferred. Hence, high *syn*-diastereoselectivity suggests kinetic control at the stages of both enolization and aldol addition. For detailed descriptions, see literature cited in [86].

Rhodium hydride addition to the enone *s-cis* conformer through a six-centered transition structure accounts for stereospecific *Z*(*O*)-enolate forma-

tion. Enones constrained in the *s-trans* configuration, such as cyclohexenone, do not participate in hydrogen-mediated reductive aldol coupling. Addition of the resulting *Z*(*O*)-enolate to the aldehyde through a Zimmerman–Traxler type transition structure stereospecifically delivers the *syn*-aldol stereoisomer [86]. To preserve high levels of *syn*-diastereoselectivity, both enolization and aldol addition should be irreversible or exhibit high levels of kinetic stereospecificity (Table 6).

Under optimum conditions employing the tri-2-furylphosphine ligated rhodium catalyst, commercially available methyl and ethyl vinyl ketone (MVK and EVK) [69] and divinyl ketones such as crotyl vinyl ketone (CVK) [70] engage in highly diastereoselective hydrogenative aldol coupling to a diverse collection of aldehydes. The hydrogenative coupling conditions are highly chemoselective, as underscored by the fact that functional groups generally considered to be "hydrogen-labile" (alkynes, alkenes, benzylic ethers, and nitroarenes) remain intact. Because hydrogen-mediated aldol coupling occurs under essentially neutral conditions in a low dielectric media at ambient temperature, substrate hydrogen bonds may be exploited as stereochemical control elements. For example, hydrogenation of MVK and EVK in the presence of *N*-Boc-α-aminoaldehydes enables formation of aldol stereotriads that embody high levels of *syn*-aldol diastereoselectivity accompanied by high levels of *anti*-Felkin-Anh control [71]. The collective data are consistent with a catalytic mechanism involving addition of the *Z*(*O*)-

Table 6 Highly *syn*-diastereoselective intermolecular Rh-catalyzed hydrogenative aldol coupling of vinyl ketones through the tri-2-furylphosphine effect[a]

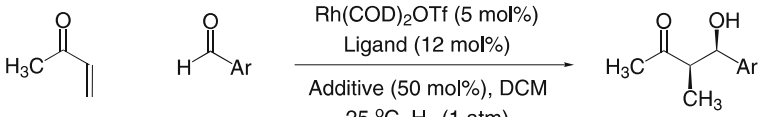

MVK 150 mol% | Ar = *p*-NO_2Ph 100 mol%

Ligand	Additive	DCM	Yield %	Dr
PPh_3	Li_2CO_3	(0.1 M)	31	3 : 1
$FurPh_2P$	Li_2CO_3	(0.1 M)	24	6 : 1
Fur_2PhP	Li_2CO_3	(0.1 M)	52	15 : 1
Fur_3P	Li_2CO_3	(0.1 M)	74	19 : 1
$AsPh_3$	Li_2CO_3	(0.1 M)	17	7 : 1
Fur_3P	–	(0.1 M)	63	19 : 1
Fur_3P	Li_2CO_3	(0.3 M)	88	16 : 1
Fur_3P	**Li_2CO_3**	**(0.1 M)**	**91**	**16 : 1**

[a] As product ratios were found to vary with surface to volume ratio of the reaction mixture, all transformations were conducted on 0.66 mmol scale in 13 × 100 mm test tubes

rhodium enolate to the sterically less-encumbered aldehyde π-face of an intramolecularly hydrogen-bonded chelate. Deletion of the intramolecular hydrogen-bond, as in the case of *N*-methyl-*N*-Boc-L-leucinal, inverts stereoselectivity to furnish the Felkin–Anh product. Notably, optical integrity of the stereochemically labile α-aminoaldehydes is preserved under the conditions of hydrogen-mediated aldol coupling, as revealed by HPLC analysis (Scheme 4).

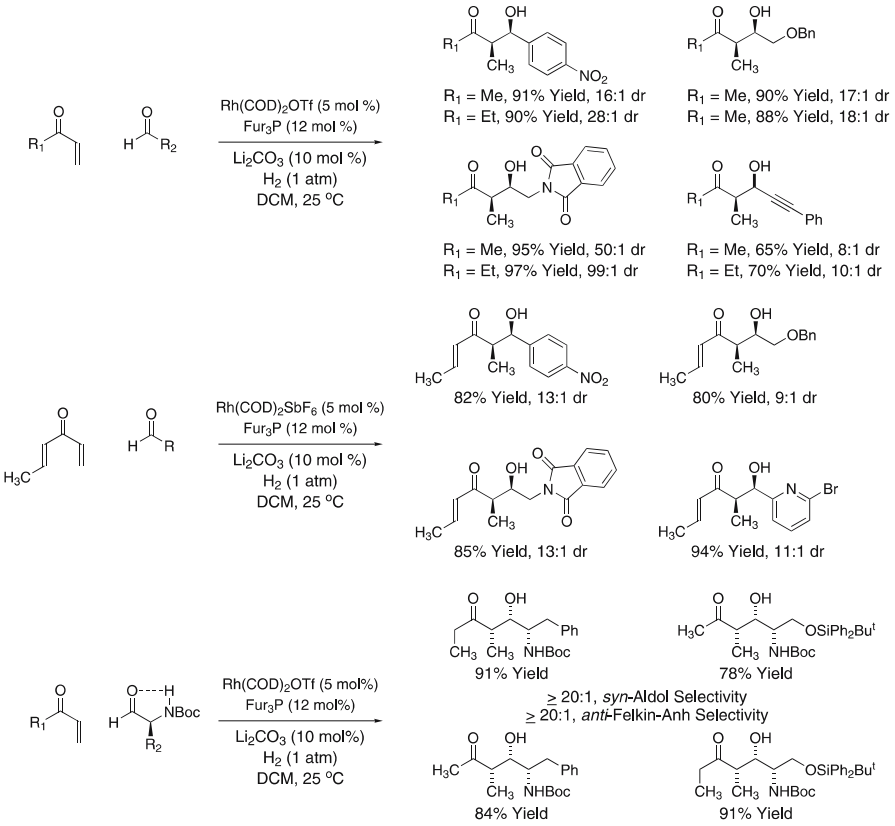

Scheme 4 *syn*-Diastereoselective intermolecular hydrogen-mediated aldol coupling employing cationic Rh catalysts ligated by tri-2-furylphosphine

Diastereoselective reductive coupling of MVK and *p*-nitrobenzaldehyde performed under an atmosphere of elemental deuterium provides an aldol adduct incorporating a single deuterium atom at the former enone β-position [69]. Deuterium incorporation at the α-carbon is not observed, excluding Morita–Baylis–Hillman pathways en route to product. Incorporation of a single deuterium atom suggests irreversible enone hydrometallation (Scheme 5).

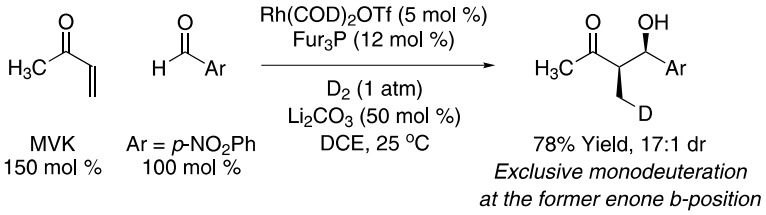

Scheme 5 Intermolecular Rh-catalyzed hydrogenative aldol coupling under an atmosphere of deuterium

While much progress in the area of hydrogen-mediated reductive aldol coupling has been made, many challenges remain. For example, an enantioselective variant of the hydrogen-mediated aldol coupling would require the design of a chirally modified monophosphine bearing 2-furyl residues. An asymmetric hydrogen-mediated aldol coupling would offer a regiochemical complement to corresponding "direct" asymmetric aldol additions. Direct aldol couplings of 2-butanone catalyzed by L-proline furnish linear adducts [94, 95]. Similarly, direct aldol couplings of 2-butanone promoted by the heterobimetallic catalyst $LaLi_3$-tris(binaphthoxide) (LLB) provide linear aldol products [96]. Under the conditions of hydrogenative coupling, the enone moiety of MVK may be exploited a regiochemical control element, directing formation of the branched aldol addition product desired for polypropionate synthesis (Scheme 6) [69].

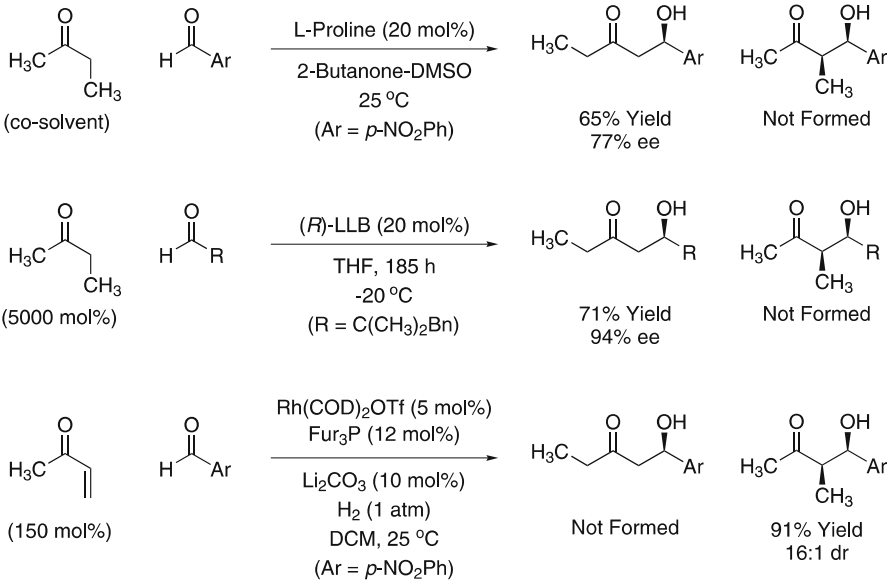

Scheme 6 Complementary regioselectivities in direct aldol couplings of 2-butanone and corresponding hydrogen-mediated reductive aldol couplings of MVK

Reductive Mannich couplings of α,β-unsaturated carbonyl compounds mediated by silane [97, 98] and the Hantzsch ester [99] support the feasibility of corresponding hydrogen-mediated transformations. In the event, hydrogenation of MVK in the presence of *N*-sulfonylimines using a tri-2-furylphosphine ligated rhodium catalyst provides the desired Mannich addition products with good levels of *syn*-diastereoselectivity (Garner and Krische, unpublished results) (Scheme 7). As product ratios were found to vary with surface-to-volume ratio of the reaction mixture, this transformation was conducted on 0.46 mmol scale in a 13 × 100 mm test tube.

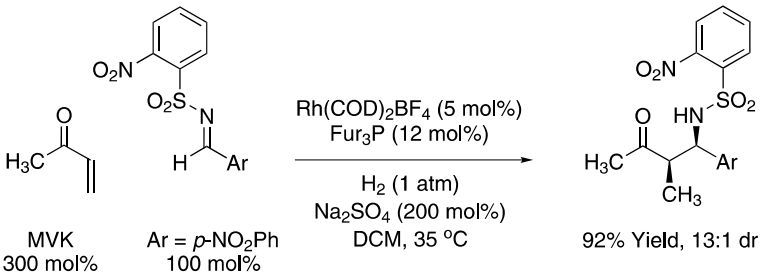

Scheme 7 *syn*-Diastereoselective intermolecular hydrogen-mediated Mannich coupling employing cationic Rh catalysts ligated by tri-2-furylphosphine

2.2 Alkyne–C=X (X=O, NR) Coupling (Reductive Carbonyl-Ene Additions)

The feasibility of hydrogenative aldol coupling prompted efforts toward the discovery of related C – C bond forming hydrogenations. A broad assay was performed in which various π-unsaturated compounds were hydrogenated in the presence of diverse carbonyl electrophiles. It was found that hydrogenation of conjugated alkenes and alkynes in the presence of phenyl glyoxal, a highly reactive vicinal dicarbonyl compound, gives rise to products of formal reductive carbonyl–ene-type coupling [100, 101]. As for the hydrogenative aldol couplings, cationic rhodium precatalysts are required. However, basic additives do not enhance the efficiency of C – C coupling. Rather, acidic additives improve rate and conversion for certain substrate combinations (vide supra) (Scheme 8).

Based on these preliminary findings, related couplings to pyruvates and iminoacetates were explored as a means of accessing α-hydroxy acids and α-amino acids, respectively. It was found that hydrogenation of 1,3-enynes in the presence of pyruvates using chirally modified cationic rhodium catalysts delivers optically enriched α-hydroxy esters [102]. However, chemical yields were found to improve upon aging of the solvent 1,2-dichloroethane (DCE), which led to the hypothesis that adventitious HCl may promote re-

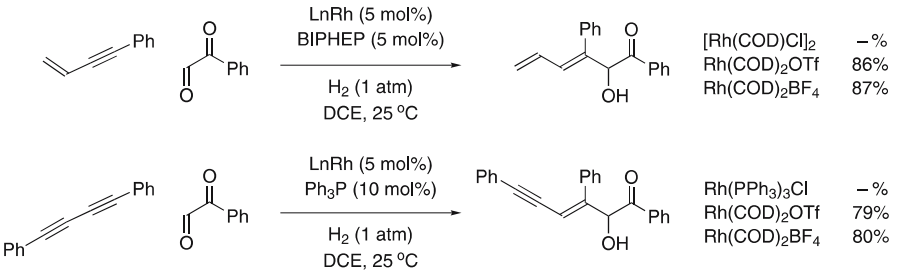

Scheme 8 Selected results from a broad assay for hydrogen-mediated C – C bond formations

ductive coupling. Using freshly distilled DCE, an assay of Brønsted acid additives reveals that reactions performed in the presence of substoichiometric quantities of triphenylacetic acid (1 mol %) exhibit enhanced rate and conversion. Through the use of a Brønsted acid co-catalyst, highly enantioselective hydrogenative couplings of conjugated alkynes to pyruvates [102] and glyoxalates [103](Hong and Krische, unpublished results) are achieved. Brønsted acid co-catalysts also facilitate couplings to heterocyclic aromatic aldehydes and ketones that are isoelectronic with respect to the vicinal dicarbonyl motif, thus providing access to optically enriched heteroaryl-substituted secondary and tertiary alcohols [104]. Finally, hydrogenation of 1,3-enynes in the presence of optically enriched ethyl (*N*-sulfinyl)iminoacetates furnishes novel nonproteogenic amino acid esters (Scheme 9) [105].

The fact that the reductive aldol and alkyne–vicinal dicarbonyl couplings both require cationic rhodium precatalysts belies substantial differences in mechanism. Rather than a hydrometallative mechanism, the collective data suggest that hydrogenative additions of alkynes to carbonyl compounds proceed via oxidative coupling to furnish cationic oxarhodacyclopentenes, which then hydrogenolytically cleave via σ-bond metathesis to deliver product and regenerate the catalyst (Scheme 2). To gain insight into the role of the Brønsted acid co-catalyst, the reductive coupling of a 1,3-enyne to 2-pyridinecarboxaldehyde was performed using an achiral rhodium catalyst in the presence of a chiral Brønsted acid co-catalyst derived from BINOL [106–108]. The coupling product was produced in highly optically enriched form (82% ee) [104], strongly suggesting that C – C coupling is accelerated by the LUMO lowering effect of substrate protonation and/or hydrogen bonding and that the Brønsted acid co-catalyst is associated with 2-pyridinecarboxaldehyde during the stereogenic C – C bond forming event (Scheme 10).

Chiral Brønsted acid co-catalysts do not promote formation of optically enriched products in analogous couplings to pyruvates, although increased rate and conversion in response to the Brønsted acid co-catalyst is unmistakably apparent. For pyruvates, protonation likely occurs subsequent to the C – C

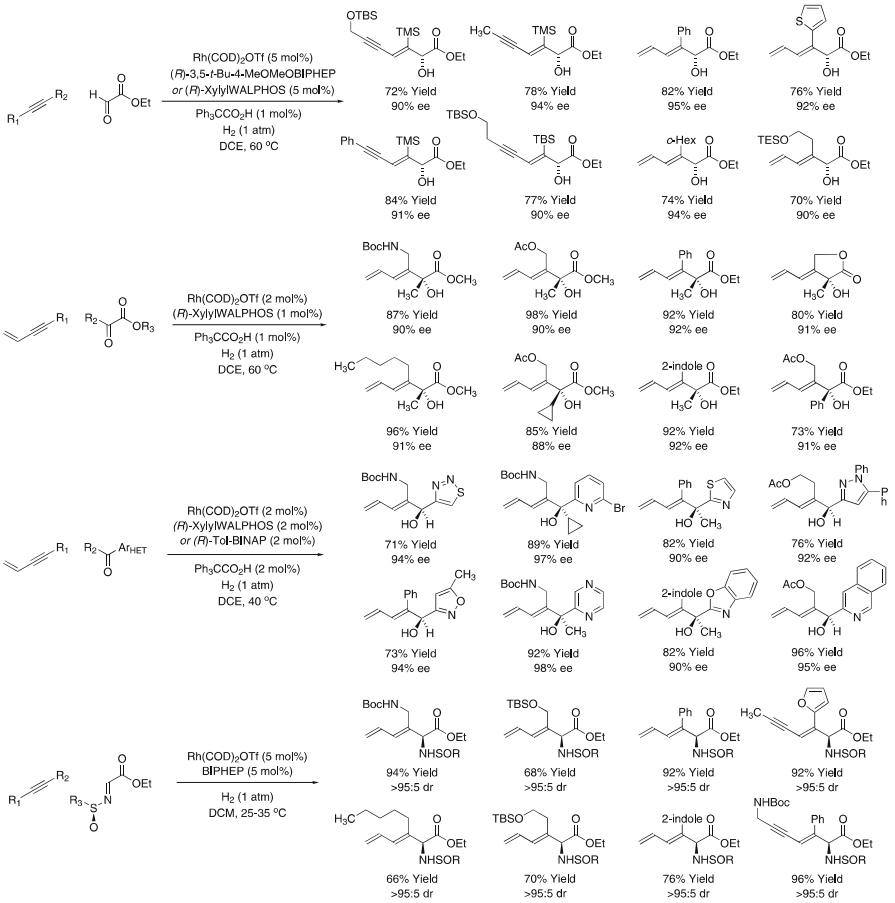

Scheme 9 Asymmetric hydrogen-mediated coupling of conjugated alkynes to carbonyl compounds and imines

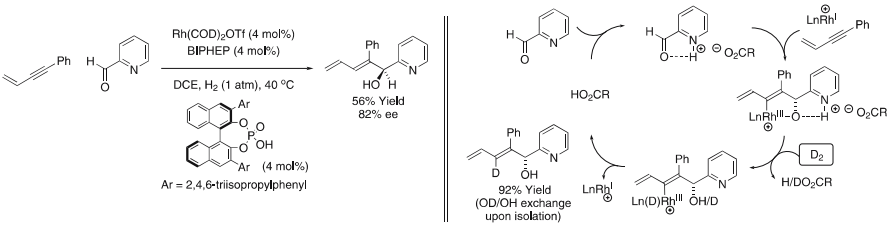

Scheme 10 Plausible catalytic mechanism for alkyne–carbonyl coupling as supported by the effect of chiral Brønsted acid catalyst and deuterium-labeling

coupling event, effecting cleavage of the intermediate oxarhodacyclopentene. Indeed, computational studies suggest that four-centered transition structures for hydrogenolysis of Rh – O bonds are higher in energy than those

occurring by way of six-centered transition structures involving rhodium carboxylates [109]. Protonolysis of the oxarhodacyclopentene, which itself may occur through a six-centered transition structure (**B**, Scheme 11), circumvents direct hydrogenolysis of the putative oxametallacyclic intermediate via σ-bond metathesis through a four-centered transition structure (**A**). Hydrogenolysis of the resulting rhodium carboxylate through the six-centered transition structure (**C**) completes the "co-catalytic cycle". ESI-mass spectrometric analyses of reactions performed in the presence and absence of the Brønsted acid co-catalyst reveal that the most abundant ions, as assigned on the basis of their m/z values, match the molecular weights of the purported oxarhodacyclopentadienes for both glyoxalate and pyruvate couplings. These data are consistent with the notion that the oxarhodacyclopentadiene is the catalyst resting state and that hydrogenolysis of the oxarhodacyclopentadiene is the slow step in the catalytic mechanism (Scheme 11).

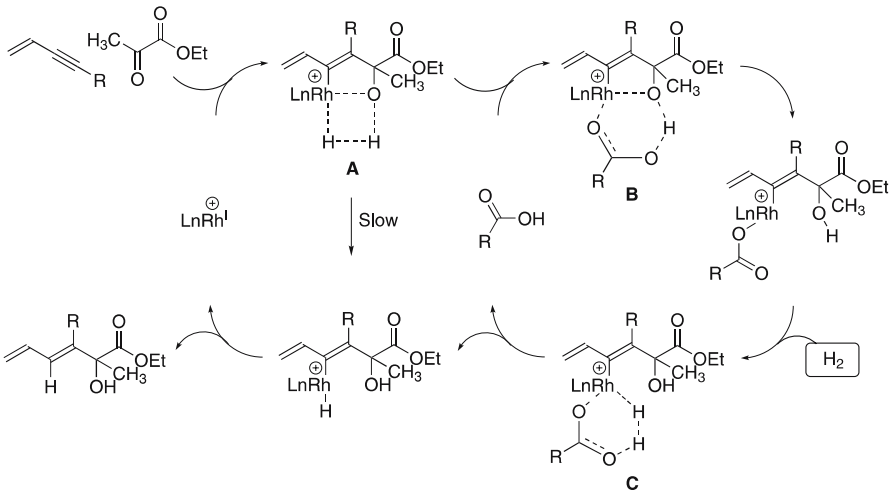

Scheme 11 Plausible role of Brønsted acid co-catalyst as supported by computational studies

Catalytic hydrogenation is eminently suited to large volume applications. Hence, the development of hydrogenative C – C couplings applicable to basic feedstocks and commodity chemicals represents an important research objective. To assess the feasibility of performing hydrogenative couplings of commercially available nonconjugated alkynes to simple unactivated aldehydes, intramolecular reductive couplings of this type were examined [110]. In the event, catalytic hydrogenation of acetylenic aldehydes using chirally modified rhodium catalysts delivers the desired products of reductive carbocyclization with uniformly high levels of optical enrichment. Brønsted acid co-catalysts again were found to enhance reaction rate and conversion (Scheme 12).

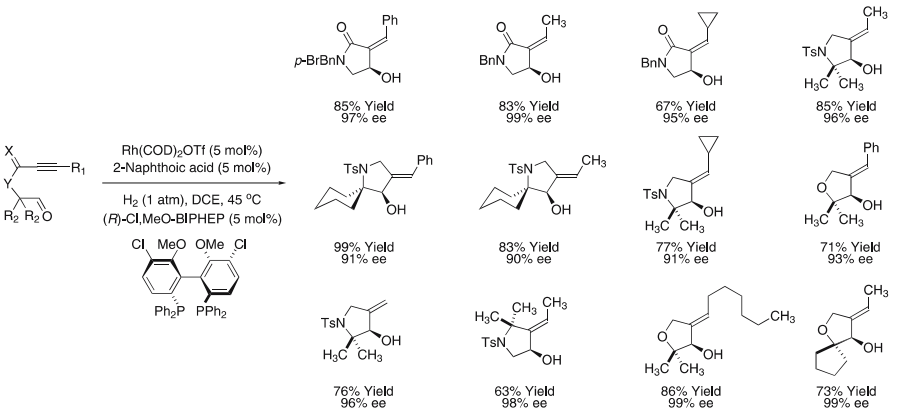

Scheme 12 Reductive cyclization of acetylenic aldehydes via Rh-catalyzed asymmetric hydrogenation

Given the preceding results, intermolecular hydrogenative couplings of commercially available nonconjugated alkynes and simple unactivated aldehydes were explored. It was found that hydrogenation of gaseous acetylene (2 cents/mol, annual US production > 500 metric kilotons) [111] in the presence of diverse aldehydes generates products of *Z*-butadienylation, which appear as single alkene geometrical isomers [112]. More recently, corresponding couplings to aldimines have been achieved (Skucas et al., unpublished results). For both aldehyde and imine couplings, the use of chirally modified rhodium catalysts enables formation of highly optically enriched allylic alcohols and allylic amines, respectively (Scheme 13).

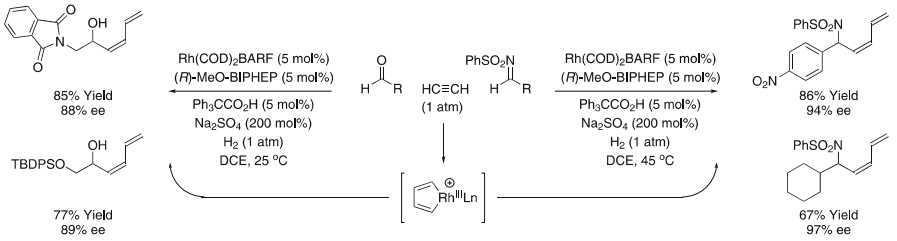

Scheme 13 Enantioselective carbonyl (*Z*)-dienylation via reductive coupling of acetylene to aldehydes and imines mediated by hydrogen

As corroborated by deuterium labeling studies, the catalytic mechanism likely involves oxidative dimerization of acetylene to form a rhodacyclopentadiene [113] followed by carbonyl insertion [114, 115]. Protonolytic cleavage of the resulting oxarhodacycloheptadiene by the Brønsted acid co-catalyst gives rise to a vinyl rhodium carboxylate, which upon hydrogenolysis through a six-centered transition structure and subsequent C – H reductive elimina-

tion delivers the product of *Z*-butadienylation. The veracity of this interpretation is supported by direct ESI-mass spectrometric analyses of reaction mixture aliquots diluted 5000-fold in methanol [116, 117]. All postulated reactive intermediates are observed, withstanding the proposed vinyl rhodium hydride, which should have a very short lifetime due to the generally rapid nature of C – H reductive elimination. Of particular interest is the ion of m/z 677 which matches the molecular weight of the rhodacyclopentadiene, and the ions matching the molecular weights of the oxarhodacycloheptadiene (m/z 900) and the intermediate obtained upon protonolytic cleavage of the oxarhodacycloheptadiene by triphenylacetic acid (m/z 1188). These data provide further support for the key role of Brønsted acid co-catalysts in hydrogenative C – C coupling (Scheme 14).

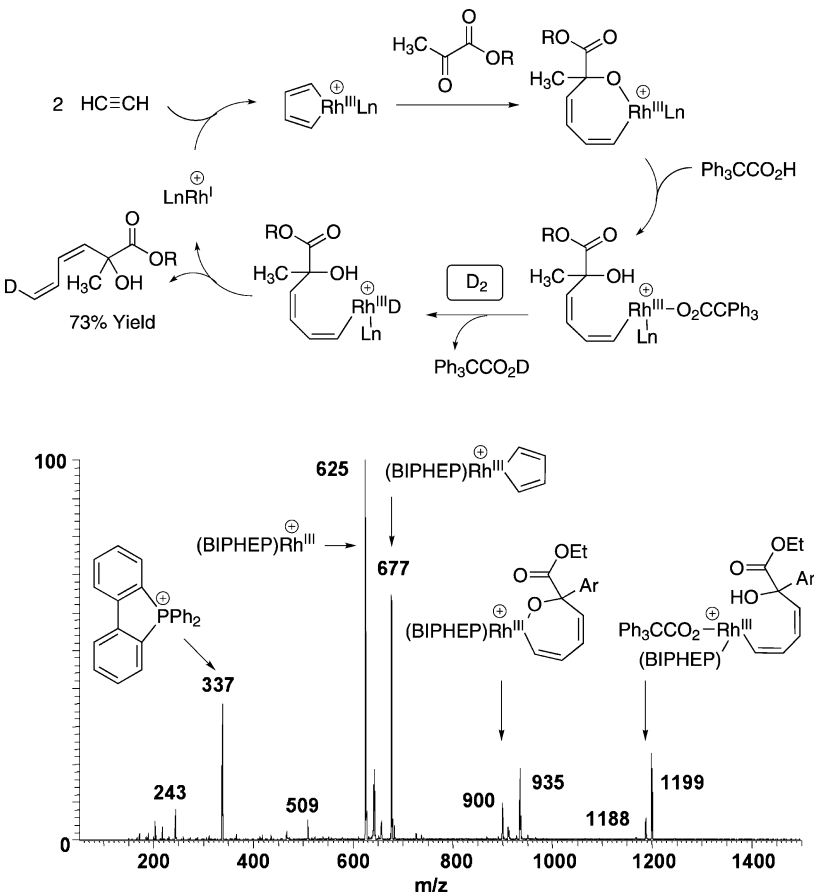

Scheme 14 *Top*: Plausible catalytic cycle as supported by deuterium labeling. *Bottom*: ESI mass spectrum of a reaction mixture aliquot diluted 5000-fold in methanol from the hydrogen-mediated coupling of gaseous acetylene to an α-ketoester (Ar = *p*-NO_2Ph)

Under the conditions of rhodium catalysis, simple nonconjugated alkyl substituted alkynes failed to provide satisfactory yields of carbonyl coupling product. The collective work on hydrogenative alkyne–carbonyl coupling suggests that alkyne–carbonyl oxidative coupling is facilitated by the formation of metal–alkyne complexes that embody a high degree of metallacyclopropene character by virtue of π-backbonding in accordance with the Dewar–Chatt–Duncanson model [118–120]. Iridium(I) complexes are stronger π-donors than rhodium [121–123] due to relativistic effects associated with the lanthanide contraction [124]. Hence, cationic iridium complexes were assayed for their ability to promote the hydrogenative C – C coupling of substituted nonconjugated alkynes to various carbonyl compounds. As anticipated, iridium-catalyzed hydrogenation of commercially available alkyl-substituted alkynes, 3-hexyne and 1-phenylpropyne, results in reductive C – C coupling to afford the corresponding β,γ-unsaturated α-hydroxyesters in excellent yield, with complete control of olefin geometry and, in most cases, excellent regiocontrol (Scheme 15) [125].

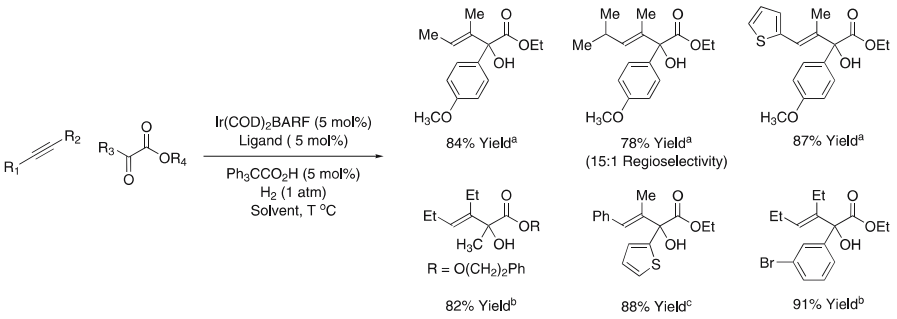

Scheme 15 Iridium-catalyzed hydrogen-mediated coupling of alkyl-substituted alkynes to activated ketones and aldehydes. Conditions: *a* ligand = BIPHEP, solvent = toluene, T = 80 °C; *b* ligand = DPPF, solvent = toluene, T = 60 °C; *c* ligand = BIPHEP, solvent = DCE, T = 80 °C

2.3 Alkene–C=X (X=O, NR) Coupling (Reductive Carbonyl-Ene and Reductive Hydroacylation)

The reductive coupling of α-olefins to simple aliphatic aldehydes to afford branched regioisomers would represent a powerful method for the generation of polypropionate substructures. With this goal in mind, the hydrogenative coupling of various alkenes to carbonyl compounds was explored. Remarkably, it was found that hydrogenation of conjugated alkenes in the presence of phenyl glyoxal provides products of formal reductive carbonyl-ene type coupling. Optimal results were obtained in connection with the use of 1,3-cyclohexadiene as the nucleophilic partner, as formation of regioisomeric

products are avoided and the *s-cis* configuration of 1,3-cyclohexadiene appears to facilitate coupling [126]. Again, cationic rhodium complexes catalyze C – C coupling, whereas neutral rhodium complexes promote conventional hydrogenation. Under optimum conditions, 1,3-cyclohexadiene was found to couple to a range of α-ketoaldehydes (Scheme 16).

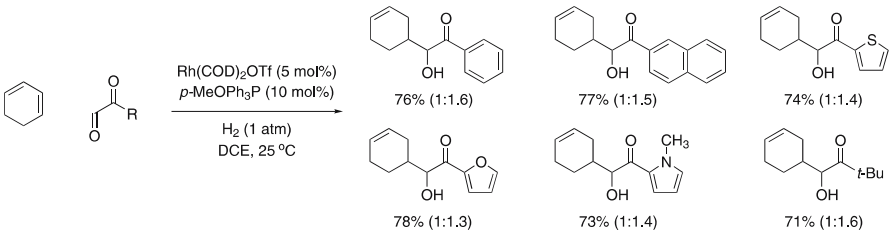

Scheme 16 Hydrogen-mediated coupling of 1,3-cyclohexadiene to α-ketoaldehydes

Reductive coupling of 1,3-cyclohexadiene with 2-naphthyl glyoxal under an atmosphere of deuterium generates coupling products that incorporate precisely two deuterium atoms as an equimolar distribution of 1,2- and 1,4-regioisomers. A relative stereochemical assignment of the deuterated adducts is currently underway. This result may be understood on the basis of a mechanism involving diene–glyoxal oxidative coupling. Specifically, diene–glyoxal oxidative coupling furnishes an oxarhodacycle, which then reacts with deuterium via σ bond metathesis to afford a rhodium alkoxide. Abstraction of an allylic hydrogen provides a rhodium π-allyl complex, which upon C – D reductive elimination delivers the dideuterated products as an equimolar distribution of regioisomers. When the diene–glyoxal coupling is performed under an atmosphere of hydrogen deuteride (HD) as the terminal reductant, the coupling product incorporates a single molecule of deuterium distributed over the same three carbons found when deuterium (D_2) is used as reductant. These data disqualify the initially disclosed hydrometallative mechanism, and strongly support the aforementioned mechanism involving diene–carbonyl oxidative coupling (Scheme 17).

The structural homology of conjugated dienes and styrene suggests the feasibility of analogous styrene–glyoxal couplings. However, under standard conditions using both rhodium- and iridium-based catalysts products of hydrogenative C – C coupling were not observed. It is possible that the LUMO of styrene is too high in energy to enable activation of the vinyl residue in the form of the π-complex, which, as previously discussed, appears to facilitate oxidative coupling to carbonyl partners. An alternate strategy involves activation of the electrophilic partner. For example, oxidative addition of rhodium(I) to carboxylic anhydrides affords acylrhodium(III)carboxylates [127], which may be induced to engage in olefin insertion. Indeed, using a neutral rhodium(I) source with triphenylphosphite as ligand, Miura reports that hydrogenation

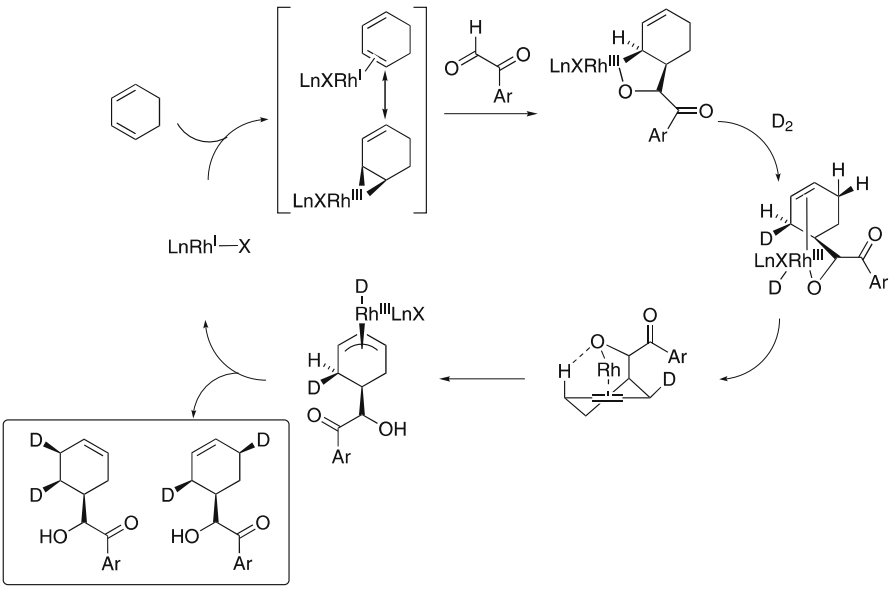

Scheme 17 A plausible catalytic mechanism for the hydrogen-mediated coupling of 1,3-cyclohexadiene to α-ketoaldehydes as corroborated by deuterium labeling

of styrene in the presence of benzoic anhydride furnishes a mixture of linear and branched hydroacylation products in modest yield [33]. Subsequent studies reveal that cationic rhodium catalysts ligated by triphenylarsine catalyze formation of branched hydroacylation products as single regioisomers in good to excellent yield using aromatic and α,β-unsaturated anhydrides as acyl donors [128]. These results are significant in view of the fact that intermolecular hydroacylation using aldehydes as acyl donors is notoriously inefficient due to competitive aldehyde decarbonylation. Consequently, to suppress aldehyde decarbonylation, aldehydes possessing adjacent sites of coordination are required (salicyladehydes and β-sulfido-aldehydes) or conventional aldehydes may be converted to the corresponding (*N*-2-pyridyl)aldimines, which are then used as acyl donors (Scheme 18) [129–141].

A potential liability associated with such reductive hydroacylations resides in the fact that only one acyl residue of the symmetric anhydride is incorporated into the coupling product. For more precious carboxylic acids, selective acyl transfer from mixed anhydrides is possible. Mixed anhydrides derived from pivalic acid are especially convenient, as they may be isolated chromatographically in most cases. In practice, mixed anhydrides of this type enable completely branch-selective hydroacylation with selective delivery of the aromatic and α,β-unsaturated acyl donors (Scheme 19).

In terms of scope, activated alkenes beyond vinyl arenes, such as norbornene, couple effectively to aromatic and α,β-unsaturated anhydrides, in-

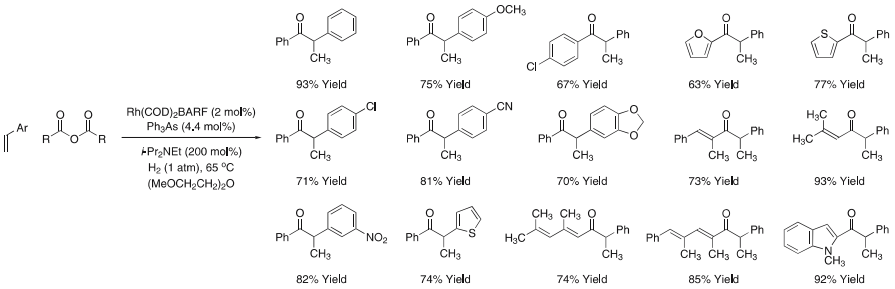

Scheme 18 Branch-selective hydroacylation via hydrogen-mediated coupling of vinyl arenes to carboxylic anhydrides

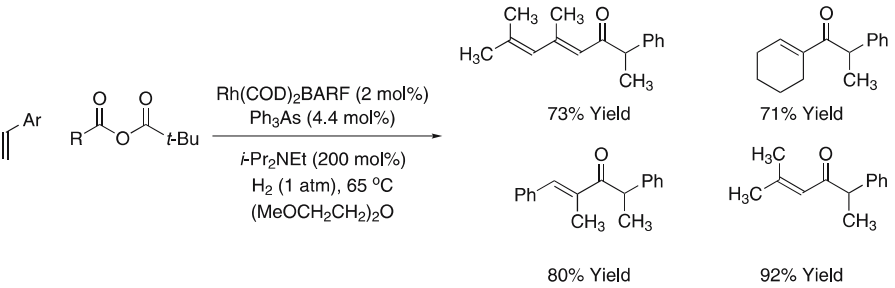

Scheme 19 Selective acyl transfer in reductive hydroacylations involving mixed carboxylic anhydrides derived from pivalic acid

cluding mixed anhydrides derived from pivalic acid (Scheme 20). Of greater interest, hydrogenation of ethylene in the presence of carboxylic anhydrides delivers the corresponding ethyl ketones. For example, simply using a balloon containing roughly equal volumes of hydrogen and ethylene gas, the indicated 2-carboxyindole anhydride (chosen due to low volatility of the product) is converted to the corresponding ethyl ketone in an unoptimized 44% isolated yield (Scheme 21). Several challenges remain. Terminal alkenes such

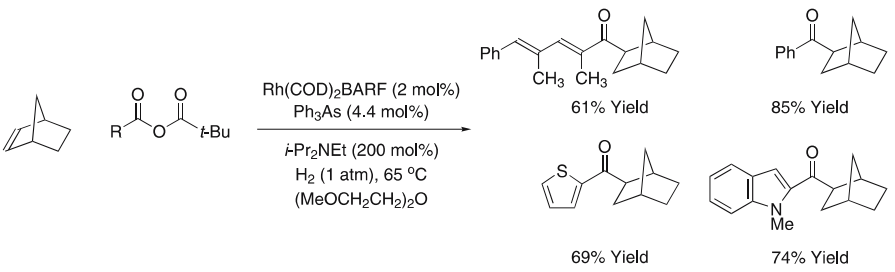

Scheme 20 Reductive hydroacylation of norbornene employing mixed carboxylic anhydrides derived from pivalic acid

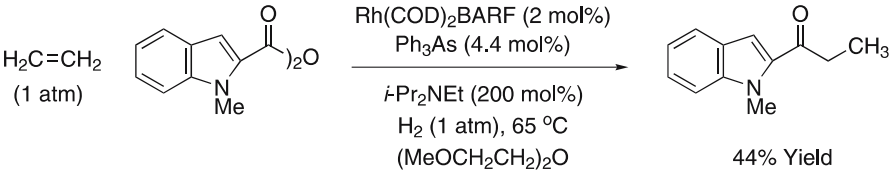

Scheme 21 Hydrogenative coupling of ethylene to a carboxylic anhydride to form an ethyl ketone

as 4-phenyl-1-butene couple to benzoic anhydride in only 34% yield with a 1 : 2.5 ratio of branched to linear regioisomers, respectively, under optimum conditions employing cationic rhodium catalysts ligated by triphenylarsine. Additionally, aliphatic ahydrides such as acetic anhydride couple to styrene in only 27% yield with a 9 : 1 ratio of branched to linear regioisomers.

In terms of mechanism, the results of isotopic labeling suggest two possible catalytic cycles. In catalytic mechanism **A** (Scheme 22) [33], heterolytic hydrogen activation with subsequent hydrometallation of styrene delivers an organorhodium intermediate that engages in formal acyl substitution to provide the hydroacylation product. In mechanism **B** [128], anhydride oxidative addition is followed by insertion of styrene and hydrogenolysis of the resulting alkyl-rhodium intermediate. In the couplings mediated by deuterium, incorporation of deuterium takes place mainly at the β-position. However, the degree of deuterium incorporation is base-dependant. Using *i*-Pr_2NEt or Li_2CO_3 as base, 0.4 and 0.8 deuterium atoms are incorporated, respectively, suggesting that incomplete deuterium incorporation may arise via dehydro-

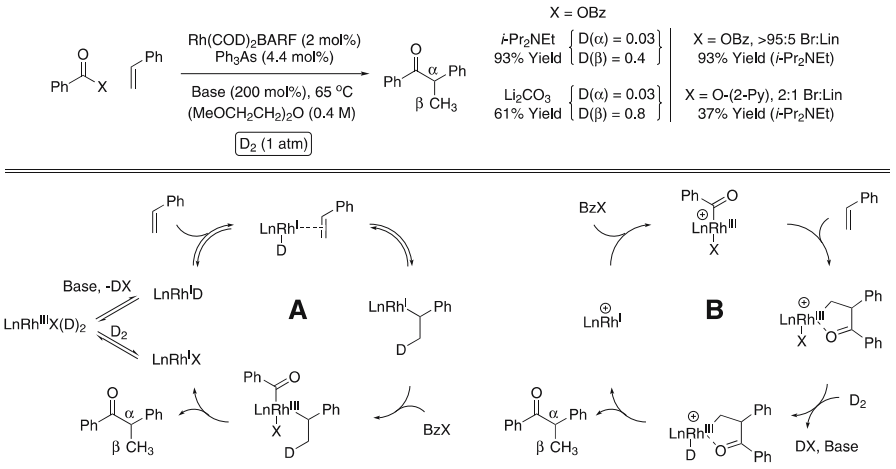

Scheme 22 Deconvoluting the catalytic mechanism in the hydrogen-mediated coupling of styrene to carboxylic anhydrides

genation of *i*-Pr_2NEt. Reversible hydrometallation of styrene through mechanism **A** also may account for incomplete deuterium incorporation. However, this should increase the extent of deuterium incorporation at the α-position of the product, which is not observed. Further mechanistic evaluation of this transformation is in underway (Scheme 22).

3 Future Challenges

Over half a century ago, seminal studies by Fischer, Tropsch and Roelen led to the prototypical hydrogen-mediated C – C bond formations. Such processes, which involve coupling to carbon monoxide, continue to rank among the largest volume metal-catalyzed reactions known [6, 7, 11]. Only recently has it been discovered that catalytic hydrogenation may induce reductive C – C bond formation between π-unsaturated reactants and conventional electrophilic partners in the form of carbonyl compounds and imines. These data suggest countless possibilities in terms of the innovative methodologies and diverse applications that will arise in the future. As catalysts for water splitting improve and hydrogen production no longer depends upon the availability of petroleum, a nonrenewable resource, the environmental and economic advantages of hydrogen-mediated transformations will be even greater.

References

1. Krische MJ (2005) Tetrahedron 61:6169
2. Hoffman R (1998) Am Sci 86:326
3. Williams WD (1999) Bull Hist Chem 24:66
4. Nobel Foundation (1966) Nobel lectures, chemistry, 1901–1921. Elsevier, Amsterdam
5. Smil V (2004) Enriching the earth: Fritz Haber, Carl Bosch, and the transformation of world food production. MIT Press, Cambridge, MA
6. Fischer F, Tropsch H (1923) Brennstoff Chem 4:276
7. Fischer F, Tropsch H (1923) Chem Ber 56B:2428
8. Storch HH, Anderson RB, Hofer LJE, Hawk CO, Anderson HC, Golumbic N (1948) Synthetic liquid fuels from hydrogenation of carbon monoxide, Part 1: review of literature. Technical paper 709. United States Department of the Interior, Washington, DC
9. United States Department of Energy (http://www.fossil.energy.gov/aboutus/history/syntheticfuels_history.html), last visited: 3 Mar 2007
10. Jacoby M (2006) C&EN News 84:57
11. Roelen O (1938) DE Patent 849 548
12. Frohning CD, Kohlpaintner CW (1996) In: Cornils B, Herrmann WA (eds) Applied homogeneous catalysis with organometallic compounds, vol 1. VCH, Weinheim, p 29
13. van Leeuwen PWNM (2004) Homogeneous catalysis, understanding the art. Kluwer, Dordrecht

14. Sabatier P, Senderens JB (1897) CR Hebd Seances Acad Sci 124:1358
15. Sabatier P, Senderens JB (1899) CR Hebd Seances Acad Sci 128:1173
16. Sabatier P, Senderens JB (1901) CR Hebd Seances Acad Sci 132:210
17. Lattes A (2000) CR Acad Sci Ser IIC: Chemie 3:705
18. Calvin M (1938) Trans Far Soc 34:1181
19. Calvin M (1939) J Am Chem Soc 61:2230
20. Halpern J, Harrod JF, James BR (1961) J Am Chem Soc 83:753
21. Halpern J, Harrod JF, James BR (1966) J Am Chem Soc 88:5150
22. Gillard RD, Wilkinson G, Osborn JA, Stockwell PB (1964) Proc Chem Soc, p 284
23. Jardine FH, Osborn JA, Wilkinson G, Young JF (1965) Chem Ind, p 560
24. Young JF, Osborn JA, Jardine FH, Wilkinson G (1965) Chem Commun, p 131
25. Knowles WS, Sabacky MJ (1968) Chem Commun, p 1445
26. Horner L, Siegel H, Büthe H (1968) Angew Chem Int Ed 7:942
27. Dang TP, Kagan HB (1971) Chem Commun, p 481
28. Miyashita A, Yasuda A, Takaya H, Toriumi K, Ito T, Souchi T, Noyori R (1980) J Am Chem Soc 102:7932
29. Thommen M (2005) Spec Chem Mag 25:26
30. Thayer AM (2005) C&EN News 83:40
31. Jakel C, Paciello R (2006) Chem Rev 106:2912
32. Molander GA, Hoberg JO (1992) J Am Chem Soc 114:3123
33. Kokubo K, Miura M, Nomura M (1995) Organometallics 14:4521
34. Moyes RB, Walker DW, Wells PB, Whan DA, Irvine EA (1992) Special Pub Royal Soc Chem 114:207
35. Bianchini C, Meli A, Peruzzini M, Vizza F, Zanobini F, Frediani P (1989) Organometallics 8:2080
36. Tolman CA, Meakin PZ, Lindner DL, Jesson JP (1974) J Am Chem Soc 96:2762
37. Halpern J, Wong CS (1973) Chem Commun, p 629
38. Halpern J, Okamoto T, Zakhariev A (1976) J Mol Catal 2:65
39. Landis CR, Halpern J (1987) J Am Chem Soc 109:1746
40. Chan ASC, Halpern J (1980) J Am Chem Soc 102:838
41. Halpern J, Riley DP, Chan ASC, Pluth JJ (1977) J Am Chem Soc 99:8055
42. Halpern J (1982) Science 217:401
43. Halpern J (1985) Asymm Synth 5:41
44. Landis CR, Brauch TW (1998) Inorg Chim Acta 270:285
45. Gridnev ID, Imamoto T (2004) Acc Chem Res 37:633
46. Schrock RR, Osborn JA (1976) J Am Chem Soc 98:2134
47. Schrock RR, Osborn JA (1976) J Am Chem Soc 98:2143
48. Schrock RR, Osborn JA (1976) J Am Chem Soc 98:4450
49. Brothers PJ (1981) Prog Inorg Chem 28:1
50. Jeske G, Lauke H, Mauermann H, Schumann H, Marks TJ (1985) J Am Chem Soc 107:8111
51. Norton JR (1992) In: Dedieu A (ed) Transition metal hydrides, chap 9. Wiley-VCH, New York
52. Jang HY, Krische MJ (2004) Acc Chem Res 37:653
53. Ngai MY, Krische MJ (2006) Chim Oggi/Chem Today 24:12
54. Ngai MY, Kong JR, Krische MJ (2007) J Org Chem 72:1063
55. Revis A, Hilty TK (1987) Tetrahedron Lett 28:4809
56. Matsuda I, Takahashi K, Sato S (1990) Tetrahedron Lett 31:5331
57. Taylor SJ, Morken JP (1999) J Am Chem Soc 121:12202
58. Taylor SJ, Duffey MO, Morken JP (2000) J Am Chem Soc 122:4528

59. Emiabata-Smith D, McKillop A, Mills C, Motherwell WB, Whitehead AJ (2001) Synlett, p 1302
60. Freiría M, Whitehead AJ, Tocher DA, Motherwell WB (2004) Tetrahedron 60:2673
61. Fuller NO, Morken JP (2005) Synlett, p 1459
62. Nishiyama H, Shiomi T, Tsuchiya Y, Matsuda I (2005) J Am Chem Soc 127:6972
63. Willis MC, Woodward RL (2005) J Am Chem Soc 127:18012
64. Ito JI, Shiomi T, Nishiyama H (2006) Adv Synth Catal 348:1235
65. Jang HY, Huddleston RR, Krische MJ (2002) J Am Chem Soc 124:15156
66. Huddleston RR, Krische MJ (2003) Org Lett 5:1143
67. Koech PK, Krische MJ (2004) Org Lett 6:691
68. Marriner GA, Garner SA, Jang HY, Krische MJ (2004) J Org Chem 69:1380
69. Jung CK, Garner SA, Krische MJ (2006) Org Lett 8:519
70. Han SB, Krische MJ (2006) Org Lett 8:5657
71. Jung CK, Krische MJ (2006) J Am Chem Soc 128:17051
72. Isayama S, Mukaiyama T (1989) Chem Lett 2005
73. Baik TG, Luis AL, Wang LC, Krische MJ (2001) J Am Chem Soc 123:5112
74. Wang LC, Jang HY, Roh Y, Lynch V, Schultz AJ, Wang X, Krische MJ (2002) J Am Chem Soc 124:9448
75. Lam HW, Joensuu PM, Murray GJ, Fordyce EAF, Prieto O, Luebbers T (2006) Org Lett 8:3729
76. Zhao CX, Duffey MO, Taylor SJ, Morken JP (2001) Org Lett 3:1829
77. Kiyooka SI, Shimizu A, Torii S (1998) Tetrahedron Lett 39:5237
78. Ooi T, Doda K, Sakai D, Maruoka K (1999) Tetrahedron Lett 40:2133
79. Lam HW, Joensuu PMA (2005) Org Lett 7:4225
80. Lam HW, Murray GJ, Firth JD (2005) Org Lett 7:5743
81. Zhao D, Oisaki K, Kanai M, Shibasaki M (2006) Tetrahedron Lett 47:1403
82. Deschamp J, Chuzel O, Hannedouche J, Riant O (2006) Angew Chem Int Ed 45:1292
83. Zhao D, Oisaki K, Kanai M, Shibasaki M (2006) J Am Chem Soc 128:14440
84. Shibata I, Kato H, Ishida T, Yasuda M, Baba A (2004) Angew Chem Int Ed 43:711
85. Miura K, Yamada Y, Tomita M, Hosomi A (2004) Synlett, p 1985
86. Zimmerman HE, Traxler MD (1957) J Am Chem Soc 79:1920
87. Evans DA, Nelson JV, Taber TR (1982) Top Stereochem 13:1
88. Heathcock CH (1982) ACS Symp Ser 185:55
89. Heathcock CH (1984) Asymm Synth 3:111
90. Heathcock CH (1991) In: Heathcock CH (ed) Additions to C – X n-bonds, part 2. Comprehensive organic synthesis, vol 2. Pergamon, New York, p 181
91. Farina V, Krishnan B (1991) J Am Chem Soc 113:9585
92. Farina V (1996) Pure Appl Chem 68:73
93. Andersen NG, Keay BA (2001) Chem Rev 101:997
94. Sakthivel K, Notz W, Bui T, Barbas CF III (2001) J Am Chem Soc 123:5260
95. Tang Z, Yang ZH, Chen XH, Cun LF, Mi AQ, Jiang YZ, Gong LZ (2005) J Am Chem Soc 127:9285
96. Yoshikawa N, Yamada YMA, Das J, Sasai H, Shibasaki M (1999) J Am Chem Soc 121:4168
97. Muraoka T, Kamiya SI, Matsuda I, Itoh K (2002) Chem Commun, p 1284
98. Townes JA, Evans MA, Queffelec J, Taylor SJ, Morken JP (2002) Org Lett 4:2537
99. Zhao GL, Córdova A (2006) Tetrahedron Lett 47:7417
100. Huddleston RR, Jang HY, Krische MJ (2003) J Am Chem Soc 125:11488
101. Jang HY, Huddleston RR, Krische MJ (2004) J Am Chem Soc 126:4664
102. Kong JR, Ngai MY, Krische MJ (2006) J Am Chem Soc 128:718

103. Cho CW, Krische MJ (2006) Org Lett 8:3873
104. Komanduri V, Krische MJ (2006) J Am Chem Soc 128:16448
105. Kong JR, Cho CW, Krische MJ (2005) J Am Chem Soc 127:11269
106. Akiyama T, Itoh J, Yokota K, Fuchibe K (2004) Angew Chem Int Ed 43:1566
107. Uraguchi D, Terada M (2004) J Am Chem Soc 126:5356
108. Hoffmann S, Seayad AM, List B (2005) Angew Chem Int Ed 44:7424
109. Musashi Y, Sakaki S (2002) J Am Chem Soc 124:7588
110. Rhee JU, Krische MJ (2006) J Am Chem Soc 128:10674
111. Kirk-Othmer (ed) (2007) Kirk-Othmer encyclopedia of chemical technology, 5th edn. Wiley, Hoboken
112. Kong JR, Krische MJ (2006) J Am Chem Soc 128:16040
113. Bianchini C, Caulton KG, Chardon C, Eisenstein O, Folting K, Johnson TJ, Meli A, Peruzzini M, Rauscher DJ, Streib WE, Vizza F (1991) J Am Chem Soc 113:5127
114. Krug C, Hartwig JF (2002) J Am Chem Soc 124:1674
115. Fujii T, Koike T, Mori A, Osakada K (2002) Synlett, p 298
116. Plattner D (2001) Int J Mass Spectrom 207:125
117. Chen P (2003) Angew Chem Int Ed 42:2832
118. Dewar MJS (1951) Bull Soc Chim Fr 18:C71
119. Chatt J, Duncanson LA (1953) J Chem Soc 2939
120. Dewar MJS, Ford GP (1979) J Am Chem Soc 101:783
121. Vaska L, Peone J Jr (1971) Chem Commun, p 418
122. Haynes A, McNish J, Pearson JM (1998) J Organomet Chem 551:339
123. Grotjahn DB, Collins LSB, Wolpert M, Bikzhanova GA, Lo HC, Combs D, Hubbard JL (2001) J Am Chem Soc 123:8260
124. Li J, Schreckenbach G, Ziegler T (1995) J Am Chem Soc 117:486
125. Ngai MY, Barchuk A, Krische MJ (2007) J Am Chem Soc 129:280
126. Jang HY, Huddleston RR, Krische MJ (2003) Angew Chem Int Ed 42:4074
127. Miller JA, Nelson JA (1991) Organometallics 10:2958
128. Hong YT, Barchuk A, Krische MJ (2006) Angew Chem Int Ed 45:6885
129. Vora KP, Lochow CF, Miller RG (1980) J Organomet Chem 192:257
130. Rode E, Davis ME, Hanson BE (1985) Chem Commun, p 716
131. Marder TB, Roe DC, Milstein D (1988) Organometallics 7:1451
132. Jun CH, Lee H, Hong JB (1997) J Org Chem 62:1200
133. Jun CH, Lee DY, Lee H, Hong JB (2000) Angew Chem Int Ed 39:3070
134. Jun CH, Chung JW, Lee DY, Loupy A, Chatti S (2001) Tetrahedron Lett 42:4803
135. Willis MC, Sapmaz S (2001) Chem Commun, p 2558
136. Tanaka M, Imai M, Yamamoto Y, Tanaka K, Shimowatari M, Nagumo S, Kawahara N, Suemune H (2003) Org Lett 5:1365
137. Imai M, Tanaka M, Tanaka K, Yamamoto Y, Imai-Ogata N, Shimowatari M, Nagumo S, Kawahara N, Suemune H (2004) J Org Chem 69:1144
138. Willis MC, McNally SJ, Beswick PJ (2004) Angew Chem Int Ed 43:340
139. Tanaka K, Tanaka M, Suemune H (2005) Tetrahedron Lett 46:6053
140. Willis MC, Randell-Sly HE, Woodward RL, Currie GS (2005) Org Lett 7:2249
141. Moxham GL, Randell-Sly HE, Brayshaw SK, Woodward RL, Weller AS, Willis MC (2006) Angew Chem Int Ed 45:7618

Top Curr Chem (2007) 279: 105–137
DOI 10.1007/128_2007_126

Published online: 12 June 2007

Reductive Aldol, Michael, and Mannich Reactions

Hisao Nishiyama (✉) · Takushi Shiomi

Graduate School of Engineering, Department of Applied Chemistry, Nagoya University, Chikusa, 464-8603 Nagoya, Japan
hnishi@apchem.nagoya-u.ac.jp

Abstract Transition metal-catalyzed conjugate reductions of α,β-unsaturated carbonyl compounds mediated by hydride sources, such as hydrosilanes or molecular hydrogen, enable in-situ generation of transition metal enolates. These are capable of coupling to aldehydes, ketones, α,β-unsaturated carbonyl compounds, or imines to furnish the corresponding aldol, Michael, or Mannich products, respectively. In these carbon–carbon coupling reactions, the transition metal catalyst and stoichiometric reductant, assisted by various ligands or chiral auxiliaries, may promote high levels of stereo- and enantioselectivity. In this review, the various metal catalysts that promote reductive aldol coupling and related processes are surveyed from the perspective of synthetic organic chemistry, from historical findings to recent developments.

Keywords Conjugate reduction · Enolate · C – C bond formation · Asymmetric catalysis · Reductive aldol · Reductive Mannich

1 Introduction

Carbon–carbon bond formation is the most important and essential subject in synthetic organic chemistry. Among the numerous carbon–carbon

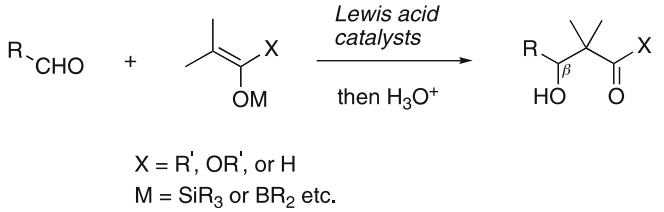

Scheme 1 Mukaiyama-type aldol reaction

bond forming reactions, the Mukaiyama-type aldol reaction, wherein Lewis acids catalyze the coupling of silyl enol ethers or silyl ketene acetals to carbonyl compounds, provides us with a valuable and practical method to access β-hydroxy carbonyl derivatives (Scheme 1) [1–3]. In 1987, Revis and Hilty reported an alternative method for the generation of β-hydroxy esters, which is a direct "one-pot" coupling reaction of α,β-unsaturated esters and carbonyl compounds mediated by Me_3SiH and catalyzed by rhodium chloride [4]. The reaction path can be thought of as follows (Scheme 2):

1. Conjugate reduction by the transition metal-hydride (TM – H) accompanied by transition metal enolate formation
2. C – C bond formation involving the transition metal enolate

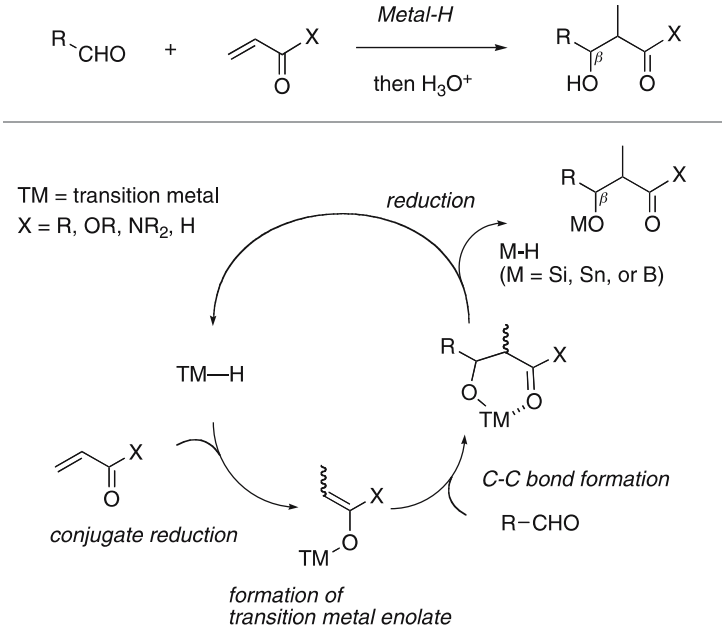

Scheme 2 Transition metal-catalyzed reductive aldol reaction

3. Reductive elimination with release of the aldol product through the action of the hydrogen source M – H (M = Si, B, etc.)

This reaction sequence of conjugate reduction followed by aldol reaction is known as the *reductive aldol reaction*. In certain instances, reductive elimination from the M-TM-enolate species may occur to furnish M-enolate, which itself may participate in the aldol reaction (Scheme 3). This detour may be described as the *background path* or stepwise path in one-pot. Indeed, it has been reported that certain cationic Rh complexes such as [Rh(COD)(DPPB)] (COD = 1,5-cyclooctadiene, DPPB = diphenylphosphinobutane) catalyze the aldol reactions of silyl enol ethers and carbonyl compounds by serving as Lewis acids [5–8].

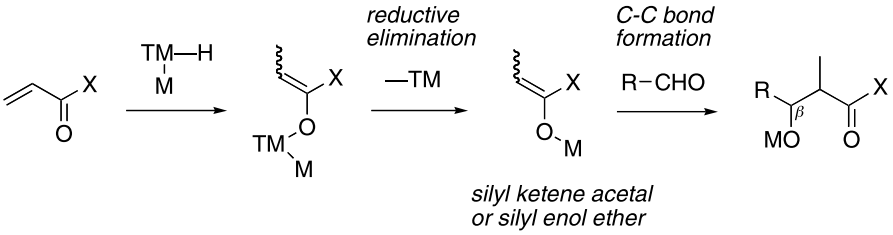

Scheme 3 Background path

After the initial two reports of Rh- and Co-catalyzed reductive aldol couplings, further studies did not appear in the literature until the late 1990s. Beyond 1998, several stereoselective and enantioselective reductive aldol reactions were developed, which are catalyzed by a remarkably diverse range of metal complexes, including those based upon Pd, Cu, Ir, and In. In this chapter, transition metal-catalyzed aldol, Michael, and Mannich reactions that proceed via transition metal hydride-promoted conjugate reduction are reviewed.

2
Reductive Aldol Reactions

2.1
Co, Rh, Ir Catalysts

2.1.1
Hydrosilane-Mediated Reactions and Related Reactions

Revis and Hilty, in 1987, first reported the direct reductive coupling reaction of methyl methacrylate (1.0 mol %) and excess acetone at 25 °C catalyzed by of $RhCl_3H_2O$ (0.09 mol %) and mediated by Me_3SiH (1.3 mol %) to give

aldol product, β-siloxy ester **1**, in 95% yield (Scheme 4) [4]. The coupling proceeded smoothly for cyclohexanone as an acceptor as well as acetaldehyde. They demonstrated that the reaction of silyl ketene acetal **2**, synthesized independently, and acetone in the presence of a catalytic amount of Rh chloride only gave a trace amount of the aldol product. This observation suggests that a background path involving the action of a Rh species as Lewis acid is not operative. Therefore, they described the coupling reaction as a *hydrosilylative condensation*. Methyl vinyl ketone was not capable of coupling to acetone, but instead formed silyl enol ether **3** in 80% yield.

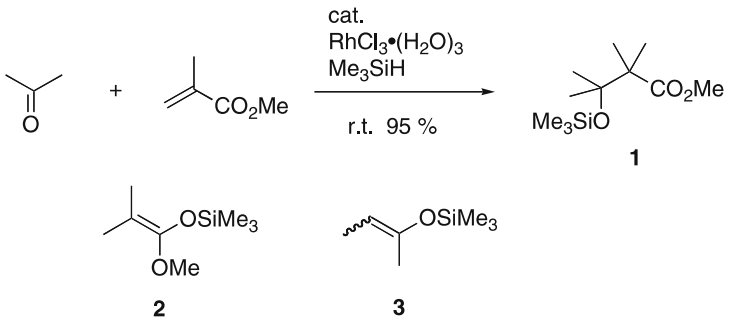

Scheme 4 Revis and Hilty's discovery

In 1989, Isayama and Mukaiyama reported a related Co-catalyzed coupling reaction that employs α,β-unsaturated nitriles, amides, and esters with $PhSiH_3$ as a hydrogen source [9]. Cobalt-bis(diketonato) complex, Co(II)(dpm)$_2$ [dpm = bis(dipivaloylmethanato)] (5 mol %), exhibited high catalytic activity at 20 °C in the coupling of excess acrylonitrile and benzaldehyde to provide β-hydroxy nitrile **4** in 93% yield (*syn* : *anti* = 50 : 50) (Scheme 5). *N,N*-Dimethylacrylamide and methyl cinnamate both reacted

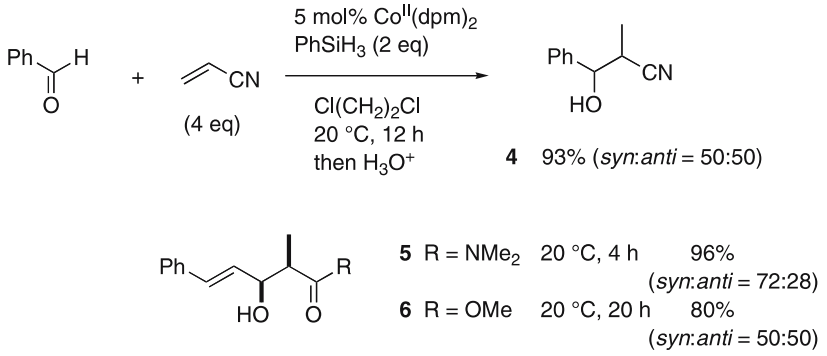

Scheme 5 Co(dpm)$_2$-catalyzed reaction

with cinnamaldehyde to give the corresponding coupling products **5** and **6** in 96% and 80%, respectively (Scheme 5).

Matsuda et al. reported in 1990 the Rh-catalyzed coupling of α,β-unsaturated ketones and aldehydes to form β-siloxy ketone aldols (Scheme 6) [10, 11]. $Rh_4(CO)_{12}$ (0.5 mol %) promoted the coupling of 3-butene-2-one (400 mol %) and benzaldehyde with Et_2MeSiH (200 mol %) in toluene at – 15 °C for 7 h to give β-siloxy ketone **7** in 98% (*syn* : *anti* = 87 : 13). Hexane, toluene, and benzene were the solvents of choice. By employing $MePh_2P$ as ligand, catalytic couplings of substituted enones to enolizable aldehydes such as hexanal were enabled.

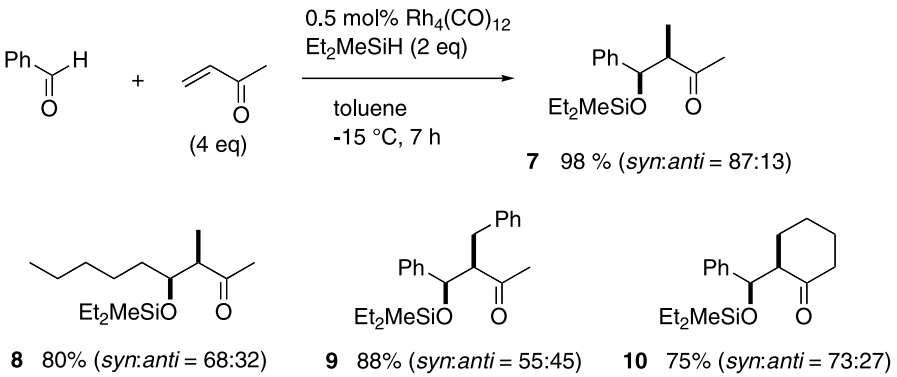

Scheme 6 $Rh_4(CO)_{12}$-catalyzed reaction

In 1999, Morken et al. disclosed an arrayed catalyst evaluation method for the reductive aldol reaction of benzaldehyde and methyl acrylate by examining four complexes, $Co(acac)_2$, $[Pd(allyl)Cl]_2$, $[Ir(COD)Cl]_2$, and $[Rh(COD)Cl]_2$, six hydride sources, and seven chiral ligands [12]. Eventually, the catalytic system $[Rh(COD)Cl]_2$ – DuPhos – Cl_2MeSiH was found to provide diastereoselectivities of up to 23 : 1 (*syn* : *anti*) in the formation of aldol product **11**. Relatively high yields, 69% for **11** and 82% for **12**, were observed (Scheme 7). $[Rh(COD)Cl]_2$-BINAP-catechol borane and $Co(acac)_2$ – MOP – $PhSiH_3$ also proved to be efficient, high yielding catalyst systems. Direct NMR analysis of reactions mixtures revealed the presence of silyl ketene acetal **13**, which is presumably generated by way of the noncatalyzed background path and serves as reactive intermediate in the aldol reaction [13]. When aldehydes were added after the conjugate reduction, the *syn*-aldol products were obtained in high yields up to 98% with diastereoselectivity up to > 60 : 1, as shown for the products **11**, **14**–**16**.

Krische et al. demonstrated intramolecular reaction with $Co(dpm)_2$ (5 mol %) and $PhSiH_3$ (120 mol %) as a hydride donor (Scheme 8) [14–16]. Addition of aldehyde-enone **17** to a solution of the Co catalyst and phenylsilane resulted in the formation of the corresponding aldol cyclization product

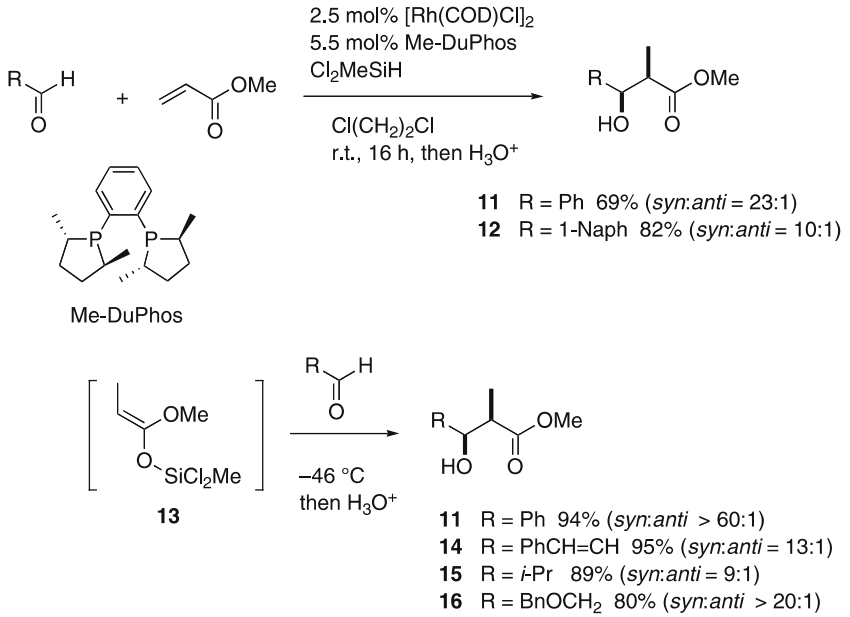

Scheme 7 Rh-catalyzed reaction and arrayed catalyst evaluation

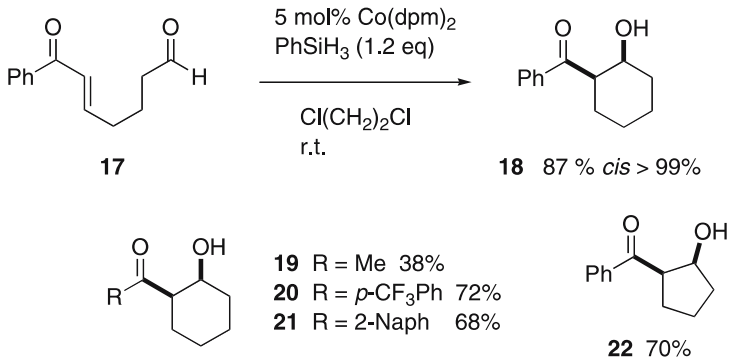

Scheme 8 $Co(dpm)_2$-catalyzed intramolecular reaction

18 in 87% yield with extremely high *cis*-selectivity > 99 : 1. Although diminished yields were obtained using aliphatic enone **19**, five- and six-membered ring formation proceeded smoothly to give the cyclic aldols **20**–**22**.

Motherwell and Whitehead et al. reported a similar intramolecular reductive aldol reaction of aldehyde-enoate derivatives. The cyclization of 6-oxoester **23** was catalyzed by $RhCl(PPh_3)_3$ (1 mol %) with Et_3SiH (210 mol %) as terminal reductant (Scheme 9) [17, 18]. The cyclization proceeded at 50 °C for 18 h to give the aldol product **24** in 81% yield with *cis*-selectivity (*cis* : *trans* =

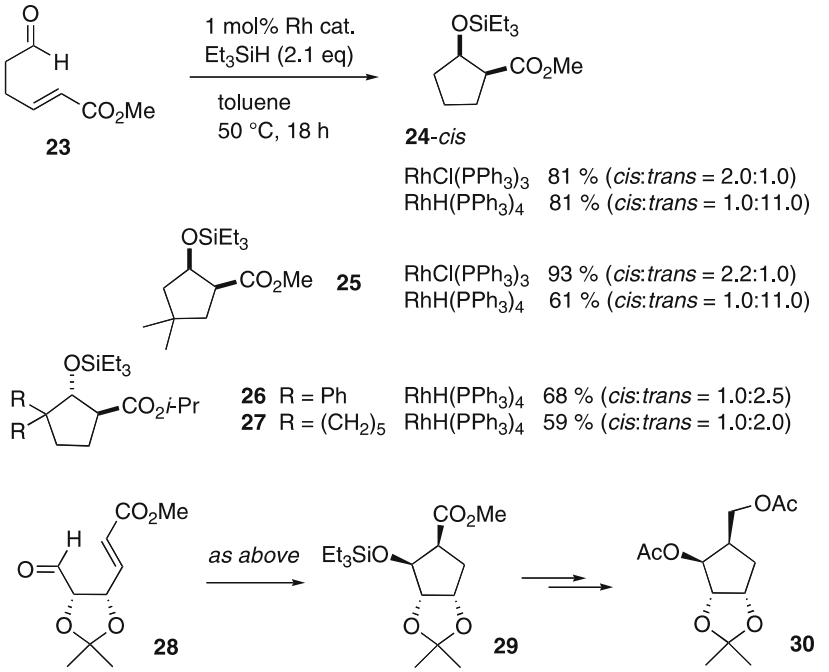

Scheme 9 Rh-catalyzed intramolecular reductive aldol reaction of 6-oxo-hex-2-enoates

2.0 : 1.0). $RhH(PPh_3)_4$ (1 mol %) exhibited higher catalytic activity and promoted a complete reversal in stereoselectivity to provide the *trans* isomer of **24** and **25** as the major reaction product. The *cis*-cyclopentane **29**, derived from optically active **28**, was converted to the differentially protected cyclopentane triol **29**, which, in turn, converted to the differentially protected tetraol **30**, a key intermediate in the synthesis of enantiopure bioactive carbocyclic nucleosides [19].

In 2005, Willis et al. disclosed a new type of catalytic reductive aldol reaction that employs aldehydes as the stoichiometric reducing agents, rather than hydride sources such as hydrosilanes [20]. The coupling of unsaturated nitriles, esters, and ketones to β-sulfide-substituted aldehydes was conducted using $[Rh(dppe)]ClO_4$ (10 mol %), which is derived from $[Rh(dppe)(NBD)]ClO_4$ and H_2. For example, the β-sulfido aldehyde **31** and acrylonitrile reacted at 70 °C to give the ester **32** in 88% yield (Scheme 10). Similarly, methyl vinyl ketone and phenyl acrylate provide the corresponding esters **33** and **34**, respectively. On the basis of isotopic labeling experiments involving deuterated aldehyde and additional evidence, a Rh-enolate was postulated as the reactive intermediate in the aldol addition event (Scheme 11). The reaction is initiated by chelation-assisted oxidative addition of the aldehyde C – H to Rh(I) to generate the Rh – H species **A**, which engages in conjugate reduction to form Rh-enolate **B**. Carbonyl addition provides the

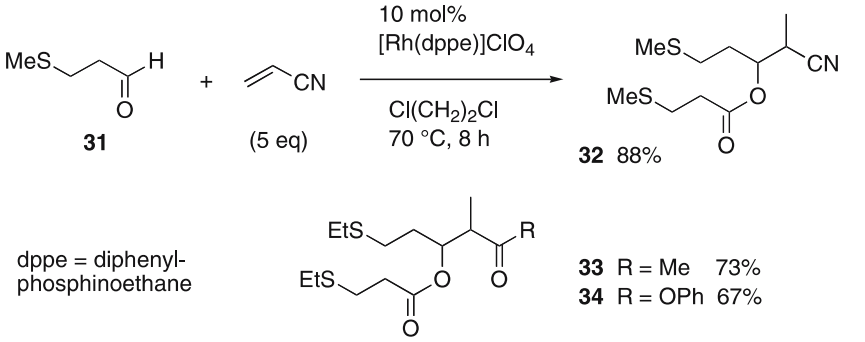

Scheme 10 Rh-catalyzed reductive aldol reaction with aldehydes as reductants

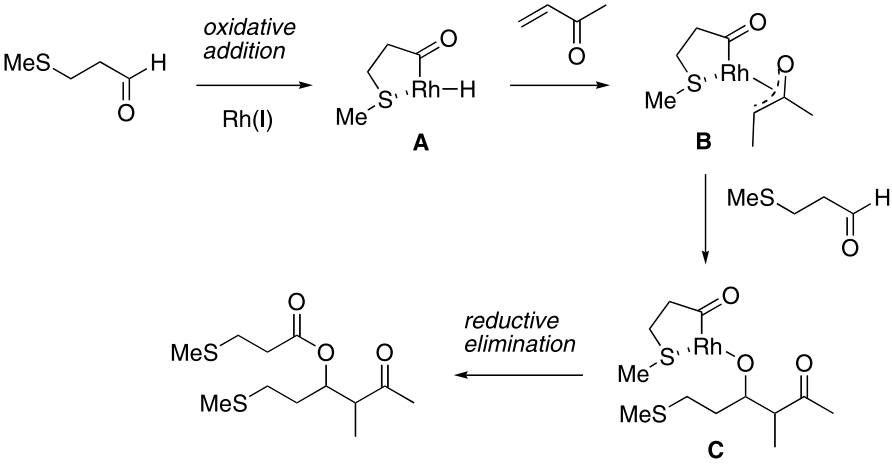

Scheme 11 Reaction path of Willis' reductive aldol reaction

Rh-aldolate **C**, which upon reductive elimination delivers the product and regenerates the rhodium catalyst.

2.1.2 Hydrosilane-Mediated Asymmetric Reactions

In 2000, Morken et al. reported the first examples of catalytic asymmetric reductive aldol reactions [21]. Using Rh(BINAP) (5 mol %) as catalyst and Et_2MeSiH as reductant, the *syn*-selective (1.7 : 1) coupling of benzaldehyde and methyl acrylate produced the diastereomers **35**-*syn* and **35**-*anti* in 91% ee and 88% ee, respectively. Using phenyl acrylate as the nucleophilic partner, a favorable yield of 72% was obtained for the aldol product **36** (Scheme 12). Several aldehydes were examined, which exhibit higher levels of *syn*-selectivity. Expanding the scope of substrates and acrylates under

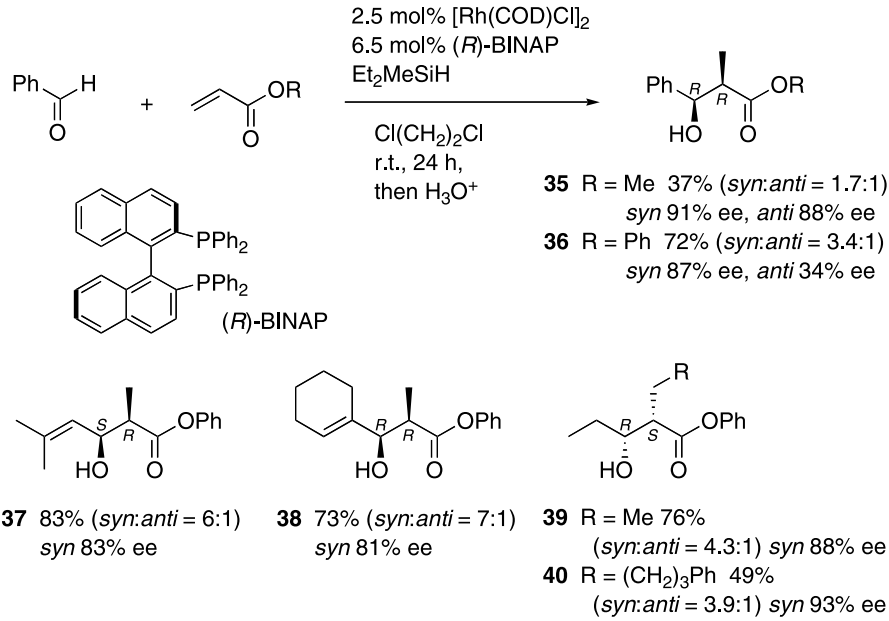

35 R = Me 37% (*syn*:*anti* = 1.7:1)
syn 91% ee, *anti* 88% ee
36 R = Ph 72% (*syn*:*anti* = 3.4:1)
syn 87% ee, *anti* 34% ee

37 83% (*syn*:*anti* = 6:1)
syn 83% ee

38 73% (*syn*:*anti* = 7:1)
syn 81% ee

39 R = Me 76%
(*syn*:*anti* = 4.3:1) *syn* 88% ee
40 R = $(CH_2)_3Ph$ 49%
(*syn*:*anti* = 3.9:1) *syn* 93% ee

Scheme 12 First catalytic asymmetric reaction

investigation was reported to show synthetic versatility, giving a variety of α,β-substituted β-hydroxyesters. For example, using Rh catalysts modified by (*R*)-BINAP, aldol products **37** and **38** are produced in highly optically enriched form. Similarly, using (*S*)-BINAP as ligand, aldol products **39** and **40** are formed with high levels of enantiomeric excess [22]. On the basis of ^{1}H- and ^{31}P-NMR analysis, a dinuclear μ-hydride bridged Rh(I) species, [(BINAP)Rh-H/H-Rh(BINAP)] was postulated as an active hydride generated by the action of $PhMe_2SiH$ at the initial stage of the catalytic cycle. The silyl-protected aldol products could be isolated [23]. The phenyl ester **39** served as a precursor in the synthesis of inostamycin natural products [24].

In 2001, Morken et al. found a new iridium catalyst system for the asymmetric reaction (Scheme 13) [25]. The coupling of benzaldehyde and methyl acrylate was carried out using $[Ir(COD)Cl]_2$ (2.5 mol %) and indane-Pybox (7.5 mmol %) with Et_2MeSiH (ca. 120 mol %) at 25 °C to selectively give *syn*-aldol product **35** in 48% yield and 92% ee for **35**-*syn* (*syn* : *anti* = 3.9 : 1). A slightly increased yield of 68% and enantioselectivity of 94% ee was observed using ethyl acrylate as the nucleophilic partner in the formation of aldol **41**. Substituted aliphatic aldehydes, such as benzyloxy- and phenylethoxyacetoaldehydes, exhibited similarly high levels of enantioselectivity, providing aldol adducts **42** and **43** in 96% ee and 82% ee, respectively. The chiral aldol product **42** was employed as a precursor for synthesis of bioactive compound borrelidin [26].

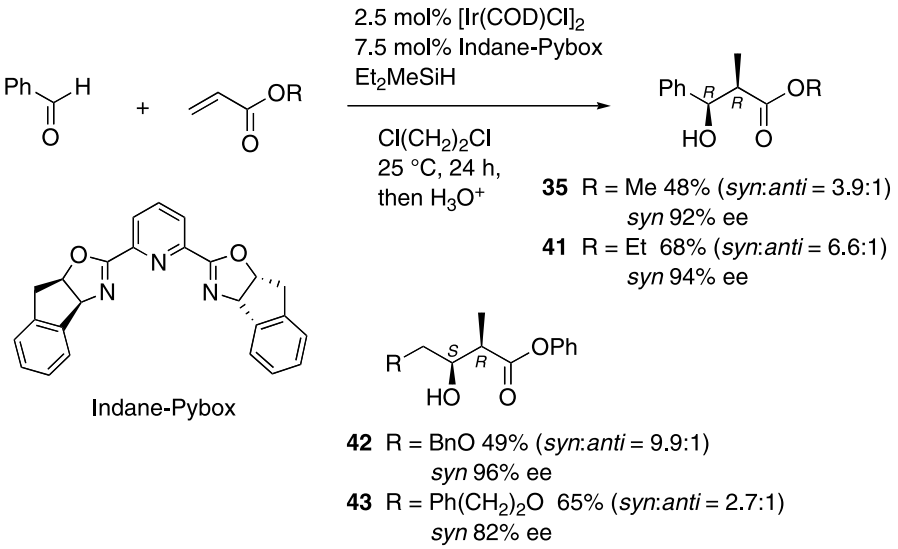

Scheme 13 Ir-catalyzed asymmetric reaction

Nishiyama et al. in 2005 disclosed that Rh(Phebox) complexes exhibit high levels of performance as catalysts for asymmetric reductive aldol coupling [27]. The coupling reaction of benzaldehyde and *tert*-butyl acrylate (150 mol %) was catalyzed at 50 °C in toluene using Rh(Phebox-Bn)$(OAc)_2$ (1 mol %) and hydrosilanes such as $(EtO)_2MeSiH$ (160 mol %). The *anti*-aldol product **44** was obtained in 98% yield with exceptional levels of stereoselection (*syn* : *anti* = 2 : 98, *syn* 94% ee) (Scheme 14). The degree of asymmetric induction was found to depend upon the choice of reductant, with Me_2PhSiH giving the highest levels of enantioselectivity, up to 96% ee for *anti*-aldol product **44**. With the appropriate choice of catalyst and hydrosilanes, aromatic, unsaturated, and aliphatic aldehydes react smoothly to provide aldol adducts that embody high levels of *anti*-selectivity. The cyclic transition state involving the Rh-(*E*)-enolate and aldehyde was postulated to account for the observed *anti*-stereoselectivity as well as the absolute configuration of the products.

Introduction of 3,5-dimethyl and 4-substituent on the Phebox skeleton revealed a weak substituent effect on the degree of asymmetric induction (Scheme 15) [28, 29]. When trimethylsilyl acrylate was used as enolate source, the β-hydroxy carboxylic acid was obtained directly upon mild acid hydrolysis. In the production of carboxylic acid **49**, an enantiomeric excess of 96% ee was attained using the NO_2-substituted Phebox-Rh catalyst.

The catalytic system of Rh(Phebox) and $MePh_2SiH$ was applied to the coupling of acetone and cinnamates under solvent-free conditions (Scheme 16) [30]. Several cinnamates and crotonates were used as enolate

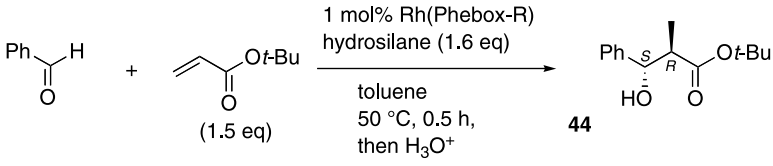

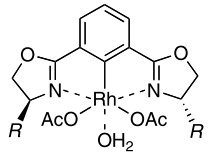

Rh(Phebox-R)$(OAc)_2(H_2O)$

R = Bn, *i*-Pr

$(EtO)_2MeSiH$ R = Bn 98% (*syn*:*anti* = 2:98)
anti 94% ee
R = *i*-Pr 91% (*syn*:*anti* = 5:95)
anti 91% ee

Me_2PhSiH R = Bn 93% (*syn*:*anti* = 6:94)
anti 96% ee
R = *i*-Pr 93% (*syn*:*anti* = 7:93)
anti 95% ee

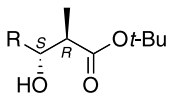

	R	yield (*syn*:*anti*)	*anti* %*ee*
45	*p*-MeOPh	98% (6:94)	94
46	1-Naph	97% (2:98)	96
47	cyclohexyl	72% (14:86)	93
48	$BnCH_2O$	81% (41:59)	91

cat.: Rh(Phebox-Bn), hydrosilane: $(EtO)_2MeSiH$

Scheme 14 Rh(Phebox)-catalyzed asymmetric reaction

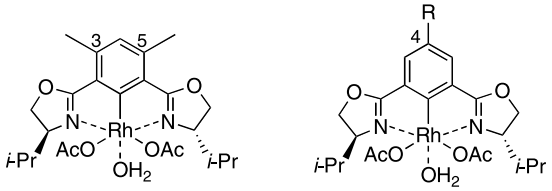

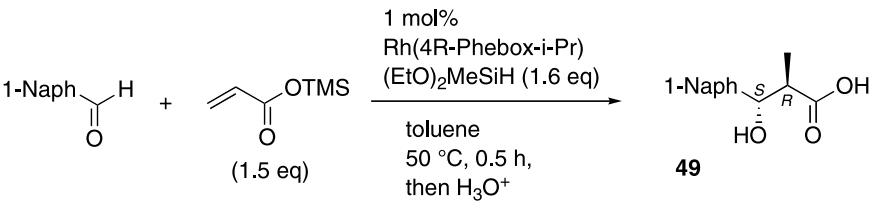

cat. R = H 92% (*syn*:*anti* = 12:88)
anti 91% ee
cat. R = NO_2 85% (*syn*:*anti* = 13:87)
anti 96% ee

Scheme 15 Asymmetric reaction catalyzed by substituted-Phebox-Rh

precursors in couplings to electrophilic partners such as cyclohexanone and acetophenone, furnishing aldol adducts with high levels of enantioselectivity and diastereoselectivity, respectively.

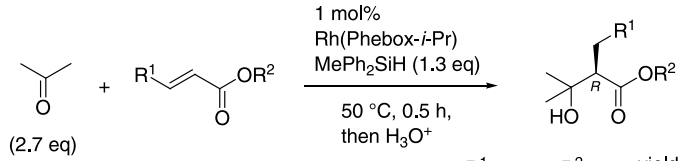

	R^1	R^2	yield	% ee
50	Ph	Et	83%	97
51	Ph	*i*-Pr	82%	98
52	*p*-CF_3Ph	Et	64%	97
53	Me	Bn	76%	95

Scheme 16 Rh(Phebox) catalytic system toward ketones

2.1.3 Hydrogen-Mediated Reactions

In 2002, Krische et al. disclosed a new method for the reductive generation of enolates from enones in inter- and intramolecular reductive aldol reactions using elemental hydrogen [31]. They employed cationic Rh(I) complexes in the conjunction with basic additives such as KOAc or K_2CO_3 to generate Rh-monohydride species by activation of hydrogen. The heterolytic cleavage of hydrogen was believed to proceed via oxidative addition of hydrogen forming metal-dihydride species followed by reductive abstraction of a proton from the dihydride species by the base (Scheme 17) [32, 33].

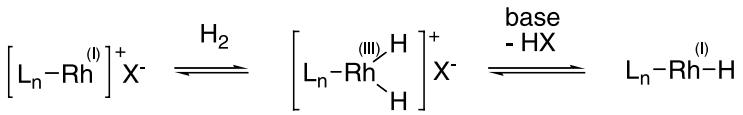

Scheme 17 Formation of Rh-monohydride and heterolytic cleavage of hydrogen

The coupling reaction of phenyl vinyl ketone (1.5 eq.) and *p*-nitrobenzaldehyde was carried out at 25 °C with $[Rh(COD)_2]OTf$ (5 mol %), PPh_3 (12 mol %), KOAc (50 mol %) under H_2 (1 atm) atmosphere to give the aldol product **54** in 92% yield (Scheme 18) [31]. Omission of KOAc decreased the yield to 79%. The aromatic aldehydes gave the corresponding aldol products in good to excellent yields, whereas aliphatic aldehydes resulted in diminished yields. Methyl vinyl ketone as an enolate source can be tolerated, giving a 70% yield of the aldol product **58**.

Under similar conditions, employing a cationic Rh complex (10 mol %) and hydrogen (1 atm), the aldehyde-enone **17** was subjected to the cyclization to give the cyclic aldol product **18** in 89% with *cis*-selectivity up to 10 : 1 (Scheme 19) [31]. Use of $(p\text{-}CF_3Ph)_3P$ as ligand accelerated the reaction

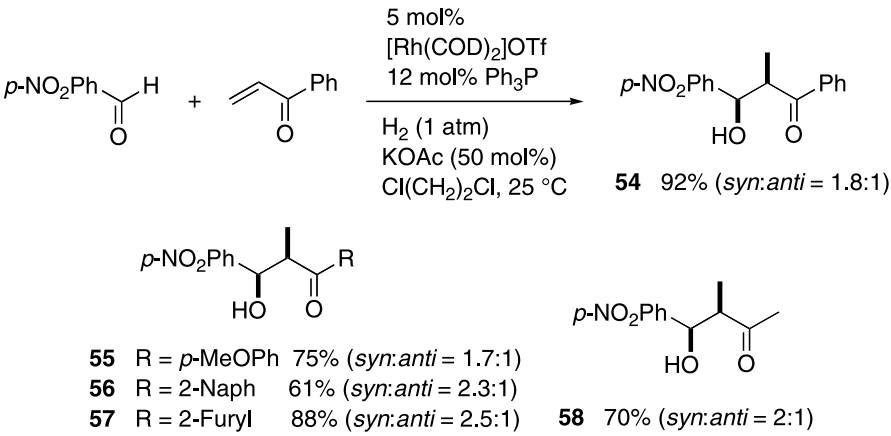

Scheme 18 Hydrogen-mediated reductive aldol reaction

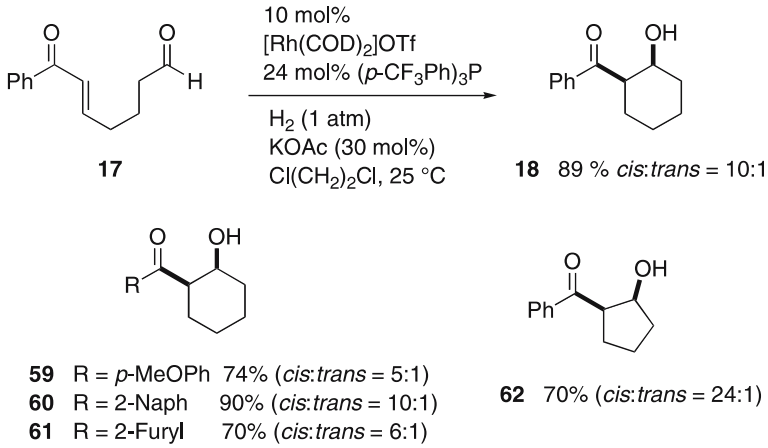

Scheme 19 Hydrogen-mediated intramolecular reaction

compared to Ph_3P. Cooperation of KOAc (30 mol %) was again crucial in obtaining optimal yields. The formation of a five-membered ring proceeded well to give **62** in 70% yield with high *cis*-ratio.

The intramolecular reductive aldol reaction of keto-enones was successfully conducted under conditions similar to those described above, employing a cationic Rh complex and Ph_3P (Scheme 20) [34]. The keto-enone **63** was cyclized in the presence of added K_2CO_3 to give the ketone-aldol **64** in 72% yield with exclusive *cis*-selectivity. Dione-enone derivatives, for example **68** and **70**, were efficiently cyclized to furnish bicyclic aldol products **69** and **71**, respectively, wherein three stereogenic centers of the bicyclic product form stereoselectivity through the intermediacy of a Rh-enolate.

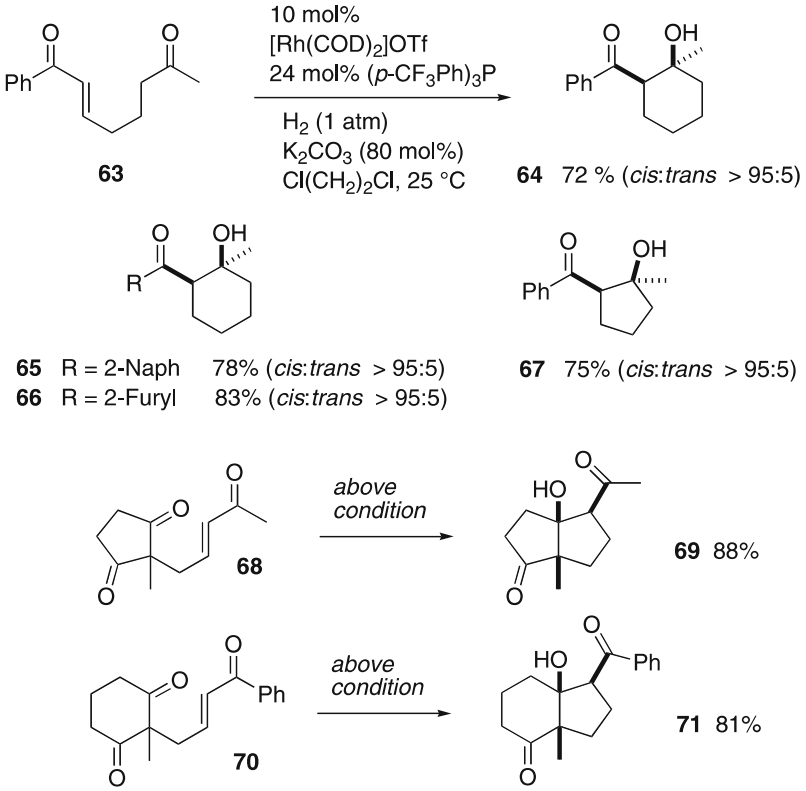

Scheme 20 Hydrogen-mediated intramolecular reaction of keto-enones

The coupling of enals and glyoxals was realized by hydrogen-mediated reaction with the cationic Rh complex and Ph_3P [35]. The intermediate aldehyde enolates derived via Rh-catalyzed hydrogenation were trapped with glyoxals to form β-hydroxy-γ-keto-aldehydes, which were treated sequentially with hydrazine to give pyridazines in a one-pot transformation to provide, for example, a 62% yield of **72** (Scheme 21).

The intramolecular cyclization of diketo-enals and keto-enals was accomplished by the combination of a cationic Rh complex and *tri*(2-furyl)phosphine ($2-Fur_3P$). The corresponding bicyclic hydroxy-aldehydes were produced in good to excellent yields, as demonstrated by the formation of **74**, **76** and **78** (Scheme 22) [36].

The catalytic system employing $(2-Fur)_3P$ as ligand was applied to the coupling of methyl vinyl ketone and ethyl vinyl ketone to aromatic, aliphatic, acetylenic, and olefinic aldehydes (Scheme 23) [37]. Despite the hydrogenation conditions, alkyne and alkene moieties, as well as benzylic ether and nitro functional groups all remained intact. Furthermore, extremely high lev-

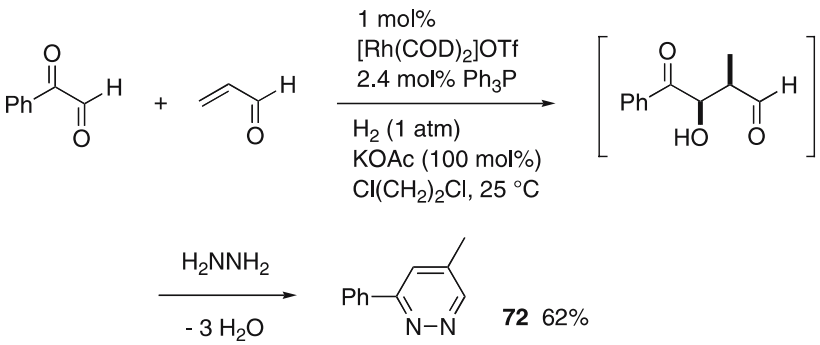

Scheme 21 Hydrogen-mediated reaction of enals and glyoxals and sequential pyridazine synthesis

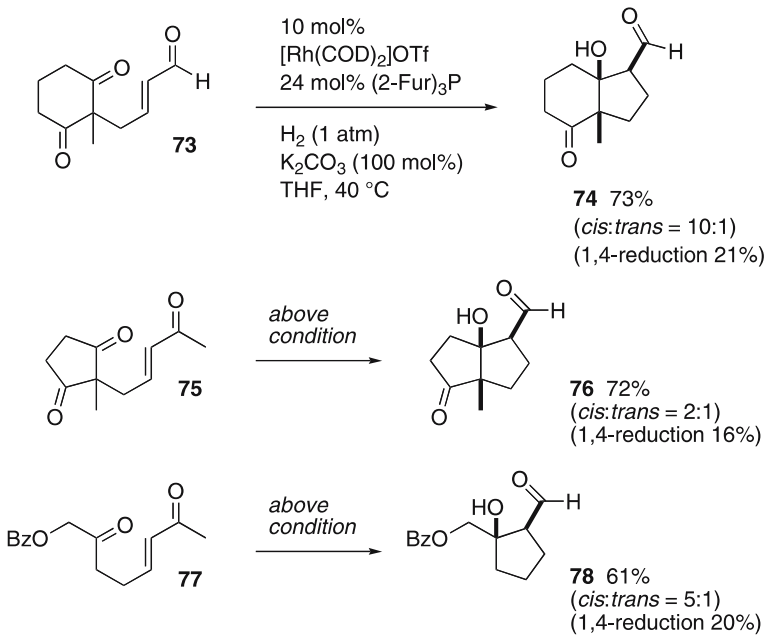

Scheme 22 Hydrogen-mediated intramolecular reaction of keto-enones

els of *syn*-selectivity of up to 99 : 1 were obtained. The *syn*-diastereoselectivity was explained on the basis of a stereochemical model involving formation of *Z*-(O)-enolate, which reacts through a Zimmerman–Traxler type transition state. Irreversible enolization and aldolization is suggested by observance of high levels of *syn*-selectivity, as acyclic *anti*-aldols are known to be thermodynamically preferred.

Nonsymmetric divinyl ketone **86** was employed as an enolate precursor en route to β-hydroxy-enones, which are formed in high yield and *syn*-selectivity

79 R^2 = Me 91% (*syn*:*anti* = 16:1) **81** R^2 = Me 90% (*syn*:*anti* = 17:1)
80 R^2 = Et 90% (*syn*:*anti* = 28:1) **82** R^2 = Et 88% (*syn*:*anti* = 18:1)

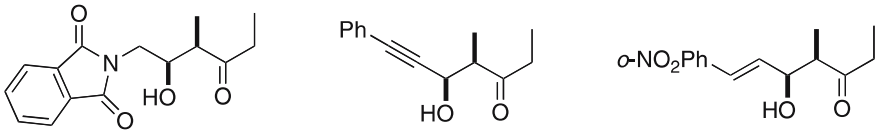

83 97% (*syn*:*anti* = 99:1) **84** 70% (*syn*:*anti* = 10:1) **85** 99% (*syn*:*anti* = 10:1)

Scheme 23 Rh-(2-Fur)$_3$P catalyst-promoted *syn*-selective reaction

(Scheme 24) [38]. Chemoselective enolization of the less substituted enone moiety under hydrogenation conditions accompanied by subsequent aldol reaction provided the corresponding hydroxyl-enones, such as **87–89**, which could be converted to various building blocks for polypropionate synthesis. *p*-Me_2N styryl vinyl enone also was employed successfully as an enolate precursor, as demonstrated by the formation of hydroxy enone **90**.

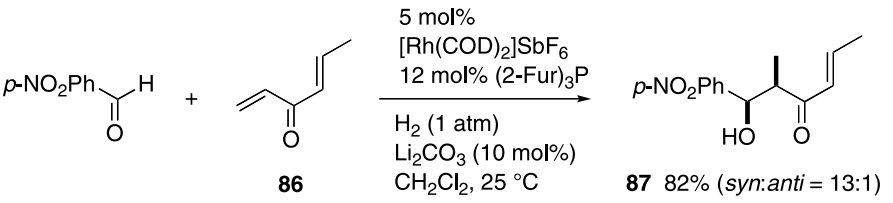

86

87 82% (*syn*:*anti* = 13:1)

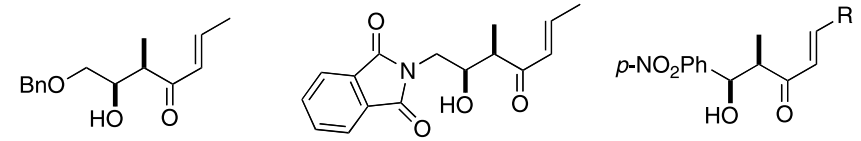

88 80% (*syn*:*anti* = 9:1) **89** 85% (*syn*:*anti* = 13:1)

90 R = *p*-Me_2NPh
93% (*syn*:*anti* = 10:1)

Scheme 24 Nonsymmetric divinyl ketones for reductive aldol reaction

α-Alkoxy and α-aminoaldehydes were readily coupled with methyl vinyl ketone by the Rh-(2-Fur)$_3$P catalyst to form *syn*-aldol products with *anti*-Felkin–Anh selectivity [39]. Upon use of the *N*-methyl derivative of **95**, which lacks the intramolecular hydrogen bond, the yield is decreased to 17% and an inversion in diastereoselectivity is observed (Scheme 25). It was suggested that the hydrogen bond directs transition state geometry and plays a important role in terms of enhancing reactivity of the aldehydes. During this reaction, which sets three contiguous stereogenic centers, optical purity of the sensitive α-aminoaldehyde was retained.

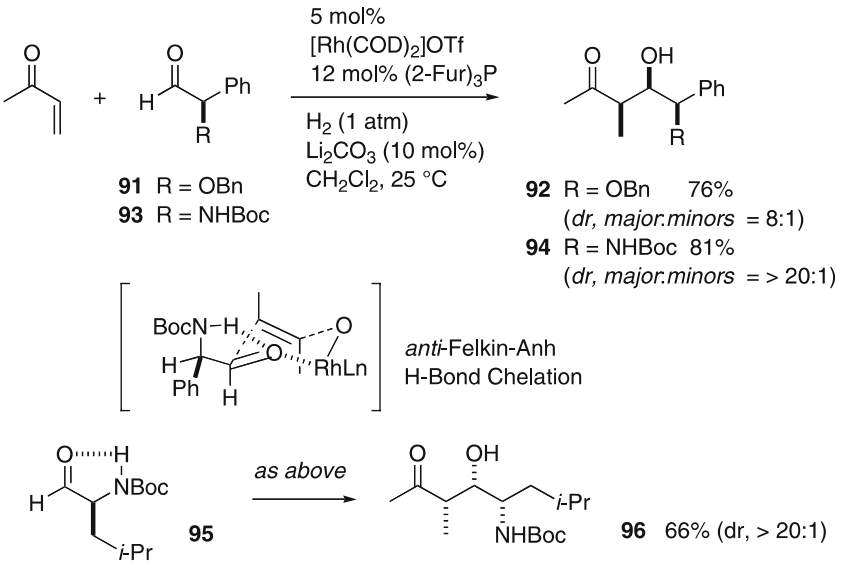

Scheme 25 Anti-Felkin–Anh selectivity in the reductive aldol reaction of α-alkoxy and α-aminoaldehydes

2.2 Pd Catalysts

Kiyooka et al. reported in 1998 the Pd-catalyzed coupling reaction of *N*,*N*-dimethylacrylamide (110 mol %) and aromatic aldehydes (100 mol % eq) in the presence of Cl_3SiH (130 mol %) (Scheme 26) [40]. Using $Pd(Ph_3Ph)_4$ (5 mol %), conjugate reduction of the acrylamide and coupling to benzaldehyde occurs at room temperature over a period of 45 h. After hydrolysis, β-hydroxy amide **97** was obtained in 87% yield with *anti*-selectivity (*syn* : *anti* = 32 : 68). Several aromatic aldehydes showed similar *anti*-selectivity, as demonstrated by the formation of adducts **98**, **99**, and **100**. In contrast, corresponding Pd-catalyzed couplings involving *tert*-butyl acrylate are *syn*-

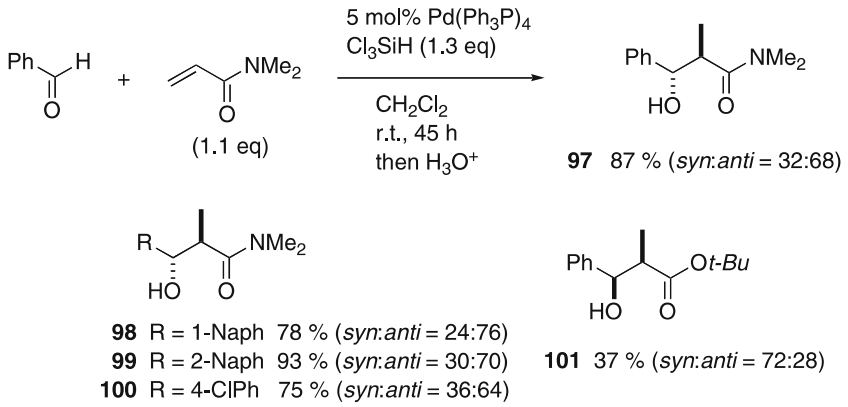

Scheme 26 $Pd(Ph_3Ph)_4$-catalyzed reaction

selective, though diminished yields are observed. For example, **101** is formed in ca. 35% yield with a *syn* : *anti* ratio of 7 : 3.

Takemoto et al. applied the Pd-catalyzed coupling reaction to *N*-phthaloyl dehydroalanine **102** and benzaldehyde (Scheme 27) [41]. Instead of hydrosilanes, *n*-Bu_3SnH was capable of serving as a hydrogen donor to promote C – C bond formation giving **103**.

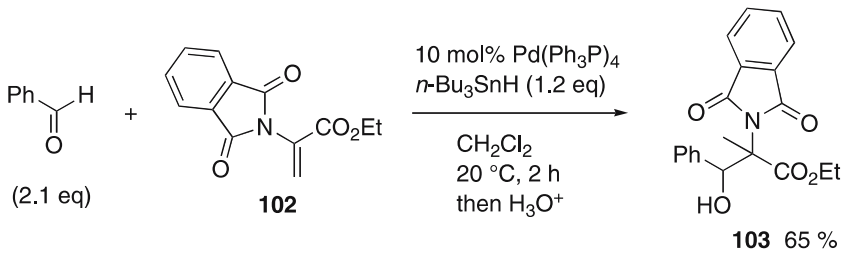

Scheme 27 Combination of $Pd(Ph_3Ph)_4$ and *n*-Bu_3SnH

2.3 Cu Catalysts

Copper hydride species, notably Stryker's reagent $[Ph_3PCuH]_6$, are capable of promoting the conjugate reduction of α,β-unsaturated carbonyl compounds [42]. Taking advantage of this trustworthy method, Chiu et al. demonstrated in 1998 an intramolecular reductive aldol reaction in the synthesis of novel terpenoid pseudolaric acids isolated from Chinese folk medicine (Scheme 28) [43]. Two equivalents of $[Ph_3PCuH]_6$ enabled cyclization of keto-enone **104** to provide the bicyclic diastereomers **105** (66%) and **106** (16%). The reaction also was applied to the transformation of **107**

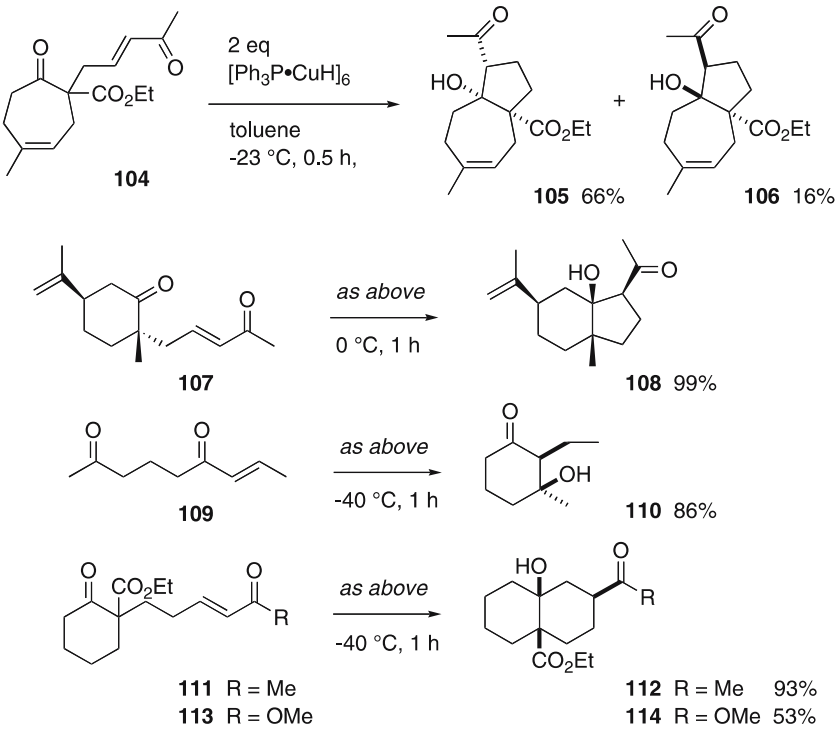

Scheme 28 Intramolecular reductive aldol reaction promoted by stoichiometric Stryker's reagent

to **108** in the asymmetric synthesis of an iphionane sesquiterpenoid lucinone [44]. Under similar reaction conditions, the scope of substrates such as keto-enones, keto-unsaturated esters, and keto-unsaturated nitriles was investigated and was shown to provide yields of aldol adduct of up to 93% with high *syn*-selectivity [45].

In this context, Lipshutz et al. reported in 2000 a catalytic reductive aldol reaction of enones and aldehydes with $[Ph_3PCuH]_6$ (5 mol %) and $PhMe_2SiH$ (150 mol %) [46]. The two-step reaction was carried out in one pot, without isolation of the intermediate silyl enol ethers, efficiently providing the β-hydroxyketones in high yield. Lewis acids such as BF_3 or $TiCl_4$ are used to promote the second step involving aldol reaction of the enol silane. In place of hydrosilanes, dialkylboranes could be employed as hydride sources, circumventing the need to introduce additional Lewis acids. Here, the aldol products are formed via intermediacy of the boron-enolates, with *syn*-selectively for acyclic enones and *anti*-selectively for cyclic enones [47–50].

Chiu et al. developed a catalytic reductive aldol cyclization of alkynediones such as **115** and **117** using $[Ph_3PCuH]_6$ (10 mol %) as catalyst and polymethylhydrosiloxane PMHS (200 mol %) as terminal reductant. The

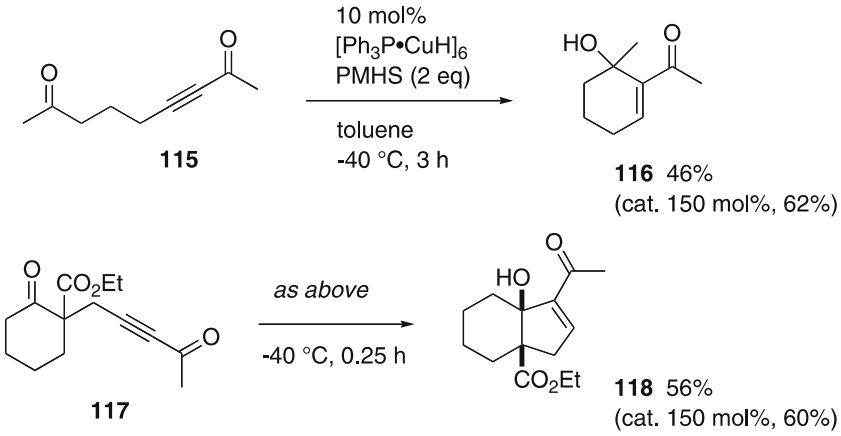

Scheme 29 Reductive aldol cyclization of alkyne-diones catalyzed by Stryker's reagent

cyclic β-hydroxy enones **116** and **118** were generate in moderate yield (Scheme 29) [51, 52].

Chiu et al. developed the first example of a reductive intramolecular Henry reaction induced by Stryker's reagent (Scheme 30) [53]. The conjugate reduction of keto-nitroalkenes with $[Ph_3PCuH]_6$ (150 mol %) triggers spontaneous nitro-aldol reaction at – 40 °C to produce β-hydroxy nitro compounds in moderate yield.

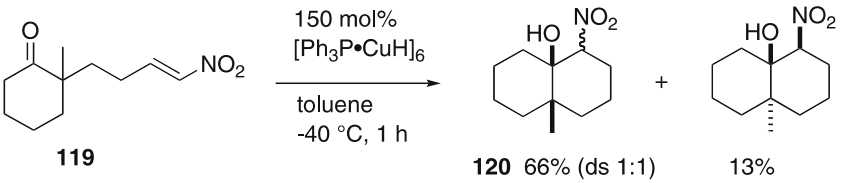

Scheme 30 Reductive intramolecular Henry reaction, nitroaldol reaction, mediated by Cu – H

In 2005, Lam et al. succeeded in developing an intramolecular reductive aldol reaction of keto-enoates catalyzed by $Cu(OAc)_2H_2O$ (5 mol %) ligated by bisphosphine ligands [54]. After surveying various combinations of copper salts, hydrosilanes, and bisphosphine ligands, they eventually identified 1,1,3,3-tetra-methylhydrosiloxane (TMDS) (100 mol %) and bis(diphenylphosphino)ferrocene (DPPF) or racemic BINAP as the ligands of choice. The reaction of keto-ester **121** was carried out at room temperature and resulted in formation of the *cis*-β-hydroxy lactone **122** in 72–73% yield (Scheme 31). This catalytic reaction was extended to asymmetric cyclizations. Using (*S*)-BINAP as ligand, the lactone **122** was produced in 62% ee, while MeO-BIPHEP ligands and SEGPHOS improved the ee to 70–77%. Sev-

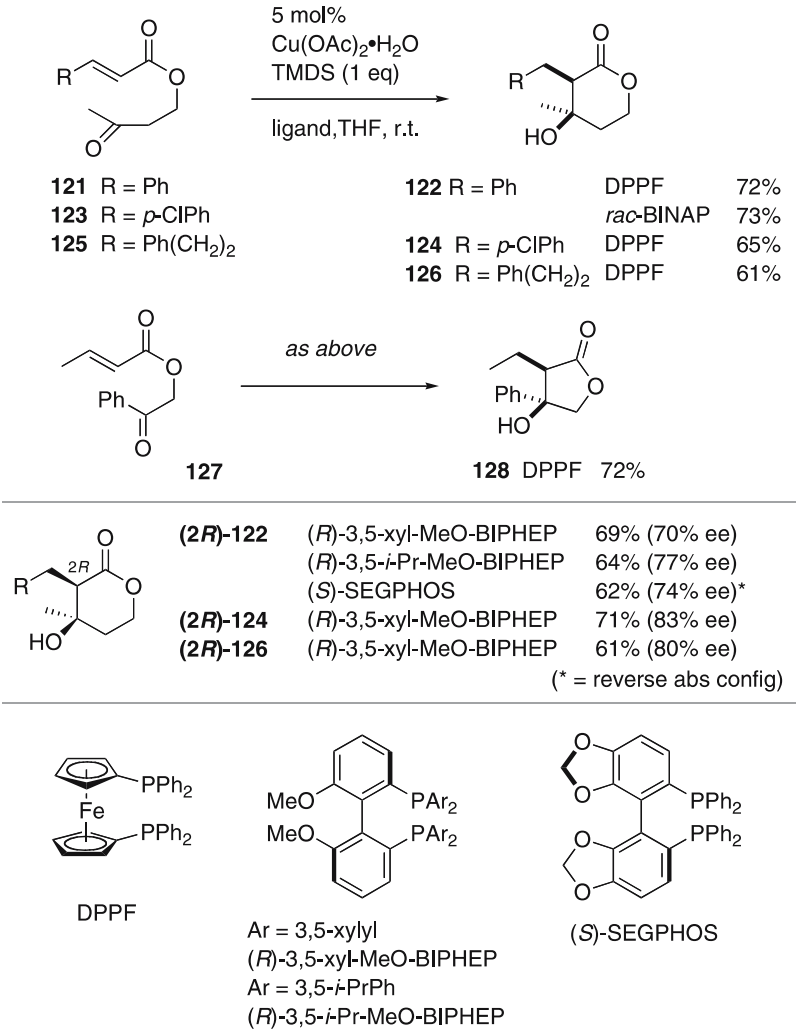

Scheme 31 Diastereoselective and enatioselective Cu-catalyzed reaction of keto-unsaturated esters

eral substrates were subjected to the conditions for catalytic asymmetric cyclization and were found to provide the aldol products with enantiomeric excesses of up to 83%. They proposed a catalytic cycle involving generation of a (bisphosphine)Cu – H species, hydrometallation (conjugate reduction) to furnish a Cu-enolate, aldol addition and, finally, liberation of the silylated product. The *cis*-stereochemistry of the products was explained by preferential formation of a chelated Cu-(*Z*)-enolate (Scheme 32).

Lam et al. applied the copper catalyst system to the diastereoselective synthesis of 4-hydroxypiperidin-2-ones, such as **130**, **132** and **134**

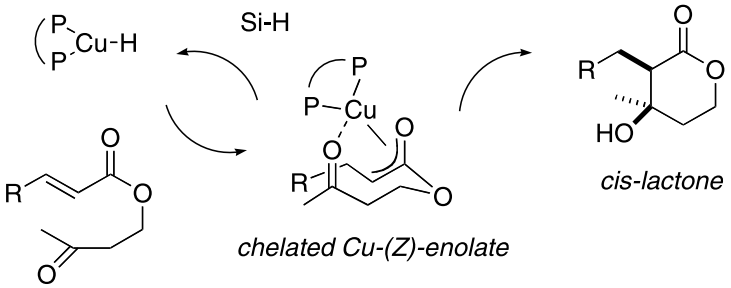

Scheme 32 Lam's proposed Cu-(*Z*)-enolate in the catalytic cycle

(Scheme 33) [55]. The keto-enamides readily gave the corresponding β-hydroxy piperidinones, which could be further transformed to biologically active polyhydroxylated piperidines, for example glycosidase inhibitor **135**. They also found that the same aldol cyclization could be catalyzed by $Co(acac)_2 2H_2O$ (5 mol %) and Et_2Zn (200 mol %) in yields of up to 99% [56]. The diethyl zinc-mediated reduction of the cobalt salt likely produces a Co – H species, which promotes conjugate reduction to initially form a Co-enolate that undergoes transmetallation to form a Zn-enolate. Aldol cyclization may be accomplished through the Zn-enolate as a stepwise one-pot procedure.

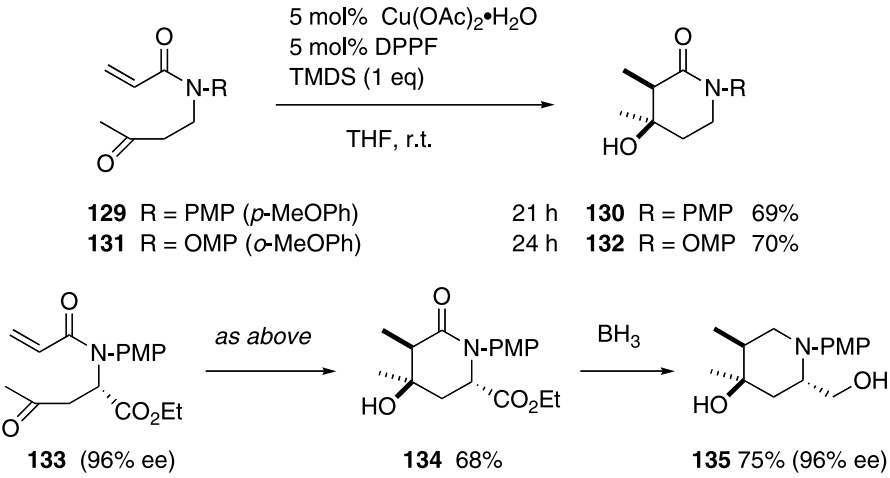

Scheme 33 Cu-catalyzed reaction of keto-unsaturated amides

Riant et al. in 2006 reported an enantioselective reductive aldol reaction of acetophenone and methyl acrylate mediated by $PhSiH_3$ (140 mol %) and catalyzed by a complex generated in situ from $[CuF(Ph_3P)_3]2MeOH$ (1–3 mol %) and a chiral bisphosphine (1–3 mol %) [57]. According to Mori's

finding, the CuF complexes were expected to generate the corresponding Cu – H species through their reaction with the hydrosilane [58–60]. The catalytic reaction employing MeO-BIPHEP as ligand took place at 0 °C in toluene and was complete within 2 h. The aldol product **136** was produced in 95% yield with a 41 : 59 ratio of *erythro* : *threo* (*e* : *t*) isomers in 2% ee and 51% ee, respectively (Scheme 34). Chiral ligand partners, such as BINAP, JOSIPHOS, TANIAPHOS, and so on, were also surveyed. The TANIAPHOS derivatives, which are ferrocenyl-based diphosphine ligands, gave the highest diastereomeric ratios, with selectivities up to 92 : 8 (*e* : *t*) and enantioselectivities of up to 95% ee for *erythro* and 94% ee for *threo*. Under optimal conditions, aromatic ketone substrates were found to participate in highly diastereo- and enantioselective couplings, as demonstrated by the formation of **137–140.**

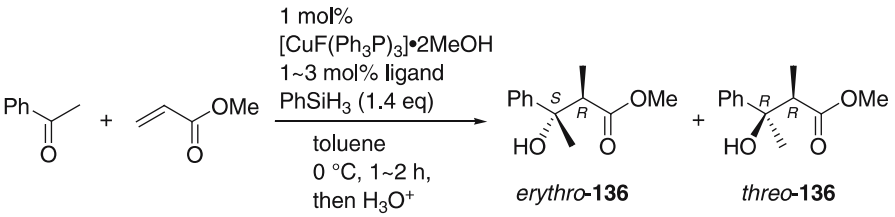

(*S*)-Ph-MeO-BIPHEP	0 °C	95%	41:59	(*e* 2% ee, *t* 51% ee)
(*R*,*S*)-*t*-Bu-JOSIPHOS	-50 °C	99%	54:46	(*e* -73% ee, *t* -63% ee)
(*R*,*S*)-Ph-TANIAPHOS	-50 °C	99%	76:24	(*e* -85% ee, *t* -94% ee)
(*R*,*S*)-Cy-TANIAPHOS	-50 °C	99%	92:8	(*e* 95% ee, *t* 72% ee)

as above condition with (*R*,*S*)-Cy-TANIAPHOS

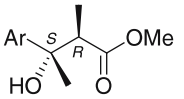

	Ar =	yield	*e*:*t*	% ee *e*	*t*
137	*p*-FPh	88%	91:9	92	73
138	*p*-ClPh	95%	86:14	90	77
139	*m*-ClPh	70%	88:12	82	-
140	3-Thienyl	95%	95:5	95	65

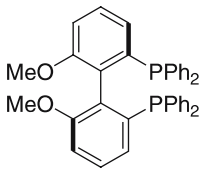

(*S*)-Ph-MeO-BIPHEP

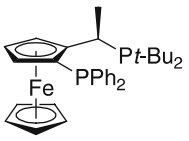

(*R*,*S*)-*t*-Bu-JOSIPHOS

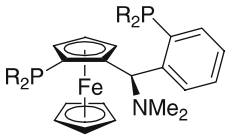

R = Ph
(*R*,*S*)-Ph-TANIAPHOS
R = Cy
(*R*,*S*)-Cy-TANIAPHOS

Scheme 34 Cu-catalyzed asymmetric reaction of aryl methyl ketones and methyl acrylate

Shibasaki and Kanai et al. reported the same coupling of acetophenone and methyl acrylate giving **136** (100%, $e:t = 45:55$, 29% ee for *e*) using $[CuF(Ph_3P)_3]2EtOH$ (2.5 mol %), (*R*)-tol-BINAP (2.5 mol %), and $(EtO)_3SiH$ (160 mol %) [61]. The coupling of diethyl ketone in THF at – 25 °C produced the corresponding β-hydroxy esters **141–143** in 71–80% ee (Scheme 35). Changing from hydrosilane to pinacolborane as the hydrogen source, they applied the Cu-catalyst system to the coupling of ketones and allenic esters to attain highly enantioselective reductive aldol reaction (Scheme 35) [62]. Remarkably, the choice of chiral ligand changed γ- and α-selectivity while maintaining high enantioselectivity.

Riant et al. applied the catalytic system $[CuF(Ph_3P)_3]2MeOH$ (0.1–1 mol %) and $PhSiH_3$ (140 mol %) in the combination with Ph-TANIAPHOS as ligand to the *syn*-selective reductive coupling of aldehydes and methyl

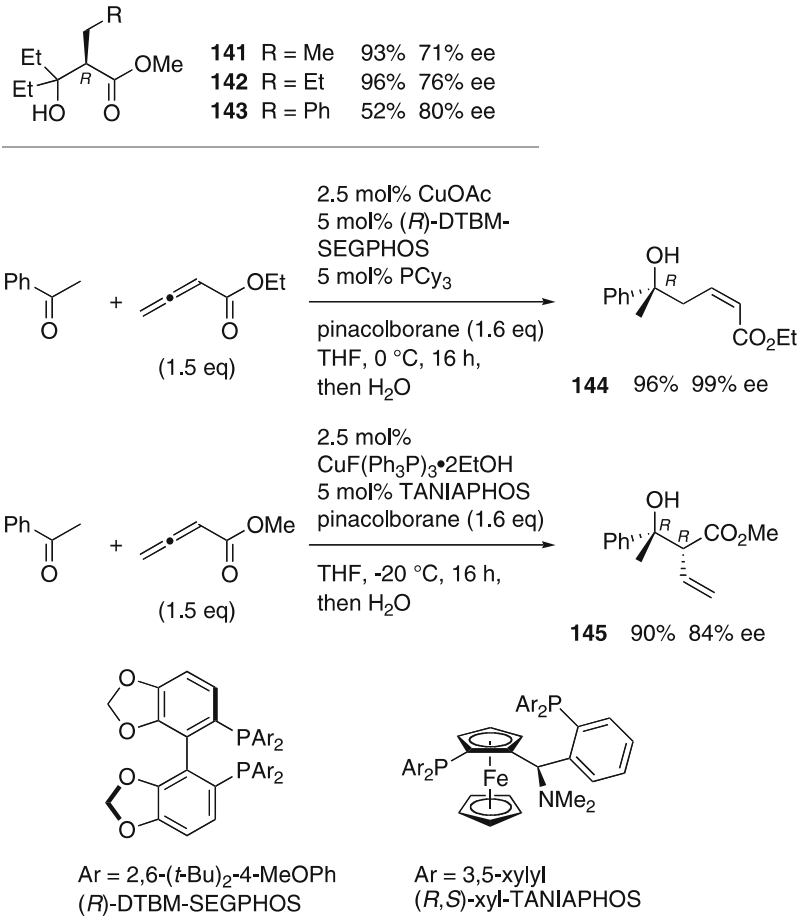

Scheme 35 Cu-catalyzed asymmetric reaction of acrylates and allenic esters to ketones

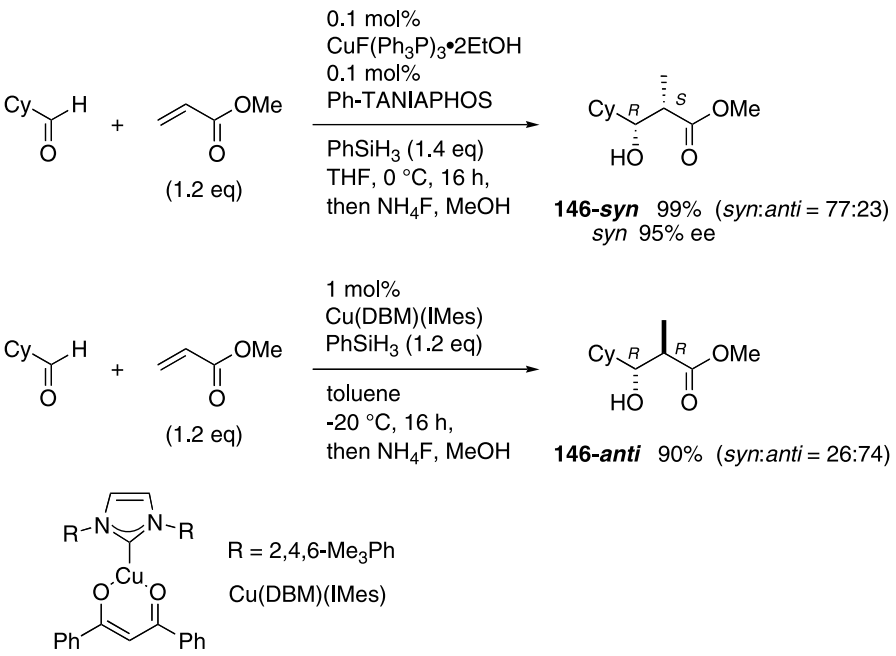

Scheme 36 Reactions catalyzed by CuF and Cu – NHC

acrylate in THF at – 78 °C. High enantioselectivities of up to 97% ee were observed for the *syn*-aldol product **146** (Scheme 36) [63]. Various chiral bisphosphines, BINAP, JOSIPHOS, TANIAPHOS, and BIPHEP etc. were examined. Among them, Ph-TANIAPHOS provided *syn*-selectivity as high as 99% with enantioselectivity reaching 95% ee. When Ph_2SiH_2 was substituted for $PhSiH_3$, the product **146** was obtained in 97% ee as a 88 : 12 ratio of *syn* : *anti* isomers. Several aromatic ketones and thienyl ketones were subjected to these conditions to give ca. 80% ee and 80% *syn*-selectivity on average. They also found that *N*-heterocyclic carbene–copper complexes such as Cu(IMes)(DBM) (DBM = dibenzolymethanoate) exhibited high activity (TOF $> 15\,000\ h^{-1}$) and *anti*-selectivity 74% [64]. Several aliphatic and aromatic aldehydes (RCHO, R = Et, *i*-Pr, *t*-Bu, Ph, 2-thienyl etc.) were subjected to conditions employing $(EtO)_2MeSiH$ as the hydride source to result in ca. 70% *anti*-selectivity in 70 ~ 80% yields. Finally, methyl vinyl ketone and acrylonitrile worked well as enolate precursors in additions to CyCHO (Cy = cyclohexyl), providing the corresponding aldol adducts in good yields, 70% (*anti* 64%) and 73% (*anti* 87%).

2.4 In Catalysts

Baba et al. found in 2002 that indium hydride species "In-H" as the stoichiometric reducing agent, generated from $InBr_3$ and *n*-Bu_3SnH, promote conjugate reduction of α,β-unsaturated ketones and subsequent aldol reaction to aromatic aldehydes. The corresponding aldol products were produced with *anti*-selectivity as high as 96% (Scheme 37) [65]. A catalytic variant of this reductive aldol reaction was developed using hydrosilane as reducing agent [66, 67]. The combination of $InBr_3$ (10 mol %) and Et_3SiH (120 mol %) promoted the coupling of enones and aldehydes with levels of *syn*-selectivity as high as 99%. The enones **147** and **149** reacted with *p*-anisaldehyde to give the aldol products **148** in 75% (*syn* : *anti* = 90 : 10) and **150** in 82% (*syn* : *anti* > 99 : 1), respectively. The *syn*-selectivity was explained by the coupling of an indium-(*Z*)-enolate to the aldehyde through a closed six-membered transition state.

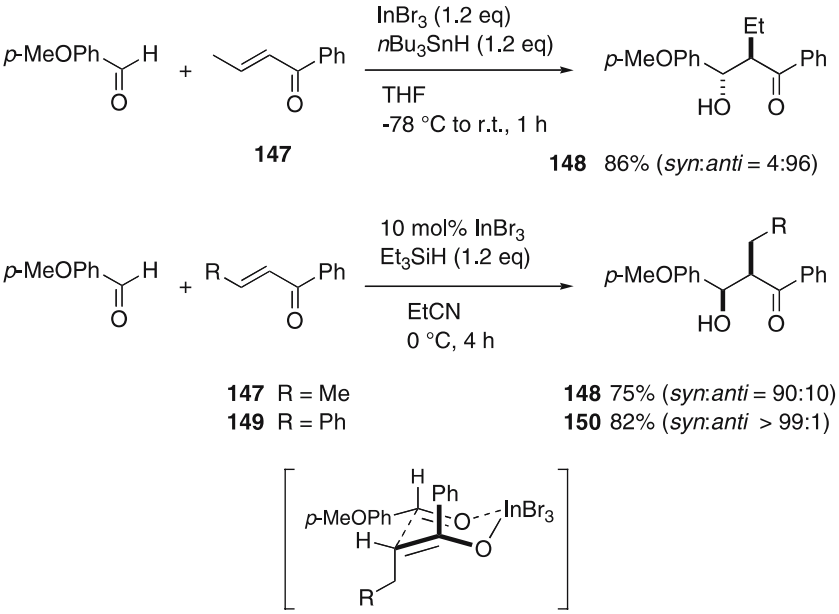

Scheme 37 In-catalyzed reaction

Hosomi et al. reported in 2004 a similar indium-catalyzed reaction employing $In(OAc)_3$ (10 mol %) and $PhSiH_3$ (100 mol %). Under these conditions, the intramolecular coupling of **63** delivers **64** in 90% yield with high *cis*-selectivity (Scheme 38) [68, 69].

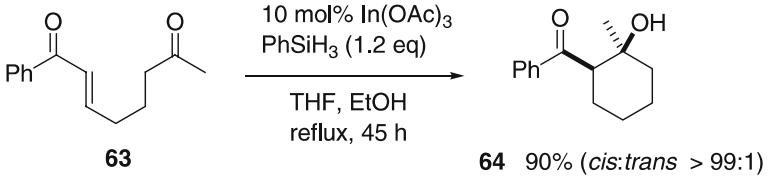

Scheme 38 In-catalyzed intramolecular reaction

3 Reductive Michael Reactions

Intermediate metal enolates generated from conjugate reduction can be trapped by α,β-unsaturated carbonyl functions to give Michael addition products. Krische et al. in 2001 devised an intramolecular Michael reaction of bis(enones) using $Co(dpm)_2$ (5 mol %) and $PhSiH_3$ at 50–70 °C (Scheme 39) [15, 16, 70]. Symmetrical bis(enones) **151** and **153** were subjected to the reductive conjugate addition to provide the cyclization products **152** and **154** in good to excellent yields. Interestingly, the reductive Michael cyclization provides the *trans*-cyclic compounds whereas the *cis* isomers are obtained in the related reductive aldol reaction described in Scheme 8.

Hosomi et al. demonstrated an intramolecular cyclization of the bis(enone) **155** with $In(OAc)_3$ and $PhSiH_3$ to produce *trans*-1,5-diketone **156** in 89% (Scheme 40) [68, 69].

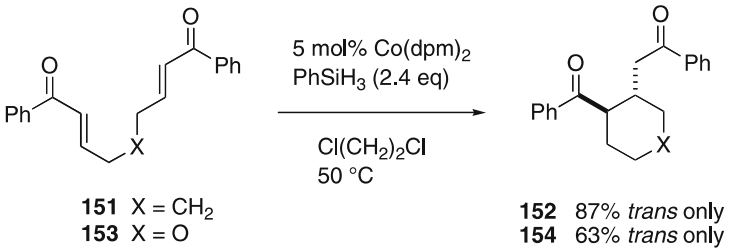

Scheme 39 Co-catalyzed intramolecular Michael reaction

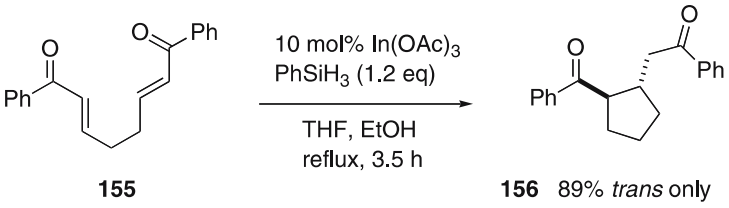

Scheme 40 In-catalyzed Michael reaction

4
Reductive Mannich Reactions

Isayama described the coupling reaction of *N*-methylimine **157** and ethyl crotonate catalyzed by $Co(acac)_2$ and mediated by $PhSiH_3$ to produce Mannich product **158** in 82% with *syn*-selectivity (Scheme 41) [71]. The β-lactam **159** was readily synthesized by heating **158**. In 2002, Matsuda et al. reported cationic Rh complex $[Rh(COD)\{P(OPh)_3\}_2]OTf$ (1 mol %) as an active catalyst for the reductive Mannich reaction [72]. *N*-Tosylaldimine **160** was coupled with methyl acrylate and Et_2MeSiH (200 mol %) at 45 °C to give the β-amino ester **161** in 96% with moderate *anti*-selectivity 68%.

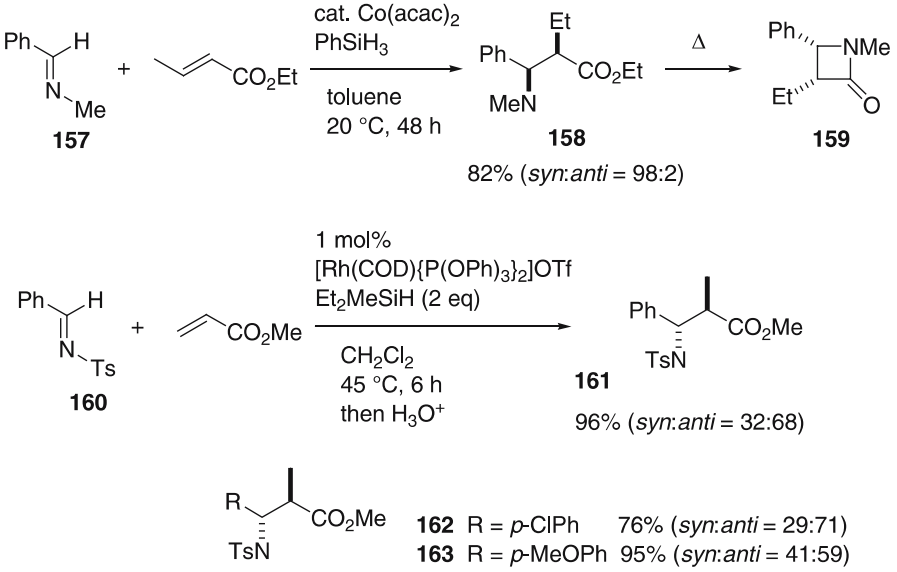

Scheme 41 Co- and Rh-catalyzed Mannich reaction

Morken et al. demonstrated that the combination of $[Ir(COD)Cl]_2$ (2.5 mol %) and $P(OPh)_3$ catalyzed the Mannich reaction of aldimine **164** and trifluorophenyl acrylate **165** at 60 °C. Under these conditions, the initially formed Mannich product undergoes cyclization to furnish the corresponding lactam **166** in 80% with high *trans*-selectivity > 20 : 1 (Scheme 42) [73].

5
Related Reactions

In 1985, Matsuda et al. reported that Rh – H species promote a reaction sequence involving conjugate reduction, aldol type C – C bond formation, and

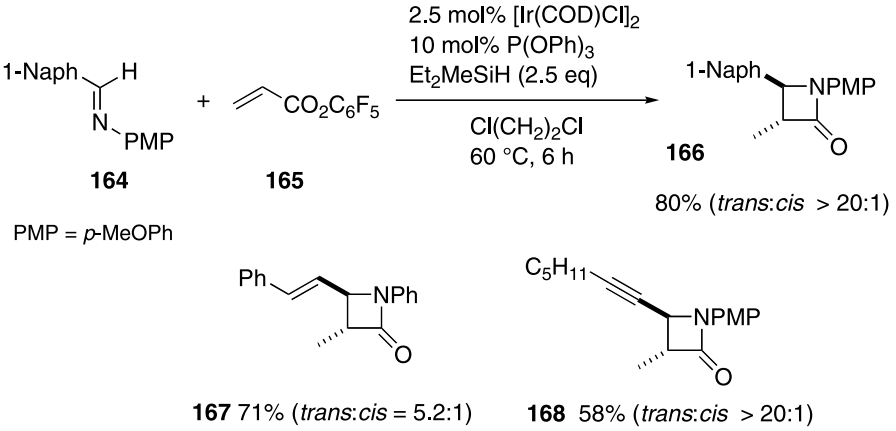

Scheme 42 Ir-catalyzed Mannich reaction

β-hydride elimination to produce Morita–Baylis–Hilman type products [74]. In addition, Ru – H species also were found to work as the same catalyst [75]. For example, the coupling of vinyl methyl ketone and propanal (200 mol %) was catalyzed with $RhH(PPh_3)_4$ (1 mol %) and $RuH_2(PPh_3)_4$ (1 mol %) at 40 °C for 40 h without solvent to form the unsaturated ketone **169** in good yields, 78% and 82%, respectively (Scheme 43). It was proposed that β-hydride elimination from metal-aldolates could release the α,β-unsaturated β′-hydroxy ketones, which were Morita–Baylis–Hilman type products.

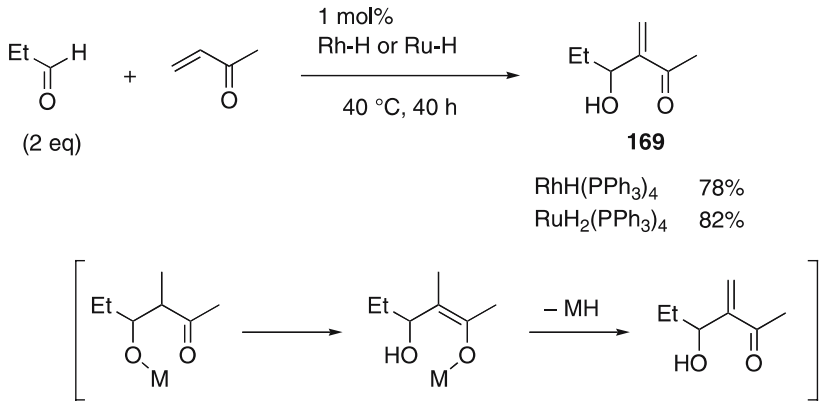

Scheme 43 Rh- and Ru-catalyzed Morita–Baylis–Hilman type reactions

Matsuda et al. applied aryl isocyanates as acceptors in reductive couplings to methyl acrylate (Scheme 44) [77]. The cationic Rh complex $[Rh(COD)\{P(OPh)_3\}_2]OTf$ (1 mol %) and Et_2MeSiH (200 mol %) catalyze the reaction in refluxing CH_2Cl_2 to provide products of hydrocarbamoylation,

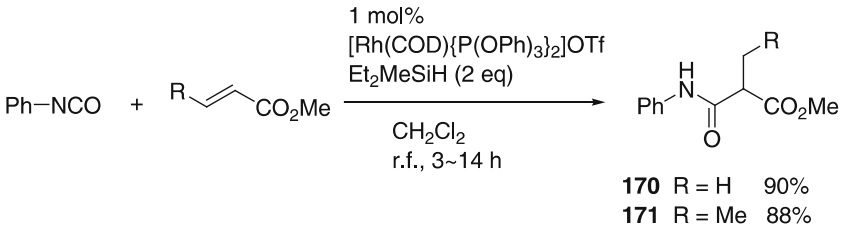

Scheme 44 Rh-catalyzed hydrocarbamoylation

such as **170** and **171**, in high yields. In place of aryl isocyanate, substituted allyl carbonate **172** was subjected to the reductive coupling conditions to deliver hydroallylation products, γ,δ-unsaturated esters, such as **173** and **174** (Scheme 45) [78, 79].

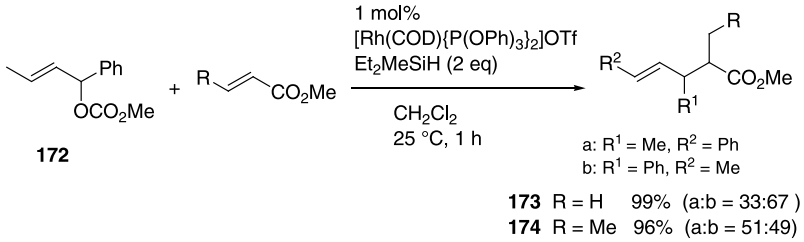

Scheme 45 Rh-catalyzed hydroallylation

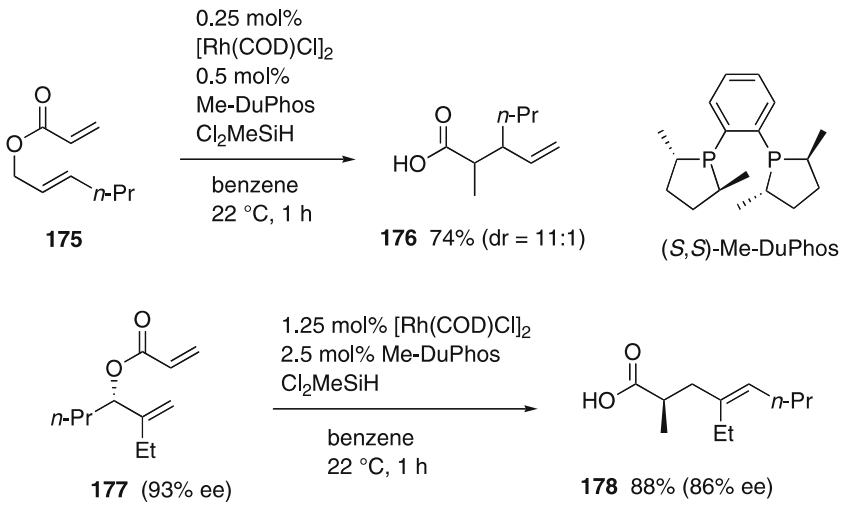

Scheme 46 Rh-catalyzed reductive Claisen rearrangement

Morken et al. developed a reductive Claisen rearrangement of substituted allyl acrylates. The reaction of (*E*)-hex-2-enyl acrylate **175** was catalyzed by $[Rh(COD)Cl]_2$ (0.25 mol %) and Me-DuPhos (0.5 mol %) with Cl_2MeSiH in benzene at 22 °C to give γ,δ-unsaturated ester **176** with high diastereoselectivity, 11 : 1 (Scheme 46) [80]. The reaction was carried out on a 10 g scale to provide a 70% yield of **176**. This reaction was applied to allylic ester **177** to provide **178**, which is a key intermediate in the total synthesis of inostamycin [24].

6 Conclusion

The catalytic reductive aldol reaction, and related reactions involving conjugate reduction mediated by transition metal-hydrides, followed by electrophilic trapping, have been demonstrated to be versatile and reliable synthetic methods. By using α,β-unsaturated carbonyl compounds as enolate precursors in couplings to carbonyl compounds, direct access to β-hydroxy carbonyl derivatives is achieved in a single manipulation. Designed transition metal complexes modified by chiral ligands are capable of catalyzing highly enantio- and diastereoselective aldol couplings, in many cases enabling control of relative and absolute stereochemistry in the formation of multiple contiguous stereogenic centers. We believe, therefore, that the full potential of these reactions will be realized in the future and will serve as practical processes for synthesis of fine chemicals on an industrial scale.

References

1. Mukaiyama T (1982) Org React 28:203
2. Mahrwald R (1999) Chem Rev 99:1095
3. Mahrwald R (ed) (2004) Modern aldol reactions. Wiley-VCH, Weinheim
4. Revis A, Hilty TK (1987) Tetrahedron Lett 28:4809
5. Sato S, Matsuda I, Izumi Y (1986) Tetrahedron Lett 27:5517
6. Reetz MT, Vouggioukas AE (1987) Tetrahedron Lett 28:793
7. Nishiyama H, Motoyama Y (1999) In: Yamamoto H (ed) Lewis acid reagents. Oxford University Press, Oxford, pp 225–243
8. Kündig EP, Saudan CM (2000) In: Yamamoto H (ed) Lewis acids in organic synthesis, vol 2. Wiley, Weinheim, pp 597–652
9. Isayama S, Mukaiyama T (1989) Chem Lett:2005
10. Matsuda I, Takahashi K, Sato S (1990) Tetrahedron Lett 31:5331
11. Matsuda I (2005) In: Evans PA (ed) Modern rhodium-catalyzed organic reactions. Wiley, Weinheim, pp 111–128
12. Taylor SJ, Morken JP (1999) J Am Chem Soc 121:12202
13. Zhao CX, Bass J, Morken JP (2001) Org Lett 3:2839
14. Baik TG, Luis AL, Wang LC, Krische MJ (2001) J Am Chem Soc 123:5112

15. Wang LC, Uang HY, Roh Y, Lynch V, Schultz AJ, Wang X, Krische MJ (2002) J Am Chem Soc 124:9448
16. Huddleston RR, Krische MJ (2003) Synlett, p 12
17. Freiría M, Whitehead AJ, Tocher DA, Motherwell WB (2004) Tetrahedron 60:2673
18. Emiabata-Smith D, McKillop A, Mills C, Motherwell WB, Whitehead AJ (2001) Synlett, p 1302
19. Freiría M, Whitehead AJ, Motherwell WB (2005) Synthesis:3079
20. Willis MC, Woodward RL (2005) J Am Chem Soc 127:18012
21. Taylor SJ, Duffey MO, Morken JP (2000) J Am Chem Soc 122:4528
22. Russell AE, Fuller NO, Taylor SJ, Aurriset P, Morken JP (2004) Org Lett 6:2309
23. Fuller NO, Morken JP (2005) Synlett, p 1459
24. Fuller NO, Morken JP (2005) Org Lett 7:4867
25. Zhao CX, Duffey MO, Taylor SJ, Morken JP (2001) Org Lett 3:1829
26. Duffey MO, LeTiran A, Morken JP (2003) J Am Chem Soc 125:1458
27. Nishiyama H, Shiomi T, Tsuchiya Y, Matsuda I (2005) J Am Chem Soc 127:6972
28. Ito J, Shiomi T, Nishiyama H (2006) Adv Synth Chem 348:1235
29. Shiomi T, Ito J, Yamamoto Y, Nishiyama H (2006) Eur J Org Chem 24:5594
30. Shiomi T, Nishiyama H (2007) Org Lett (in press)
31. Jang HY, Huddleston RR, Krische MJ (2002) J Am Chem Soc 124:151157
32. Jang HY, Krische MJ (2004) Acc Chem Res 37:653
33. Jang HY, Krische MJ (2004) Eur J Org Chem 19:3953
34. Huddleston RR, Krische MJ (2003) Org Lett 5:1143
35. Marriner GA, Garner SA, Jang HY, Krische MJ (2004) J Org Chem 69:1380
36. Koech PK, Krische MJ (2004) Org Lett 6:691
37. Jung CK, Garner SA, Krische MJ (2006) Org Lett 8:519
38. Han SB, Krische MJ (2006) Org Lett 8:5657
39. Jung CK, Krische MJ (2006) J Am Chem Soc 128:17051
40. Kiyooka S, Shimizu A, Torii S (1998) Tetrahedron Lett 39:5237
41. Miyabe H, Asada R, Takemoto Y (2005) Tetrahedron 61:385
42. Mahoney WS, Stryker JM (1989) J Am Chem Soc 110:291
43. Chiu P, Chen B, Cheng KF (1998) Tetrahedron Lett 39:9229
44. Chiu P, Szeto CP, Geng Z, Cheng KF (2001) Tetrahedron Lett 42:4091
45. Chiu P, Szeto CP, Geng Z, Cheng KF (2001) Org Lett 3:1901
46. Lipshutz BH, Chrisman W, Noson K, Papa P, Sclafani JA, Vivian RW, Keith JM (2000) Tetrahedron 56:2779
47. Lipshutz BH, Papa P (2002) Angew Chem Int Ed 41:4580
48. Evans DA, Fu GC (1990) J Org Chem 55:5678
49. Huddleston RR, Cauble DF, Krische MJ (2003) J Org Chem 68:11
50. Ooi T, Doda K, Saki D, Maruoka K (1999) Tetrahedron Lett 40:2133
51. Chiu P, Leung SK (2004) Chem Commun, p 2308
52. Chiu P (2004) Synthesis:2210
53. Chung WK, Chiu P (2005) Synlett, p 55
54. Lam HW, Joensuu PM (2005) Org Lett 7:4225
55. Lam HW, Murray GJ, Firth JD (2005) Org Lett 7:5743
56. Lam HW, Joensuu PM, Murray GJ, Fordyce EA, Prieto O, Luebbers T (2006) Org Lett 8:3729
57. Deschamp J, Chuzel O, Hannedouche J, Riant O (2006) Angew Chem Int Ed 45:1292
58. Mori A, Fujita A (1997) Chem Commun, p 2159
59. Mori A, Fujita A, Kaniro H, Nishihara Y, Hiyama T (1999) Tetrahedron 55:4573
60. Ito H, Ishizuka T, Arimoto K, Miura K, Hosomi A (1999) Tetrahedron Lett 38:8887

61. Zhao D, Oisaki K, Kanai M, Shibasaki M (2006) Tetrahedron Lett 47:1403
62. Zhao D, Oisaki K, Kanai M, Shibasaki M (2006) J Am Chem Soc 128:14440
63. Chuzel O, Deschamp J, Chausteur C, Riant O (2006) Org Lett 8:5943
64. Welle A, Díez-González S, Tinant B, Nolan SP, Riant O (2006) Org Lett 8:6059
65. Inoue K, Ishida T, Shibata I, Baba A (2002) Adv Synth Catal 344:283
66. Shibata I, Kato H, Ishida T, Yasuda M, Baba A (2004) Angew Chem Int Ed 43:711
67. Baba A, Shibata I (2005) Chem Rec 5:323
68. Miura K, Yamada Y, Tomita M, Hosomi A (2004) Synlett, p 1985
69. Suwa T, Nishino K, Miyatake M, Shibata I, Baba A (2000) Tetrahedron Lett 41:3403
70. Baik TG, Luis AL, Wang LC, Krische MJ (2001) J Am Chem Soc 123:6716
71. Isayama S (1992) J Synth Org Chem 50:190
72. Muraoka T, Kamiya S, Matsuda I, Itoh K (2002) Chem Commun, p 1284
73. Townes JA, Evans MA, Queffelec J, Taylor SJ, Morken JP (2002) Org Lett 4:2537
74. Sato S, Matsuda I, Izumi Y (1985) Chem Lett:1875
75. Matsuda I, Shibata M, Sato S (1988) J Organometal Chem 340:C5
76. Sato S, Matsuda I, Shibata M (1989) J Organometal Chem 377:347
77. Muraoka T, Matsuda I, Itoh K (2001) Organometallics 20:4676
78. Muraoka T, Matsuda I, Itoh K (2000) J Am Chem Soc 122:9552
79. Muraoka T, Matsuda I, Itoh K (2000) Tetrahedron Lett 41:8807
80. Miller SP, Morken JP (2002) Org Lett 4:2743

Top Curr Chem (2007) 279: 139–172
DOI 10.1007/128_2007_136

Published online: 2 June 2007

Recent Advances in Alkene Hydroformylation

Bernhard Breit

Institut für Organische Chemie und Biochemie, Albert-Ludwigs Universität Freiburg, Albertstr. 21, 79104 Freiburg im Breisgau, Germany
bernhard.breit@chemie.uni-freiburg.de

Abstract Recent advances in synthetic aspects of the rhodium-catalyzed hydroformylation of alkenes are reviewed. Emphasis is given to practical improvements, efficient new catalysts for regioselective and enantioselective hydroformylation, and to applications of the reaction in organic synthesis. Furthermore, new developments in directed hydroformylation are covered as well as new approaches toward efficient hydroformylation catalysts employing the concept of self-assembly.

1 Introduction

The hydroformylation of alkenes, which was originally discovered by Otto Roelen in 1938 [1], has developed into one of the most important applications of homogeneous catalysis in industry (Scheme 1) [2, 3]. Today, more than 9 million tons of so-called oxo-products are produced per year, a number which is still rising continuously. The majority of these oxo-products stem

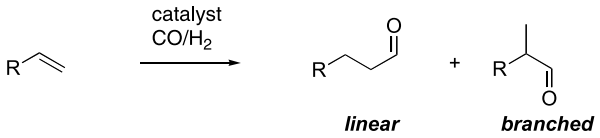

Scheme 1 Hydroformylation of alkenes

from hydroformylation of propene, which is a fraction of the steam-cracking process. The resulting products *n*-butanal and isobutyraldehyde are important intermediates for the production of esters and acrylates etc. [2].

From a synthetic point of view the reaction is a one-carbon chain elongation caused by the addition of carbon monoxide and hydrogen across the π system of a C = C double bond [4–6]. As a pure addition reaction, the hydroformylation reaction meets all requirements of an atom economic process [7, 8]. Furthermore, the synthetically valuable aldehyde function is installed which allows for subsequent skeleton expanding operations, which may even be achieved in one-pot sequential transformations [5, 6, 9]. As an industrially important process hydroformylation in all of its facets has been reviewed many times [2–6, 9–26]. This review will focus on the most recent progress in application of hydroformylation in organic synthesis, for which selectivity control is a major aspect. The review separates traditional ways of selectivity control through application of improved catalysts based on classical ligand modifications (Sects. 2 to 5) from new concepts for selectivity control in the course of hydroformylation (Sects. 6 and 7). The latter include approaches such as directed hydroformylation employing substrate-bound catalyst-directing groups as well as new and selective catalysts through self-assembly [6, 27, 28].

2
Chemoselective Hydroformylation of Internal Alkenes

In 1968 Wilkinson discovered that phosphine-modified rhodium complexes display a significantly higher activity and chemoselectivity compared to the first generation cobalt catalyst [29]. Since this time ligand modification of the rhodium catalyst system has been the method of choice in order to influence catalyst activity and selectivity [10].

Despite significant research efforts in the past, one of the remaining problems to be solved in industry is the chemoselective (and simultaneously regioselective) low-pressure hydroformylation of internal alkenes. The problem originates from the exponential drop of alkene reactivity with increasing number of alkene substituents. The known hydroformylation catalysts for internal alkene hydroformylation operating under low-pressure conditions rely on the use of strong π-acceptor ligands, such as bulky

phosphites and phosphabenzene systems [30–35]. However, the high hydroformylation activity of the corresponding rhodium catalysts is always associated with a high tendency toward alkene isomerization, which renders a position-selective hydroformylation of an internal alkene so far impossible.

Recently, a new class of phosphabarrelene/rhodium catalysts has been developed, which for the first time allows for hydroformylation of internal alkenes with very high activity and which proceeds essentially free of alkene isomerization [36–38]. Two examples, results of hydroformylation of an acyclic and a cyclic internal alkene substrate, are depicted in Scheme 2.

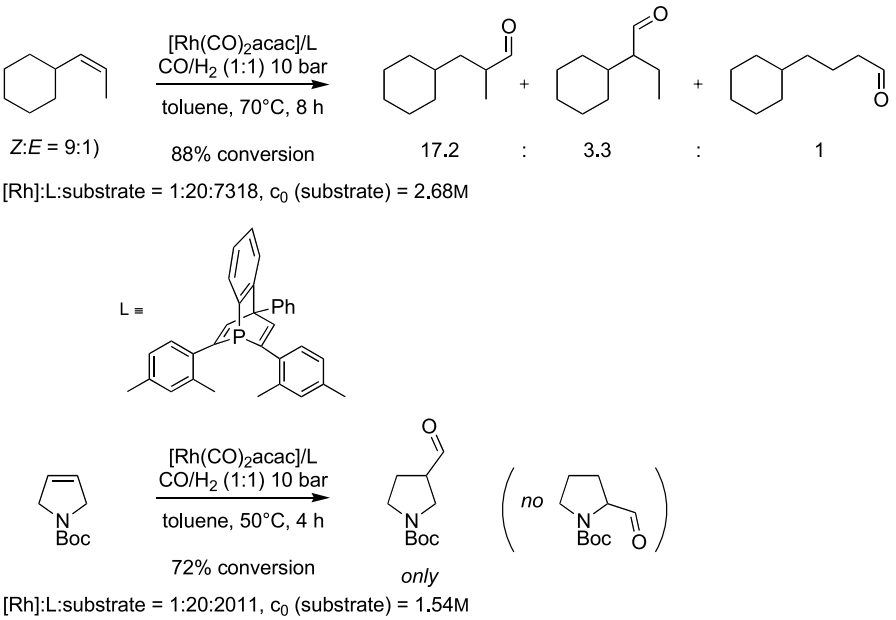

Scheme 2 Position-selective hydroformylation of internal alkenes with a rhodium(I)/-phosphabarrelene catalyst

3 Regioselective Hydroformylation

The regioselectivity of the hydroformylation of alkenes is a function of many factors. These include inherent substrate preferences, directing effects exerted by functional groups as part of the substrate, as well as catalyst effects. In order to appreciate substrate inherent regioselectivity trends, alkenes have to be classified according to the number and nature of their substitution pattern (Scheme 3) [4].

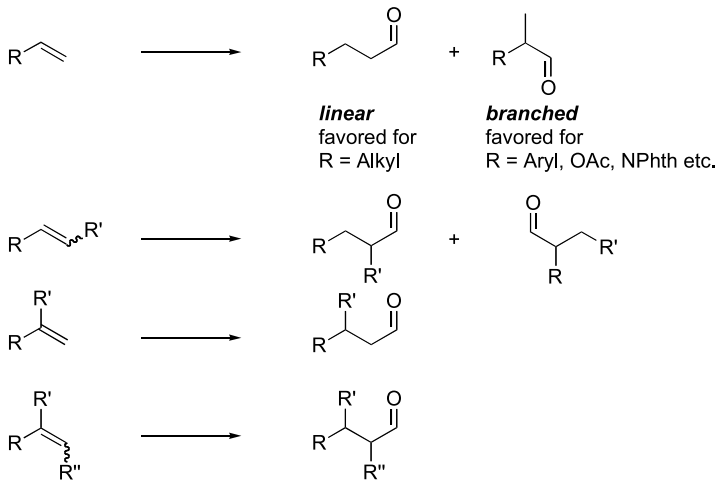

Scheme 3 Regioselectivity trends on hydroformylation of different alkene classes

The problem of regioselectivity arises in general only for terminal and 1,2-disubstituted alkenes. For alkyl-substituted terminal alkenes there is a slight preference for the linear product. Today good solutions for the selective formation of linear aldehydes employing tailor-made bidentate (this chapter) or self-assembled ligands exist (Sect. 7). For terminal alkene functions attached to an inductively electron-withdrawing substituent the branched regioisomer is preferred, and sometimes even the exclusive product. This tendency is more or less unaffected by the catalyst structure. Both 1,1-disubstituted and trisubstituted alkenes generally provide only one regioisomer based on Keuleman's rule, which states that the formyl group is attached such as to avoid the formation of a quaternary carbon center [39].

3.1 Branched-Regioselective Hydroformylation

Most recently new applications for substrate-controlled branched-selective hydroformylation of alkenes substituted with inductively electron-with drawing substituents have emerged. A recent example is the hydroformylation of acrylamide with a standard rhodium/triphenylphosphine catalyst, which yields the branched aldehyde exclusively (Scheme 4) [40]. Reduction of the aldehyde function furnishes 3-hydroxy-2-methylpropionamide, which is an intermediate en route to methyl methacrylate.

Branched-regioselective hydroformylation of unsaturated esters has been achieved [41]. The use of the phosphaadamantane ligand **1**, which is readily available from acetylacetone and phenylphosphine (Eq. 1), proved particularly useful in terms of reaction rate, regio-, and chemoselectivity [42–44].

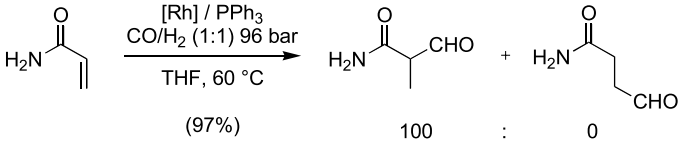

Scheme 4 Branched-regioselective hydroformylation of acrylamide

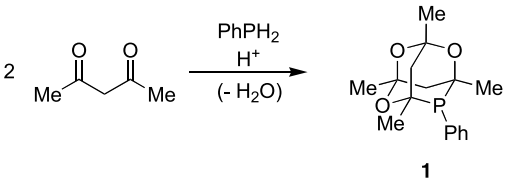

Equation 1

Hydroformylation of a range of 1,1-di- and 1,1,2-trisubstituted unsaturated esters yields quaternary aldehydes (Table 1, entries 1–8). Hence, the regiochemistry-directing influence of the electron-withdrawing ester function overcompensates Keuleman's rule. Furthermore, hydroformylation of 1,2-disubstituted unsaturated esters occurred with high α-selectivity and chemoselectivity (Table 1, entries 9 and 10). As a side reaction hydrogenation of the alkene has been observed [41].

Table 1 Results of branched-selective hydroformylation of α,β-unsaturated esters with a rhodium/phosphaadamantane (**1**) catalyst

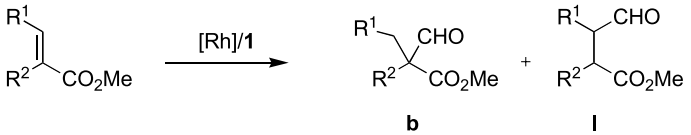

Entry	R^1	R^2	**b**ranched	**l**inear
1	H	Me	50	1
2	H	Ph	> 100	1
3	H	MeO_2CCH_2	99	1
4	H	$NC(CH_2)_2$	22	1
5	H	$MeO_2C(CH_2)_2$	56	1
6	Me	*n*-Pr	10	1
7	Me	Ph	7.5	1
8	Me	Me	48	1
9	Me	H	> 100	1
10[a]	Ph	H	6	1

[a] 16% hydrogenation

From a library of mixtures of monodentate ligands an excellent catalyst for branched-selective hydroformylation of methacrylic esters was identified (Scheme 5) [45]. The best catalyst employs a 1:1 mixture of triphenylphosphine and a phosphabenzene ligand **2** [32].

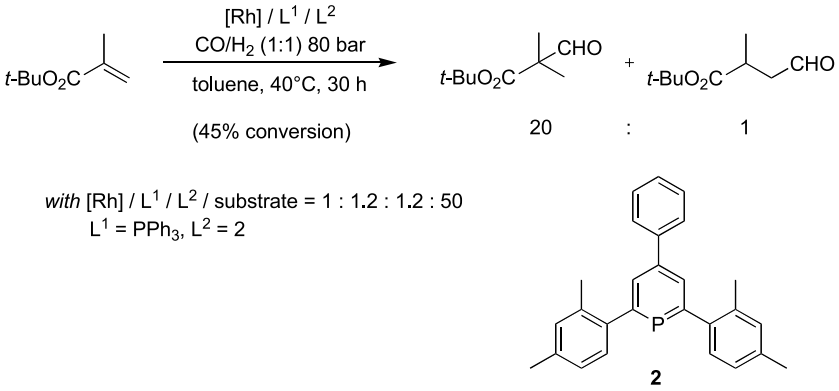

Scheme 5

On hydroformylation of styrene derivatives, in general high regioselectivity in favor of the branched regioisomeric aldehyde is observed [4]. This has been used in order to develop a useful synthetic access to indoles from *o*-haloanilines by employing a two-step sequence consisting of a Heck coupling with allylic amine derivatives and a branched-selective hydroformylation step (Scheme 6). A variety of tryptamines and tryptophols have been prepared according to this protocol [46].

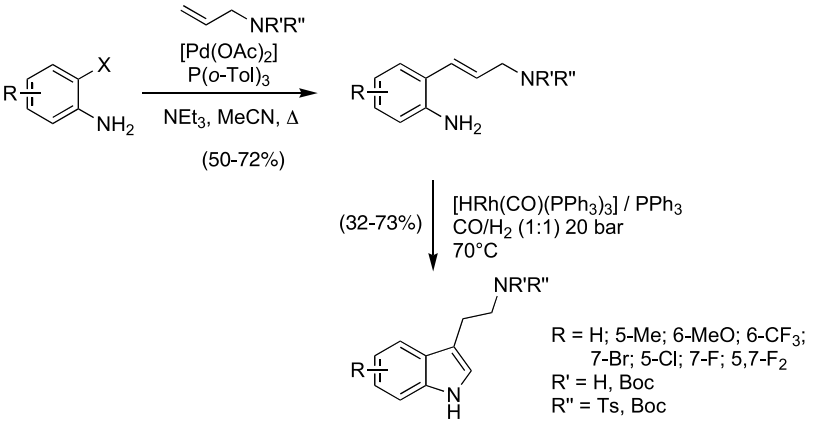

Scheme 6 Indoles from *o*-haloanilines: synthesis of tryptamines and tryptophols via regioselective hydroformylation of functionalized anilines

3.2
Linear-Regioselective Hydroformylation

Alkyl-substituted terminal alkenes favor upon hydroformylation the linear regioisomer. This regiochemical preference originates from steric interactions in the course of the selectivity-determining hydrometalation step [4]. In the case of sterically demanding alkyl substituents, regioselecitivities may become very high without employing catalyst/ligand control. A recent example is a sequential regioselective hydroformylation/intramolecular aldol addition (Scheme 7) [47, 48]. Simple diastereoselectivity in the course of the aldol addition reaction was observed. In the case of silyl enol ether derivative **3**, a *Z*-rhodium enolate reacting via a Zimmerman–Traxler transition state furnishes the *syn*-aldol **4**. Conversely, employing the preformed *E*-configured boron enolate **5** furnished the *anti*-aldol **6**.

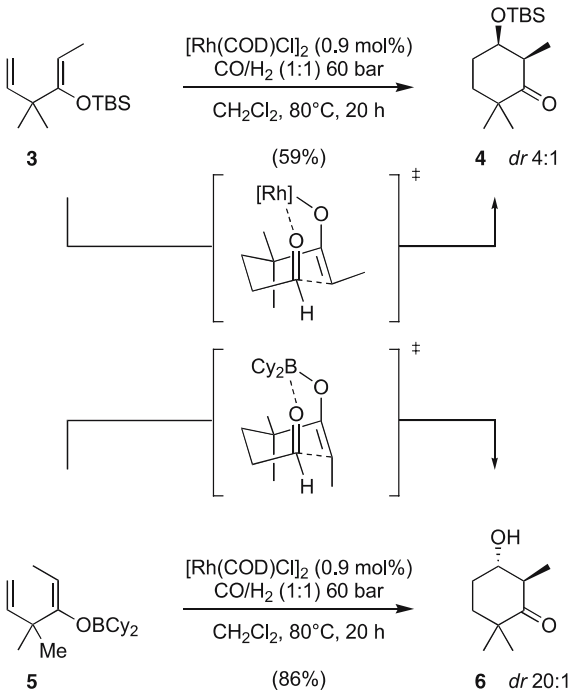

Scheme 7

Much progress has been made on regioselective hydroformylation of terminal alkenes in favor of the linear product. In particular bidentate phosphine or phosphite ligands, which have a natural bite angle θ of about 110°, will favor the linear product. The most successful ligand types are BISBI [49, 50], BIPHEPHOS [51, 52], and XANTPHOS systems (Scheme 8) [53].

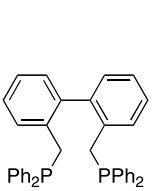

BISBI
l:b = 66 : 1 for 1-hexene

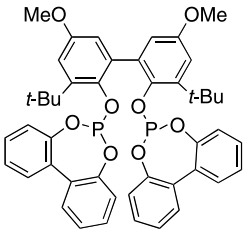

BIPHEPHOS
l:b > 40 : 1 for a wide range of alkenes

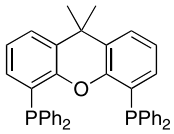

XANTPHOS
l:b = 53 : 1 for 1-octene

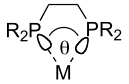

θ = Natural Bite Angle

Scheme 8 Bidentate ligands for regioselective hydroformylation of terminal alkenes

Recently, a new bidentate hemispherical chelating bisphosphite ligand based on a calixarene backbone has been designed for linear selective hydroformylation of alkenes (Scheme 9) [54]. Excellent levels of regioselectivity have been observed, and even the intrinsic branched-selective hydroformylation of styrene could be overruled by this system. However, the system suffers from low catalytic activity.

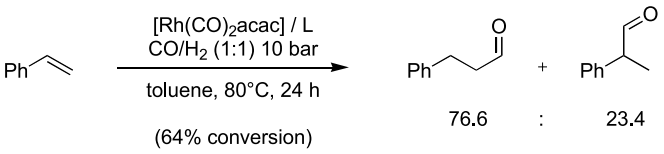

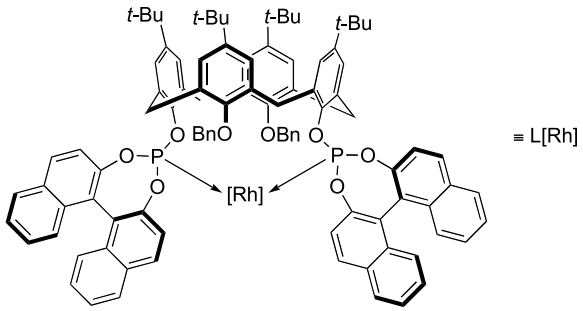

Scheme 9

Two recent exemplary applications in organic synthesis employing either a rhodium(I)/BIPHEHOS or a rhodium(I)/XANTPHOS catalyst to achieve a linear-regioselective hydroformylation of terminal alkenes are summarized in Schemes 10 and 11. The hydroformylation of an aldehyde allylation product has served as a key step during the course of a synthesis of a BC-ring subunit of the anticancer agent bryostatin (Scheme 10) [55].

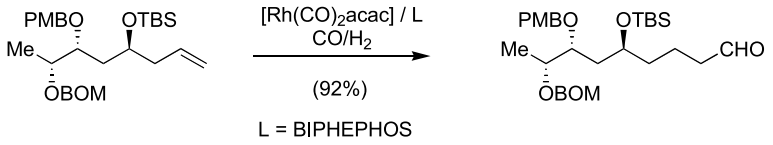

Scheme 10

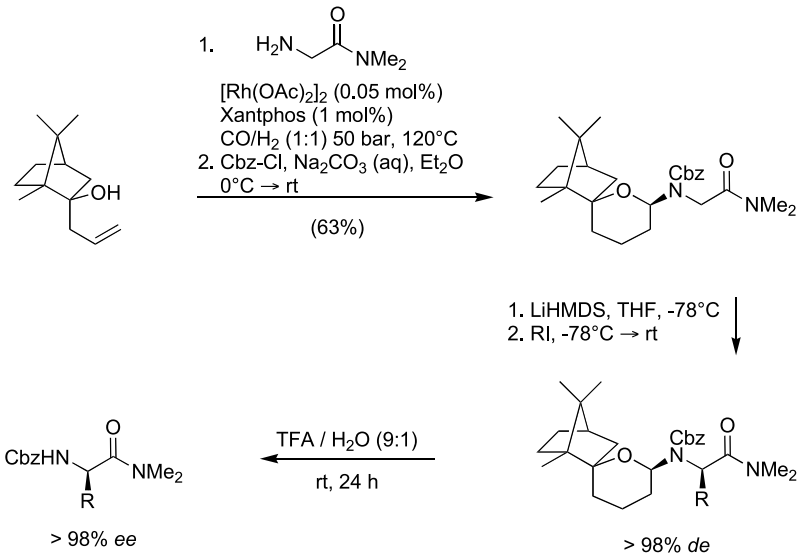

Scheme 11

A new chiral auxiliary based on a camphor-derived δ-lactol has been developed for the stereoselective alkylation of glycine enolate in order to give enantiomerically pure α-amino acid derivatives. As a key step for the synthesis of this useful auxiliary has served the *n*-selective hydroformylation of a homoallylic alcohol employing the rhodium(I)/XANTPHOS catalyst (Scheme 11) [56].

Hydroformylation of alkenes can be carried out in a few minutes under microwave activation at a relatively low pressure (2.7 bar) employing the rhodium(I)/XANTPHOS catalyst. The presence of the ionic liquid butylmethylimdazolium tetrafluoroborate ([bmim][BF_4]) was crucial. Unfortu-

nately, a relatively high catalyst loading is required (Scheme 12) [57]. A significantly more active catalyst which allows for room-temperature, ambient-pressure, regioselective hydroformylation of terminal alkenes is obtained with self-assembly ligands based on hydrogen bonding (see Sect. 7.1).

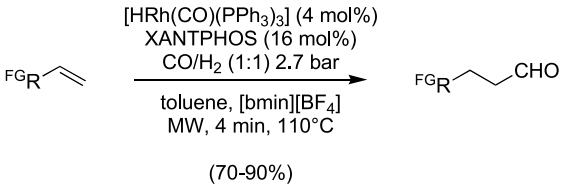

Scheme 12

A variant of the BISBI ligand system is the NAPHOS ligand, which as expected gives similar levels of *n*-selectivity in the course of the hydroformylation of terminal alkenes. Interesting is a hydroformylation in the presence of secondary amines which allows a mild and selective one-pot hydroformylation/enamine formation (Scheme 13) [58].

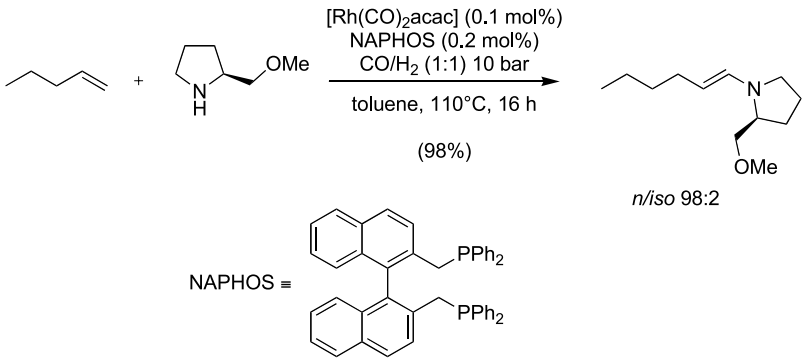

Scheme 13

Increasing the hydrogen partial pressure enables a subsequent enamine/immonium hydrogenation and thus leads to an *n*-regioselective hydroaminomethylation of terminal alkenes. In this case the optimal results were obtained with the rhodium(I)/XANTPHOS catalyst (Scheme 14) [59].

The reaction can be combined with an alkene isomerization, which requires the use of the more electron-withdrawing XANTPHENOXAPHOS ligand. Thus, starting from internal alkenes, linear amines can be obtained in quite reasonable yields and high *n*/*iso* selectivity (Scheme 15) [60].

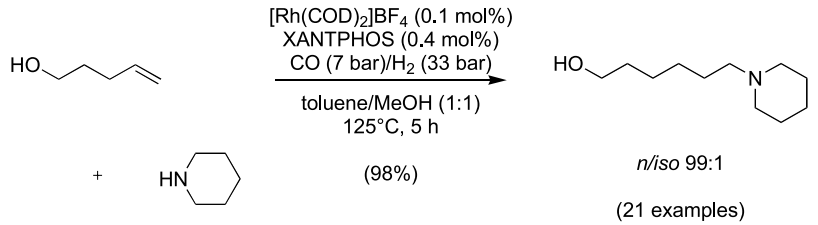

Scheme 14

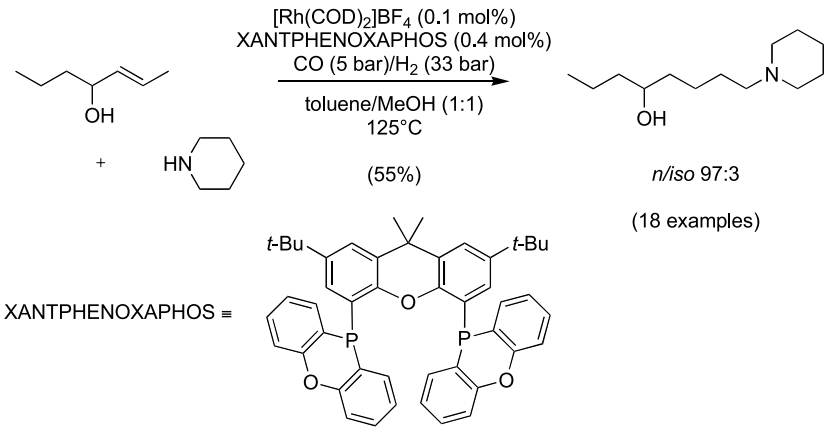

Scheme 15

An interesting one-pot hydroformylation/Fischer indole sequence can be achieved by running the hydroformylation in the presence of a phenylhydrazine. This protocol gave access to the methyl ester of the plant growth regulator 3-indole butanoic acid (IBA) (Scheme 16) [61–63]. A review on related tandem processes involving the hydroformylation as a key step has appeared recently [9].

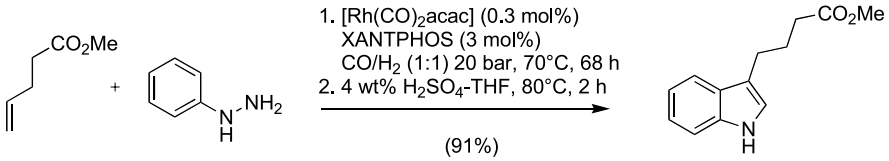

Scheme 16

4
Diastereoselective Hydroformylation

Diastereoselective hydroformylation can be achieved in special cases through "passive" substrate control in which conformational preferences are transferred in the corresponding selectivity-determining hydrometalation step [4–6]. A recent example is the highly diastereoselective hydroformylation of a kainic acid derivative (Scheme 17) [64]. The selective formation of the major diastereomer has been explained via a reactive substrate conformation in which allylic 1,2-strain has been minimized. In this situation the *cis*-positioned methylene carbonylmethoxy group controls the catalyst attack to occur from the si face exclusively.

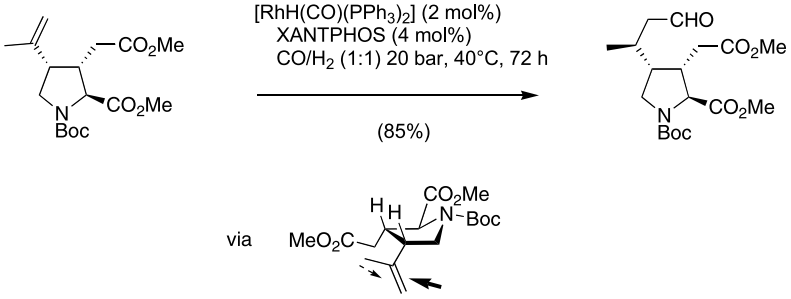

Scheme 17 Diastereoselective hydroformylation of a kainic acid derivative relying on passive substrate control

Alternatively, substrate control of diastereoselectivity can rely on attractive catalyst substrate interactions. This requires in general special functional groups which allow for a directed hydroformylation, which is summarized in Sect. 6 (vide infra).

5
Enantioselective Hydroformylation

Many chiral diphosphine ligands have been evaluated with regard to inducing enantioselectivity in the course of the hydroformylation reaction [25, 26]. However, a real breakthrough occurred in 1993 with the discovery of the BINAPHOS ligand by Takaya and Nozaki [65]. This was the first efficient and rather general catalyst for the enantioselective hydroformylation of several classes of alkenes, such as aryl alkenes, 1-heteroatom-functionalized alkenes, and substituted 1,3-dienes, and is still a benchmark in this area [66, 67]. But still a major problem in this field is the simultaneous control of enantio-

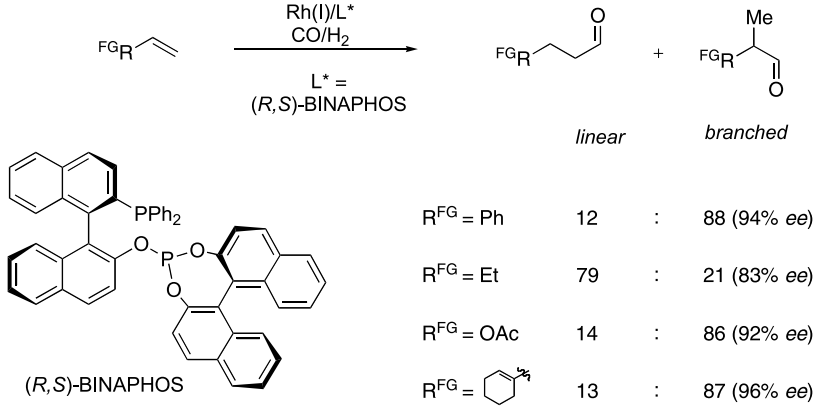

Scheme 18

and regioselectivity, which limits the structural variety of suitable alkenes for enantioselective hydroformylation significantly (Scheme 18).

Second generation BINAPHOS-type ligands have been developed recently. Placing 3-methoxy substituents on the aryl phosphine unit furnishes a catalyst which allows for an enantioselective hydroformylation of vinylfurans (Scheme 19) [68].

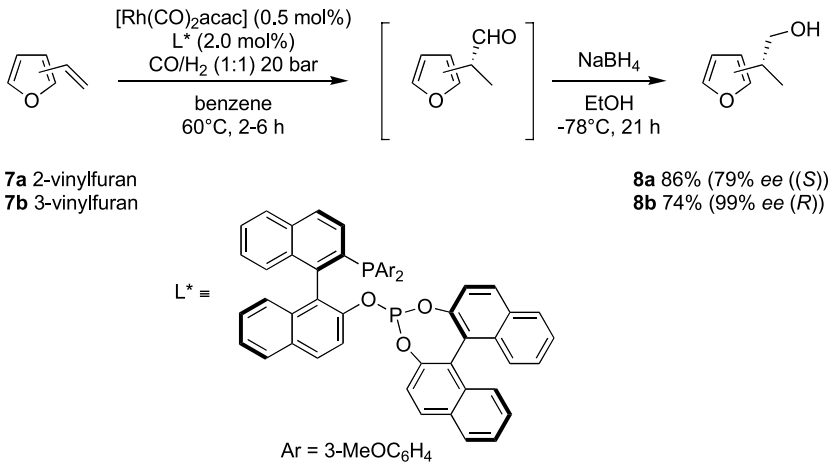

Scheme 19

A new structural feature is obtained by replacement of the phosphite donor within BINAPHOS by a phosphoramidite system. Improved enantioselectivities were noted, albeit the problem of regioselectivity persists (Scheme 20) [69].

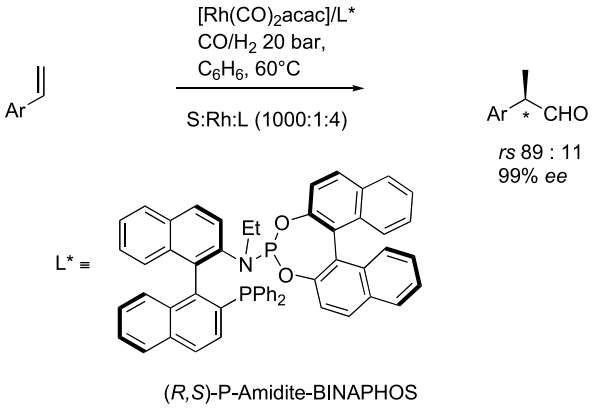

Scheme 20

A set of 47 phosphorus-based chiral ligands, which are known as efficient ligands for asymmetric hydrogenation, were evaluated in asymmetric hydroformylation. Most of the ligands exhibited poor enantio- and regioselectivity as well as low catalyst activity. However, two ligands, (*S*)-Binapine and (*S*,*S*,*R*,*R*)-TangPhos, were found to give excellent enantioselectivities for hydroformylation of styrene, allyl cyanide, and vinyl acetate (Scheme 21). (*S*)-Binapine gave 94, 94, and 87% *ee*, whereas (*S*,*S*,*R*,*R*)-TangPhos gave 90, 93, and 83% *ee* for hydroformylation products of styrene, allyl cyanide, and vinyl acetate, respectively. The enantioselectivities achieved for the allyl cyanide product with these ligands are the highest ever reported for this substrate [70].

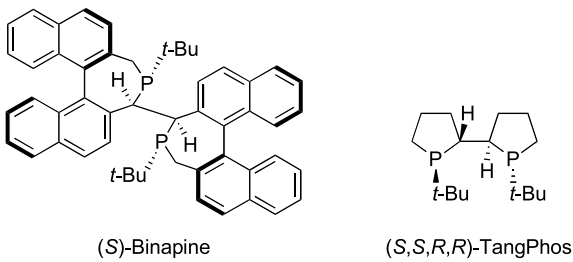

Scheme 21

The discovery of the bisphospholane scaffold as a new privileged structure for asymmetric induction in alkene hydroformylation has triggered research for new and improved bisphospholane-type ligands. In this context (*R*,*R*)-Ph-bpe has been identified as an excellent ligand for asymmetric hydroformylation, which gives state-of-the-art regio- and enantioselectivities

for styrene, allyl cyanide, and vinyl acetate, while maintaining commercially viable turnover rates over 4000 h^{-1} at 80 °C (Scheme 22) [71].

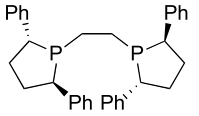

(*R*,*R*)-Ph-bpe

styrene **b**:**l** = 45:1, 94% ee (57% conversion)
allyl cyanide **b**:**l** = 7.1:1, 90% *ee* (96% conversion)
vinyl acetate **b**:**l** = 340:1, 82% *ee* (52% conversion)

all reactions at 80°C, CO/H_2 (1:1) 10 bar,
Rh:L:substrate = 1:1.2:5000, c (catalyst) = 0.037 mol%

Scheme 22

Related systems are the bis-diazaphospholane ligands of which ESPHOS has proved optimal. Best results were obtained upon hydroformylation of vinyl acetate with *ee* values up to 89% for the branched lactaldehyde acetate (Scheme 23) [72]. Even more efficient variations are bis-3,4-diazaphospholane ligands, which furnished up to 96% *ee* upon hydroformylation of vinyl acetate [73].

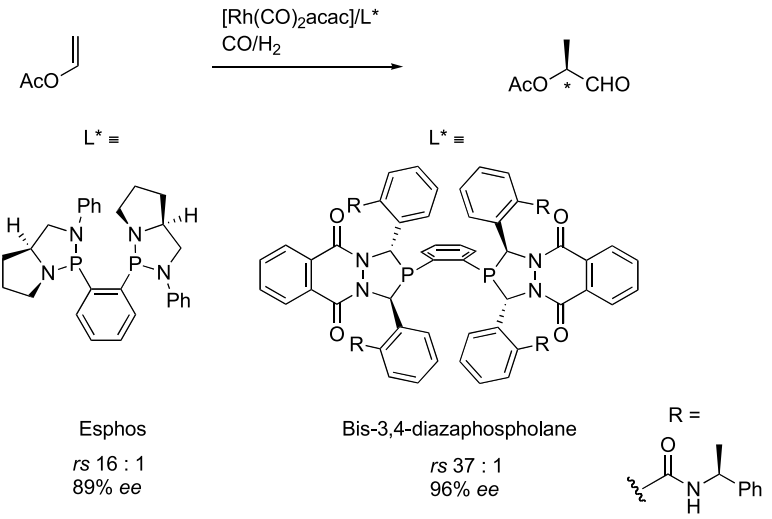

Scheme 23

The major problem remains control of regioselectivity in favor of the branched regioisomer. While aryl alkenes as well as heteroatom-substituted alkenes favor the chiral branched isomer, for aliphatic alkenes such an intrinsic element of regiocontrol is not available. As a matter of fact branched-selective and asymmetric hydroformylation of aliphatic alkenes stands as an unsolved problem. In this respect regio- and enantioselective hydroformy-

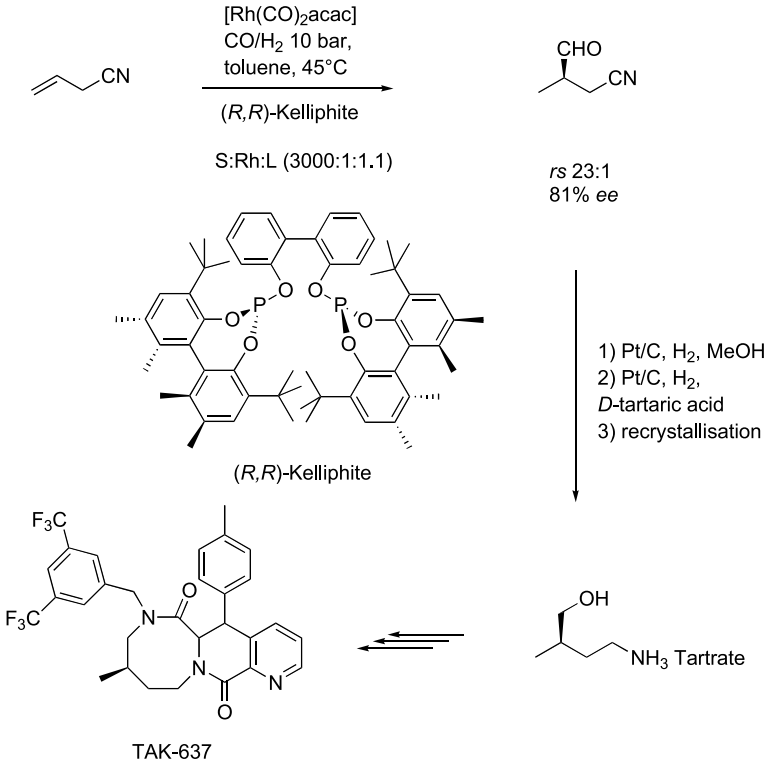

Scheme 24

lation of allyl cyanide employing a chiral bisphosphite(Kelliphite)/rhodium catalyst is a remarkable result (Scheme 24) [74]. After successive reduction of aldehyde and nitrile function the resulting amino alcohol could serve as a potential intermediate for the construction of TAK-637, a compound in development at Takeda Chemical Industries for urinary continence.

The asymmetric hydroformylation of a 1,3-diene has been recently used in the course of a total synthesis of the antifungal natural product ambruticin. The retrosynthesis as well as the hydroformylation key step are depicted in Scheme 25 [75].

6
Directed Hydroformylation

Although significant progress in the field of asymmetric hydroformylation has been made, it is limited to a rather narrow substrate scope. An alternative approach to a stereoselective hydroformylation might employ substrate control of a chiral alkenic starting material. Of particular use

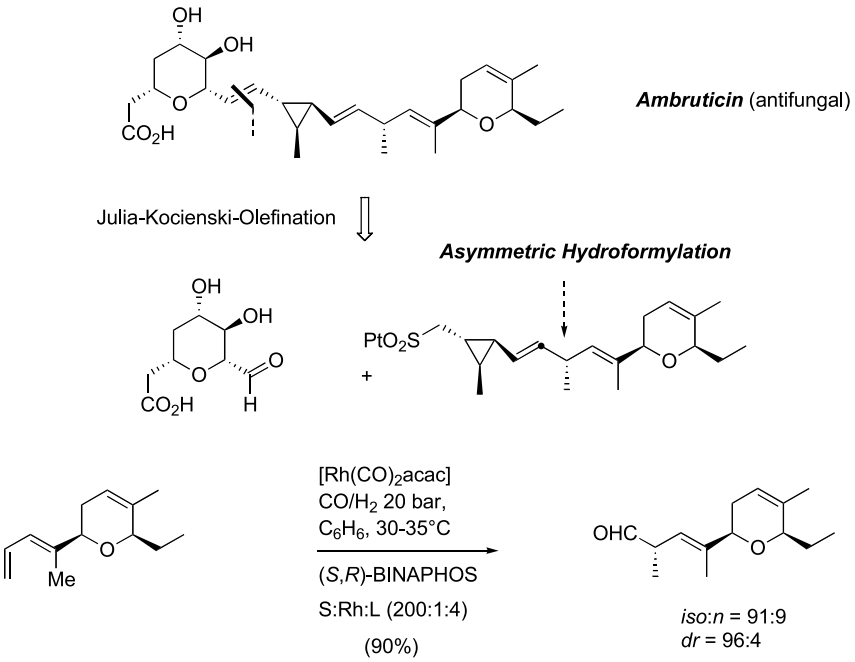

Scheme 25

have proved directed hydroformylation variants making use of attractive substrate–catalyst interactions by way of substrate-bound catalyst-directing groups (Scheme 26) [27]. An ideal catalyst-directing group incorporates three major features: (1) it must contain a donor function to allow for a reversible coordination of the rhodium(I) catalyst under hydroformylation conditions; (2) it must be equipped with the correct geometry to allow it to pass a cyclic transition state enabling the energetic discrimination of diastereotopic alkene faces; and (3) it should be readily attachable to and removable from a substrate. A system which has proved to be efficient and practical uses the *ortho*-diphenylphosphanyl function. Transformation of an allylic or homoallylic alcohol into a corresponding *ortho*-diphenylphosphanylbenzoate ester (*o*-DPPB) allows the regio- and stereoselective hydroformylation of a wide range of substrates in good to excellent levels of diastereoselectivity [76–82]. Scheme 26 summarizes the substrate scope of the *o*-DPPB-directed hydroformylation. This chemistry has been reviewed previously [5, 6, 27], and for all details the reader's attention is drawn to these summaries, which allows this chapter to focus on the latest developments.

A new chiral variant of the *o*-DPPB catalyst-directing group, the *ortho*-diphenylphosphanylferrocene-carboxylate (*o*-DPPF) has been developed. Employing this chiral directing group, a desymmetrizing hydroformylation of

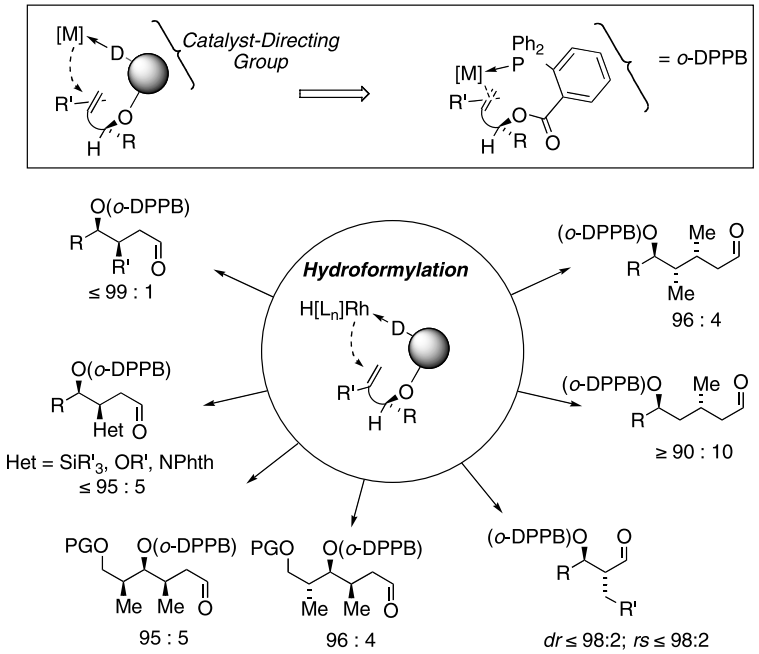

Scheme 26

bis-alkenyl- and bis-allyl carbinols could be achieved with excellent chemo-, regio-, and stereoselectivity (Scheme 27) [83–86].

A stereochemical model has been proposed, which is based on comparison of the relative stabilities of the diastereomorphic chelating trigonal bipyramidal rhodium hydrido alkene complexes leading to the selectivity-determining hydrometalation transition states. Removal of the substrate-bound catalyst-directing *o*-DPPF group can be achieved through saponification after protection of the aldehydes as a dimethylacetal with recovery of the *o*-DPPFA. Alternatively, clean reductive removal of the *o*-DPPF group is achieved upon DIBAL reduction [85, 86].

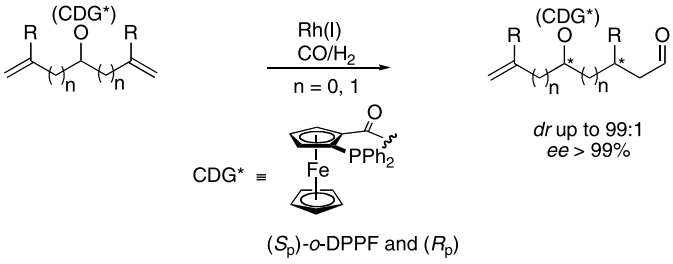

Scheme 27

7
Selective Hydroformylation Catalysts Through Self-Assembly

Bidentate ligands are important for selectivity control in homogeneous metal complex catalysis. However, the quest for the ultimate ligand which gives a catalyst with optimal activity and selectivity is difficult. Since rational design still does not allow the ligand of choice for a given reaction and substrate to be predicted, the combinatorial synthesis of ligand libraries and their subsequent use has become an additional strategy. However, the rate-determining step in catalyst development is in most cases the time-consuming ligand synthesis required to generate the ligand library.

An alternative way for the generation of a bidentate ligand makes use of a self-assembly process of monodentate to bidentate ligands employing non-covalent interactions [87].

7.1
Self-Assembly of Hydroformylation Catalysts Through Complementary Hydrogen Bonding

Among the possible modes of supramolecular interaction, hydrogen bonding has proved particularly efficient [88]. Upon mixing two equivalents of 6-diphenylphosphinopyridone **9** with a transition metal, salt complex **10** is formed (Scheme 28). The bidentate nature of **1** in these complexes has been proven in solution (NMR) as well as in the crystalline state (X-ray). Interestingly, rhodium complexes derived from **9** displayed excellent regioselectivity and actitivity upon hydroformylation of terminal alkenes [89]. These catalysts allowed the first room-temperature, ambient-pressure, regioselective hydroformylation, which is of particular use to synthetic organic chemistry (Table 2) [90].

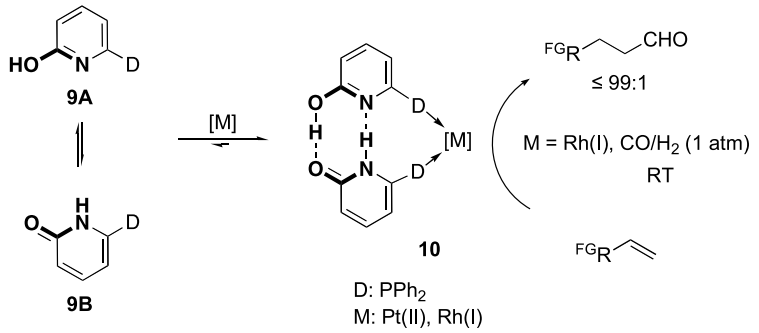

Scheme 28

The advantage of the self-assembly approach is its inherent possibility for combinatorial ligand library generation through mixing of two differ-

ent ligands. However, since both tautomers of **9**—the hydroxypyridine **9A** and the pyridone **9B**—are energetically almost equivalent and show rapid equilibration, mixing of two different ligands **9** would furnish a mixture of the two homodimeric and the heterodimeric ligand complexes. In order to generate selectively the unsymmetrical heterodimeric ligand, a self-assembly platform based on the Watson–Crick base pairing of A and T in DNA has been developed [91]. As an A-T base pair analogue, the 2-aminopyridine (**11**)/isoquinolone (**12**) platform proved suitable. Thus, mixing of two monodentate ligands based on this platform in the presence of a transition metal salt led to the selective formation of the heterodimeric complexes **13** featuring a bidentate coordination mode, as proved by NMR and X-ray

Table 2 Results of room-temperature/ambient-pressure hydroformylation of functionalized terminal alkenes with the rhodium/6-DPPon (**10**) catalyst

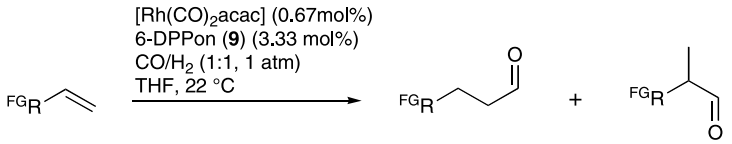

Entry[a]	Substrate	l : b	Isom. (%)	*t* (h)	Yield (%)
1		99 : 1	5	20	quant.
2		97 : 3	10	20	85
3	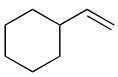	> 99 : 1	–	20	84
4	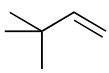	> 99 : 1	–	44	91
5	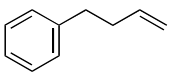	96 : 4	< 2	20	85
6	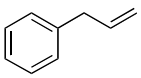	91 : 9	< 4	20	90
7	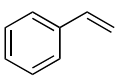	23 : 77	–	20	quant.

Table 2 (continued)

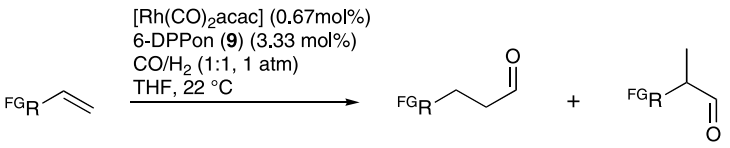

linear branched

Entry[a]	Substrate	l : b	Isom. (%)	*t* (h)	Yield (%)
8	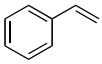 solvent: MeOH	4 : 96	–	37	quant.
9	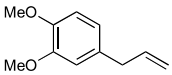	90 : 10	< 5	20	98
10	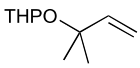	> 99 : 1	–	90	89
11	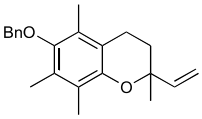	99 : 1	–	63	90
12	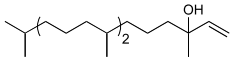	99 : 1	–	20	quant.
13	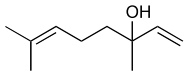	99 : 1	–	20	quant.
14	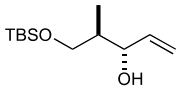	95 : 5	–	44	90
15	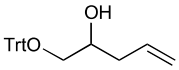	99 : 1	< 3	20	95
16	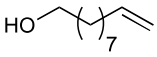	96 : 4	5	20	98
17	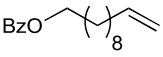	96 : 4	5	20	97

Table 2 (continued)

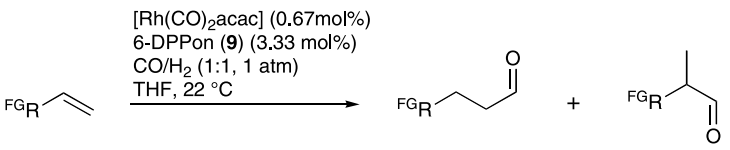

Entry[a]	Substrate	l : b	Isom. (%)	*t* (h)	Yield (%)
18	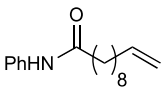	99 : 1	5	20	65
19	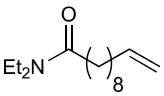	99 : 1	5	20	36
20	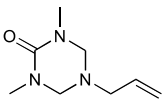	92 : 8	5	20	82
21	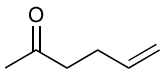	99 : 1	5	20	88
22	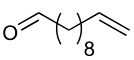	99 : 1	< 4	20	quant.
23	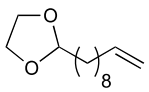	97 : 3	5	20	98
24	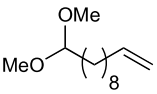	97 : 3	5	20	quant.
25	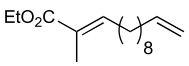	97 : 3	5	20	97
26	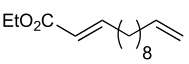	91 : 9	9	85	88

Table 2 (continued)

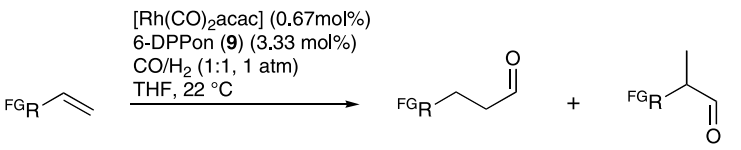

Entry[a]	Substrate	l : b	Isom. (%)	*t* (h)	Yield (%)
27	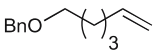	97 : 3	5	20	99
28	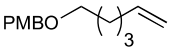	98 : 2	5	20	quant.
29	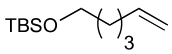	96 : 4	5	20	97
30	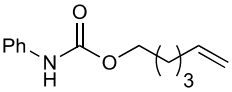	98 : 2	4	20	98
31	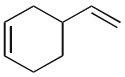	99 : 1	-	20	95

[a] Conditions: [Rh(CO)$_2$acac]/6-DPPon(**10**)/alkene (1:5:150), 1 atm CO/H$_2$ (1:1), THF (c_0(alkene)= 0.97 M; C_M = 6.5 mM), 22 °C

diffraction analysis (Scheme 29). Thus, on the basis of this platform the first 4×4 self-assembled ligand library based on hydrogen bonding was generated and explored for regioselective hydroformylation of terminal alkenes (exemplarily for 1-octene). This study allowed identification of a catalyst (**11d/12d**) which operated with truly outstanding activity and regioselectivity (see Table 3) [91].

Additional combinatorial variation sites allow the heterocyclic self-assembly units. Thus, it has been shown that heterocycles **11** and **14–17** can serve as A-analogous donor–acceptor ligands self-assembling with the T-analogous acceptor–donor ligands isoquinolone **12** and 7-azaindole **18** (Scheme 30) [92]. All combinations form the heterobidentate ligands exclusively upon simple mixing in the presence of a transition metal salt (proven by X-ray, NMR).

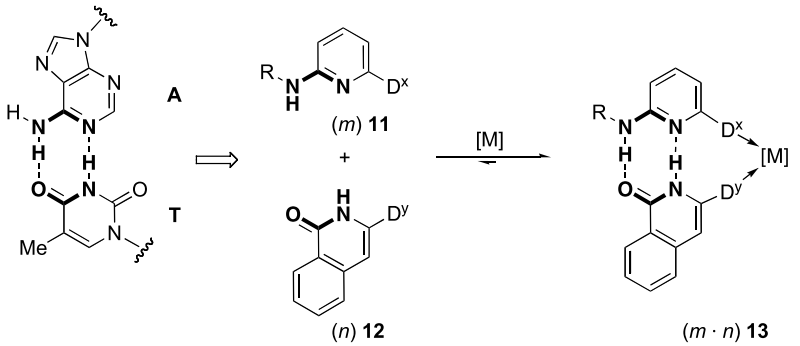

Scheme 29

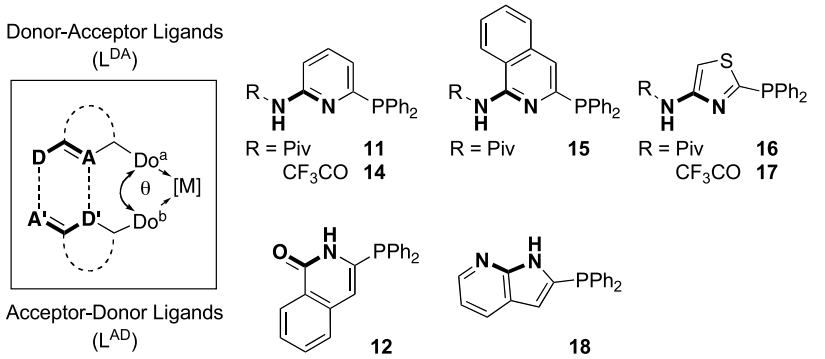

Scheme 30 Library of ligands with complementary hydrogen-bonding motifs analogous to the AT base pair

Screening of this 5×2 catalyst library for regioselective hydroformylation of 1-octene allowed elucidation of the influence of the heterocyclic self-assembly platform on catalyst properties. Thus, while all catalysts displayed higher catalyst activity compared to the industrially applied rhodium/triphenylphosphine system, regioselectivity varied from 89 : 11 to up to > 99 : 1. Hence, the nature of the heterocyclic self-assembly platform has a profound influence on catalyst performance, presumably due to changes in coordination geometry and hydrogen bond strength. The best catalyst **17/12** is based on the five-membered thiazole heterocycle and gave a regioselectivity of > 99 : 1 in favor of the linear aldehyde (Table 4). This catalyst operates even in protic solvents such as methanol as a bidentate system, in contrast to the first generation self-assembly systems which behave in methanol as monodentate ligands (Table 5) [92].

Table 3 4 × 4 ligand matrix of aminopyridine (**4a–d**)/isoquinolone (**5a–d**) derived self-assembled bidentate ligands in the [Rh]-catalyzed hydroformylation of 1-octene[a]

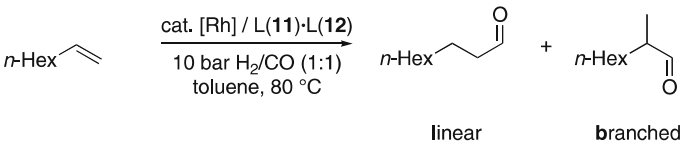

L	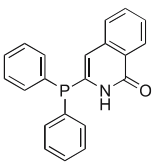 **12a**	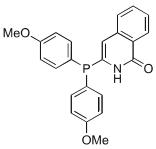 **12b**	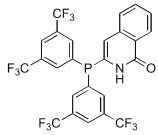 **12c**	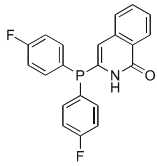 **12d**
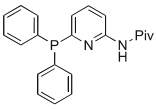 **11a**	2425 h^{-1} [b] 94 : 6	1040 h^{-1} 94 : 6	2732 h^{-1} 96 : 4	2559 h^{-1} 95 : 5
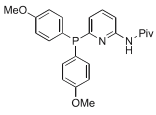 **11b**	2033 h^{-1} 93 : 7	1058 h^{-1} 92 : 8	1281 h^{-1} 96 : 4	1772 h^{-1} 94 : 6
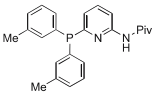 **11c**	3537 h^{-1} 94 : 6	1842 h^{-1} 93 : 7	1808 h^{-1} 96 : 4	2287 h^{-1} 94 : 6
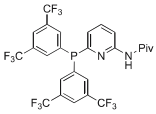 **11d**	7439 h^{-1} 96 : 4	2695 h^{-1} 95 : 5	7465 h^{-1} 94 : 6	8643 h^{-1} 96 : 4

[a] Reaction conditions: [$Rh(CO)_2$acac], [Rh]:L(**4**):L(**5**):1-octene = 1:10:10:7500, 10 bar H_2/CO(1:1), toluene (c_0(1-octene)= 2.91 M), 5 h.
Catalyst preformation: 5 bar CO/H_2 (1:1), 30 min, RT to 80 °C

[b] Turnover frequency (TOF) was calculated as (mol aldehydes) × (mol catalyst)$^{-1}$ × (t/h^{-1})$^{-1}$ at 20–30% conversion

Table 4 Turnover frequencies and regioselectivities (in parentheses) for a 5×2 ligand matrix of DA ligand (**11**, **14**–**17**)/AD ligand (**12**, **18**) derived self-assembled bidentate ligands in the [Rh]-catalyzed hydroformylation of 1-octene[a]

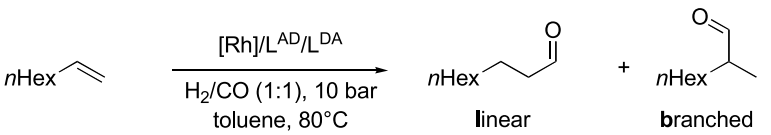

L	**11**	**14**	**15**	**16**	**17**
12	2465 h^{-1} [b] (94 : 6)	3396 h^{-1} (96 : 4)	2341 h^{-1} (95 : 5)	3890 h^{-1} (98 : 2)	3888 h^{-1} (**>99:1**)
18	2713 h^{-1} (89 : 11)	4356 h^{-1} (96 : 4)	3205 h^{-1} (95 : 5)	3233 h^{-1} (95 : 5)	2318 h^{-1} (**99:1**)

[a] Reaction conditions: $[Rh(CO)_2(acac)]$, [Rh]:L^{AD}:L^{DA}:1-octene = 1:10:10:7500, 10 bar H_2/CO (1:1), toluene, 80 °C, 5 h.
Catalyst preformation: 5 bar H_2/CO (1:1), 30 min, RT → 80 °C
[b] Turnover frequency (TOF) = (mol aldehydes) × (mol catalyst)$^{-1}$ × (t/h^{-1})$^{-1}$ at 30 min reaction time

Table 5 Regioselectivities of rhodium-catalyzed hydroformylation of 1-octene using toluene and MeOH as solvents[a]

Entry	Ligand	**l**:**b**[b] in toluene	**l**:**b**[b] in MeOH
1	**11/12**	94 : 6	82 : 18
2	**14/12**	96 : 4	79 : 21
3	**17/18**	99 : 1	85 : 15
4	**16/12**	98 : 2	97 : 3
5	**17/12**	99 : 1	96 : 4

[a] Reaction conditions: $[Rh(CO)_2(acac)]$, [Rh]:L^{AD}:L^{DA}:1-octene = 1:10:10:1000, 10 bar H_2/CO (1:1), 80 °C, 20 h
[b] Regioselectivity: linear to branched determined at complete conversion after 20 h

7.2 Self-Assembly of Hydroformylation Catalysts Through Coordinative Bonding

Zinc(II) porphyrins form stable complexes with nitrogen donors. This complementary binding motif has been used in a number of variations for the self-assembly combinatorial construction of phosphine and phosphite ligand libraries.

An example is the interaction of template **20** with nitrogen-donor functionalized monodentate phosphine and phosphite ligands **21a,b** to give bidentate self-assembly ligands **22** (Scheme 31) [93]. As a test reaction hydroformylation of 1-octene was studied. The best catalyst in terms of regioselectivity (**l** : **b** 17 : 1) was derived from mixing of **20**/2×**21b** and $[Rh(CO)_2acac]$ (Table 6, entry 1). Unfortunately, catalyst activity was low. Additionally, chiral ligands of this library were screened against asymmetric hydroformylation of styrene. However, enantioinduction was low.

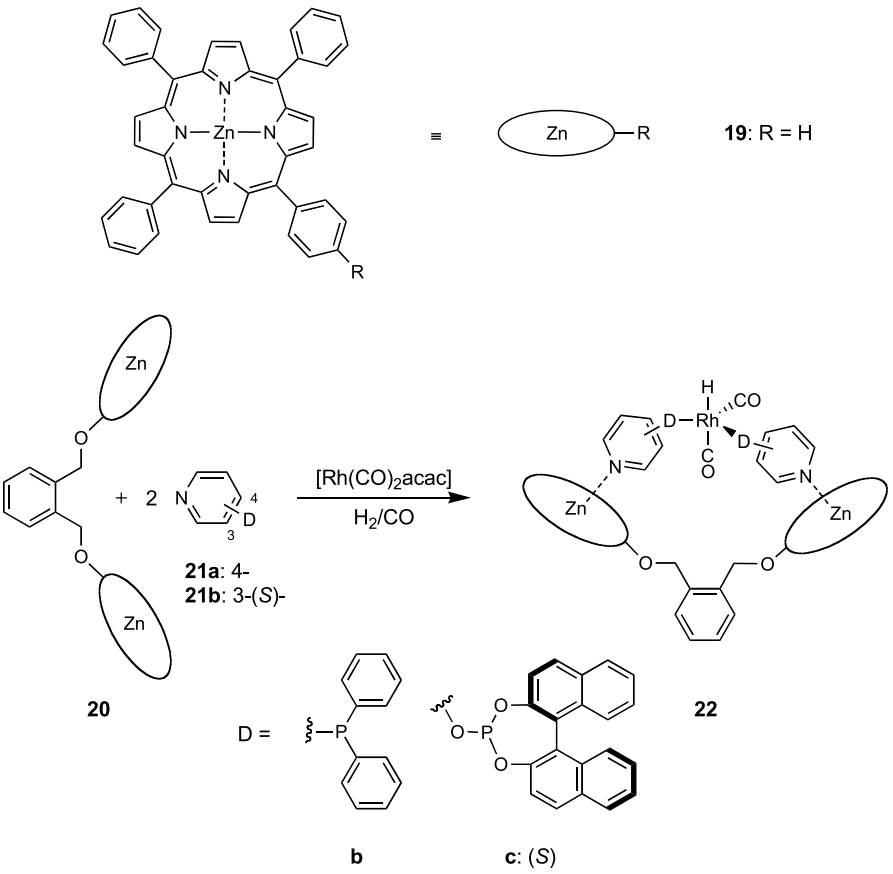

Scheme 31

Switching the roles of the zinc porphyrin template and N-donor adapter provides an alternative mode for the supramolecular construction of bidentate ligands (Scheme 32). Complex **26** derived from mixing three equivalents of template **24** with two equivalents of monodentate phosphite ligands **23** furnished a rhodium catalyst which displayed good regioselectivity toward

Table 6 Rhodium-catalyzed hydroformylation of 1-octene with catalysts **26**

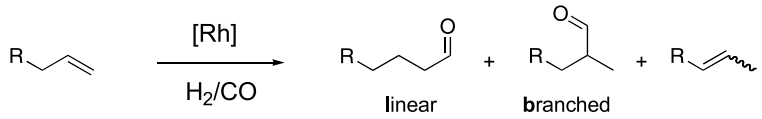

Entry [a]	Ligand	T (°C)	TOF [b]	2-octene (%)	**l**:**b**
1 [c]	**20**/2·**21b**	25	0.9	0.0	83.5 : 16.5
2 [d]	3·**24**/2·**23**	30	25	10.3	77.2 : 22.8

[a] [$Rh(CO)_2acac$]= 0.084 mM in toluene, 20 bar CO/H_2 (1 : 1), 1-octene : [Rh] = 5200
[b] TOF (turnover frequency) = (mol aldehyde)(mol [Rh])$^{-1}h^{-1}$
[c] 1-octene/Rh = 5200
[d] 1-octene/Rh = 5160

n-nonanal on hydroformylation of 1-octene (Table 6, entry 2) [94]. However, catalyst activity was also rather low.

Ligand self-assembly through coordinative bonding has been used to increase the bulkiness of a monodentate tris-3-pyridyl phosphine ligand employing the zinc porphyrin/pyridine interaction (Scheme 33) [95–97]. The corresponding rhodium catalyst allowed for regioselective hydroformylation of 2-octene [95].

As an alternative bis-Zn(II) template the bis-salphen-type system **29** has been introduced (Scheme 34). This template has two identical binding sites which allow for coordination of nitrogen donor functionalized phosphines and phosphites **37**. The identical binding sites allow formation of homoleptic-type self-assembly ligands. But heteroleptic self-assembly ligands can also be obtained when a small ligand and large ligand are combined (e.g., **30**/**32** with template **29**). The catalysts have been evaluated for asymmetric hydroformylation of styrene. However, asymmetric induction of even the best ligands from this library cannot compete with the state-of-the-art classical bidentate ligand systems described in Sect. 5.

8 Conclusions and Outlook

The hydroformylation of alkenes, one of the largest applications of homogeneous catalysis in industry, is also an ideal synthetic transformation meeting all criteria of atom economy. The reaction is becoming increasingly interesting for the synthetic organic chemist due to the development of new catalysts that have appeared during the last few years, which allow either

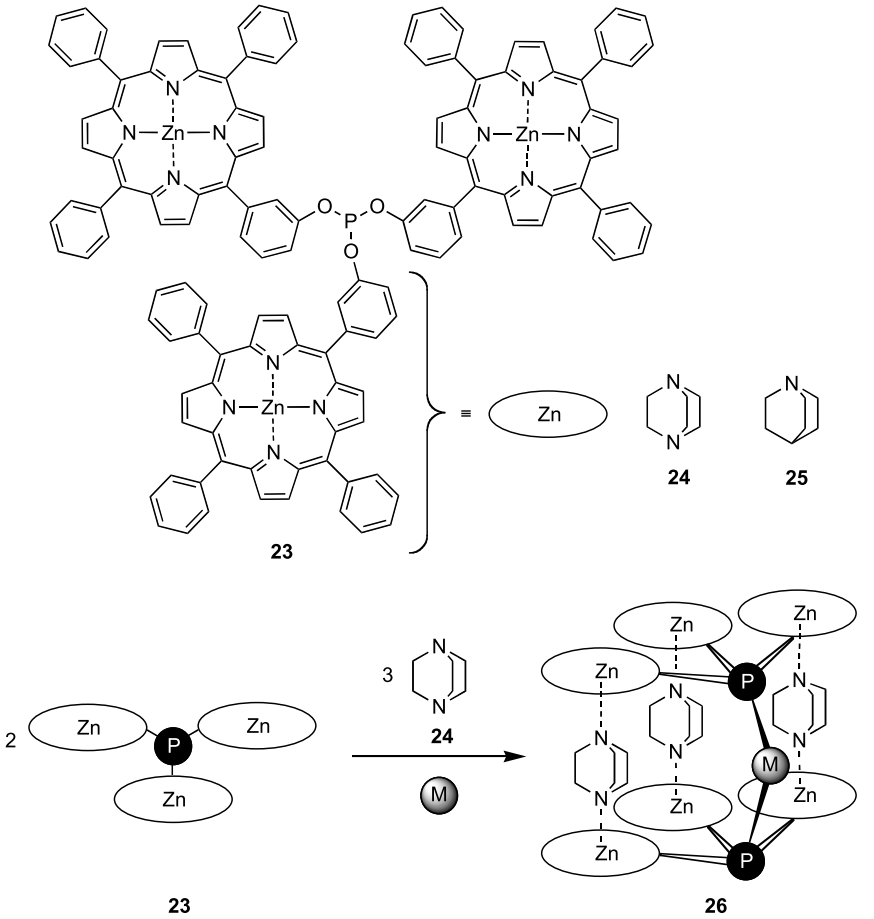

Scheme 32

for a linear-regioselective hydroformylation of terminal alkenes or in special cases for highly enantioselective hydroformylation. Unfortunately, the latter is restricted to a narrow class of alkenes, for which regioselectivity is under substrate control. Here, the use of directed stereoselective hydroformylation has proved an attractive alternative employing substrate-bound catalyst-directing groups. With chiral directing groups today even desymmetrizing hydroformylation is possible. A very promising approach for the future is the use of self-assembly principles to arrive at better hydroformylation catalysts. Thus, self-assembly of monodentate to bidentate ligands based on self-assembly of complementary hydrogen-bonding platforms according to the role model of DNA base pairing has provided new hydroformylation catalysts that allow for highly regioselective hydroformylation of terminal alkenes. The catalysts display very high activity, which enables the first prac-

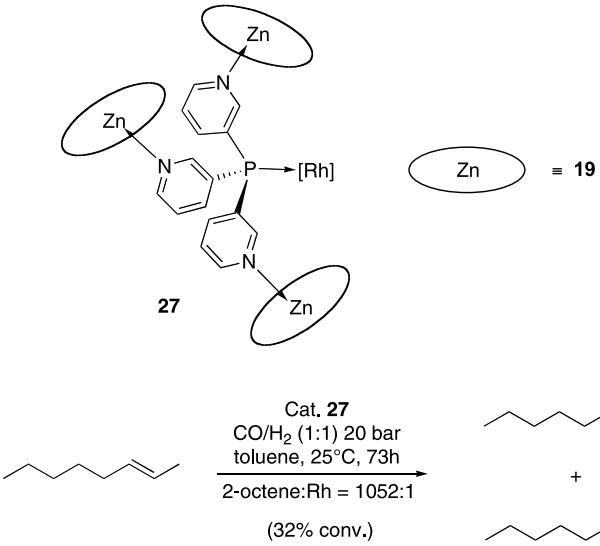

Scheme 33

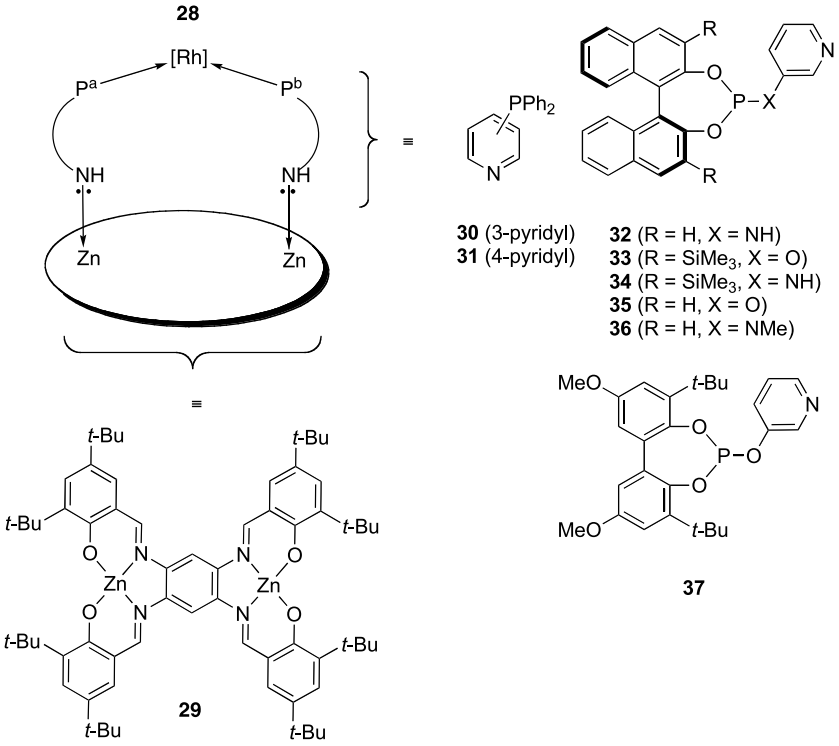

Scheme 34

Table 7 Asymmetric Rh-catalyzed hydroformylation of styrene[a]

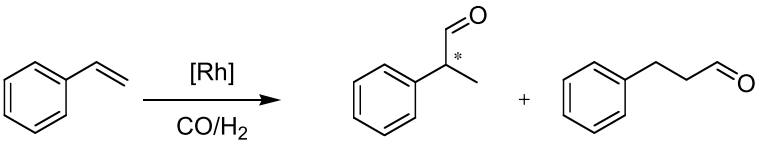

Entry	Ligands	Without template			Template **29**		
		Conv. (%)[b]	**b**:**l**[c]	*ee* (%)[d]	Conv. (%)[b]	**b**:**l**[c]	*ee* (%)[d]
homocombinations							
1	**32/32**	< 1	–	–	< 1	–	–
2[e]	**33/33**	> 99	12.2	11	> 99	13.5	13
heterocombinations							
3	**32/33**	> 99	12.0	10	66	9.90	55
4	**32/30**	33	8.02	0	19	9.20	72
5	**32/37**	28	7.56	0	20	8.21	55
6	**32/31**	–	–	–	12	3.92	57
7[f]	**32/34**	–	–	–	2.0	4.20	61
8[f]	**34/35**	–	–	–	1.3	4.20	53
9[f]	**33/35**	–	–	–	84	16.0	6
10[g]	**33/36**	97	11.3	3	21	5.3	4

[a] $[Rh(CO)_2acac]$=1.0 mmol/l in toluene, [phosphorus]=10 mmol/l, styrene/rhodium = 1000, pressure= 20 bar CO/H_2 (1 : 1), temperature= 40 °C
[b] Percentage conversion; the reaction was stopped after 87 h
[c] Ratio of branched to linear product
[d] In all cases the (*S*)-enantiomer of the product was formed
[e] 16 h; [f] 20 h; [g] 48 h

tical room-temperature/ambient-pressure regioselective hydroformylation of a broad substrate scope.

References

1. Roelen O (1944) Chem Abstr 38:550 (Chemische Verwertungsgesellschaft, mbH Oberhausen, (1938/1952) DE Patent 849 584)
2. Weissermel K, Arpe HJ (2003) Industrial organic chemistry. VCH, Weinheim, p 127
3. Wiese KD, Obst D (2006) Top Organomet Chem 18:1–33
4. Breit B (2007) Aldehydes: synthesis by hydroformylation of alkenes. In: Brückner R (ed) Science of synthesis, vol 25. Thieme, Stuttgart, pp 277–317

5. Breit B, Seiche W (2001) Synthesis p 1
6. Breit B (2003) Acc Chem Res 36:264
7. Trost BM (1991) Science 254:1471
8. Trost BM (1995) Angew Chem Int Ed Engl 34:259
9. Eilbracht P, Schmidt AM (2006) Top Organomet Chem 18:65–95
10. van Leeuwen PWNM, Claver C (2000) Rhodium catalyzed hydroformylation. Kluwer, Dordrecht
11. Claver C, Diéguez M, Pamiès O, Castillón S (2006) Top Organomet Chem 18:35–64
12. Nozaki K, Ojima I (2000) Asymmetric carbonylation. In: Ojima I (ed) Catalytic asymmetric synthesis. Wiley-VCH, New York, p 429
13. Beller M, Seayad J, Tillack A, Jiao H (2004) Angew Chem Int Ed Engl 43:3368
14. Adams DJ, Cole-Hamilton DJ, Hope EG, Pogorzelec PJ, Stuart AM (2004) J Organomet Chem 689:1413
15. Bohnen HW, Cornils B (2007) Adv Catal 47:1–64
16. Cornils B, Herrmann WA (1998) Aqueous-phase organometallic catalysis—concepts and applications. Wiley-VCH, Weinheim
17. Ojima I, Tsai CY, Tzamarioudaki M, Bonafoux D (2000) Org React 56:1
18. Torrent M, Solà M, Frenking G (2000) Chem Rev 100:439
19. van Leeuwen PWNM, Kamer PCJ, Reek JNH, Dierkes P (2000) Chem Rev 100:274
20. Beller M, Cornils B, Frohning CD, Kohlpaintner CW (1995) J Mol Catal A Chem 104:17
21. Ojima I, Eguchi M, Tzamarioudaki M (1995) Hydroformylation. In: Abel EW, Stone FGA, Wilkinson G (eds) Comprehensive organometallic chemistry. Elsevier, Oxford, p 9
22. Stille JK (1991) Hydroformylation and related additions of carbon monoxide to alkenes and alkynes. In: Trost BM, Fleming I, Paquette LA (eds) Comprehensive organic synthesis. Pergamon, Oxford, p 913
23. Diéguez M, Pàmies O, Claver C (2004) Tetrahedron Asymmetry 15:2113
24. Kalck P, Peres Y, Jenck J (1991) Adv Organomet Chem 32:121
25. Agbossou F, Carpentier JF, Mortreux A (1995) Chem Rev 95:2485
26. Gladiali S, Bayon JC, Claver C (1995) Tetrahedron Asymmetry 6:1453
27. Breit B (2007) Directed Rhodium Catalyzed Hydroformylation of Alkenes. Top Organomet Chem, published online
28. Breit B (2005) Angew Chem Int Ed 44:6816
29. Evans DA, Osborn JA, Wilkinson G (1968) J Chem Soc A 3133
30. Jongsma T, Challa G, van Leeuwen PWNM (1991) J Organomet Chem 421:121
31. Selent D, Wiese KD, Röttger D, Börner A (2000) Angew Chem Int Ed 39:1639
32. Breit B, Winde R, Mackewitz T, Paciello R, Harms K (2001) Chem Eur J 7:3106
33. Breit B (1999) J Mol Catal A 143:143
34. Breit B, Winde R, Harms K (1997) J Chem Soc Perkin Trans 1:2681
35. Breit B (1996) J Chem Soc Chem Commun p 2071
36. Breit B, Fuchs E (2004) Chem Commun p 694
37. Piechaczyk O, Doux M, Ricard L, le Floch P (2005) Organometallics 24:1204
38. Fuchs E, Keller M, Breit B (2006) Chem Eur J 12:6930
39. Keulemans AIM, Kwantes A, van Bavel T (1948) Recl Trav Chim Pays Bas 67:298
40. García L, Claver C, Diéguez M, Masdeu-Bultó AM (2006) Chem Commun p 191
41. Clarke ML, Roff GJ (2006) Chem Eur J 12:7978
42. Baber RA, Clarke ML, Heslop K, Marr A, Orpen AG, Pringle PG, Ward AM, Zambrano-Williams DA (2005) Dalton Trans p 1079
43. Gee V, Orpen AG, Phetmung H, Pringle PG, Pugh RI (1999) Chem Commun p 901

44. Pugh RI, Pringle PG, Drent E (2001) Chem Commun p 1476
45. Reetz MT, Li X (2005) Angew Chem Int Ed 44:2962
46. Dong Y, Busacca CA (1997) J Org Chem 62:6464
47. Keränen MD, Eilbracht P (2004) Org Biomol Chem 2:1688
48. Keränen MD, Kot K, Hollmann C, Eilbracht P (2004) Org Biomol Chem 2:3379
49. Devon TJ, Phillips GW, Puckette TA, Stavinoha JL, Vanderbilt JJ (1987) US Patent 4 694 109
50. Casey CP, Whiteker GT, Melville MG, Petrovich LM, Gavey JA, Powell DR (1992) J Am Chem Soc 114:5535
51. Billig E, Abatjoglou AG, Bryant DR (1988) US Patent 4 769 498
52. Cunny GD, Buchwald SL (1993) J Am Chem 114:5535
53. Kranenburg M, van der Burgt YEM, Kamer PCJ, van Leeuwen PWNM, Goubitz K, Fraanje J (1995) Organometallics 14:3081
54. Séméril D, Jeunesse C, Matt D, Toupet L (2006) Angew Chem Int Ed 45:5810
55. Keck GE, Truong AP (2005) Org Lett 7:2149
56. Dixon DJ, Horan RAJ, Monck NJT (2004) Org Lett 6:4423
57. Petricci E, Mann A, Schoenfelder A, Rota A, Taddei M (2006) Org Lett 8:3725
58. Ahmed M, Seayad AM, Jackstell R, Beller M (2003) Angew Chem Int Ed 42:5615
59. Ahmed M, Seayad AM, Jackstell R, Beller M (2003) J Am Chem Soc 125:1031
60. Ahmed M, Bronger RPJ, Jackstell R, Kamer PCJ, van Leeuwen PWNM, Beller M (2006) Chem Eur J 12:8979
61. Schmidt AM, Eilbracht P (2005) Org Biomol Chem 3:2333
62. Schmidt AM, Eilbracht P (2005) J Org Chem 70:5528
63. Köhling P, Schmidt AM, Eilbracht P (2003) Org Lett 5:3213
64. Rodriquez M, Bassarello C, Bifulco G, Gomez-Paloma L, Mann A, Marchetti M, Schoenfelder A, Taddei M (2005) Synlett p 1581
65. Sakai N, Mano S, Nozaki K, Takaya H (1993) J Am Chem Soc 115:7033
66. Nozaki K, Sakai N, Nanno T, Higashijima T, Mano S, Horiuchi T, Takaya H (1997) J Am Chem Soc 119:4413
67. Nozaki K, Itoi Y, Shibahara F, Shirakawa E, Ohta T, Takaya H, Hiyama T (1998) J Am Chem Soc 120:4051
68. Nakano K, Tanaka R, Nozaki K (2006) Helv Chim Acta 89:1681
69. Yan Y, Zhang X (2006) J Am Chem Soc 128:7198
70. Axtell AT, Klosin J, Abboud KA (2006) Organometallics 25:5003
71. Axtell AT, Cobley CJ, Klosin J, Whiteker GT, Zanotti-Gerosa A, Abboud KA (2005) Angew Chem Int Ed 44:5834
72. Clarkson GJ, Ansell JR, Cole-Hamilton DJ, Pogorzelec PJ, Whittell J, Wills M (2004) Tetrahedron Asymmetry 15:1787
73. Clark TP, Landis CR, Freed SL, Klosin J, Abboud KA (2005) J Am Chem Soc 127:5040
74. Cobley CJ, Gardner K, Klosin J, Praquin C, Hill C, Whiteker GT, Zanotti-Gerosa A, Petersen JL, Abboud KA (2004) J Org Chem 69:4031
75. Liu P, Jacobsen EN (2001) J Am Chem Soc 123:10773
76. Breit B (1996) Angew Chem Int Ed Engl 35:2835
77. Breit B (1997) Liebigs Ann Recl 1841
78. Breit B, Heckmann G, Zahn SK (2003) Chem Eur J 9:425
79. Breit B, Dauber M, Harms K (1999) Chem Eur J 5:2819
80. Breit B, Demel P, Gebert A (2004) Chem Commun p 114
81. Breit B (1997) Chem Commun p 591
82. Breit B (1998) Eur J Org Chem 6:1123
83. Breit B, Breuninger D (2004) J Am Chem Soc p 10244

84. Breit B, Breuninger D (2005) Synthesis p 2782
85. Breit B, Breuninger D (2005) Eur J Org Chem p 3916
86. Breit B, Breuninger D (2005) Eur J Org Chem p 3930
87. Breit B (2005) Angew Chem Int Ed 44:6816
88. Breit B, Seiche W (2006) Pure Appl Chem 78:249
89. Breit B, Seiche W (2003) J Am Chem Soc 125:6608
90. Seiche W, Schuschkowski A, Breit B (2005) Adv Synth Catal 347:1488
91. Breit B, Seiche W (2005) Angew Chem Int Ed 44:1640
92. Waloch C, Wieland J, Keller M, Breit B (2007) Angew Chem Int Ed 46:3037
93. Slagt VF, van Leeuwen PWNM, Reek JNH (2003) Chem Commun p 2474
94. Slagt VF, van Leeuwen PWNM, Reek JNH (2003) Angew Chem Int Ed 42:5619
95. Kuli M, Solter T, van Leeuwen PWNM, Reek JNH (2006) J Am Chem Soc 128:11344
96. Slagt VF, Kamer PCJ, van Leeuwen PWNM, Reek JNH (2004) J Am Chem Soc 126:1526
97. Slagt VF, Reek JNH, Kamer PCJ, van Leeuwen PWNM (2001) Angew Chem Int Ed 40:4271
98. Kuil M, Goudriaan PE, van Leeuwen PWNM, Reek JNH (2006) Chem Commun p 4679

Top Curr Chem (2007) 279: 173–207
DOI 10.1007/128_2007_121

Published online: 14 June 2007

Nickel-Catalyzed Reductive Coupling of Dienes and Carbonyl Compounds

Masanari Kimura[2] · Yoshinao Tamaru[1] (✉)

[1]Department of Applied Chemistry, Faculty of Engineering, Nagasaki University, 1-14 Bunkyo, 852-8521 Nagasaki, Japan
tamaru@nagasaki-u.ac.jp

[2]Graduate School of Science and Technology, Nagasaki University, 1-14 Bunkyo, 852-8521 Nagasaki, Japan

Abstract Nickel-catalyzed allylation and homoallylation of carbonyl compounds with conjugated dienes promoted by a several kind of organometallic reagents are described. In the presence of $Ni(cod)_2$, trialkylsilanes (R_3SiH) serve as reducing agents and promote ω-dienyl aldehydes to undergo intramolecular allylation with high regio- and stereoselectivity. In the presence of indium(I) iodide, $Ni(acac)_2$ catalyzes double allylation of aldehydes with 1,3-butadiene to provide 3-hexene-1,6-diols and/or 2-vinyl-1,4-butanediols. The combination of $Ni(acac)_2$ and triethylborane selectively promotes homoallylation of aromatic aldehydes and α,β-unsaturated aldehydes. The reaction shows high regio- and stereoselectivity. Isoprene, for example, provides 1-substituted 3-methyl-4-pentenols with excellent 1,3-*anti* stereoselectivity. Diethylzinc, in place of Et_3B, nicely promotes the homoallylation of less reactive carbonyl compounds (sterically congested aliphatic

aldehydes and ketones). 1,3-Cyclohexadiene is one exception among the dienes examined and undergoes allylation instead of homoallylation under the catalysis of Ni-Et_2Zn. Aldimines prepared in situ from aldehydes and *p*-anisidine undergo homoallylation with 2-substituted-1,3-deines under Ni-Et_2Zn catalysis to afford bis-homoallyl amines with excellent 1,3-*syn* stereoselectivity.

Keywords Allylation · Carbonyl compound · Dienes · Homoallylation · Nickel catalysis · Reductive coupling

Abbreviations

acac	Acetylacetonato
Bn	Benzyl
CDT	1,5,9-Cyclododecatriene (cdt as a ligand)
COD	1,5-Cyclooctadiene (cod as a ligand)
Cy	Cyclohexyl
DBA	*trans*,*trans*-Dibenzylideneacetone
DIBAL	Diisobutylaluminum
DMF	*N*,*N*-Dimethylformamide
DMI	1,3-Dimethyl-2-imidazolidinone
DPPB	1,4-Bis(diphenylphosphino)butane
Fur	2-Furanyl
PMP	*p*-Methoxyphenyl
TBDMS	*tert*-Butyldimethylsilyl
TIPS	Triisopropylsilyl
Tol	Tolyl

1 Introduction

Conjugated dienes are among the most significant building blocks both in laboratories and in the chemical industry [1]. Especially, 1,3-butadiene and isoprene are key feedstocks for the manufacture of polymers and fine chemicals. Since the discovery of the Ziegler–Natta catalyst for the polymerizations of ethylene and propylene, the powerful features of transition metal catalysis has been widely recognized, and studies in this field have been pursued very actively [2–7].

In the last decade, a new aspect of nickel-catalyzed reactions has been disclosed, where nickel serves to selectively activate dienes as either an allyl anion species or a homoallyl anion species (Scheme 1). These anionic species are very important reactive intermediates for the construction of desired molecules. Traditionally they have been prepared in a stoichiometric manner from the corresponding halides and typical metals, e.g., Li, Mg. In this context, the catalytic generation method of allyl anions and homoallyl anions disclosed here might greatly contribute to synthetic organic chemistry and organotransition metal chemistry.

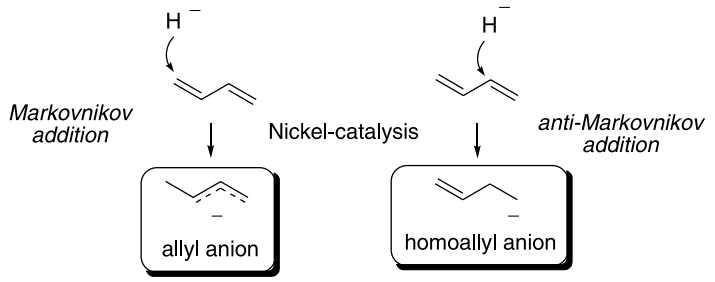

Scheme 1 Selective formation of allyl anion and homoallyl anion under nickel catalysis

This review focuses on the recent developments in nickel-catalyzed functionalizations of conjugated dienes as allyl anions and homoallyl anions.

2
Nickel-Catalyzed Reductive Allylation of Carbonyl Compounds with 1,3-Dienes

2.1
Allylation of Aldehydes via Dimerization of 1,3-Dienes Promoted by Nickel Complexes

Nickel(0) complexes are extremely effective for the dimerization and oligomerization of conjugated dienes [8, 9]. Two molecules of 1,3-butadiene readily undergo oxidative cyclization with a Ni(0) metal to form bis-allylnickel species. Palladium(0) complexes also form bis-allylpalladium species of structural similarity (Scheme 2). The bis-allylpalladium complexes show amphiphilic reactivity and serve as an allyl cation equivalent in the presence of appropriate nucleophiles, and also serve as an allyl anion equivalent in the presence of appropriate electrophiles. Characteristically, the bis-allylnickel species is known to date only as a nucleophile toward carbonyl compounds (Eq. 1) [10, 11].

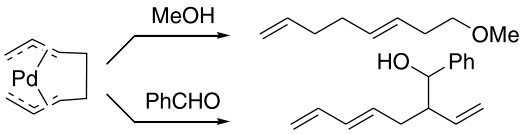

Scheme 2 Amphiphilic reactivity of bis-π-allylpalladium

Representative results for the Ni-catalyzed allylation of acetaldehyde with 1,3-butadiene in the presence of phosphine ligands are shown in Table 1. The reaction is rather complex and four kinds of products are formed: two

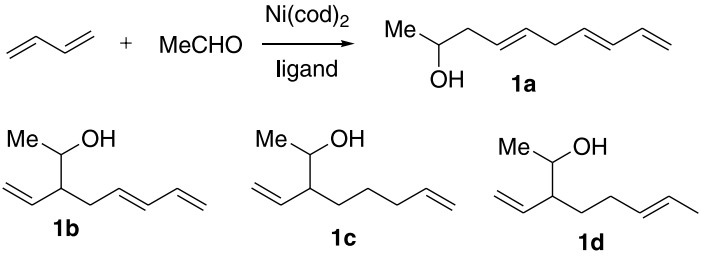

Equation 1

Table 1 Ni-catalyzed allylation of acetaldehyde with butadiene

Run	Ligand	%Yield			
		1a	**1b**	**1c**	**1d**
1	PPh_3	71	12	5	4
2	$P(n-Bu)_3$	40	19	26	8
3	$P(c-Hex)_3$	3	29	40	18

trienyl alcohols **1a** and **1b**, and two dienyl alcohols **1c** and **1d**. The effects of phosphine ligands on the product distribution are remarkable. Triphenylphosphine shows high selectivity in favor of **1a**, whereas trialkylphosphine, especially tricyclohexylphosphine, tends to provide dienyl alcohols **1c** as a major product. The straight-chain isomer **1a** may be formed via an intermediate **3**, which undergoes β-H elimination to give a trienyl-ONiH intermediate **4**. Reductive elimination of the OH group with regeneration of a Ni(0) species completes one catalytic cycle of the reaction (Scheme 3). In a similar way, an intermediate **6**, formed by allylation of at the internal allylic terminus of **5**, lead to a branched isomer **1b** via intermediates **6** and **7**.

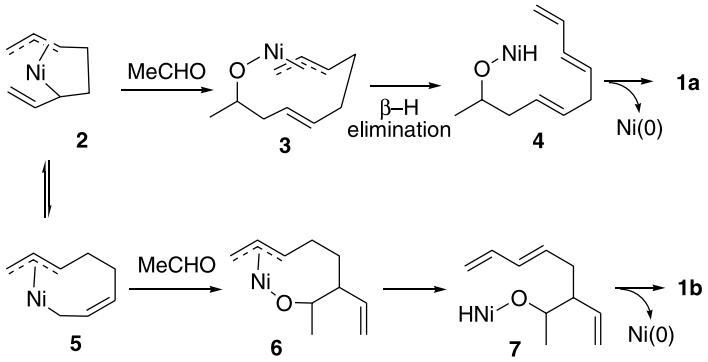

Scheme 3 Catalytic cycle for the formation of trienyl alcohols **1** via bis-allylnickel(II) intermediates **2** and **5**

The formation of trienyl alcohols **1a** and **1b** can be rationalized as above, but it is difficult to explain the formation of the dienyl alcohols **1c** and **1d**; the stoichiometric balance of the starting materials and products requires one molecule of hydrogen for the formation of these alcohols (starting materials: $2C_4H_6 + CH_3CHO = C_{10}H_{16}O$, products **1c**,**d**: $C_{10}H_{18}O$). The origin of one of the molecules of hydrogen in the product is not clear.

Isoprene does not participate in the reaction under the above-optimized conditions. The combination of Ni(cdt) and *c*-Cy_3P promotes the reaction. Unfortunately, however, the reaction results in a very complex mixture consisting of 1 : 1 and 1 : 2 adducts of acetaldehyde and isoprene. The 1 : 1 adducts (**8a**,**b**) are the minor products (Eq. 2) [12]. Except for **8e**, all the products are out of material balance (vide supra, requiring one molecule of H_2) and it is difficult to give any mechanistic rationale for their formation.

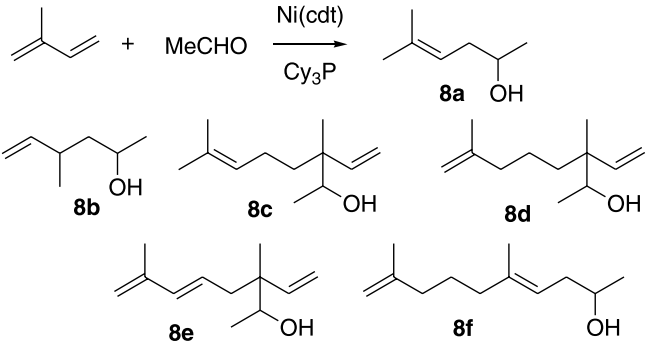

Equation 2

2.2 Allylation of Aldehydes with Dienes Promoted by Trialkylsilanes

π-Allylnickel species can be formed by the Markovnikov-type addition of a Ni – H species upon a 1,3-diene, in a specific way to provide the most substituted allyl nickel species of the possible two regioisomers for 1-substituted 1,3-dienes. The Ni – H complex can be generated readily by oxidative addition of a Ni(0) species upon the Si – H bond of trialkylsilanes (R_3SiH).

A Ni(0)-catalyzed 1,ω-hydrosilylation across the two dienyl moieties of 1,3,8,10-undecatetraene **9** proceeds regioselectively and stereoselectively and provides vic-*trans*-divinyl cyclopentane products **10** in modest yield (Eq. 3) [13]. The reaction shows an interesting stereoselectivity with respect to the substituent geometry; both of the vinyl groups of **10a** and **10b** are stereoisomeric to each other, and one of the two double bonds is *cis* and the other is *trans*.

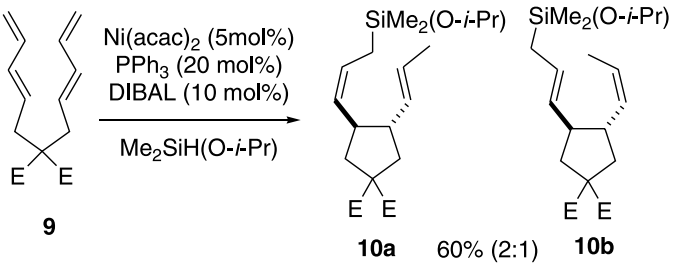

Equation 3

The π-allylnickel bearing a silyl group on nickel(II) is expected to be nucleophilically activated toward addition upon an aldehyde, since the oxophilic silyl group might activate the aldehyde by coordination to the oxygen atom. Based on this idea, Mori et al. have first demonstrated the stoichiometric cyclization reaction of ω-dienyl aldehyde **11** with R_3SiNiH (Eq. 4) [14]. A reaction mixture of ω-dienyl aldehyde **11**, $Ni(cod)_2$ (100 mol %), PPh_3 (200 mol %), and Et_3SiH (150 mol %) dissolved in toluene at 0 °C provides **12** exclusively as a single diastereomer.

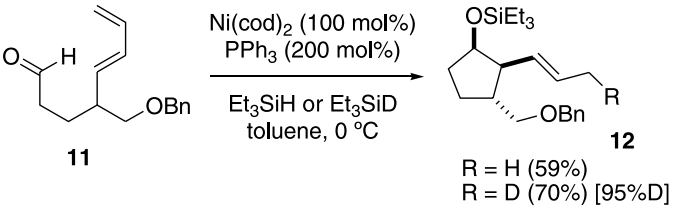

Equation 4

The reaction can be conducted successfully using $Ni(cod)_2$ as a catalyst in the presence of an excess amount of Et_3SiH (5 equiv.). Deuteriotriethylsilane (Et_3SiD) delivers the D atom exclusively at the terminal carbon of the diene (95% D content). A possible reaction mechanism is outlined in Scheme 4. A silylnickel hydride complex, Et_3SiNiH, generated by oxidative addition of a Ni(0) complex upon Et_3Si-H, adds to the diene moiety of **11** in the Markovnikov fashion to provide an allylnickel species **13**. Intramolecular nucleophilic attack of the allylnickel upon the aldehyde affords **14**, which undergoes reductive elimination to give rise to a final product **12** along with a Ni(0) active species. An alternative reaction mechanism is also possible, which involves a concerted silyl group transfer to the aldehyde oxygen, nucleophilic allylation, and regeneration of Ni(0) species via a transition state **I**.

This strategy is successfully applied to the synthesis of the indolizidine framework of an Elaeocarpus alkaloid, (–)-elaeokanine C (Eq. 5) [15, 16]. Fur-

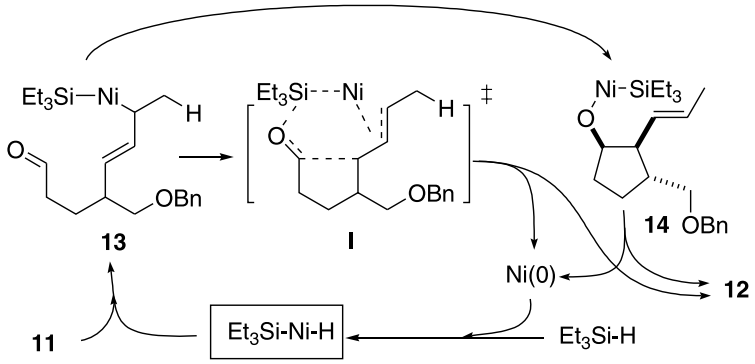

Scheme 4 Ni(0)-catalyzed intramolecular allylic cyclization of ω-dienyl aldehydes **11** using hydrosilanes as a reducing agent

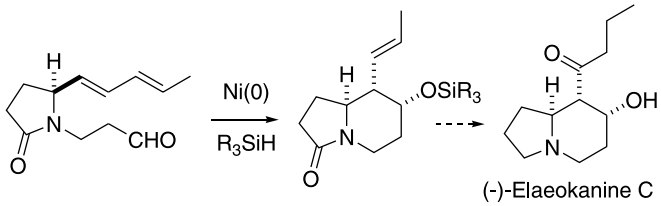

Equation 5

thermore, the reductive coupling reaction can be extended to an asymmetric version. By using a chiral monodentate cyclic phosphine ligand, a carbocyclic compound is prepared in 86% ee (Eq. 6) [17, 18]. In all reactions forming five- and six-membered rings (Eqs. 4 ~ 6), the vicinal hydroxy and vinyl groups are placed *cis* stereoselectively.

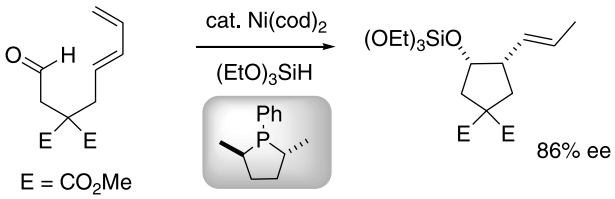

Equation 6

Dienes incorporated in a cyclohexane skeleton show different reaction features from acyclic dienes. Under the reductive allylation conditions, ω-(2,4-cyclohexadienyl)alkanals **15** react to provide a homoallylation product **16a** ($n = 1$) as a major product or **16a** ($n = 2$) exclusively (Eq. 7) [19]. The expected allylation product is obtained as a minor product only for the reaction of **15** ($n = 1$).

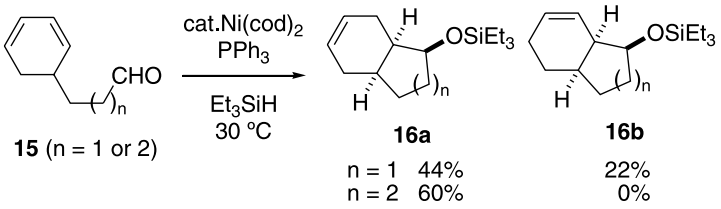

Equation 7

The homoallylation product **16a** presumably stems from oxidative cycloaddition of a Ni(0) species across the diene and aldehyde moieties of **15**, leading to an oxanickellacycle intermediate **17** (path A, Scheme 5), which undergoes σ-bond metathesis with triethylsilane giving rise to a σ-allylnickel **19**. On the other hand, formation of **16b** may start with addition of a Ni – H species upon the diene followed by intramolecular nucleophilic allylation as described in Eqs. 4–6 (path B). Alternatively, allylic transposition of the NiH group providing **20** from **19** may be related to the formation of **16b**. The different reactivity between cyclohexadiene and many other acyclic dienes is also observed for the reaction undertaken under typical homoallylation conditions (see Scheme 14).

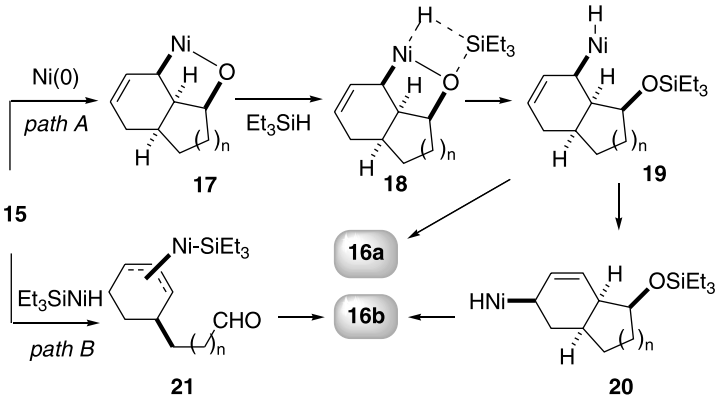

Scheme 5 Ni-Et_3SiH promoted intramolecular reductive coupling of **15**

Intermolecular allylation of aldehydes with 1-trialkylsilyl-1,3-dienes **22** in the presence of a stoichiometric amount of triethylsilane and a catalytic amount of $Ni(cod)_2$ and PPh_3 shows novel regio- and stereoselectivity (Scheme 6) [20–22]. When a toluene solution of a 1-silyl-1,3-diene and an aldehyde is refluxed in the presence of trialkylsilane under the catalysis of $Ni(cod)_2$ and PPh_3, (*E*)-allylsilane (*E*)-**23** is obtained exclusively. On the other hand, when the reaction is carried out in THF upon heating at 50 °C as

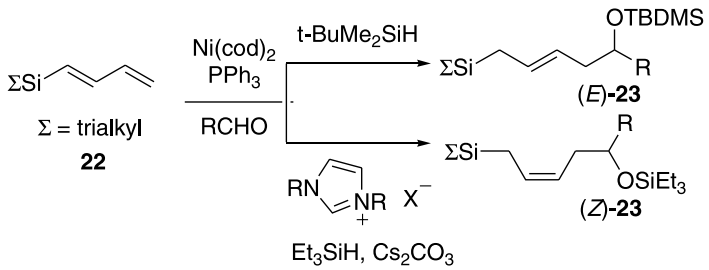

Scheme 6 Stereoselective synthesis of *E*- and *Z*-allylsilanes

a mixture of trialkylsilane, $Ni(cod)_2$, PPh_3, an imidazolium salt, and Cs_2CO_3, (*Z*)-allylsilane (*Z*)-**23** is formed as a sole product.

The possible reaction pathways for the stereoselective *E*- and *Z*-allylation are illustrated in Scheme 7. 1-Silyl-1,3-dienes **22** react with a Ni – H species in the presence of PPh_3 to provide a *syn*-π-allylnickel species **24**, *the least substituted allylnickel species*, which undergoes nucleophilic addition to an aldehyde at *the least substituted allylic terminus* to provide (*E*)-allylsilane (*E*)-**23**. It should be noted that the regioselectivities observed for the Ni – H addition to a diene **22** and nucleophilic addition of **24** to aldehydes are opposite to those observed so far in many precedents in this review (e.g., Eqs. 4 and 6).

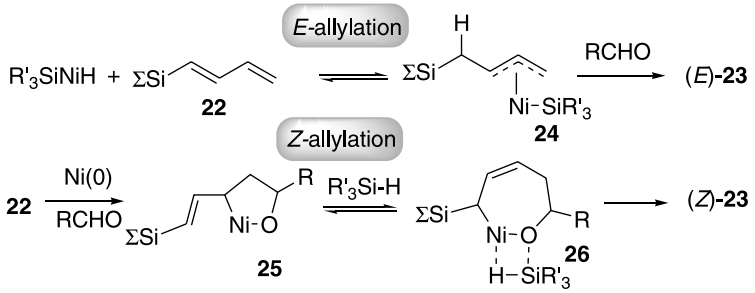

Scheme 7 A rationale for the *E*- and *Z*-selective allylation of aldehydes

In the presence of an imidazolium salt and a base, oxidative cyclization of a Ni(0) species upon the diene and an aldehyde takes place first and forms an oxanickellacycle **25**, which equilibrates with a seven-membered oxanickellacycle **26**, naturally possessing a *cis* double bond. σ-Bond metathesis through **26** with hydrosilane affords (*Z*)-allylsilane (*Z*)-**23**. The role of NHC ligand (*N*-heterocyclic carbene, generated by H^+ elimination from imidazolium C_2H by a base) is not clear at present; a Ni(0)–NHC complex is believed to effectively produce **26**.

2.3
Double Allylation of Aldehydes with Dienes Promoted by Indium(I)

Indium(I) iodide serves as a two electron reducing agent to promote a Ni-catalyzed allylation of benzaldehyde with 1,3-dienes [23]. In the presence of a catalytic amount of $Ni(acac)_2$ and a stoichiometric amount of InI, 1,3-butadiene reacts with 2 equiv. of benzaldehyde to provide a mixture of a 1,4-diol **28** and 1,6-diol **29** and/or with 1 equiv. of benzaldehyde to give **27** (Eq. 8). The product distribution of **27**–**29** markedly depends on the solvent, the ligand, and the additive employed (Table 2). The combination of $Ni(acac)_2$, PPh_3, and 3 equiv. of water in DMI provides the 1,4-diol **28** as the major product (run 1). Under similar conditions, dppb dramatically changed the reaction course and the mono-allylation product **27** is produced exclusively (run 2). In contrast to these, the reaction in dry THF provides the 1,6-diol **29** in excellent yield (run 3).

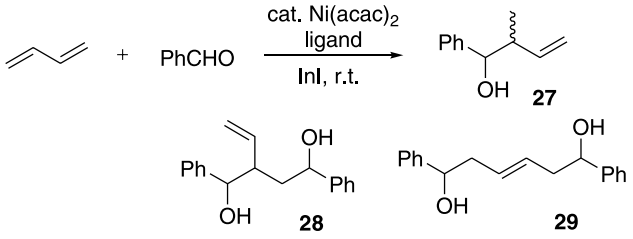

Equation 8

Table 2 Ni-catalyzed, InI-mediated allylation of benzaldehyde with 1,3-butadiene

Run	Solvent	Ligand	Additive (equiv.)	Time (h)	%Yield 27	28	29
1	DMI	PPh_3	H_2O (3)	3	21	63	11
2	DMI	dppb	H_2O (3)	18	74	Trace	Trace
3	THV	PPh_3	None	4	5	5	87

Despite the complexity caused by unsymmetrical substitution, isoprene shows more favorable results than 1,3-butadiene under the DMI-PPh_3-H_2O conditions (c.f., run 1, Table 2) and reacts with benzaldehyde regioselectively at C2 and C4 carbons and provides a diol **31** in remarkably good yield (Eq. 9).

The catalytic role of a Ni(0) species in this reaction may be attributed to oxidative addition of a Ni(0) species to isoprene in conjunction with protonation (leading to **33**) or nucleophilic addition to benzaldehyde (leading to **35**). Reduction of Ni(II) to Ni(0) by In(I) and metal exchange may form an

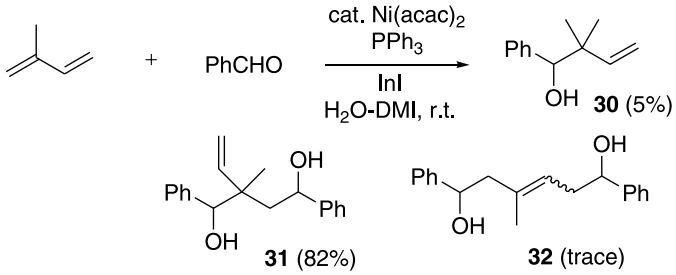

Equation 9

allylindium(III) intermediate **34**, which reacts with benzaldehyde at the most substituted allylic terminus to provide **30** regioselectively (Scheme 8). Here it is supposed that **34** reacts with benzaldehyde through a six-membered cyclic transition state. Similar redox between Ni(II) and In(I) and transmetallation would lead **35** to an equilibrium mixture of **36** and **37**. In a dipolar solvent, especially in the presence of water, a less congested and primary allylindium species **36** would be favored over a more congested, tertiary allylindium species **37** and hence 1,4-diols **31** and **28** would be formed selectively. On the other hand, in a less polar solvent like anhydrous THF, **37** would predominate in the equilibrium, and hence 1,6-diols **32** and **29** would be formed as the major products.

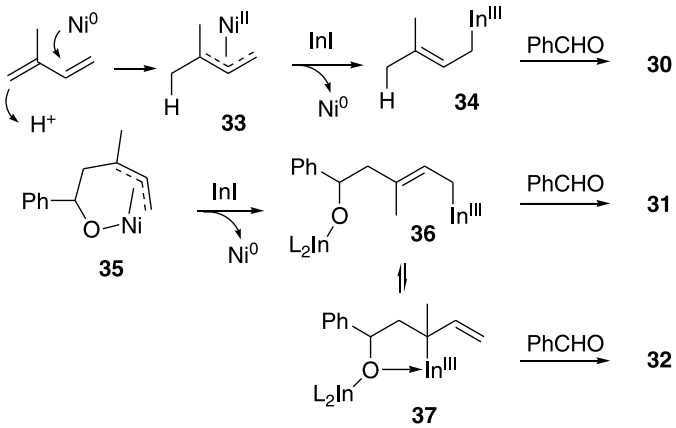

Scheme 8 Plausible reaction mechanism for the Ni-catalyzed mono- and bis-allylation of aldehyde with butadiene, promoted by In(I)I

The synthetic utility and generality of the reaction is demonstrated by an intramolecular/intermolecular double allylation using an ω-dienyl aldehyde **38** as a probe. The internal diene terminus selectively undergoes nucleophilic allylation intramolecularly to form a cyclopentanol structure. The terminal

diene terminus reacts with benzaldehyde to provide a diol, which is isolated as a di-acetate **39** in reasonable yield after esterification (Eq. 10). The relative stereochemistry of the vicinal hydroxy and vinyl groups is not specified.

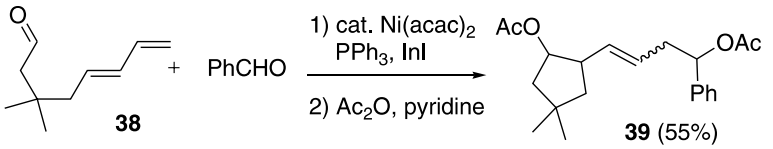

Equation 10

3
Nickel-Catalyzed Reductive Homoallylation of Carbonyl Compounds with 1,3-Dienes

3.1
Homoallylation of Aldehydes with Dienes Promoted by Triethylborane

Compared with allylation, homoallylation has received little attention both in stoichiometric organometallic chemistry and in catalytic transition metal chemistry [24–26]. This is apparently owing to the difficult availability and the poor reactivity of a homoallyl metal species as compared with an allyl metal species.

Remarkably, 1,3-dienes have been shown to serve as homoallyl anion equivalents and react with aldehydes in the presence of a catalytic amount of $Ni(acac)_2$ and a stoichiometric amount of triethylborane to provide bis-homoallyl alcohols, 4-pentenols **40**, exclusively (Eq. 11) [27, 28].

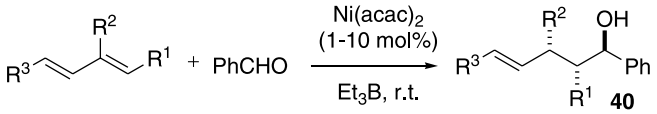

Equation 11

The reaction is quite general for dienes with a variety of combinations of substituents R^1–R^3. Some representative examples for the reaction with benzaldehyde are summarized in Table 3. The reaction is performed uniformly using benzaldehyde (1 equiv.), a diene (4 equiv.), $Ni(acac)_2$ (0.1 equiv.), and triethylborane (2.4 equiv.) in THF at room temperature under nitrogen atmosphere.

The homoallylation shows remarkably high regioselectivity and stereoselectivity, yielding a 1 : 1 adduct of a diene and benzaldehyde. The parent 1,3-butadiene is only one exception and provides the homoallylation product

as the major product, along with the allylation product as the minor product (run 1, Table 3). This exceptional result may be attributed to isomerization of the primary-formed homoallylation product to the thermodynamically more stable internal double bond isomer.

Table 3 Ni-catalyzed homoallylation of benzaldehyde with a variety of 1,3-dienes promoted by Et_3B

Run	Diene	Time (h)	Products	%Yield [ratio]
1	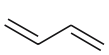	21	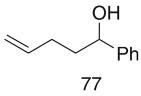 77	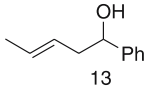 13
2	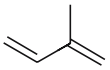	35	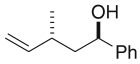	90[15:1]
3	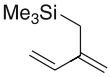	45	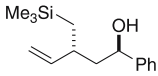	90[exclusive]
4	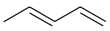	50	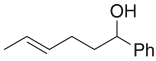 55	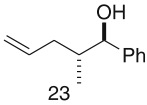 23 [*anti*:*syn*= 5.5 : 1]
5	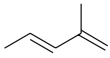	5	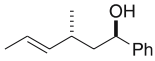	82[exclusive]
6	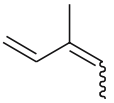 [*Z*:*E* = 1.9 : 1](4 eq)	46	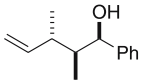	94 [1, 2-*anti*:*syn*= 1 : 8]
7	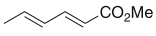	29	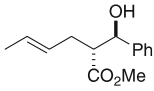	79[exclusive]
8		34	No reaction	

As for the regioselectivity, C2 electron-donating substituents strongly direct dienes to react with benzaldehyde at the C1 position (runs 2, 3, and 5). C1 substituents are not so influential as the C2 substituents and tend to promote the reaction at the distal C-4 diene terminal. For example, piperylene forms a mixture of the C4 and C1 adducts in ca. 2 : 1 ratio (run 4). The relative directing ability of the C1 and C2 substituents may be demonstrated by the reaction of 1,2-dimethyl-1,3-butadiene, where both substituents work oppositely, the former directing the reaction at C1, while the latter at C4 (run 6). The exclusive formation of the C1 adduct clearly indicates that C2-Me overrides C1-Me in controlling the regioselectivity.

As for the stereoselectivity, C2-substituted dienes generally provide 1,3-*anti* isomers with excellent stereoselectivity. The stereoselectivity of C1-substituted dienes depends on the geometry of the starting dienes: (*E*)-dienes provide 1,2-*anti* isomers exclusively (run 6) and (*Z*)-dienes yield 1,2-*syn* isomers exclusively. The stereocontrol by the C1 and C2 substituents may be best demonstrated by the examples shown in run 6, where (*Z*)-1,2-dimethyl-1,3-butadiene furnishes the 1,2-*syn*-2,3-*anti* isomer exclusively and (*E*)-1,2-dimethyl-1,3-butadiene provides the 1,2-*anti*-2,3-*syn* isomer exclusively.

Notably, not only electron-rich dienes, but also electron-deficient dienes nicely participate in the reaction and react benzaldehyde with similar ease and in a similar sense of stereoselectivity. For example, methyl sorbate provides the 1,2-*anti* isomer exclusively in good yield with excellent regio- and stereoselectivity (run 7). The regioselectivity reacting at C1 of the diene skeleton might stem from electronic factors rather than from other factors such as coordination: the coordination of the ester oxygen to nickel metal center, since (*E*,*E*)-1-(methoxymethyl)-4-methyl-1,3-butadiene and (*E*,*E*)-1-(hydroxymethyl)-4-methyl-1,3-butadiene furnish the C4 adducts selectively together with the C1 adducts as minor products (not shown). Notably, 1,3-cyclohexadiene is unreactive and no reaction is observed at all under similar reaction conditions (run 8).

1,3-Butadienes bearing trialkylsiloxy group at C1 and/or C2 positions also undergo the homoallylation with benzaldehyde with high regio- and stereoselectivity (Table 4). C2-siloxy-1,3-butadienes react at the C1 position and provide 1,3-*anti* isomers exclusively (runs 1–3, Table 4), while C1-siloxy-1,3-butadienes react regioselectively at the distal C4 position and provide 1,3-*anti* isomers exclusively (runs 5 and 6, Table 4).

The present homoallylation with siloxy- and methoxy-substituted dienes may be of great synthetic use. The product **42** is easily converted to *anti*-5-phenyl-5-hydroxy-3-methylpentanal (Scheme 9); hence the diene **41f** may be regarded as a synthetic equivalent of a bis-homoenolate of 3-methylbutanal, being capable of introducing 1,3-*anti* relationship between the methyl and hydroxy groups in the product.

The relative reactivity of dienes has been estimated on the basis of competition experiments performed using two kinds of dienes (2 mmol each) and

Table 4 Ni-catalyzed homoallylation of benzaldehyde with siloxy-1,3-butadienes promoted by Et_3B

Run	Diene	Time (h)	Products	%Yield
1	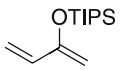	68	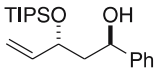	65
2	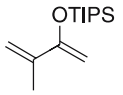	35	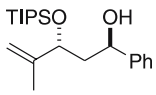	84
3	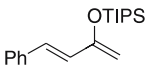	46	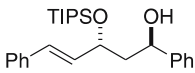	81
4	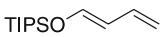	43	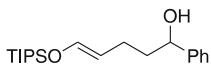	92
5	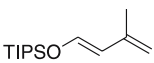	43	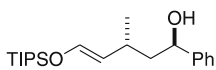	92
6	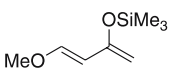	24	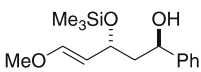	69

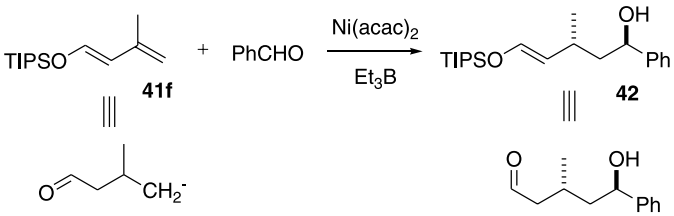

Scheme 9 1-Siloxy-1,3-butadienes as synthetic equivalents of bishomoenolate of butyraldehydes

benzaldehyde (1 mmol) in the presence of $Ni(acac)_2$ catalyst and triethylborane (Scheme 10). Interestingly, 2-siloxydiene **41d** is about three times as reactive as isoprene, while 1-siloxybutadiene **41e** is more than 100 times less

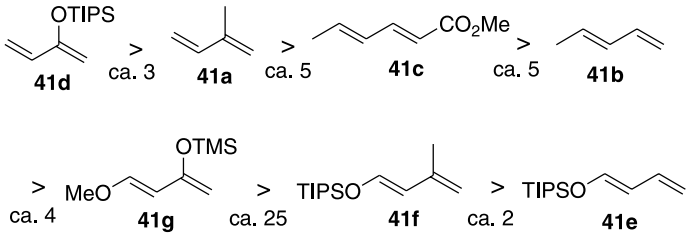

Scheme 10 Relative reactivity of dienes toward homoallylation of benzaldehyde under the Ni-Et_3B catalysis

reactive than isoprene. Furthermore, electron-deficient methyl sorbate (**41c**) is five times as reactive as piperylene (**41b**). These data apparently indicate that the relative reactivity is far from the one expected from electronic effects. It should be noted that *2-siloxy-1,3-butadiene is 15 000 times as reactive as 1-siloxy-1,3-butadiene*, and the former is the most reactive and the latter is the least reactive among the 1,3-dienes examined. Generally, the 2-siloxy group slightly accelerates the reaction, while the 1-siloxy group significantly retards the reaction. A rationale for the poor reactivity associated with the 1-siloxy substituent is given in a full account in [28].

Table 5 summarizes the reactions of isoprene with aromatic aldehydes and unsaturated aldehydes. Salicylaldehyde provides the expected product as a cyclic boric ester derivative and shows apparently lower stereoselectivity, giving a mixture of 1,3-*anti* and 1,3-*syn* isomers in a ratio of 6 : 1 (run 1, Table 5). 2-Furfural reacts as usual and provides a 1,3-*anti* isomer as a single diastereomer in good yield (run 2). Unsaturated aldehydes, irrespective of their substitution patterns, undergo homoallylation selectively with excellent 1,3-*anti* selectivity, the geometry of the double bond of the starting aldehydes remaining intact (runs 3–5). 1,2-Addition to unsaturated aldehyde takes place selectively and no 1,4-addition is observed.

Not only because of their diminished electrophilic reactivity but also because of their propensity to undergo enolization and many other side reactions, nucleophilic alkylation of aliphatic aldehydes often suffers from low yields. Accordingly, the reaction that is successful for aromatic aldehydes is not necessarily successful for aliphatic aldehydes.

The present homoallylation with isoprene under Ni-Et_3B catalysis shows marginal success for the reaction with aliphatic aldehydes. Results are summarized in Table 6. Primary alkyl aldehydes (bearing no α-substituents) and sterically less-hindered secondary alkyl aldehydes undergo the homoallylation successfully to provide the expected products in good yields with excellent stereoselectivity (runs 1–5). The results in runs 3–5 indicate that the present reaction shows almost no diastereofacial selectivity with respect to the α-stereocenters of secondary alkyl aldehydes. Sterically demanding aldehydes, such as cyclohexanecarbaldehye and pivalaldehyde, provide the

Table 5 Ni-catalyzed homoallylation of aromatic and unsaturated aldehydes with isoprene promoted by Et_3B

Run	Diene	Time (h)	Products	%Yield [*anti* : *syn*]
1	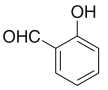	50	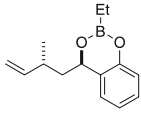	90[6:1]
2	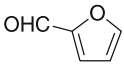	22	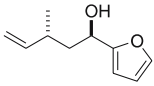	77[single]
3	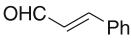	70	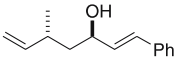	81[single]
4	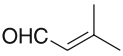	21	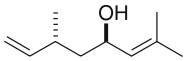	69[single]
5	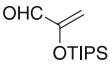	44	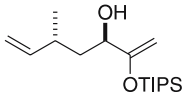	77[single]

expected homoallylation product in poor yields (runs 6 and 7). The yield for less-reactive aldehydes have been improved under the Et_2Zn-Ni catalysis (Table 7).

Triethylborane is unique among organometallic reagents and is stable toward hydrolysis with water. In this context, the synthetic utility of the Ni-Et_3B catalysis may be best demonstrated by the homoallylation of aldehydes that are only storable and stable in an aqueous solution. Glutaraldehyde is one of such aldehydes and is commercially available as an aqueous solution. Under the catalysis of Ni-Et_3B, isoprene reacts with a commercial 50% aqueous solution of glutaraldehyde as usual and provides a hemiacetal **43** as a single diastereomer, being 1,3-*anti* with respect to the THP oxygen and methyl group (Eq. 12) [29].

The compatibility of Et_3B with a hydroxy group is demonstrated by the reaction with cyclic hemiacetals ($n = 1$ or 2). Here again the reaction proceeds smoothly without using any extra amount of Et_3B and provides ω-hydroxy bishomoallyl alcohols **44** with an excellent 1,3-asymmetric induction (Eq. 13).

Table 6 Ni-catalyzed homoallylation of aliphatic aldehydes with isoprene promoted by Et_3B

Run	Diene	Time (h)	Products	%Yield
1	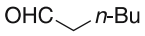	31	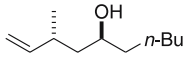	80
2	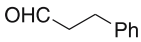	24	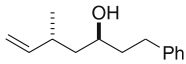	48
3	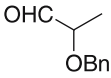	24	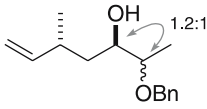	92
4	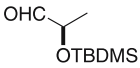	40	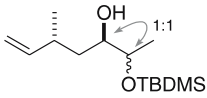	76
5	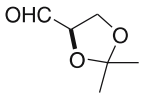	47	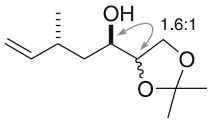	66
6	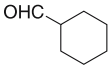	24	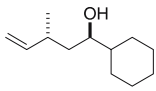	28
7	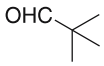	48	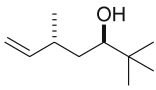	16

A plausible reaction mechanism for the nickel-catalyzed and Et_3B-promoted homoallylation of an aldehyde with isoprene is outlined in Scheme 11. The regioselectivity of an unsymmetrical diene reacting either at C1 or C4 with an aldehyde might be mainly under the control of the electron densities on the diene termini C1 and C4, and the terminal bearing the highest electron density would enter into the reaction with an aldehyde. A transition state **II** might lead to an intermediate **45** and/or **50** through oxidative cyclization of a Ni(0) species across isoprene and an aldehyde, as

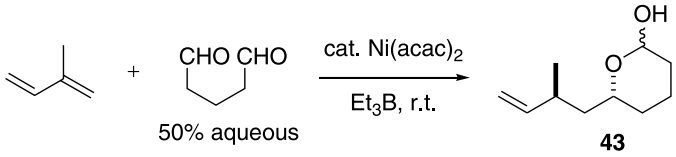

Equation 12

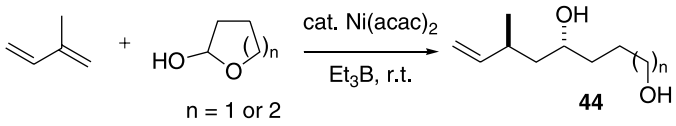

Equation 13

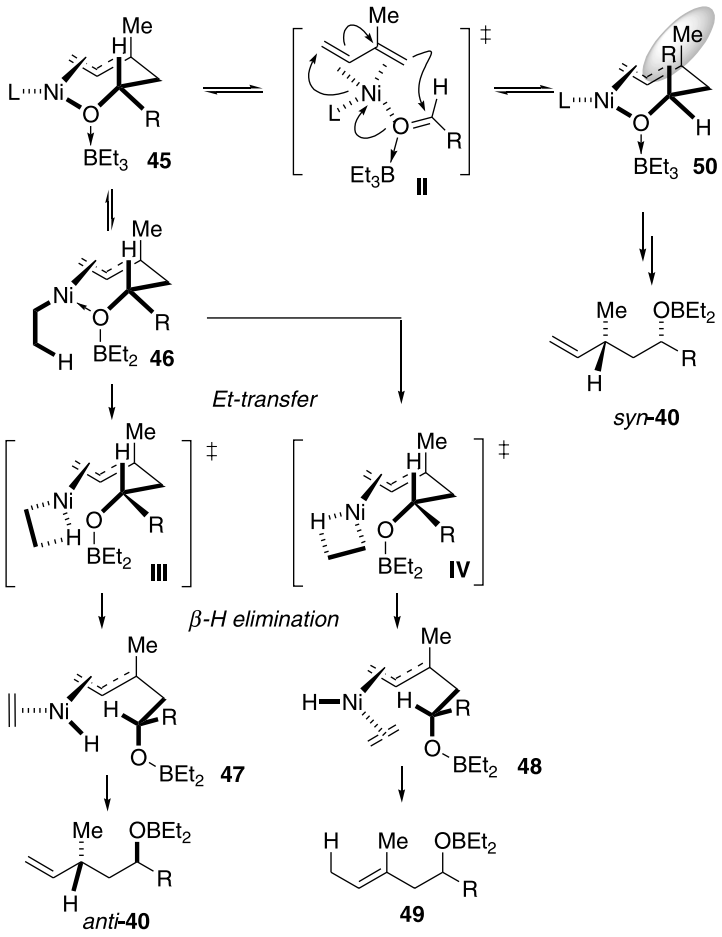

Scheme 11 Plausible reaction pathway leading to a 1,3-*anti* isomer, *anti*-**40**

indicated by arrows. The oxidative cyclization might be accelerated by coordination of Et_3B to an aldehyde oxygen. In this process, isoprene might serve not only as an electron-push toward an aldehyde but also as an electron-pull from a Ni(0) species. For the electron-rich dienes the former factor might be important, and for the electron-deficient dienes the latter factor might be crucial. This is one of the reasons why the relative reactivity of dienes does not straightforwardly follow the electronic characters of the dienes (Scheme 10).

The intermediates **45** and **50** are diastereomeric to each other. The latter suffers from 1,3-diaxial repulsion between an aldehyde R and isoprene Me (indicated by shading), and hence the reaction proceeds selectively through **45**. Ethyl group transfer from B to Ni, accompanying the change of the Ni – O bond from an ionic bond to a coordination bond, would form an allylethylnickel complex **46**, which then might undergo β-H elimination in the following two pathways. The route leading to an intermediate **47** is expected to be much favored over the one leading to **48**, since β-agostic interaction of the Et group with the vacant site on Ni, created by dissociation of an oxygen ligand, would readily take place via a transition state **III**. On the other hand, in order to arrive at the transition state **IV**, three distinctive steps are required: (1) dissociation of Ni – O coordination, (2) migration of the Et group to the position previously occupied by O, and (3) β-agostic interaction. Reductive *cis*-elimination of Ni(0) from an intermediate **47** might provide a homoallylation product, *anti*-**40**, regenerating a Ni(0) species. The same process via the transition state **IV** might result in the formation of an allylation product **49**. Thus, this reaction mechanism invokes that Et_3B not only accelerates the formation of **45** by acting as a Lewis acid but also serves as a reducing agent delivering a formal hydride regioselectively in the anti-Markovnikov fashion at the C2 position of C2-substituted unsymmetrical dienes.

3.2 Homoallylation of Aldehydes and Ketones with Dienes Promoted by Diethylzinc

Et_2Zn also participates in the reductive coupling as a formal hydride source. Results for the Ni-catalyzed, Et_2Zn-promoted homoallylation of carbonyl compounds with isoprene are summarized in Table 7 [30]. Et_2Zn is so reactive that for the reaction with reactive aromatic aldehydes it causes direct ethylation of aldehydes, and the yields of homoallylation are diminished (runs 1 and 2). Unsaturated aldehydes seem to be subject to the Michael addition of Et_2Zn. Accordingly, for the reaction with cinnamaldehyde, none of the expected homoallylation product is produced; instead, the 1,4-addition product of Et_2Zn, 3-phenylpentanal is produced exclusively (run 3).

The combination of Et_2Zn and $Ni(acac)_2$ is particularly effective for the homoallylation of less-reactive aliphatic aldehydes (runs 4–6). For example,

Table 7 Ni-catalyzed homoallylation of aliphatic aldehydes with isoprene promoted by Et_2Zn[a]

Run	Diene	Time (h)	Products	%Yield[b] [*anti* : *syn*]
1	PhCHO	1	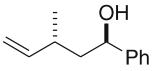	71 (90) [15:1]
2	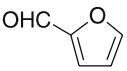	1	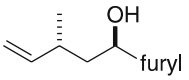	65 (77) [15:1]
3	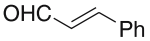	0.5	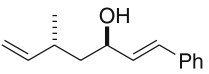	0 (81) [15:1]
4	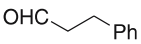	1	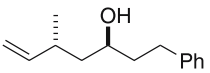	73 (48) [15:1]
5	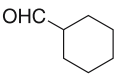	0.5	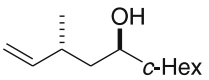	83 (28) [30:1]
6	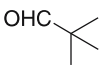	1	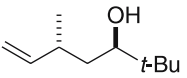	66 (16) [20:1]

[a] Isoprene (4 mmol), aldehyde (1 mmol), $Ni(acac)_2$ (10 mol %), Et_2Zn (240 mol %, M in hexane) in THF at room temperature

[b] Yields for the reactions promoted by Et_3Zn are shown in parathensis

for the reaction with cyclohexanecarbaldehyde, Et_2Zn-$Ni(acac)_2$ and Et_3B-$Ni(acac)_2$ provide the expected homoallylation product in 83% and 28% yield, respectively. Thus, Et_2Zn-$Ni(acac)_2$ and Et_3B-$Ni(acac)_2$ are complementary to each other and the former catalytic system is recommended for the homoallylation of non-reactive aldehydes and the latter for the homoallylation of reactive aldehydes (e.g., aromatic and unsaturated aldehydes).

Whereas Et_3B fails to promote the Ni-catalyzed homoallylation of ketones, Et_2Zn successfully promotes the reaction. Some results are illustrated in Scheme 12. Isoprene, for the first time, loses its regioselectivity and reacts with acetone both at C1 and C4 positions to provide a mixture of ho-

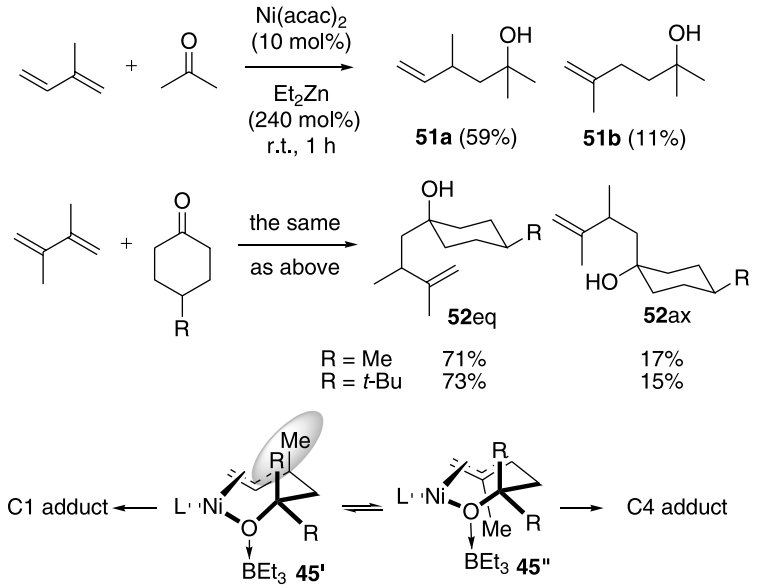

Scheme 12 Ni(0)-catalyzed homoallylation of ketones with 1,3-dienes promoted by Et_2Zn

moallylation products **51a** and **51b** in a ratio of ca. 6 : 1. The reaction with cyclohexanone also shows a similarly poor regioselectivity.

As observed in runs 3–5 (Table 6) the reaction shows poor diastereofacial selectivity. For example, the reaction with 4-substituted cyclohexanone provides a mixture of an equatorial approach product **52eq** and an axial approach product **52ax** in a ration of ca. 6 : 1, irrespective of the steric size of the substituents

The erosion in regioselectivity observed for ketones may be due to 1,3-diaxial repulsion in an intermediate **45′** (indicated by shading in Scheme 12), that is inevitable when isoprene reacts with ketones at C1 position. Accordingly, the reaction may optionally proceed through an intermediate **45″**, which is formed by the reaction of a ketone with isoprene at the C4 position and may be sterically less congested than **45′**.

Another advantage of the Et_2Zn-Ni catalysis over the Et_3B-Ni catalysis is that only the former can promote the reductive coupling of 1,3-cyclohexadiene with aldehydes (c.f., run 8, Table 3). For example, under the Et_2Zn-Ni catalysis, 1,3-cyclohexadiene smoothly reacts with benzaldehyde at room temperature and provides **53** in 61% isolated yield (Scheme 13). Curiously, however, the product **53** is not the expected homoallylation product, but an allylation product.

A rationale for the exceptionally low reactivity and the unusual reductive coupling pattern, allylation not homoallylation, associated with 1,3-cyclohexadiene is outlined in Scheme 13. In contrast to *syn-trans* dienes

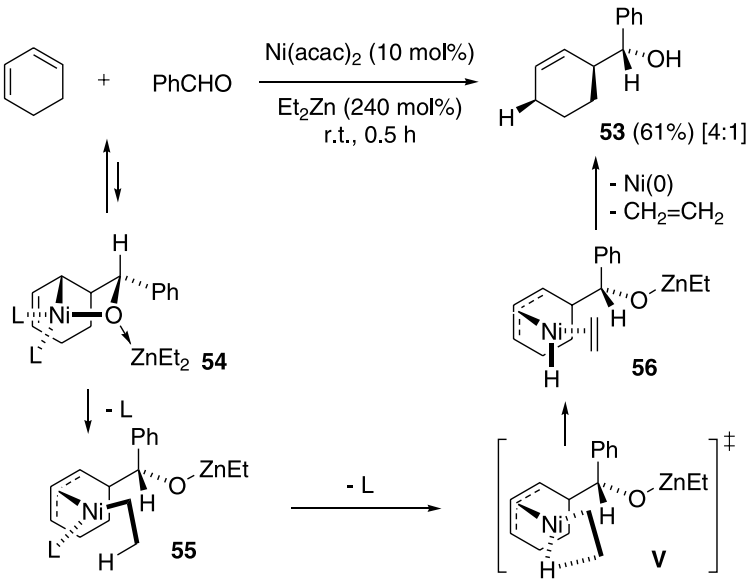

Scheme 13 Ni-catalyzed allylation (not homoallylation) of benzaldehyde with 1,3-cyclohexadiene promoted by Et_2Zn

as described in Scheme 11, *syn-cis* dienes might be sterically obliged to form a less stable cyclic sigma-oxanickellacycle **54**. Facile formation of a π-allyl(ethyl)nickel(II) intermediate **55**, via Ni – O bond cleavage and ethyl group transfer from Zn to Ni, concomitant with dissociation of one of the two ligands L, is essential to put the reaction forward; otherwise, **54** might fragment into the starting materials through which 1,3-cyclohexadiene would be able to restore its conjugate stabilization. Diethylzinc might contribute to promoting the reaction by its ability to facilely transfer the ethyl group to nickel(II). The π-allyl(ethyl)nickel(II) intermediate **55**, being *cis* with respect to the ethyl and alkoxy groups, might undergo β-H elimination via a transition state **V** and provide a hydridonickel intermediate **56**, which might be destined to undergo reductive *cis*-elimination to selectively provide an allylation product **53**.

3.3
Homoallylation of Aldimines with Dienes Promoted by Diethylzinc

In general, an aldimine is among the least reactive carbonyl compounds and is by far less reactive than an aldehyde [31–33]. Nevertheless, the Et_2Zn-Ni catalytic system is successfully extended to the homoallylation of aldimine. Aldimine prepared in situ from an aldehyde and a primary aromatic amine undergoes the homoallylation smoothly under the essentially identical con-

ditions applied to aldehydes and ketones and provides bis-homoallyl amines **57** in good to excellent yields (Eq. 14) [34, 35]. Results for the reaction of isoprene and *p*-anisidine-imine are shown in Table 8.

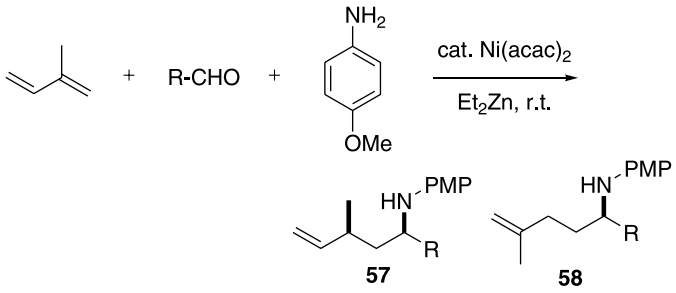

Equation 14

Table 8 Ni-catalyzed homoallylation of anisidine-imine with isoprene promoted by Et_2Zn

Run	Aldehyde	Time (h)	%Yield [*anti* : *syn*] **57**	**58**
1	*p*-Tol-CHO	1	89[8 : 1]	6
2	*p*-ClPh-CHO	1	89[7 : 1]	7
3	2-FurCHO	0.5	82[20 : 1]	4
4	$(CH_2O)_n$	1	78	1
5	*i*PrCHO	0.5	62[>30 : 1]	20

The reaction can be performed in one flask with great operational ease; a mixture of an aldehyde and *p*-anisidine is stirred in THF for 5–10 h at 50 °C. Then, without removing the water produced, $Ni(acac)_2$, isoprene, and Et_2Zn are added in this order at room temperature. The mixture is stirred at the same temperature for the period of time indicated (Table 8). The products **57** and **58** are isolated as a mixture by column chromatograph after the usual work-up. Table 8 demonstrates the scope regarding the kind of aldehyde that encompasses not only aromatic aldehydes but also aliphatic aldehydes and even the parent formaldehyde. Despite the diminished electrophilic reactivity of aldimines, the reaction is complete at room temperature within a reasonable reaction time. The reaction of aldimines proceeds in an opposite sense of stereoselectivity to that of aldehydes and selectively provides 1,3-*syn* isomers **57**.

Regioselectivity with respect to the reaction site of dienes (C1 or C4) is the same as, but slightly lower than that observed for aldehydes. The C4-adducts **58** are produced as minor products in varying amounts, seemingly depending

on the steric size of the aldimine substituents; the bulkier the substituents, the greater amounts of **58** result.

The reaction is also applicable to a wide structural variety of 1,3-dienes, as demonstrated by the reaction of 2-furfural-*p*-anisidine imine (Table 9). All dienes react with the aldimine regioselectively at the diene termini bearing the highest electron densities and provide bis-homoallyl amines with excellent 1,3-*syn* diastereoselectivity. No C4-adducts are formed in these reactions.

Table 9 Ni-catalyzed homoallylation of 2-furfural-*p*-anisidine imine with a variety of dienes

Run	Diene	Product	%Yield [*syn*:*anti*]
1	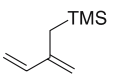	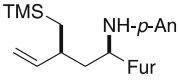	81[> 30 : 1]
2	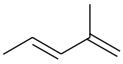	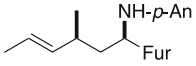	98[> 30 : 1]
3	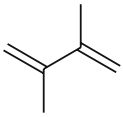	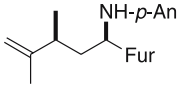	94[15 : 1]
4	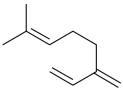	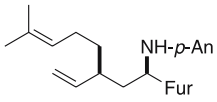	98[15 : 1]

Scheme 14 outlines a rationale for the opposite stereoselectivity between aldehydes and aldimines using isoprene as a representative unsymmetrical diene. As described in Scheme 11, the 1,3-*anti* stereoselectivity for aldehydes stems from a quasi-equatorial orientation of an aldehyde substituent in an intermediate **59**. In an intermediate **60**, however, placing an aldimine substituent in the same equatorial position causes steric repulsion between *p*-anisyl and a ligand on Ni(II), which has a square planar configuration. Hence, as a second choice, the aldimine substituent R would take a quasi-axial configuration in an intermediate **61**, which leads to 1,3-*syn*-**63** via ethyl group transfer and β-H elimination and *cis*-reductive elimination of a hydridonickel(II) intermediate **62**. Owing to 1,3-diaxial repulsion between methyl and R in the intermediate **61** (indicated by shading), sterically demanding

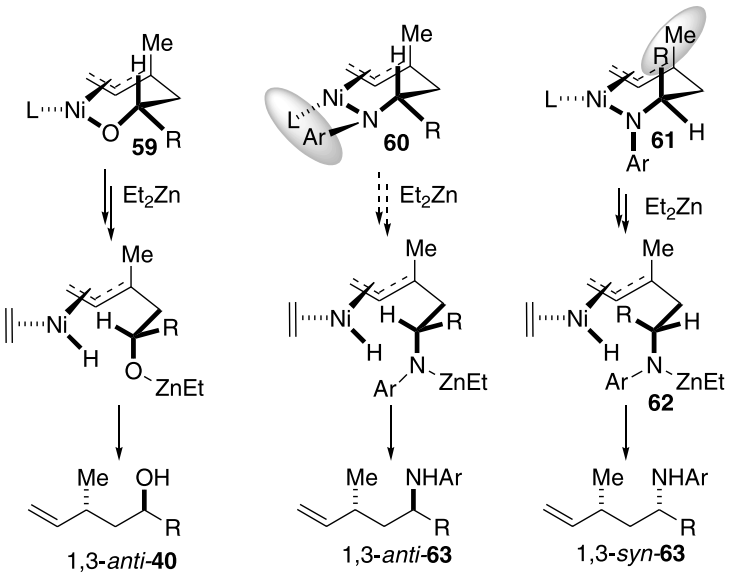

Scheme 14 Possible intermediates for the stereoselective and regioselective formation of 1,3-*syn*-**63**

aldimines might tend to give the C4-regioisomer **58** in considerable amounts, according to the mechanism described in Scheme 12 (c.f., **45″**).

3.4 Application to Multigram-Scale Experiments

The homoallylation is applicable to multigram-scale experiments (Scheme 15) [36]. In the presence of 3 mol % of $Ni(acac)_2$, a mixture of 25 mmol of benzaldehyde, 50 mmol of Et_3B, and 50 mmol of isoprene provides *anti*-3-methyl-1-phenyl-4-pentenol in 92% yield (4.1 g) with excellent 1,3-*anti* stereoselectivity. The product is purified by means of a single Kugelrohr distillation of the reaction mixture after an appropriate aqueous workup.

The reaction of isoprene (200 mmol) and dihydrocinnamaldehyde (50 mmol) using 1.5 mol % of $Ni(acac)_2$ as a catalyst is undertaken as usual, which yields the desired bis-homoallyl alcohol in 85% yield (8.7 g) contaminated by the ethylation product (10%). In large-scale experiments, both the yield and diastereoselectivity are significantly improved as compared with those recorded for the usual millimolar-scale reaction conditions. However, the ethylation of aldehydes with Et_2Zn becomes a serious side reaction. After many experimentations in pursuit of suppressing the ethylation in large-scale experiments, a satisfactory procedure has been developed. This consists of a pretreatment of $Ni(acac)_2$ (3 mol %) with 1 equiv. of Et_2Zn (3 mol %) at ambient temperature, followed by addition of Et_3B (240 mol %), an aldehyde,

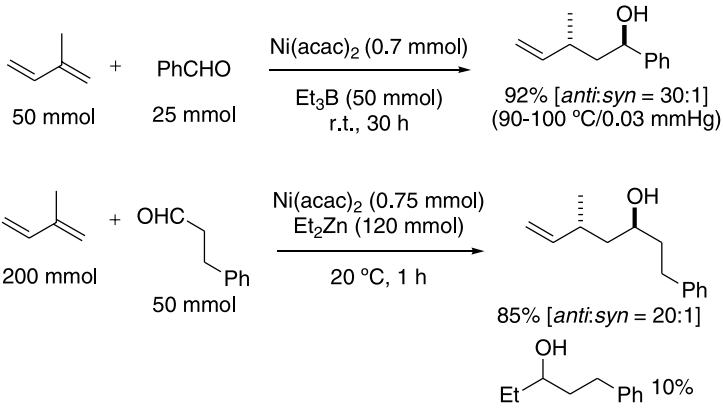

Scheme 15 Multigram-scale experiments: Et_3B-Ni catalysis for aromatic aldehydes and Et_2Zn-Ni catalysis for aliphatic aldehydes and their variation (Eq. 15)

and isoprene (300 mol %) at ambient temperature. According to this protocol, the homoallylation product is obtained in 80% yield with excellent 1,3-*anti* selectivity without contamination by the ethylation product (Eq. 15).

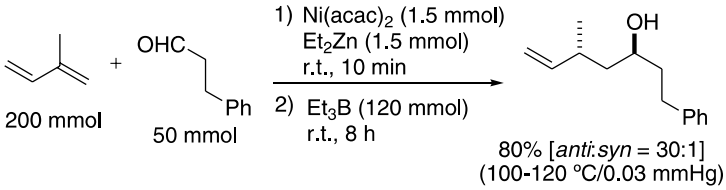

Equation 15

3.5 Intramolecular Homoallylation of ω-Dienyl Aldehydes

The protocol for the intermolecular homoallylation of aldehyde with 1,3-dienes is applied successfully to an intramolecular version of ω-dienyl aldehydes forming five- and six-membered rings. Generally, aliphatic ω-dienyl aldehydes **64** show remarkably high regio- and stereoselectivity irrespective of the carbon chain lengths, and provide *cis*-2-allylcycloalkanols **65** as a single isomer (Eq. 16, Table 10) [37]. All the reactions proceed very quickly with Et_2Zn, being complete within half an hour at room temperature. However, in some cases, simple addition reaction of Et_2Zn upon an aldehyde takes place as a side reaction (run 3 in Table 10). On the other hand, although the reaction with Et_3B requires a longer reaction time for completion of the reaction ($1 \sim 2$ days), no ethylation takes place at all. As for the stereoselectivity, no significant difference is observed between the reactions with Et_2Zn and Et_3B.

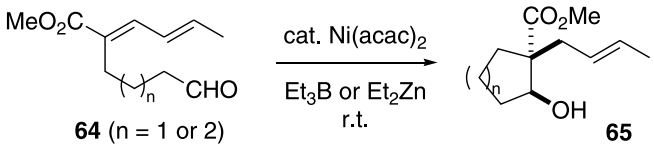

Equation 16

Table 10 Ni-catalyzed reductive cyclization of ω-dienyl aldehydes **64** at room temperature

Run	n in **64**	Et_nM	Time	%Yield of **65**
1	1	Et_2Zn	15 min	72
2	1	Et_3B	34 h	67
3	2	Et_2Zn	30 min	57[a]
4	2	Et_3B	24 h	68

[a] 1,2-Addition product of Et_2Zn upon **64** (16% yield)

A rationale for the *cis*-selective cyclization for the intramolecular homoallylation of ω-dienyl aldehyde **64** is illustrated in Scheme 16. The scenario is essentially the same as the one proposed for the intermolecular reaction, and a Ni(0) species undergoes oxidative addition upon the diene and the aldehyde moieties through a conformation placing the aldehyde substituent and the diene *anti* to each other. An intermediate **66** undergoes β-H elimination and *cis*-reductive elimination of the thus-formed Ni – H complex to produce **65**.

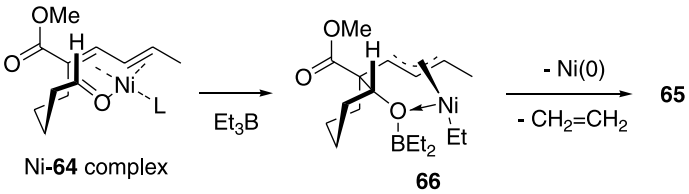

Scheme 16 Intramolecular reductive homoallylation of ω-dienyl aldehydes

A palladium(0) species nicely catalyzes the Grob-type decarboxylative ring-opening reaction of cyclic carbonate **67** (Eq. 17) [38, 39].

The reaction proceeds at room temperature and is rationalized invoking oxidative addition of a Pd(0) species upon the allylic C – O bond of **67**, followed by decarboxylation to form an oxapalladacyclopentane intermediate **66′** (Pd in place of Ni), which undergoes a facile β-C elimination to finally give an ω-dienyl aldehyde **68′** (Scheme 17). Recently, it has been revealed that a combination of $Ni(cod)_2$ and a phosphine ligand also catalyzes the same

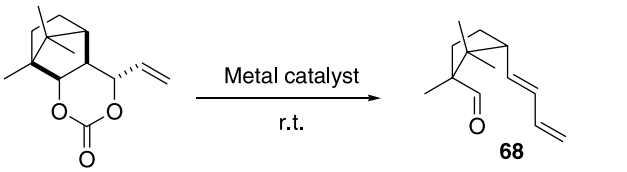

Equation 17

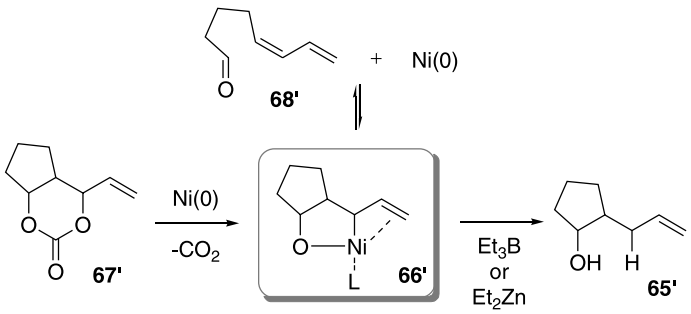

Scheme 17 Ni-catalyzed reversible C – C bond formation and C – C bond cleavage

fragmentation and furnishes ω-dienyl aldehydes **68′** in the better yield than the palladium catalyst does [40].

It should be noted that the Grob fragmentation reaction and the reductive cyclization (homoallylation) discussed in this section involve the same oxanickellacyclopentane **66′** as a common intermediate (Scheme 17). The reversibility of these C – C bond cleavage reaction and C – C bond formation reaction is also supported by the isolation and characterization (by X-ray analysis) of an oxanickellacyclopentane-like **66′** (without a tether), which is prepared from a stoichiometric amount of $Ni(cod)_2$, a diene, an aldehyde, and a monodentate phosphine ligand [41].

3.6 Homoallylation of Aldehydes Promoted by Diisobutyl(acetylacetonato)aluminum(III)

The kind of reducing agents determines the course of the reductive coupling reaction of aldehydes with dienes: either allylation or homoallylation. As discussed in Sect. 2.2, in the presence of $Ni(cod)_2$-PPh_3 catalyst, triethylsilane promotes an ω-dienyl aldehyde **69** to undergo the intramolecular *allylation* to provide a homoallyl alcohol **70** (Scheme 18) [42]. On the other hand, DIBAL(acac), like Et_3B and Et_2Zn (Sect. 3.5), guides the same ω-dienyl aldehyde **69** to selectively undergo homoallylation to afford a bis-homoallyl alcohol **71** as a sole product [43].

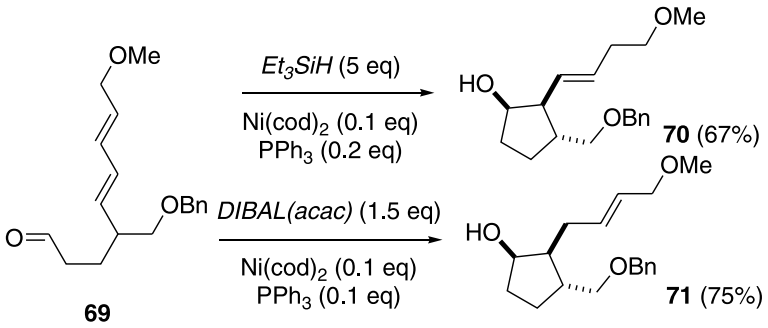

Scheme 18 Ni-catalyzed allylation vs. homoallylation using different reducing agents

Intermolecular reductive coupling of 1-phenyl-1,3-diene and benzaldehyde in a 1 : 1 ratio in the presence of a catalytic amount of $NiCl_2(PPh_3)_2$ and a stoichiometric amount of DIBAL(acac) shows poor selectivity. 1-Phenyl-1,3-butadiene reacts with benzaldehyde at the C4 and C1 positions, providing a mixture of linear and branched isomers **72** and **73**, respectively. The reaction is complicated by the formation of a bis-allylation product **74** (Eq. 18) [44]. In this reaction, a Ni(0) species is generated in situ from $NiCl_2(PPh_3)_2$ by treatment with *n*-BuLi. The relative amount of the linear and branch isomers (e.g., **72**/**73**) depends on the kind of aldehydes and ranges from 9.8 : 1 (*p*-methoxybenzaldehyde) to 1 : 2.3 (butyraldehyde).

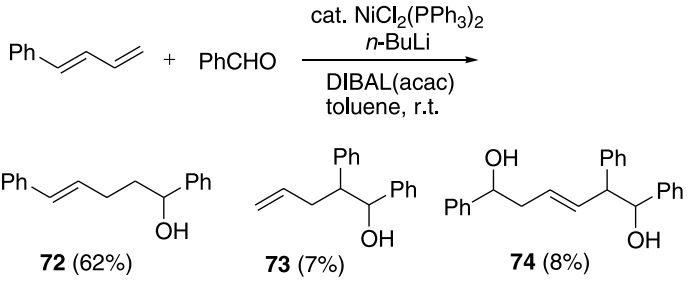

Equation 18

4 Other Related Reactions

The event, oxidative addition of a Ni(0) species upon dienes and aldehydes activated by coordination with Lewis acids to provide oxanickellacycles **45**, has proven to take place quite generally, and many variations making the best use of the intermediate **45** have been developed. The key issue of the reactions discussed in Sect. 3 is a regioselective and stereoselective hydrogen delivery

via a transition state **III**. The hydrogen stems from either ethyl group (from Et_2Zn, Et_3B) or isobutyl group (from $(i-Bu)_2Al(acac)$) via β-hydrogen elimination.

When β-elimination is impossible, e.g., Me_2Zn and Ph_2Zn, Me and Ph groups are introduced at the distal allylic terminus of an intermediate **46′** via *cis*-reductive elimination, overall establishing difunctionalization of dienes at C1 and C4 positions (Scheme 19). The following equations summarize examples demonstrating 1,4-difunctionalization of dienes currently developed [45–57]. The reaction shown in Eq. 25 is stoichiometric with respect to Ni, and the other examples are all catalytic with respect to Ni.

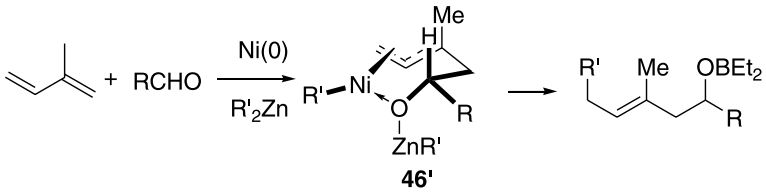

46'

Scheme 19 Ni(0)-catalyzed 1,4-difunctionalization of dienes

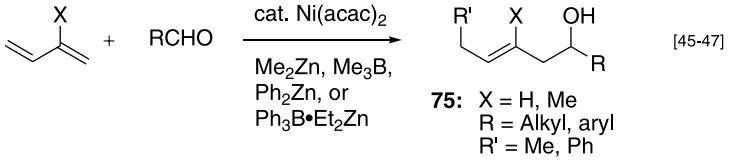

75: X = H, Me
R = Alkyl, aryl
R' = Me, Ph

Equation 19

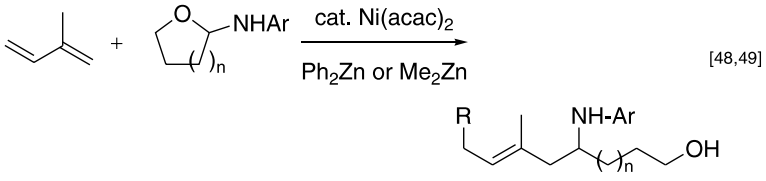

76: R = Me, Ph
n = 1, 2

Equation 20

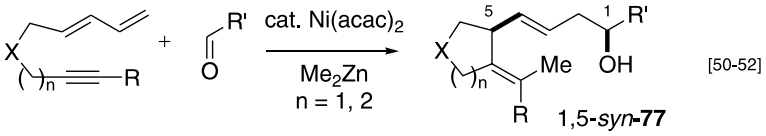

1,5-*syn*-**77**

Equation 21

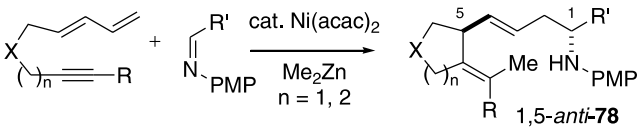

[53]

Equation 22

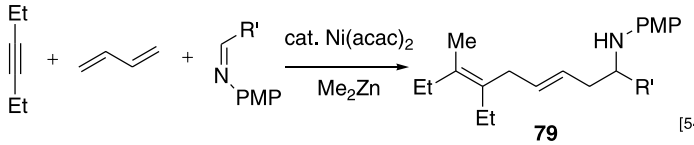

[54]

Equation 23

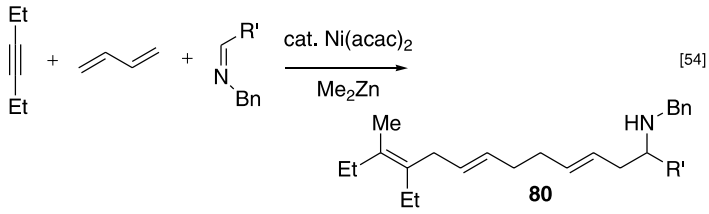

[54]

Equation 24

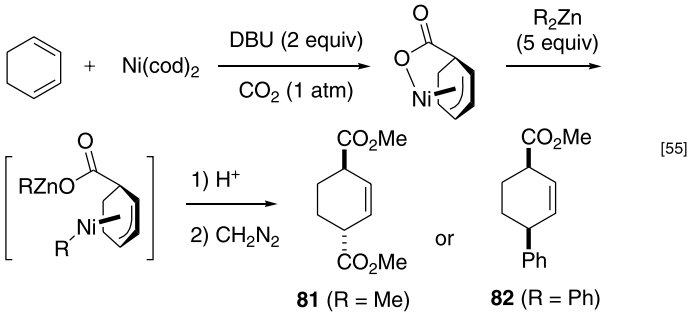

[55]

Equation 25

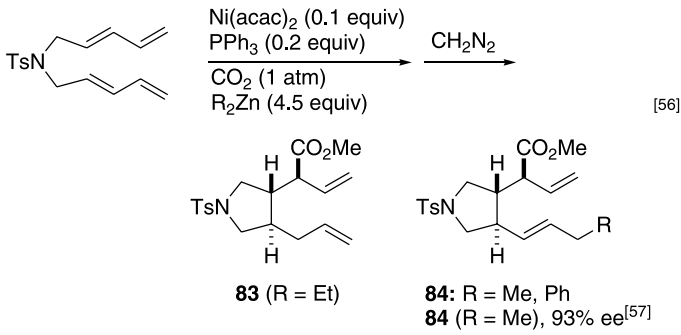

[56]

Equation 26

5 Conclusion

In this review, the reductive coupling reactions of dienes and carbonyl compounds promoted by Ni complexes, activating dienes as allyl anions and as homoallyl anions, have been described. In the presence of an excess amount of trialkylsilane as a reducing agent, a nickel(0) species catalytically generates allyl anion equivalents from dienes, which react with aldehydes to provide homoallyl alcohols. The reaction shows high regioselectivity and stereoselectivity. In the presence of a stoichiometric amount of indium(I) iodide, $Ni(acac)_2$ catalyzes the double additions of aldehydes with 1,3-butadienes to afford either 3-hexene-1,6-diols and/or 2-vinyl-1,4-butanediols depending on the ligands and solvent systems.

The combination of $Ni(acac)_2$ and triethylborane promotes the generation of homoallyl anion equivalents from dienes. Homoallylation of aromatic aldehydes and α,β-unsaturated aldehydes with a variety of conjugated dienes provides 4-pentenols in high yields with excellent regioselectivity and stereoselectivity. 2-Substituted 1,3-dienes provide 1,3-*anti* adduct selectively, and 1-substituted dienes furnish the 1,2-*anti* adduct exclusively. Aliphatic aldehydes and ketones undergo the homoallylation with 1,3-dienes by using diethylzinc as a reducing agent. Aldimines prepared in situ from aldehydes and *p*-anisidine undergo the homoallylation with 2-substituted 1,3-dienes in the presence of diethylzinc and a Ni(0) catalyst, and provide bis-homoallyl amines with excellent 1,3-*syn* stereoselectivity, the stereoselectivity being opposite to that of aldehydes. These homoallylations are applicable to the multigram-scale experiments. The reactions are so clean that the products can be purified by means of single distillation. DIBAL(acac) works similarly well to triethylborane and diethylzinc.

Recent advancements involving oxanickellacycles as common intermediates, which are formed by oxidative addition of a Ni(0) species upon dienes and aldehydes, is also reviewed very briefly.

References

1. Trost BM (1991) In: Paquette LA (ed) Combining C – C n-bonds. Comprehensive organic synthesis, vol 5, chap 4. Pergamon, Oxford
2. Wilke G (2003) Angew Chem Int Ed 42:5000
3. Parshall GW (1978) J Mol Catal 4:243
4. Baker R (1973) Chem Rev 73:487
5. Müller H, Wittenberg D, Seibt H, Scharf E (1965) Angew Chem Int Ed 4:327
6. Reed HWB (1954) J Am Chem Soc 76:1931
7. Tamaru Y (2005) Modern organonickel chemistry. Wiley-VCH, Weinheim
8. Wilke G (1988) Angew Chem Int Ed 27:185

9. Benn R, Büssemeier B, Holle S, Wolly PW, Mynott R, Tkatchenko I, Wilke G (1985) J Orgnomet Chem 279:63
10. Baker R, Crimmin MJ (1976) J Chem Soc Perkin Trans 1 1264
11. Baker R, Blackett BN, Cookson RC, Cross RC, Madden DP (1972) J Chem Soc Chem Commun, p 343
12. Akutagawa S (1976) Bull Chem Soc Jpn 49:3646
13. Tamao K, Kobayashi K, Ito Y (1992) Synlett, p 539
14. Sato Y, Takimoto M, Hayashi K, Katsuhara T, Takagi K, Mori M (1994) J Am Chem Soc 116:9771
15. Sato Y, Saito N, Mori M (1997) Tetrahedron Lett 38:3931
16. Sato Y, Saito N, Mori M (1998) Tetrahedron 54:1153
17. Sato Y, Saito N, Mori M (2000) J Am Chem Soc 122:2371
18. Sato Y, Saito N, Mori M (2002) J Org Chem 67:9310
19. Yeh MCP, Liang JH, Jiang YL, Tsai MS (2003) Tetrahedron 59:3409
20. Takimoto M, Hiraga Y, Sato Y, Mori M (1998) Tetrahedron Lett 39:4543
21. Sawaki R, Sato Y, Mori M (2004) Org Lett 6:1131
22. Sato Y, Sawaki R, Mori M (2001) Organometallics 20:5510
23. Hirashita T, Kambe S, Tsuji H, Araki S (2006) Chem Commun, p 2595
24. Kong JR, Ngai MY, Krische MJ (2006) J Am Chem Soc 128:718
25. Jang HY, Krische MJ (2004) Eur J Org Chem 2004(19):3953
26. Bertelo CA, Schwaltz J (1976) J Am Chem Soc 98:262
27. Kimura M, Ezoe A, Shibata K, Tamaru Y (1998) J Am Chem Soc 120:4033
28. Kimura M, Ezoe A, Mori M, Iwata K, Tamaru Y (2006) J Am Chem Soc 128:8559
29. Kimura M, Ezoe A, Mori M, Tanaka S, Tamaru Y (2001) Angew Chem Int Ed 40:3600
30. Kimura M, Fujimatsu H, Ezoe A, Shibata K, Shimizu M, Matsumoto S, Tamaru Y (1999) Angew Chem Int Ed 38:397
31. Tamaru Y (2005) Eur J Org Chem 2005(13):2647
32. Wei C, Li Z, Li CJ (2004) Synlett, p 1472
33. Kobayashi S, Ishitani H (1999) Chem Rev 99:1069
34. Kimura M, Miyachi A, Kojima K, Tamaru Y (2004) J Am Chem Soc 126:14360
35. Kimura M, Miyachi A, Kojima K, Tamaru Y (2005) J Am Chem Soc 127:10117
36. Tamaru Y, Kimura M (2006) Org Synth 83:88
37. Shibata K, Kimura M, Shimizu M, Tamaru Y (2001) Org Lett 3:2181
38. Harayama H, Kuroki T, Kimura M, Tanaka S, Tamaru Y (1997) Angew Chem Int Ed 36:2352
39. Harayama H, Kimura M, Tanaka S, Tamaru Y (1998) Tetrahedron Lett 39:8475
40. Mori M, Kimura M, Takahashi Y, Tamaru Y (2006) Chem Commun, p 4303
41. Ogoshi S, Tonomori K, Oka M, Kurosawa H (2006) J Am Chem Soc 128:7077
42. Sato Y, Takanashi T, Hoshiba M, Mori M (1998) Tetrahedron Lett 39:5579
43. Sato Y, Takimoto M, Mori M (2000) J Am Chem Soc 122:1624
44. Sato Y, Sawaki R, Saito N, Mori M (2002) J Org Chem 67:656
45. Kimura M, Matsuo S, Shibata K, Tamaru Y (1999) Angew Chem Int Ed 38:3386
46. Kimura M, Shibata K, Koudahashi Y, Tamaru Y (2000) Tetrahedron Lett 41:6789
47. Shibata K, Kimura M, Kojima K, Tanaka S, Tamaru Y (2001) J Organomet Chem 624:348
48. Kojima K, Kimura M, Tamaru Y (2005) Chem Commun, p 4717
49. Kojima K, Kimura M, Ueda S, Tamaru Y (2006) Tetrahedron 62:7512
50. Ezoe A, Kimura M, Inoue T, Mori M, Tamaru Y (2002) Angew Chem Int Ed 41:2784
51. Kimura M, Ezoe A, Mori M, Tamaru Y (2005) J Am Chem Soc 127:201

52. Kojima K, Kimura M, Tamaru Y (2004) Synthesis 3089
53. Kimura M, Mori M, Mukai N, Kojima K, Tamaru Y (2006) Chem Commun, p 2813
54. Kimura M, Kojima K, Tatsuyama Y, Tamaru Y (2006) J Am Chem Soc 128:6332
55. Takimoto M, Mori M (2001) J Am Chem Soc 123:2895
56. Takimoto M, Mori M (2002) J Am Chem Soc 124:10008
57. Takimoto M, Nakamura Y, Kimura K, Mori M (2004) J Am Chem Soc 126:5956

Top Curr Chem (2007) 279: 209–248
DOI 10.1007/128_2007_123

Published online: 9 June 2007

Reductive Coupling of Unactivated Alkenes and Alkynes

Richard D. Broene

Department of Chemistry, Bowdoin College, 6600 College Station,
Brunswick, ME 04011-8466, USA
rbroene@bowdoin.edu

Abstract Significant advances have been made in the study of catalytic reductive coupling of alkenes and alkynes over the past 10 years. This work will discuss the progress made in early transition metal and lanthanide series catalytic processes using alkyl metals or silanes as the stoichiometric reductants and the progress made in the use of late transition metals for the same reactions using silanes, stannanes and borohydrides as the reductant. The mechanisms for the reactions are discussed along with stereoselective variants of the reactions.

Keywords Metal-catalyzed · Reductive coupling · Cyclization

Abbreviations

Acac	Acetylacetonate
Ar	Aromatic
BArF	Tetra(perfluorophenyl)borate or tetra(3,5-trifluoromethylphenyl)bortate
BINAP	2,2′-Bis(diphenylphosphino)-1,1′-binaphthalene
BINOL	1,1′-Binaphthalene-2,2′-dioate
Bn	Benzyl
Bz	Benzoate
Bu	*n*-Butyl
*i*Bu	Isobutyl
*t*Bu	*tert*-Butyl
Cat	1,2-Benzenedioate
cod	1,5-Cyclooctadiene
Cp	1,3-Cyclopentadienyl anion
Cp*	1,2,3,4,5-Pentamethyl-1,3-cyclopentadienyl anion
Cy	Cyclohexyl
dba	Dibenzylideneacetone
DMF	*N*,*N*-Dimethylformamide
dppe	1,2-(Diphenylphosphino)ethane
dr	Diastereomeric ratio
ee	Enantiomeric excess
Et	Ethyl
Et2O	Diethyl ether
L	Ligand
Ln	Lanthanide or Group 3 metal
OAc	Acetate
Ph	Phenyl
*i*Pr	Isopropyl
*n*Pr	*n*-Propyl
R	Alkyl group
Sol	Solvent
oTol	2-Methylphenyl
THF	Tetrahydrofuran
TMS	Trimethylsilyl
Ts	Tosyl, 4-methylphenylsulfonyl

1 Introduction and Scope

Metal-mediated reductive coupling of alkenes and alkynes affords access to complicated organic structures, including carbocyclic and heterocyclic molecules, from readily available starting materials. While most of these coupling reactions were initially developed as stoichiometric processes, many selective, catalytic versions have been developed over the past decade; these advancements have made reductive coupling much more attractive to synthetic chemists.

This review will explore reductive coupling reactions using early (Group 3, 4, and lanthanides) and late (Groups 9 and 10) transition metals. The reac-

tions of unactivated alkenes, alkynes, and allenes with stoichiometric reductants that leave at least one hydrogen atom in the product will be discussed. Reactions that are terminated without hydrogen atoms (e.g., diborations, distannylations, and disilylations) [1] will not be covered within this review in order to more fully explore the reductive homo- and heterocoupling of alkenes and alkynes. Areas that are covered by other chapters of this volume are intentionally omitted; these include reactions catalyzed by nickel and reactions terminated with dihydrogen. Finally, the review is organized by catalyst rather than by substrate so that mechanistic parallels can be highlighted.

2
Reactions Catalyzed by Early Transition Metals or Lanthanides

2.1
Group 4 Metals

2.1.1
Zirconium-Catalyzed Intermolecular Reactions

Zirconium complexes are very effective promoters of both intra- and intermolecular couplings of alkenes and alkynes, but they generally require a stoichiometric quantity of the metal for effective reaction. Typically, the metallocene "Cp_2Zr" (Cp = $C_5H_5^-$) or an equivalent is employed in these processes. Zirconium-mediated reductive coupling can be employed in the cross-coupling of a wide variety of alkenes and alkynes, leading to zirconacyclopentanes, zirconacyclopentenes, or zirconacyclopentadienes [2]. The metal complexes employed in reductive coupling reactions are closely related to those used as alkene polymerization catalysts [3]. The key to using them as reductive coupling catalysts is to intercept the "polymerization" after coupling of two unsaturated hydrocarbons with an appropriate reducing agent or to transfer the growing chain via transmetallation.

In the mid-1980s, Dzhemilev [4] reported that strained or α-olefins could be carbomagnesiated intermolecularly using a catalytic amount of Cp_2ZrCl_2. For example, excellent chemo- and regioselective addition of Et_2Mg to *Z*-1,4-hexadiene gave a 90% yield of *Z*-5-methyl-2-heptene, with Markovnikov addition of ethyl group to the less substituted alkene (Eq. 1). Several research

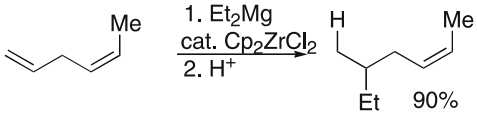

Equation 1

groups explored this reaction in greater detail in the early 1990s with the consensus mechanism described below.

The mechanism for this reaction follows a route very similar to that observed in the stoichiometric reaction, in which Cp_2ZrEt_2 (**1**) forms the intermediate **2** after loss of ethane (Scheme 1) [2]. Complex **2** can be described as either an ethene complex of Zr(II) or as a Zr(IV) zirconacyclopropane; this species is formally a 16-electron complex, and can coordinate to and insert into an olefin to give zirconacyclopentane **3** with the bulky group at the sterically less hindered position *beta* to the Zr [5]. Under conditions of excess EtMgX (X = halide or Et), an ethyl anion adds to the coordinatively unsaturated Zr center to provide complex **4**, which is in equilibrium with bimetallic species **5**. Depending on conditions, complex **5** can either undergo β-abstraction to regenerate zirconacyclopropane (**2**) and the carbometallated product **6** or can form **1** and the bis-Grignard reagent **7** through a second *ate* complex. In either case, the final product after hydrolysis is best described as the result of formal addition of an ethyl group and a hydrogen atom to the olefin [2].

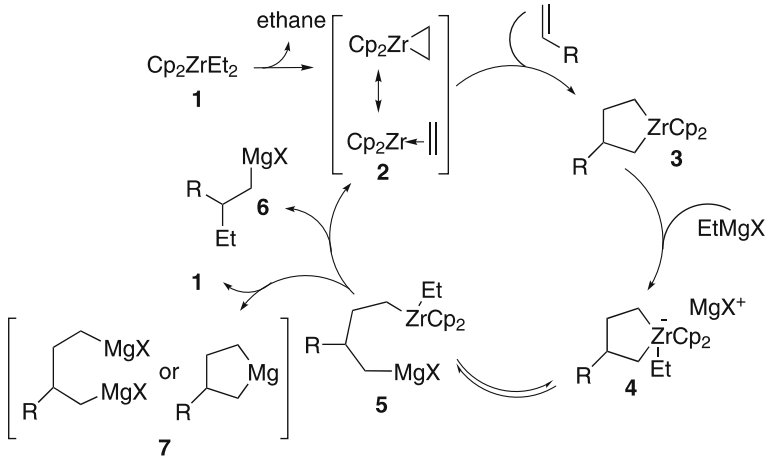

Scheme 1 Mechanism of the zirconocene-catalyzed ethyl magnesiation reaction

The ratio of products resulting from the competing pathways detailed above changes depending on the solvent and on the nature and concentration of the alkylating agent used for the reaction (Scheme 2). The ratio of deuterated products resulting from the treatment of alkene **8** with **1** and Et_2Mg, followed by addition of D_2O, reduced the ratio of **9**:**10** from 2 : 3 to 1 : 3 upon doubling the concentration of alkylating agent [6]. Use of THF as solvent in place of diethyl ether increased the ratio of **9**:**10** from 2 : 3 to 19 : 1 under otherwise identical conditions. These results are consistent with coordinating solvents suppressing the β-abstraction of **5** [6]. The

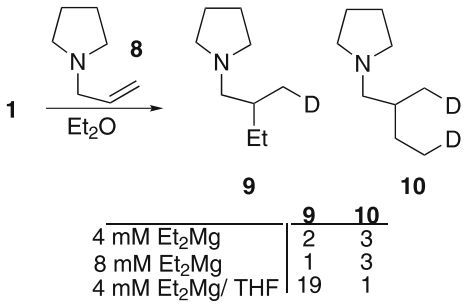

Scheme 2 Dependence of product ratio on concentration and solvent

turnover-limiting step of the catalytic process is the formation of zirconacyclopropane **2** from Cp_2ZrEt_2. It should be noted that this reaction is facile only for EtMgX species, with longer chain alkyl Grignards providing mixtures of products [7].

2.1.1.1 Asymmetric Alkene Coupling Reactions

A variety of chiral, non-racemic zirconium complexes were explored in attempts to develop an enantioselective variant of this reaction (Scheme 3) [7–9]. For example, when allylic amines **11a,b** were treated with EtMgCl and 10% of C_2-symmetric BINOL-zirconium bis(tetrahydroindenyl)ethane (**12**, Brintzinger's catalyst [10], BINOL is 1,1′-binaphthalene 2,2′-dioate), chiral ethylated products **13a,b** were obtained in 34–39% yield with enantiomeric excesses (ee) of ca. 26% [8]. Use of a (neomenthylindene)$ZrCpCl_2$ catalyst **14**, designed to improve the steric differentiation of the diastereomeric transition states, improved the chemical yields of amines at lower catalyst loadings (2–4%) and increased the ees of the reactions by a factor of three in the case of **11a** [8, 9]. Similar reactivity is observed in zirconocene dichloride-catalyzed cyclization of 1,6- and 1,7-enynes with 12.5% Cp_2ZrCl_2 using Et_3Al as the stoichiometric reductant. For these substrates, the alkyne coordinates

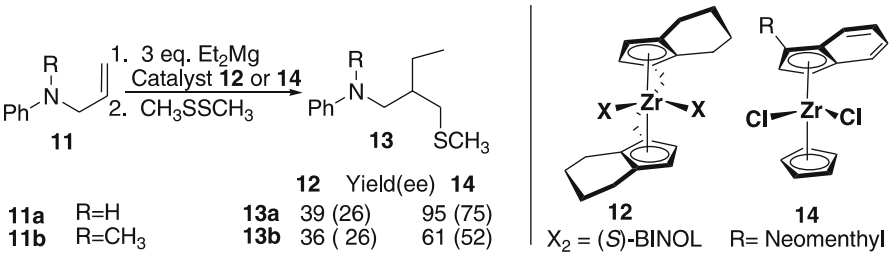

Scheme 3 Enantioselectivity within the ethyl magnesiation reaction induced by **12** or **14**

and displaces the ethene, followed by oxidative cyclization and transmetallation to give a cyclic alane. The mechanism for this reaction is not yet clear cf. [11, 12].

2.1.2 Zirconium-Catalyzed Diene Cyclizations

The reaction described above forms one of the coupling partners by β-abstraction of a hydrogen atom on the ethyl group to formally generate the second alkene-coupling partner. This reaction has also been used to reductively couple 1,6- and 1,7-dienes to generate cyclopentane and cyclohexane derivatives **17** and **18** [13, 14]. When 1 eq. of 1,7-octadiene was treated with 10 mol % Cp_2ZrCl_2 and 3 eq. of Bu_2Mg in diethyl ether (Eq. 2), followed by acidification, a 96% yield of 1,2-dimethylcyclohexane (**18**) is formed with a ca. 1 : 4 *trans* to *cis* ratio [15]. Intermediate dimagnesium species such as **23** (Scheme 4) could be oxidized with iodine or oxygen to give diiodide or diol products [13, 14]. Alkenes with substitution at either the 1 or 2 positions were tolerated under the reaction conditions, as was the presence of tertiary amine groups within the connecting chain (Z = NCH_2Ph in Eq. 2).

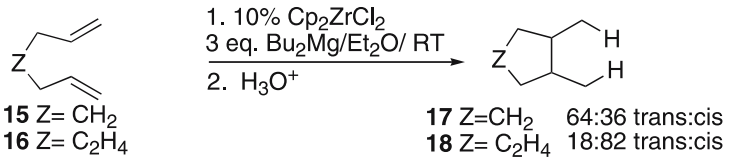

Equation 2

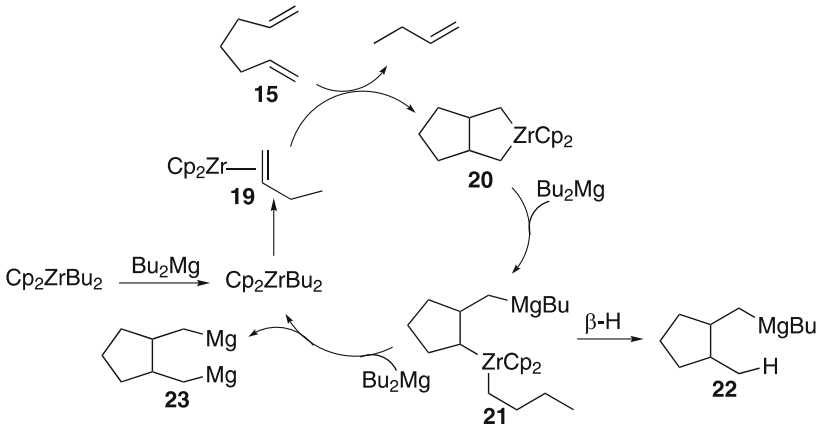

Scheme 4 Mechanism of the zirconocene-catalyzed reductive cyclization of dienes

Extensive mechanistic experiments have revealed that the reductive cyclization reaction is very sensitive to the experimental conditions employed: *cis/trans* selectivity and mono- or di-magnesiated selectivity depends on the identity and concentration of the Grignard reagent, as well as the solvent and temperature for the reaction [13, 14]. The mechanism for this reaction closely mirrors that seen in the intermolecular case; the 16-electron bicyclic zirconacyclopentane **20** is formed by generation of the zirconocene equivalent CpZr(1-butene) **19** [16] from initially formed Cp_2ZrBu_2 followed by ligand exchange with **15** and coupling of the olefins. Zirconacyclopentane **20** undergoes transmetallation with Bu_2Mg to give complex **21**. Subsequent β-abstraction affords the mono-magnesium product **22**, whereas reaction with a second equivalent of alkylmagnesium reagent gives the di-magnesium product **23**.

The ratio of **23** to **22** is larger in diethyl ether than in THF due to a faster second transmetallation of **21** relative to the β-abstraction reaction [13]. This hypothesis is supported by kinetic studies revealing that transmetallation of the metallacycle **20** is rate-limiting at low concentrations of RMgX, while at high [RMgX] the β-abstraction reaction of Cp_2ZrBu_2 becomes the rate-limiting step. The diastereoselectivity of the reaction depends on the temperature, the concentration of Bu_2Mg, as well as the size of the ring formed and the functional groups present. For the formation of six-membered rings, the *cis* metallacycle is kinetically favored (82 : 18 *cis* : *trans*) but the *trans* isomer is thermodynamically favored (1 : 10 *cis* : *trans*). In contrast, cyclization to five-membered rings shows that the *trans* isomer is typically both kinetically (4 : 6) and thermodynamically (3 : 97) favored (with the exception of 3,4-dimethylpyrrolidene formed by the cyclization of diallylaniline). The ratios of diastereomers obtained from the reaction depend on the concentration of the RMgX and the rate of the transmetallation step, as it is not reversible and leads to isolation of the kinetic products at high RMgX concentrations [13, 14].

These methods were applied to the synthesis of heterocycles such the perhydroindene in Eq. 3 [17]. The reductive coupling of diene **24** catalyzed by Cp_2ZrCl_2 in the presence of BuMgBr demonstrates the ability of the coupling to generate contiguous stereogenic centers in an effective fashion.

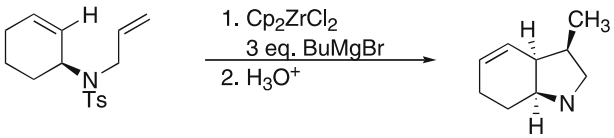

24

Equation 3

2.1.2.1
Enantioselective Diene Cyclization Reactions

An enantioselective variant of the diene cyclization reaction has been developed by application of chiral zirconocene derivatives, such as Brintzinger's catalyst (**12**) [10]. Mori and co-workers demonstrated that substituted diallylbenzylamine **25** could be cyclized to pyrrolidines **26** and **27** in a 2 : 1 ratio using chiral complex **12** in up to 79% yield with up to 95% ee (Eq. 4) [17, 18]. This reaction was similarly applied to 2-substituted 1,6-dienes, which provided the analogous cyclopentane derivatives in up to 99% ee with similar diastereoselectivities [19]. When cyclic, internal olefins were used, spirocyclic compounds were isolated. The enantioselection in these reactions is thought to derive from either the *ate* or the transmetallation step. The stereoselectivity of this reaction has been extended to the selective reaction of enantiotopic olefin compounds to form bicyclic products such as **28**, in 24% yield and 59% ee after deprotection (Eq. 5) [20].

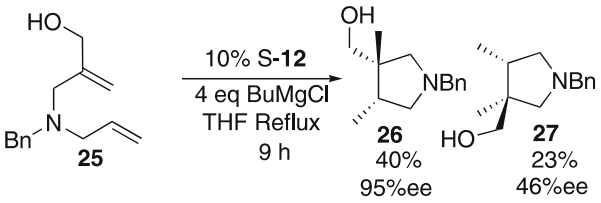

Equation 4

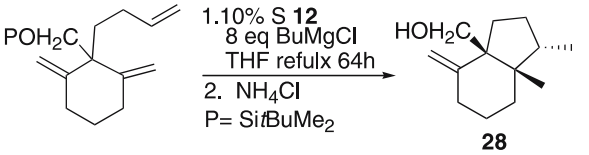

Equation 5

2.1.3
Diastereocontrol via Proximal Oxygen

The zirconocene catalysts described above are very oxophilic, which provides several synthetically useful transformations. Oxygen substitution at the allylic or homoallylic position of an olefin substrate allows for excellent regio- and diastereocontrol in the ethyl magnesiation reactions of α-olefins and dienes [21]. When **29** is substituted with a hydroxyl group (**29a**), *syn* **30a** is favored over *anti* in a 95 : 5 ratio, while substitution with OCH_3 (**29b**) reversed the diastereoselectivity to 11 : 89 (Eq. 6). Use of THF in place of diethyl ether as the reaction solvent for the reaction of **29a** lowered the overall diastereo-

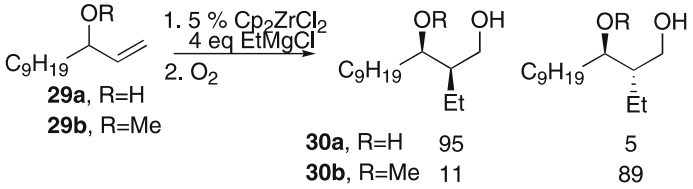

Equation 6

selectivity of the reaction to favoring the *syn* diastereomer in an 85 : 15 ratio. Both of these observations are consistent with the selectivity arising from coordination of magnesium alkoxide, formed by deprotonation of **29a**, to the Zr center, leading to the major product. The authors propose that this effect would be diminished in the more Lewis basic THF solvent relative to diethyl ether [22].

Homoallylic oxygen substitution of the olefins **31** and **33** gave coupled products **32** and **34** with addition of the new alkyl group *anti* to the methyl group, regardless of the oxygen orientation (Scheme 5) [22]. This result strongly suggests that α-substitution controls the stereoselectivity of the reaction. Similar results were observed in the cyclization of diene **35** with 0.1 eq. Cp_2ZrCl_2 and BuMgCl [21]; the kinetically formed *cis* zirconacycle **36** reacts to give a 60% yield of **37** after oxidation (Scheme 6). In this case, the mech-

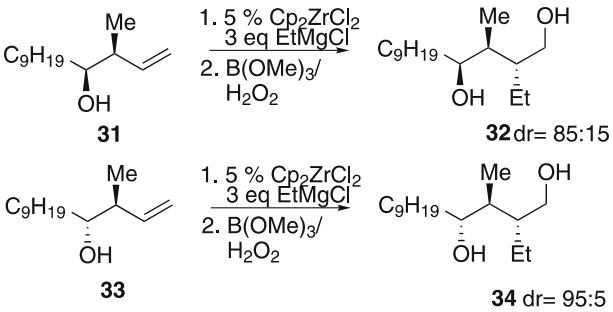

Scheme 5 Diastereoselectivity of the ethyl magnesiation reaction

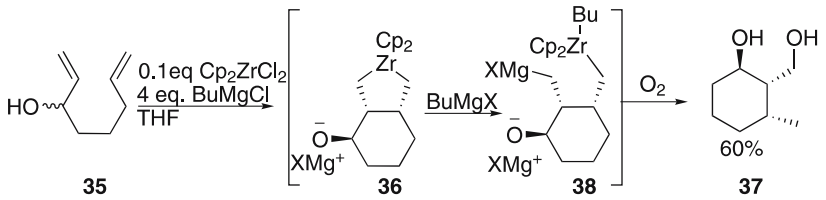

Scheme 6 Diastereoselectivity within the reductive cyclization reaction

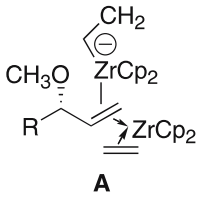

Fig. 1 Proposed bimolecular zirconocene complex leading to reductive coupling

anism favors transmetallation at the C proximal to the hydroxyl group to give the alkyl magnesium intermediate **38** prior to β-abstraction.

Interestingly, Hoveyda and coworkers observed a second-order dependence of the reaction rate on the concentration of zirconium in these reactions, suggesting that the zirconacyclopentane is formed from a bimetallic alkene–zirconate complex such as **A** in Fig. 1 [21]. This finding suggests that olefin alkylations and substitutions occur via reaction of a nucleophilic alkene unit [23].

2.1.4 β-Alkoxide Elimination Processes

Reductive coupling of substrates with allylic oxygen or nitrogen substitution may undergo related reactions via β-alkoxide or β-amide elimination pathways. Hoveyda and coworkers demonstrated that the reductive coupling of ethene to cyclic allylic ethers or amines resulting in the formation of enols and amines [7, 24–26]. Using the Brintzinger catalyst (R)-**12** and EtMgCl, dihydrofuran **39** is carbometallated to provide alkoxide **40** in > 97% ee and 65% yield (Scheme 7) [26]. The diene complex initially formed in the reaction favors alkene coordination as illustrated in **41** such that the oxygen is

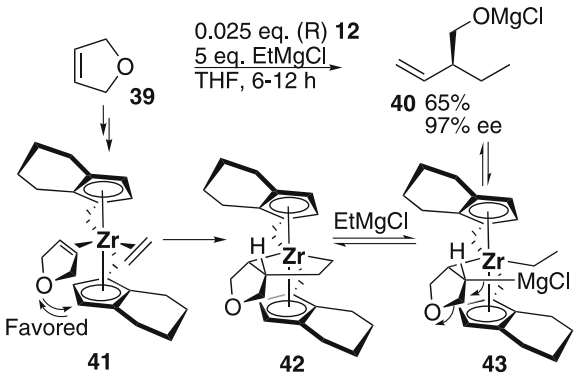

Scheme 7 Enantioselective coupling, β-alkoxide elimination sequence

orientated away from the sterically encumbered cyclohexane portion of the tetrahydroindene ligand and closer to the Cp end of the ligand. Complex **41** reductively couples enantioselectively to give **42**, which undergoes transmetallation to **43**. β-Alkoxide elimination then occurs to form the open chain product **40**. The reaction is general for five-, six-, and seven-membered cyclic allylic ethers giving good yields and > 90% ee, as well as protected five- and six-membered 3-azacyclohexenes to provide amino alkene products (72–75% yield, > 98% ee) [25].

An interesting extension of this reaction is shown in the asymmetric kinetic resolution of cyclic allylic ether **44** under alkene coupling conditions. Use of (*R*)-**12** as the catalyst gives (*R*)-**45** in > 99% ee at 58% conversion. The ethylated product **46** is also formed in the reaction in 94% ee (Eq. 7) [25]. The reaction is effective for six- to eight-membered 3-oxacycloalkenes **47** as well as for a wide variety of alkoxycycloalkenes **48** [27], with some resolution dependency on the ring size of **47** (Fig. 2) [26].

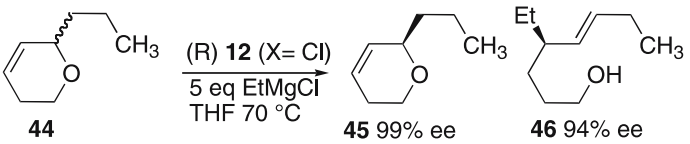

Equation 7

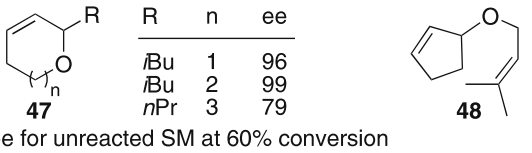

Fig. 2 Effect of ring size on ee in kinetic resolution of racemic allylic ethers. For $n = 3$, the material is 2,3-benzo-1-oxacyclo-2,6-octadiene

Both Waymouth [28, 29] and Takahashi [30] have taken advantage of zirconium's high oxophilicity to cyclize 1,6-dienyl allylic ethers **49** (R = CH_3, Ph) to give vinyl substituted cyclopentanes **50** with high *trans* to *cis* ratios in diethyl ether (Scheme 8) [29]. The reaction presumably goes through the zirconabicyclic intermediate **51**, followed by elimination of the alkoxide, transmetallation of the Zr alkoxide with BuMgCl, and regeneration of the catalyst via β-abstraction. Barluenga and coworkers provided 4-penten-1-ol derivatives **52** without diastereoselectivity through a similar β-alkoxide elimination reaction process [31]. Zirconabicyclic ether **53** was formed by oxidative cyclization of enol ether **54**; β-alkoxide elimination, followed by transmetallation with PrMgCl, provided **52** after protonation. Quenching the reaction with ketones gave **55**, supporting a mechanism wherein magnesium has replaced the zirconium by transmetallation.

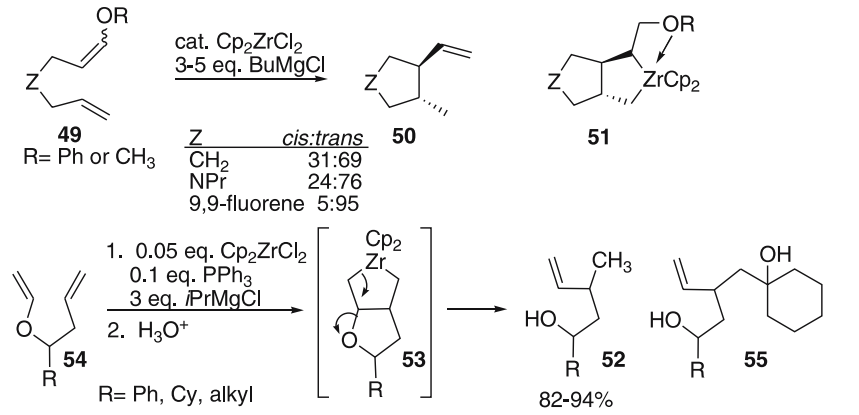

Scheme 8 Diene cyclization followed by β-alkoxide elimination

Waymouth and coworkers used chiral zirconocene complexes such as **56** with Et_3Al as the stoichiometric reductant to enantioselectively desymmeterize oxabicyclic compounds (Scheme 9) [29]. A reductive coupling mechanism to give **57** followed by β-alkoxide ring opening and transmetallation is consistent with the experimental results. Neither direct insertion of the alkene into the M – C bond nor nucleophilic attack mechanisms can be ruled out, however [12].

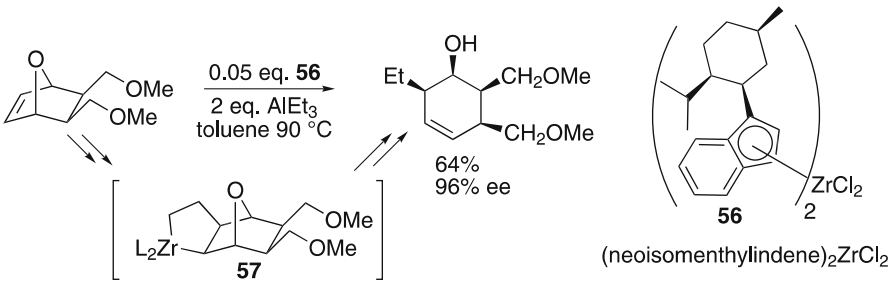

Scheme 9 Catalytic desymmetrization of *meso* compounds using **56**

2.1.5 Cationic Zirconium-Catalyzed Reactions

All of the reactions described above use *anionic* alkyl metal complexes as stoichiometric reductants. Cationic zirconium catalyst **58** was shown to reductively cyclize a variety of 1,5-dienes to give both mono- and bicyclic silane products when H_3SiPh was employed as the stoichiometric reductant (Scheme 10) [32]. Poor yields due to competing polymerization processes were observed when less substituted dienes were employed. It is likely that

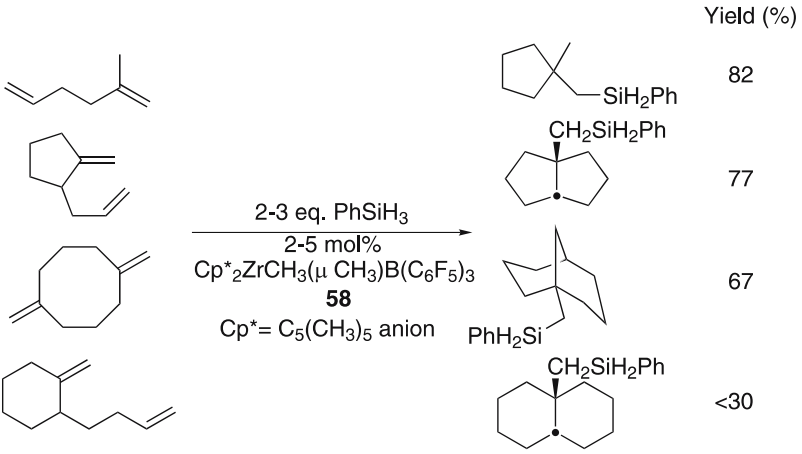

Scheme 10 Cyclization of dienes using a cationic zirconocene **58** and phenylsilane

the reaction generates the active catalyst by metathesis of the Zr – CH_3 bond with the silane Si – H bond. The Zr – H species formed by this process then hydrometallates the less hindered alkene. Finally, a second equivalent of alkene inserts into the resulting Zr – R bond to give a cyclic product. σ-Bond metathesis of the final zirconium alkyl gives the silylmethyl product and the Zr – H species, similar to the reactions observed with lanthanide metals (vide infra).

2.2 Titanium-Catalyzed Reactions

Despite many coupling reactions promoted by Ti(II), few have been developed into catalytic processes [12]. Negishi and coworkers developed the first catalytic system for the reductive coupling of unactivated 1,6- and 1,7-enynes, based on Ti(IV) tri- or tetra-alkoxide complexes **59**, using Et_2Zn as the stoichiometric reductant (Scheme 11) [33, 34]. Good yields of the methylenecycloalkanes **60** were obtained after hydrolysis or iodinolysis of the zinc anions. A mechanism similar to that detailed for the reductive coupling with Cp_2ZrCl_2 was proposed; it was suggested that **61** functions as the

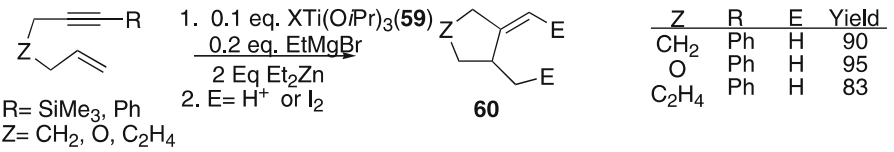

Scheme 11 Reductive coupling of enynes using **59** and diethylzinc

active catalyst to generate, after cyclization and transmetallation, cyclic zinc intermediate **62** (Scheme 12) [33].

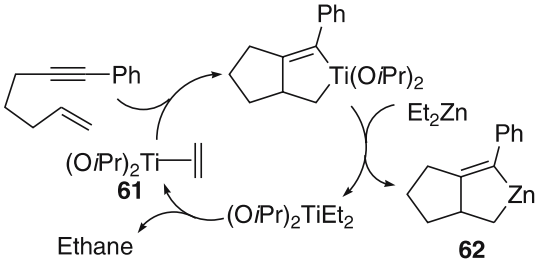

Scheme 12 Mechanism of the titanium alkoxide catalyzed cyclization of enynes

One limitation of this methodology is that unprotected terminal alkynes are incompatible with the strongly basic ethyl zinc reagents required for this reaction. Livinghouse and coworkers found that a similar Ti(IV)tetraaryloxide/cyclohexylmagnesium chloride system catalytically cycloisomerized dienes to methylenecyclopentanes **63** with the formation of some reduced product **64** (Eq. 8) [35].

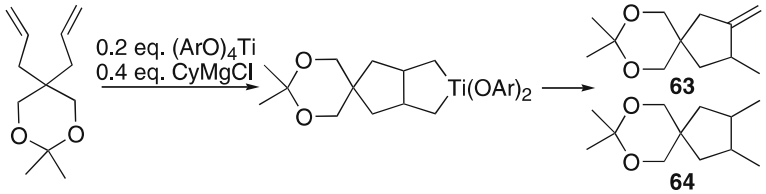

Equation 8

In reactions similar to those observed with the Zr species **56** (Scheme 9), Waymouth used both chiral (e.g., **66**) and achiral constrained geometry Ti complexes to desymmeterize the oxabicycloheptane **65** achieving good yields with modest enantioselectivity (Eq. 9) [29].

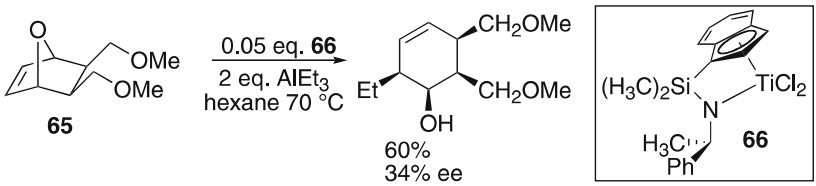

Equation 9

2.3
Group 3 and Lanthanide Catalyzed Reactions

Metallocenes of lanthanide and Group 3 metals (Cp_2M-R) are also active Ziegler–Natta polymerization catalysts, suggesting they should be active for reductive coupling reactions [36]. These complexes are typically oxo- and electrophilic, which decreases their functional group compatibility in many cases. However, variability in ionic radius of the lanthanide metals (the lanthanide contraction renders early lanthanides larger than later metals in the series [37]) allows for more flexible bonding options for the substrate by varying ancillary ligands or the size of the metal atom. This flexibility allows the metals to serve as very effective catalysts for a wide variety of reactions, most notably, hydrosilylations, hydroborations, and hydrostannations [36].

The metallocenes used for these reactions are typically d^0 at the metal and react through σ-bond metathesis and π-bond insertion mechanisms (Scheme 13). A stable precatalyst is treated with a stoichiometric reductant to give the metal hydride, which inserts a π-bond. The regiochemistry of this insertion reaction depends on the size of the metal and supporting ligands [36, 38]. σ-Bond metathesis of the resulting metal-carbon bond regenerates the catalyst, concomitantly providing a functionalized product that can be reacted further.

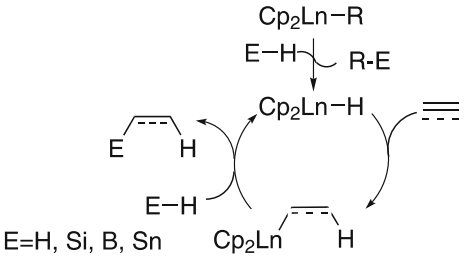

Scheme 13 Generalized mechanism for the alkene insertion and σ-bond metathesis reactions catalyzed by lanthanocenes

2.3.1
Diene Cyclization

A 1990 patent reported the quantitative cyclization of 1,5-hexadiene **66** to **67** with $Cp^*_2LuCH_3$ (Cp^* = C_5Me_5 anion) in the presence of $PhSiH_3$ (Scheme 14) [39]. This result was followed by reports that $Cp^*_2NdCH(SiMe_3)_2$ reductively cyclized both **66** and 1,6-heptadiene (**68**) under similar conditions [40] and that $Cp^*_2SmCH(SiMe_3)_2$ also served as a precatalyst for the cyclization of 1,5-hexadiene [41]. In the case of the neodymium and samarium catalysts competitive alkene hydrosilylation was observed.

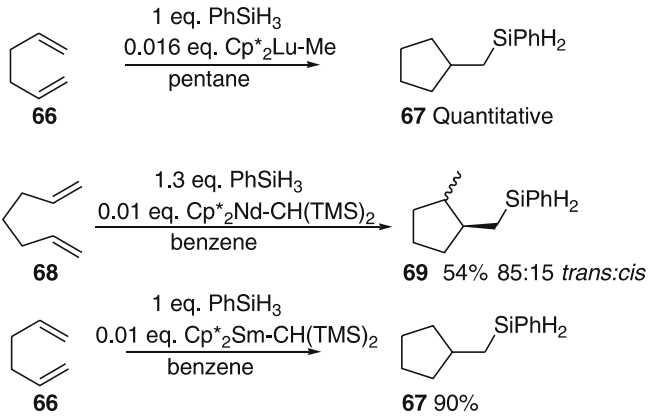

Scheme 14 Cp^*_2Ln-R catalyzed reductive cyclizations of dienes in the presence of silanes

The scope of the cyclization/silylation sequence was greatly expanded by Molander and coworkers, who found that $Cp^*_2YCH_3THF$ (**70**) was an effective catalyst for the diene cyclization [42]. Using 5 mol % **70** and either $PhMeSiH_2$ or $PhSiH_3$ as the stoichiometric reductant, excellent yields of cyclized products were obtained from both 1,5- and 1,6-dienes (Scheme 15). 1,6-Dienes provided better yields with the bulkier silane, as these bulky silanes suppressed formation of Si-bridged diene dimers. The reductive coupling reaction tolerated tertiary amine, protected alcohol, and sulfide functional groups within the chain of the diene and gave good diastereoselectivity with allylically substituted dienes. The authors proposed that the reaction proceeds via insertion of the less hindered alkene into the Y – H bond. In the case of the homoallylic alkoxy diene **71** the authors argued that the insertion pro-

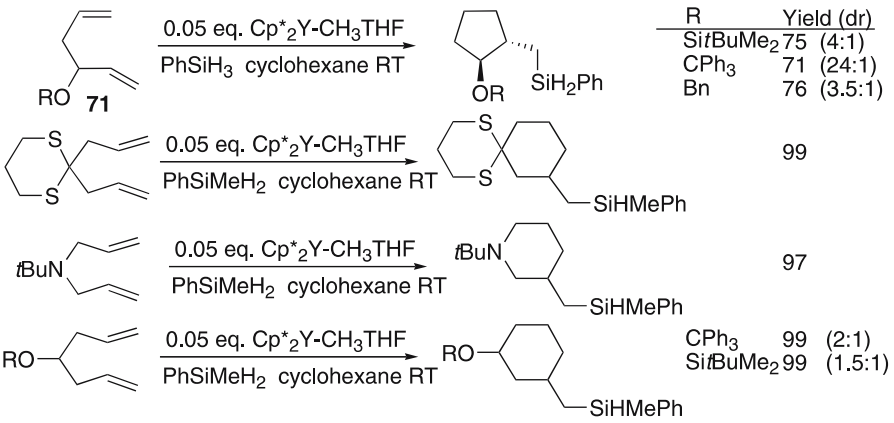

Scheme 15 $Cp^*_2Y - CH_3THF$-catalyzed diene cyclization

ceeds with excellent regiocontrol, then cyclizes through a chair-like transition structure (**72**) to achieve the diastereoselection observed (Scheme 16) [42]. The terminal silane products can be oxidized to give alcohol products in good overall yields [43].

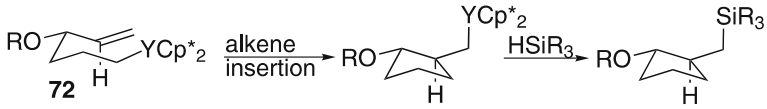

Scheme 16 Origin of the diastereoselectivity in the cyclization of dienes with **70**

The reductive coupling/silylation reaction was extended to more complicated polyenes, such as the triene-substituted cyclopentanol **73**, which cyclizes to provide **74** with a 72% yield and 6 : 1 dr after oxidation (Eq. 10) [44]. The reaction is chemoselective: the initial insertion occurs into the allyl substituent, which then inserts into the less hindered of the two remaining olefins, leaving the most hindered alkene unreacted.

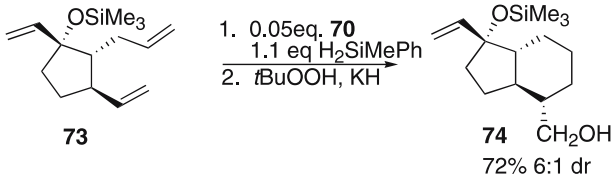

Equation 10

For most dienes, π-bonds adjacent to quaternary centers do not undergo insertion reactions. One notable exception is 1,5-diene (**75**) (Scheme 17) [44]. For this substrate, the observed selectivity is inconsistent with a chair-like (in this case a *trans* decalin-like) transition structure (**76** top) leading to the insertion product, which is typically seen in diene cyclizations with **70** [36].

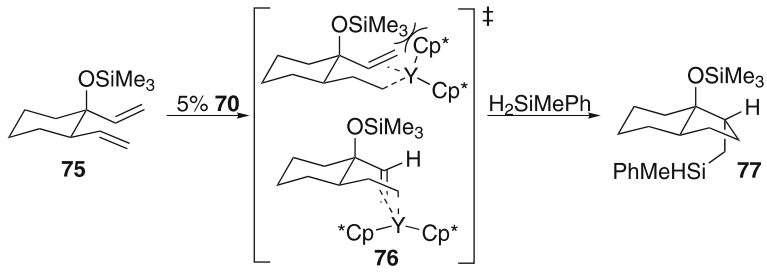

Scheme 17 Proposed transition structures for the diastereoselective bicyclization of dienes

Instead, transannular strain between the silylether and one of the Cp* ligands leads to a product **77** from a boat-like insertion transition structure (**76** bottom).

Catalyst **70** is very effective for the reaction of terminal alkenes, however 1,1-disubstituted olefins provide hydrosilylation products; presumably, this is due to steric hindrance [45]. When a catalyst with an open geometry (**78** or **79**) is employed, 1,1-disubstituted alkenes are inserted into C – Y bonds to give quaternary carbon centers with high diastereoselectivities (Scheme 18). As before, initial insertion into the less hindered alkene is followed by cyclic insertion into the more hindered alkene (entry 1) [45]. Catalyst **79** is more active than is **78**, operating with shorter reaction times (entries 2 and 3) and reduced temperatures. Transannular cyclization was possible in moderate yield (entry 4), as was formation of spirocyclic or propellane products

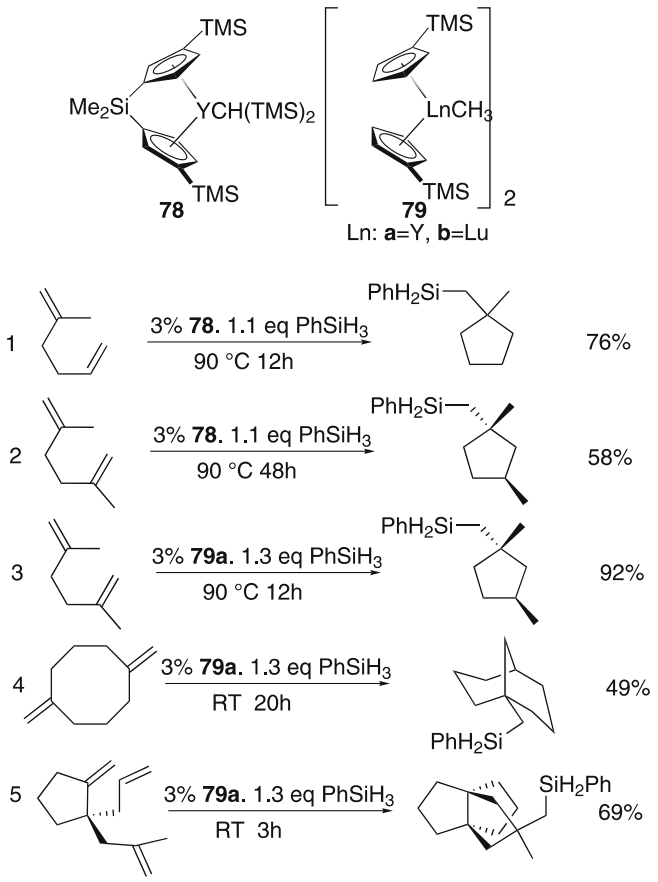

Scheme 18 Cyclization of substituted dienes using the "open" catalysts **78** and **79**

(entry 5). The reaction could be performed with as little as 0.5 mol % of **79a** when performed with 20 mmol of diene [45].

The reductive coupling of of dienes containing amine groups in the backbones allows for the production of alkaloid skeletons in relatively few steps [36, 46, 47]. Epilupinine **80** was formed in 51% yield after oxidation by treatment of the tertiary amine **81** with $PhMeSiH_2$ in the presence of catalytic **70** [46]. Notably, none of the *trans* isomer was observed in the product mixture (Eq. 11). The $Cp^*_2LuMeTHF$ was found to catalyze cyclization of unsubstituted allyl amine **82** to provide **83**. This reaction proceeded in shorter time and with increased yield relative to the same reaction with **70** (Eq. 12) [47]. Substitution of either alkene prevented cyclization, possibly due to competitive intramolecular stabilization of the metal by nitrogen preventing coordination of the substituted olefin, and resulted in hydrosilylation of the less substituted olefin.

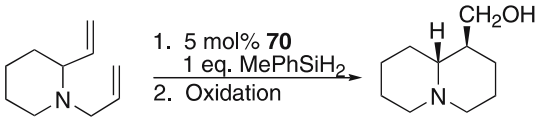

81 **80** 51-62%

Equation 11

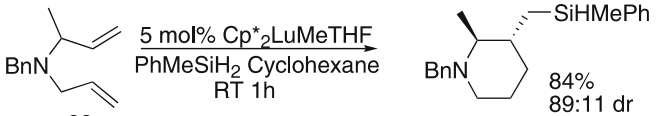

82 **83**

Equation 12

Electronic factors also influenced the outcomes of these cyclization reactions; cyclization of pyrrole **84** to bicyclic amine **85** is catalyzed by the sterically open complex **79a**. In this reaction, initial insertion into the Y – H bond occurred in a Markovnikov fashion at the *more hindered* olefin (Scheme 19) [48]. The authors proposed that the Lewis basic aromatic ring stabilizes the electrophilic catalyst during the hydrometallation step, overriding steric factors. In the case of pyrroles and indenes, the less Lewis basic nitrogen contained in the aromatic systems allowed for the cyclization of 1,1-disubstituted alkenes.

One example of asymmetric diene silylation was reported using the binaphthalenediol-based yttrocene catalyst (Fig. 3) [49]. A variety of 1,5- and 1,6-dienes were cyclized in 70–95% yields, but with < 5–50% ees. Due to the slower cyclization of 1,6-diene substrates, $PhMeSiH_2$ was in place of $PhSiH_3$ to prevent hydrosilylation of the olefins.

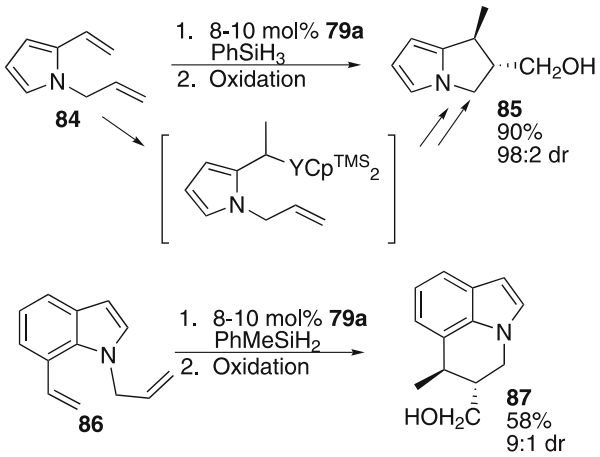

Scheme 19 The "aryl affect" directs Y – H insertion

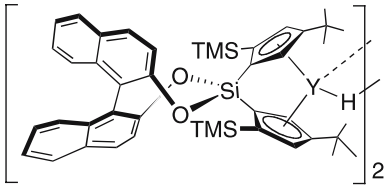

Fig. 3 An asymmetric yttrocene catalyst

Metal complexes of lanthanides beyond lanthanocenes were used to catalyze the reductive coupling reaction of dienes. $La[N(TMS)_2]_3$ was found to effect the cyclization of 1,5-hexadiene in the presence of $PhSiH_3$ (Eq. 13) [50]. Cyclized products **88** and **89** were isolated in a combined yield of 95% (**88** : **89** = 4 : 1). It was suggested that the silacycloheptane **89** resulted from competitive alkene hydrosilylation followed by intramolecular hydrosilylation.

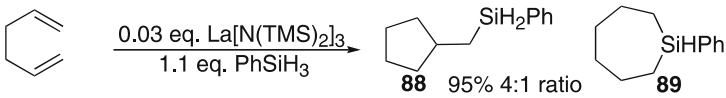

Equation 13

2.3.1.1 Reductants other than Silanes

Other metal hydrogen donors can be used in place of silanes. For instance, cyclization of substituted 1,5- and 1,6-dienes in the presence of Cp^*_2SmTHF, using a borohydride as the stoichiometric reductant, has been reported; other

lanthanide metal complexes, such as **79b**, provided lower yields than those shown by the samarium catalyst (Eq. 14) [51]. The catalytically active species in this reaction is presumed to be a Sm(III) species generated through allylic C – H activation by Sm(II) [52].

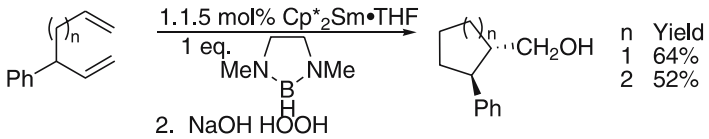

Equation 14

2.3.2 Enyne Cyclization Reactions

Similar reactivity is observed in the cyclization of enynes in the presence of the yttrium-based catalyst **70** and a silane reductant [53, 54]. The 1,6- and 1,7-enynes **90** and **91** provide *E*-alkylidene-cyclopentanes **92** and -cyclohexanes **93** in very good yield (Eq. 15, Scheme 20) [55]. These transformations likely proceed by *syn* hydrometallation of the π-basic alkyne, followed by insertion of the alkene and σ-bond metathesis. The reaction of 1,6-enynes tolerated

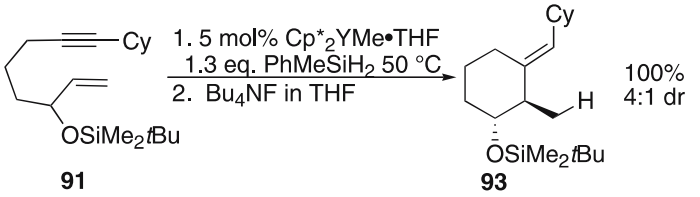

Equation 15

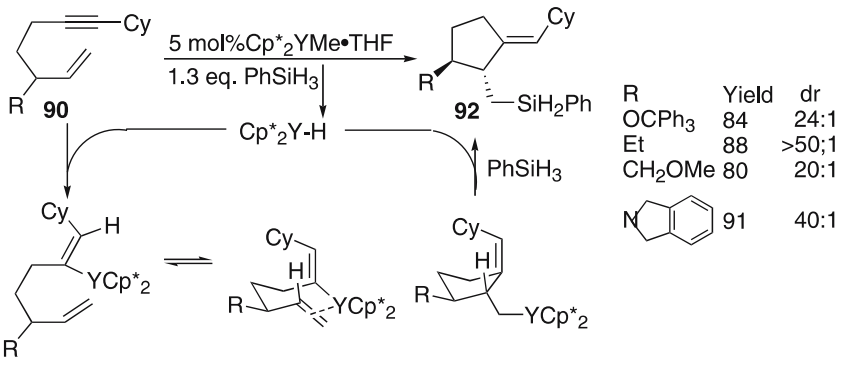

Scheme 20 Mechanism, functional group compatibility, and selectivity within enyne cyclizations catalyzed by **70**; Cy = cyclohexyl

bulky allylic ethers and allylic tertiary amines, but required secondary alkyl substitution at the alkyne terminus to allow for complete regiocontrol of the alkyne hydrometallation. When substituted at the allylic position, excellent diastereoselection (dr > 50 : 1) was observed. The diastereoselectivity of the reaction did not depend on either the reaction temperature or the use of the smaller $Cp^*_2LuCH_3 \cdot THF$ [55].

Cyclization to six-membered rings (Eq. 15) provided modest diastereoselectivity and required the use of bulkier $PhMeSiH_2$ to prevent olefin hydrosilylation. Propargyl and homopropargyl amines **94** afforded a variety of heterocycles (Scheme 21), if the catalyst was added slowly over the reaction course to diminish side reactions resulting from metal coordination to the basic amine [56]. The reaction procedure was extended to the diastereoselective bicyclization of dienyne substrate **95**, giving **96** as product in a cascade fashion (Eq. 16) [57].

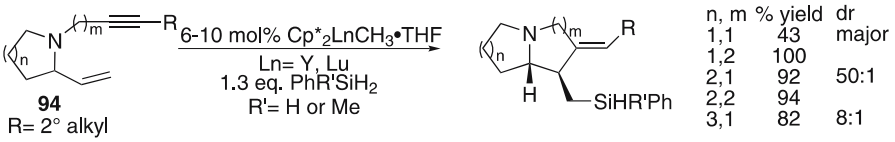

Scheme 21 Formation of five- and six-membered ring heterocycles by lanthanocene complexes

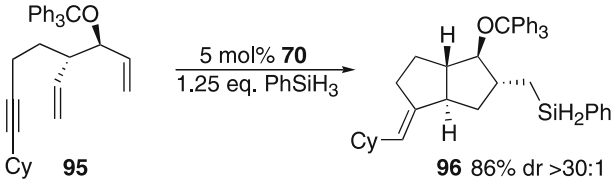

Equation 16

3
Late Transition Metal Catalysts

3.1
Palladium-Catalyzed Reactions

3.1.1
Alkene Coupling Reactions

The mechanistic similarity between Ziegler–Natta polymerization of olefins and the alkene cyclization reactions described above suggested that early transition metal catalysts would be effective catalysts for the coupling of

alkenes and alkynes. A significant obstacle to the application of these catalysts to organic transformations is that many functional groups are incompatible with these highly Lewis acidic metals. In the mid-1990s, Brookhart and coworkers reported that cationic Pd(II) complexes with non-coordinating anions were effective for the dimerization [58], polymerization [59], and hydrosilylation [60] of α olefins. The electrophilic catalysts described by Brookhart are less oxophilic than the d^0 early transition metals described in the preceding section and show greater functional group compatibility.

3.1.1.1 Dienes

In 1998, two research groups reported reductive cyclization of 1,6-dienes in the presence of Pd catalysts, using silanes as the stoichiometric reductant [61–63]. Hayashi and coworkers demonstrated that allyl vinyl benzene **97** was reductively coupled by $[(\eta^3\text{-}C_3H_5)PdCl]_2/PR_3$ (R = oTol) to give **98** in 78% yield using Cl_3SiH as the stoichiometric reductant (Eq. 17) [61]. Hydrosilylation of the vinyl group to give **99** competed with the cyclization/reduction route; bulky phosphines provided better yields of the cyclized product. Initial insertion of the alkene into the Pd – H bond, placing the metal to the benzylic position, is consistent with the formation of both **98** and **99**.

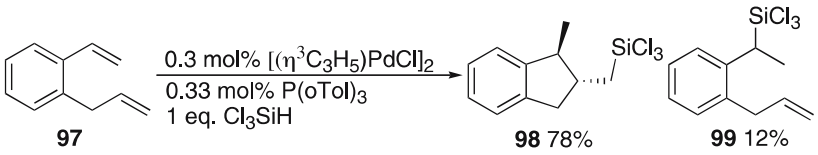

Equation 17

Widenhoefer and coworkers showed that 5 mol % of cationic Pd complex **100** provided excellent yields of the silylated cyclopentane derivatives **101** from 1,6-dienes in the presence of tertiary silanes; these reactions often afforded excellent selectivity for the *trans* diastereomer (Scheme 22) [62, 63]. (Use of the non-coordinating BArF anion allowed for complete dissociation of the ion pair). The reaction tolerated ester, amide, ketone, and nitrile functional groups in the homoallylic position of the diene, although the diastereoselectivity suffered with substitution at the allylic position (**102**). Diallyl amine derivatives afforded pyrrolidine derivatives (e.g., **101d**) with similar diastereoselectivities, but lower yields. In general, the reductive cyclization was most efficient for substrates with two ketone, ester, or ether groups homoallylic to the diene [63], though the origin of this phenomenon is unclear. The cyclization reaction tolerated alkyl substitution on one of the alkenes: substrates **102** and **104** provided good yields of **103** and **105**. These substrates were treated with bulky silane $PhMe_2SiH$ to slow the rate of competitive hy-

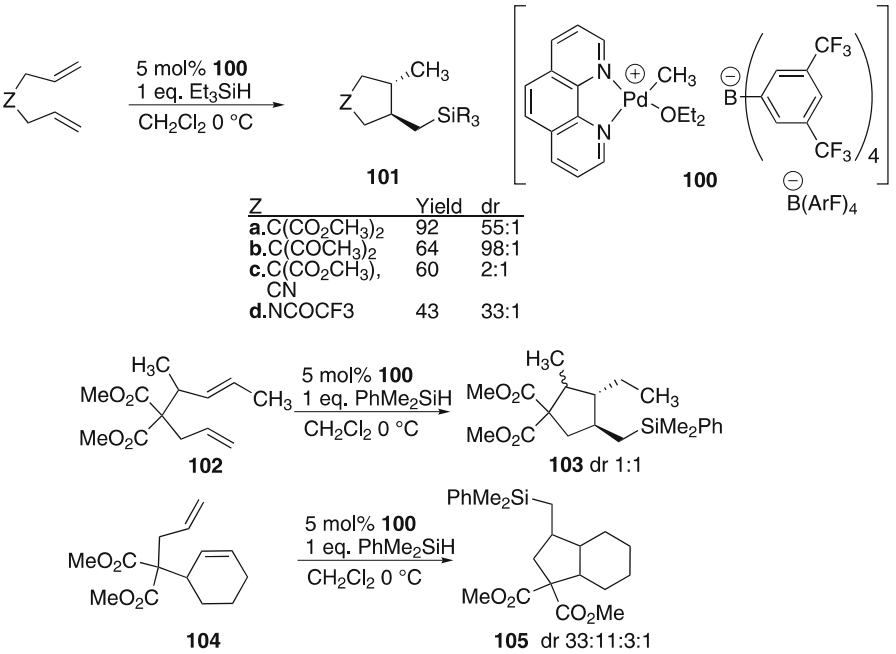

Scheme 22 Functional group compatibility and diastereoselectivity within diene cyclizations catalyzed by **100**

drosilylation. Suitably arranged trienes provided tricyclic products in a cascade reaction catalyzed by **100** [64].

Six-membered rings were formed in good to excellent yields via cyclization of 1,7-dienes **107** and **109** when the reaction was performed in 1,2-dichloroethane at room temperature (Scheme 23) [65]. Similar functional group compatibility and olefin substitution tolerance was observed as found

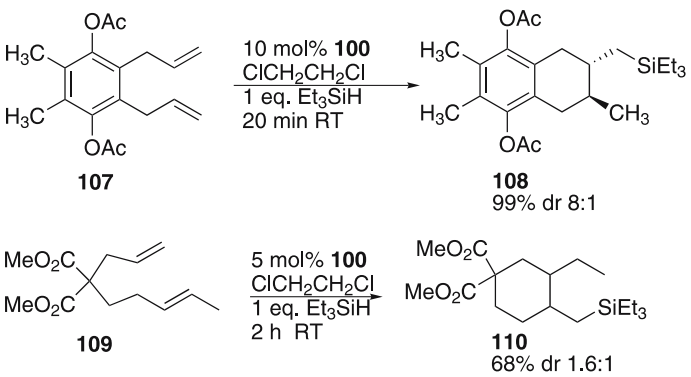

Scheme 23 Formation of cyclohexane rings from 1,7-dienes

in the formation of five-membered rings, but the reactions were slower and less diastereoselective.

3.1.1.2 Asymmetric Diene Cyclization Reactions

An asymmetric variant of this reaction was developed using chiral Pd complex **111** with either silanes or disiloxanes [66–68]. Both relative and absolute stereochemistries were controlled in this system and good yields (60–85%) were obtained after oxidation (Eq. 18). Formation of the silane-containing product was inhibited by the presence of water due to competitive formation of the palladium hydrides and silanols [68]. The use of disiloxanes as reductants, however, provided expedient oxidation to the alcohol products without decreasing the isolated yields; enantioselectivity was 5–15% lower in this more robust system [66]. Benzhydryldimethylsilane proved to be a good compromise between high yield and facile oxidation [66]. Palladium com-

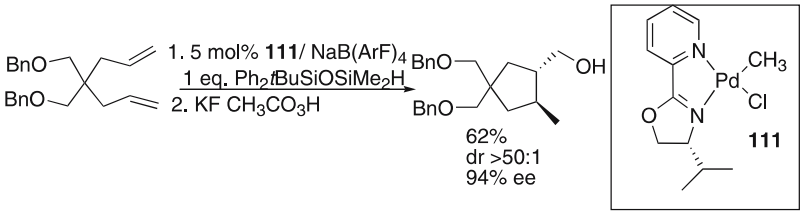

Equation 18

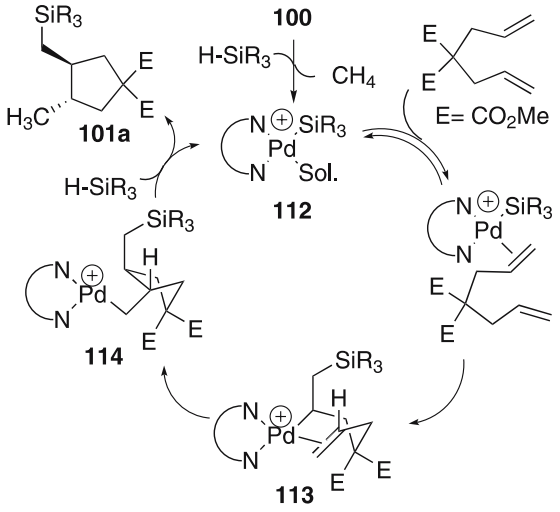

Scheme 24 Mechanism of the reductive diene cyclization with precatalyst **100**

plexes of bis-oxazoline ligands also functioned as asymmetric catalysts, but gave lower enantioselectivity [68].

The mechanism for the reaction catalyzed by cationic palladium complexes (Scheme 24) differs from that proposed for early transition metal complexes, as well as from that suggested for the reaction shown in Eq. 17. For this catalyst system, the alkene substrate inserts into a Pd – Si bond a rather than a Pd – H bond [63]. Hydrosilylation of methylpalladium complex **100** then provides methane and palladium silyl species **112** (Scheme 24). Complex **112** coordinates to and inserts into the least substituted olefin regioselectively and irreversibly to provide **113** after coordination of the second alkene. Insertion into the second alkene through a boat-like transition state leads to *trans* cyclopentane **114**, and σ-bond metathesis (or oxidative addition/reductive elimination) leads to the observed *trans* stereochemistry of product **101a** with regeneration of **112** [69].

3.2 Enyne Cyclization Reactions

Palladium complexes are effective catalysts for the reductive cyclization of enyne substrates [53, 54]. The first report of catalytic cyclization of 1,6- and 1,7-enynes **115a,b** to cyclopentane **116a** and cyclohexane **116b** derivatives appeared in 1987 (Eq. 19) [70]. The authors proposed that the Pd(II) species **117** forms by oxidative addition of acetic acid to Pd(0) (Scheme 25). Complex **117** hydrometallates the alkyne to give **118**, which cyclizes to provide

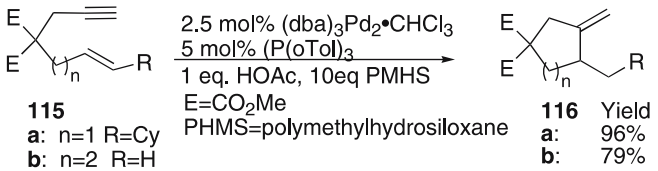

Equation 19

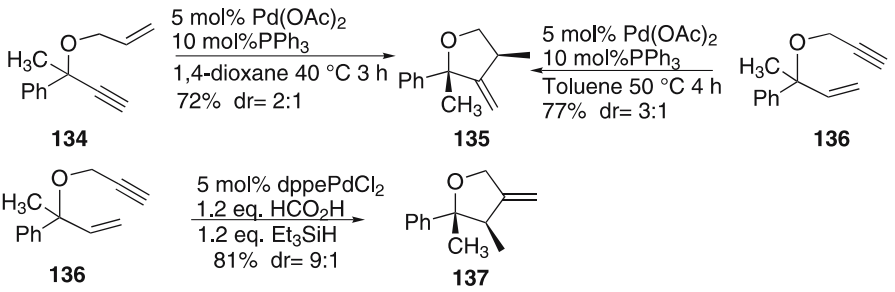

Scheme 25 Mechanism of the reductive enyne cyclization promoted by Pd and silane

119. Silane reduces the palladium acetate in **119** to the palladium hydride **120**, which undergoes reductive elimination to provide the organic product and the catalytic Pd(II) species. This mechanistic hypothesis was supported by the use of Et_3SiD as the reductant: product was formed with D incorporation at only the methyl group [70]. This reaction is best performed with a Pd(0) precatalyst in the presence of acetic acid and 10 eq. of silane, which suppresses the competitive cycloisomerization reaction [70].

Cationic palladium complex **121** reductively coupled enynes (Eq. 20) using trichlorosilane as the stoichiometric reductant [71]. This combination of catalyst and silane afforded silylated methylenecyclopentanes such as **122** in good yield from enynes such as **123**. Attempts to develop an enantioselective version of this reaction were not successful [71]. When enediyne **124** was cyclized in the presence of trichlorosilane, the reaction favored enyne cyclization **126** by a 3 : 1 ratio over diyne cyclization to **125** (Eq. 21). In contrast, when the more electron-rich dichloromethylsilane was used as the reductant, diyne cyclization product **125** was preferred in a ratio of 4 : 1 [71]. Selectivities of up to 10 : 1 for enyne cyclization were observed, depending on the substrate employed [72].

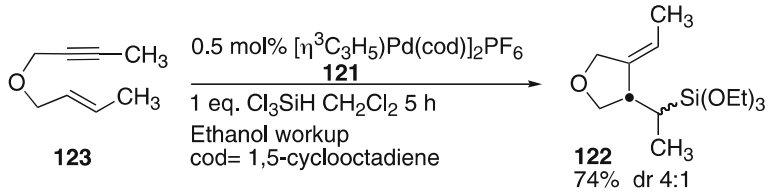

123 **122**
74% dr 4:1

Equation 20

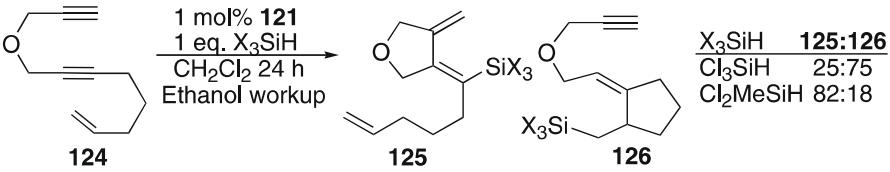

124 **125** **126**

Equation 21

The authors propose that this reaction proceeds by initial insertion of the π-bond into a Pd – H bond, in contrast to the Pd – Si insertion seen in the reaction between Et_3SiH and dienes catalyzed by **100** (Scheme 24) [71]. A weak bond between the cationic palladium and the electron-poor Cl_3Si group favoring Pd – H formation accounts for the change in mechanism.

The **121**/Cl_3SiH combination selectively cross-couples alkenes with alkynes intermolecularly to give acyclic homoallylic silanes **127** and **128** (Eq. 22) [73].

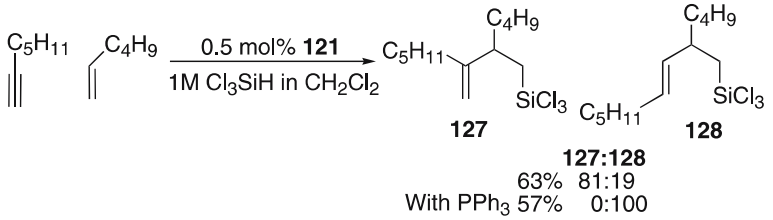

Equation 22

The moderate level of regioselectivity seen in the alkyne insertion is dependent on added PPh_3, but the alkene insertion occurs with excellent regioselectively. This is the only catalytic, late transition metal system shown to intermolecularly couple alkenes with alkynes.

3.2.0.3 Reductants Other than Silanes

Stannanes [74] and formic acid [75, 76] were used as the stoichiometric reductants with palladium catalysts. Using H-$SnBu_3$ as the reductant (Eq. 23), homoallylic stannanes were formed through a mechanism similar to that shown in Scheme 25 [74]. Sn – H oxidative addition to an in situ generated Pd(0) gave an H – Pd – Sn species analogous to **117**. Regioselective alkyne insertion into the Pd – H bond, olefin carbometallation, and finally C – Sn reductive elimination regenerates Pd(0). A variety of Pd catalysts were active, with $PdCl_2$ and $Pd(OAc)_2$ being most effective; phosphine ligands retarded the reaction. This reaction was tolerant of ether, ester, and sulfonamide substitution within the backbone of **129**, but the reaction was limited to the cyclization of 1,6-enynes. It was necessary to add the tin hydride slowly over the course of the reaction to avoid the formation of hydrostannylation products [74].

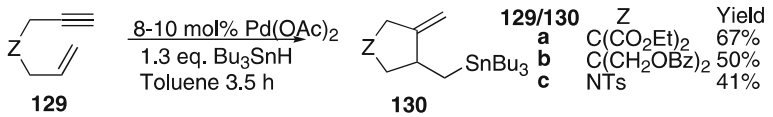

Equation 23

In the presence of formic acid, $Pd(OAc)_2$ and PPh_3, 1,6-enyne **129a** is reductively coupled to provide methylenecyclopentane **131**, along with **132** and **133** (Eq. 24) [75, 77]. The reaction tolerated substitution at either the 1- or 2-positions of the alkene and the terminal position of the alkyne. 1,7-Enynes gave methylenecyclohexane products. This catalytic system gave regioisomeric products depending on the reaction conditions (Scheme 26). When the

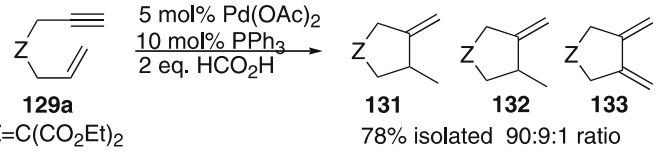

Equation 24

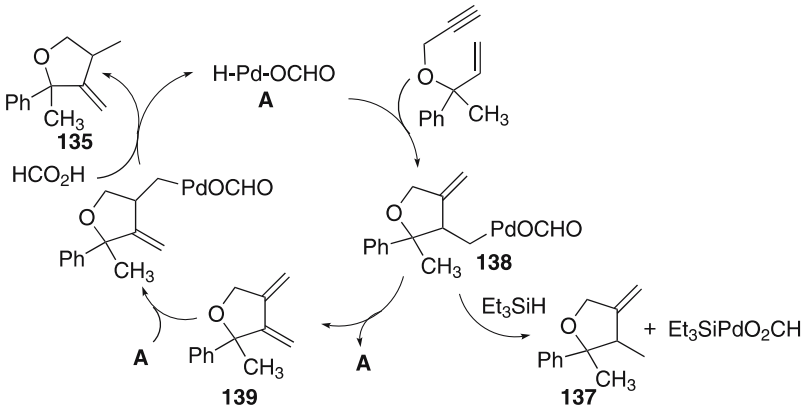

Scheme 26 Dependence of Pd(II)-catalyzed enyne cyclization upon solvent and added silane

reaction was carried out in 1,4-dioxane at 40 °C, **134** provides **135**, as does **136** when the reaction is carried out using toluene as the solvent at 50 °C. However, when **136** was treated with a stoichiometric amount of Et_3SiH in toluene under similar conditions **137** was produced [78].

The results shown in Scheme 26 are consistent with the mechanism shown in Scheme 27. Alkyne hydrometallation by catalytic intermediate A and

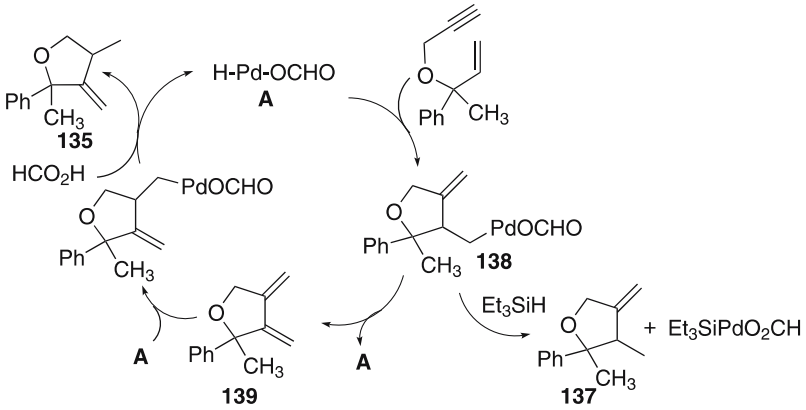

Scheme 27 Mechanism of the Pd(II)-catalyzed enyne cyclization with formate or silane as reductant

olefin insertion generate **138**, through a mechanism similar to that seen in Scheme 25 [78]. The silane directly reduces intermediate **138** to give the silylated Pd species and the methylene cyclopentane **137**. Without added silane, β-elimination to provide **139** and A is followed by regioselective reduction of the diene at the less hindered alkene. Reductive elimination of the Pd-alkyl provides **135** and a Pd(0) species, which is reoxidized by formic acid to give **A**.

This Pd(0)/formic acid system was effective for the cyclization of substituted 5-allene-1-ynes to give diene **140** (Eq. 25) through initial insertion into the internal π-bond of the allene followed by insertion into the alkyne [79]. All of the examples provided were geminally substituted within the backbone to facilitate cyclization. Intramolecular allene–alkyne reductive couplings to generate six-membered rings were not achieved.

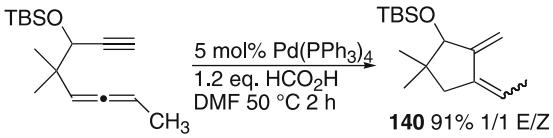

Equation 25

3.2.0.4 Applications to Synthesis

The palladium-catalyzed reductive coupling reactions were used in the synthesis of several natural products, including laurene [75], ceratopicanol [80], and dihydrostreptazolin **141** [81]. The cyclization leading to dihydrostreptazolin shown in Eq. 26 highlights the diastereoselectivity and functional group compatibility seen with this catalytic system.

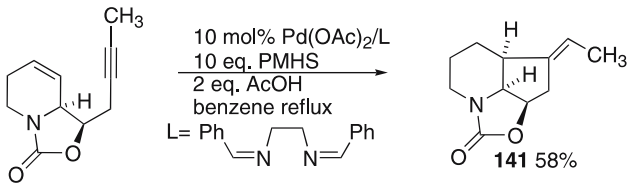

Equation 26

An enantioselective variant of the enyne cyclization has been reported. For example, cationic palladium oxalzoline catalyst **111** and Et_3SiH reductively cyclized **129a** to **130a** (shown in racemic form in Eq. 24) in 88% yield of the cyclized products with 24% ee [76].

3.2.1
Alkyne–Alkyne Coupling Reactions

While the early transition metals have been very effective at coupling two alkynes stoichiometrically [2], no examples of a catalytic, alkyne coupling process have been reported with these metals. Late transition metals, however, effectively catalyze reductive coupling reactions between alkynes in both intra- and intermolecular fashion. In 1988, the first example of intramolecular coupling of 1,6-diynes was reported, using catalytic $Pd_2(dba)_3CHCl_3$ in acetic acid with Et_3SiH as the reductant [82]. Exocyclic 1,3-dienes (e.g. **142**) were produced with excellent *E*/*Z* selectivity (Eq. 27) in very good yields. The mechanism is similar to that shown for the enyne reductive coupling reaction within Scheme 25.

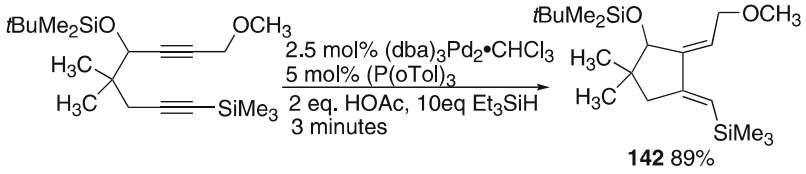

Equation 27

Two examples of alkyne couplings using palladium and trichlorosilane are known. Using $[\eta^3\text{-}C_3H_5PdCl]_2/POAr_3$ as the precatalyst, phenylacetylene is coupled in a head-to-tail fashion to provide **143** (Eq. 28) [83]. Similarly, a cationic palladium catalyst, $(\eta^3\text{-}C_3H_5)Pd(cod)^+PF_6^-$ (**145**), was effective for the reductive cyclization of 1,6- (**146a–d**), 1,7- (**146e**), and 1,8-diynes (**146f**) in moderate yields and up to 100% *Z* selectivity (Scheme 28) [84]. When a substituted alkyne **146b** was used, substituted silane product **147b** was formed,

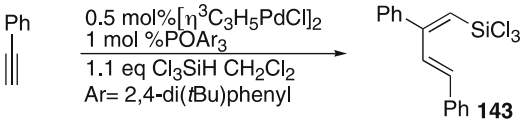

Equation 28

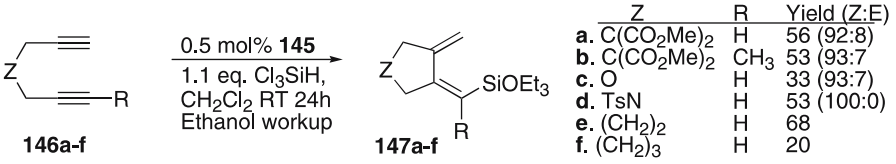

	Z	R	Yield (Z:E)
a.	$C(CO_2Me)_2$	H	56 (92:8)
b.	$C(CO_2Me)_2$	CH_3	53 (93:7
c.	O	H	33 (93:7)
d.	TsN	H	53 (100:0)
e.	$(CH_2)_2$	H	68
f.	$(CH_2)_3$	H	20

Scheme 28 Scope and selectivity of the diyne cyclization catalyzed by **145**

implicating initial insertion of the least substituted alkyne into a Pd – H bond [63, 84].

3.2.1.1
Reductants other than Silane

Tin hydrides are effective stoichiometric reductants for the coupling of diynes in the presence of palladium [85]. Dienes **148** are formed through the cyclization of diynes **146** in up to 95% yield using heterogeneous $Pd(OH)_2$ as the catalyst (Scheme 29). For this combination, it was necessary to add the Bu_3SnH slowly by syringe pump during the reaction to suppress competitive alkyne hydrostannylation reactions. Addition of phosphine to the catalyst suppressed cyclization and gave products resulting from hydrostannylation. Ester, alcohol, sulfide, and amine substitution were tolerated within the substrate, as was substitution of one of the two alkyne termini, although large substituents prevented cyclization.

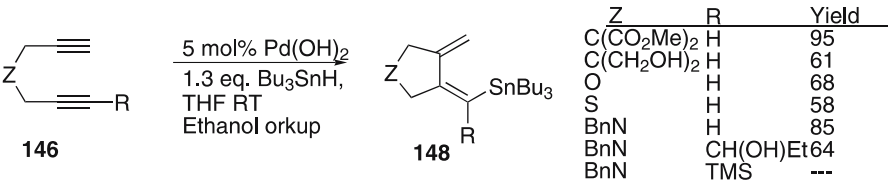

Scheme 29 Scope and selectivity of the diyne cyclization catalyzed by $Pd(OH)_2$ in the presence of Bu_3SnH

3.2.1.2
Applications to Synthesis

The palladium-catalyzed cyclization reaction was used in the syntheses of several natural products such as siccanin [86], streptazolin [87], and ceratopicanol (through a diyne, diene cascade) [80]. The production of the streptazolin precursor **149** through reductive cyclization of **150** is illustrative of the complexity that the reaction can provide (Eq. 29) [87].

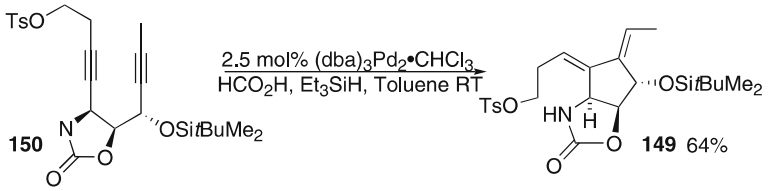

Equation 29

3.3
Platinum-Catalyzed Cyclizations

Cationic platinum bis-imine complexes were shown to reductively cyclize diynes in the presence of alkyl silanes [88, 89]. Phenanthroline (phen) complex **152**, generated by the in situ methyl abstraction of (phen)$Pt(CH_3)_2$ with $B(C_6F_5)_3$ [60], cyclized 1,6- (**151a–d**) and 1,7-diynes (**151e**) to provide dienes in 71–92% yield and excellent *E*/*Z* ratios (Scheme 30). Better *E*/*Z* ratios were seen when bis-imine **153** was used for the cyclization [89]. The reaction showed good functional group tolerance and did not require geminal disubstitution within the backbone for effective cyclization (**151d**). Terminal alkyne substitution with electron-donating groups led to mixtures of products while electron-withdrawing groups gave good yields of products resulting from insertion of the less substituted alkyne into the Pt – Si bond [89].

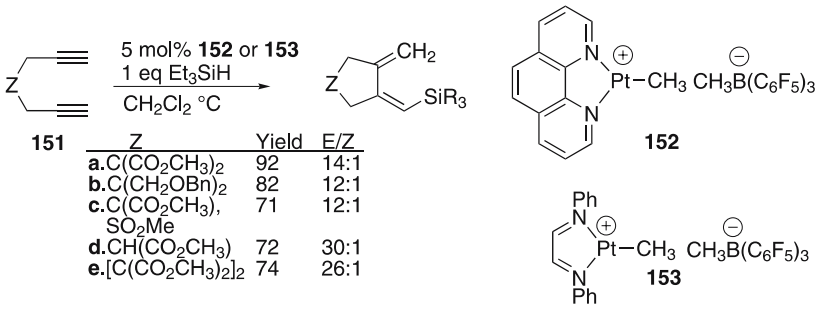

Scheme 30 Scope and selectivity of diyne cyclization catalyzed by cationic Pt species **151**

3.4
Group 9 Metal Catalysts

3.4.1
Enyne Cyclization Reactions

Rhodium and rhodium–cobalt based catalysts using silanes as the stoichiometric reductant were initially reported in 1992 to reductively couple enyne substrate (Eq. 30) [90, 91]. Further investigation showed this reaction to be an effective method for the cyclization of enyne substrates **129** to

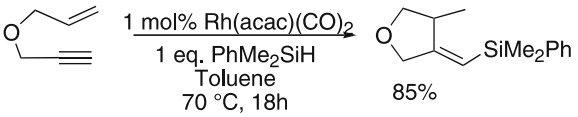

Equation 30

methylenecyclopentanes **154** (Scheme 31) using several Rh or Rh/Co catalysts with $PhMeSiH_2$ or Me_2PhSiH as the reductant [91–93]. These reactions were very fast, with cyclization of 1,6-enynes occurring in less than a minute. The formation of the six-membered ring and furan derivatives were considerably slower [93]. Cyclohexene substrate **155** gave the cycloisomerization product **156** in the presence of $Rh(acac)(CO)_2$ and Me_2PhSiH, suggesting that β-elimination was faster than σ-bond metathesis under these conditions (Scheme 32). The catalysts tolerated methyl substitution on the alkyne terminus, but not the alkene (**157** and **158** do not cyclize). The authors hypothesize that the initial step of the reaction is oxidative addition of Si – H to the rhodium followed by regioselective insertion of the alkyne into a Si – Rh bond [93].

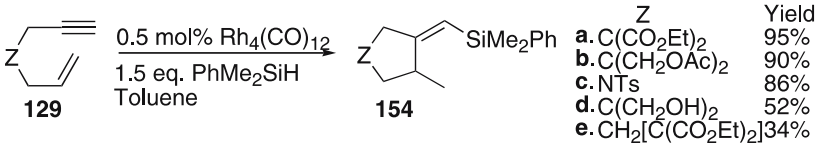

Scheme 31 Scope and selectivity of reductive enyne cyclization by $Rh_4(CO)_{12}$

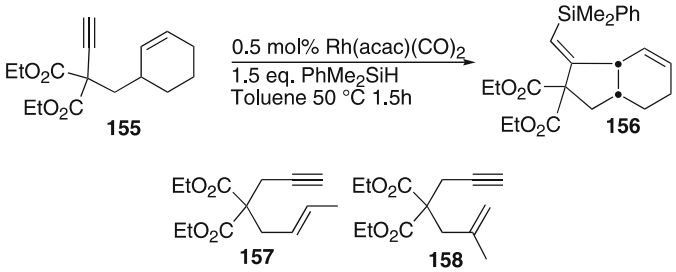

Scheme 32 Dependence of enyne cyclizations on alkene substitution

When the rhodium-catalyzed reaction is performed under a high pressure of CO in the presence of phosphite ligands, aldehyde products (**159**) are formed by insertion of CO into the rhodium–alkyl bond followed by reductive elimination (Eq. 31) [90]. The bimetallic catalysts were immobilized as nanoparticles, giving the same products and functional group tolerance, with the advantage that the catalyst could be recovered and reused without loss of

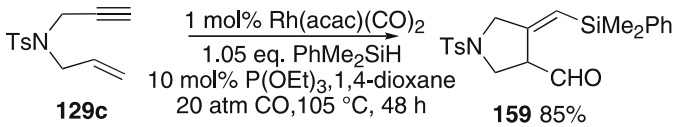

Equation 31

activity [94]. A rhodium *N*-heterocyclic carbene (Rh – NHC) catalyst has also been used to produce the cyclized products such as **152** using Me_2PhSiH as the reductant [95]. This Rh – NHC complex was not compatible with terminal alkenes.

Allenynes **160** were also cyclized chemo- and regioselectively to methylenecyclopentane derivatives **161** and **162** using $Rh(acac)(CO)_2$ as the catalyst and silanes or alkoxysilanes as the reductant (Eq. 32) [96]. The major product resulted from initial insertion of the internal π-bond of the allene into the Rh – Si bond. Only 1,1-disubstituted allenes were used for this reaction; others may show less selectivity for the internal π-bond of the allene.

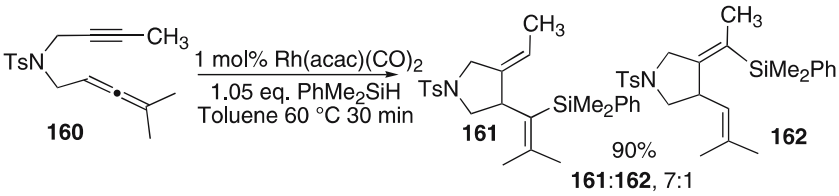

Equation 32

3.4.2
Enantioselective Enyne Cyclization Reactions

Enantioselective variants of the rhodium-catalyzed reductive cyclization reaction using both cationic and neutral complexes have been reported. When 5 mol % of $[Rh(cod)_2]_2$ SbF_6 was reacted with **129a**, $MeEt_2SiH$, and chiral ligand **163** a 76% yield of **154a** was achieved with 88% ee (Scheme 33) [97]. Other substrates gave 50–75% chemical yields and 77–89% ee [97, 98].

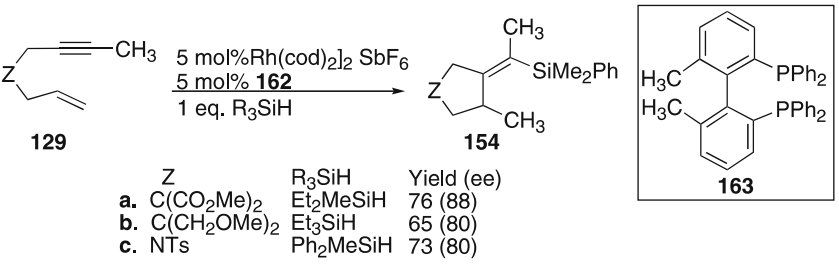

Scheme 33 Enantioselective enyne cyclizations with rhodium in the presence of **163**

Using cationic $[Rh(cod)_2]_2$ SbF_6 and (*S*)-BINAP (BINAP = 2,2′-bis(diphenylphosphino)-1,1′-binaphthalene) as the chiral ligand, the substrates **129** can be reductively coupled using HBCat (Cat = 1,2-benzenediolate) as the

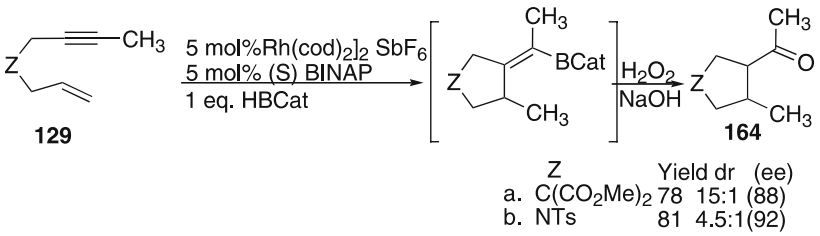

Scheme 34 Enantioselective enyne cyclizations with rhodium in the presence of (S) BINAP using HBCat as the reductant

reductant to give the corresponding ketones **164** with 88–90% ee after oxidation (Scheme 34) [99]. Under these conditions neither terminal alkynes nor substituted olefins were cyclized.

3.4.3 β-Alkoxide Reactions

In a reaction similar to the β-alkoxide elimination reactions seen with zirconocenes, catalytic $Rh(OH)(cod)_2$ and 2 eq. of arylboronic acids gave cyclic products **165** from enynes **166** (Scheme 35) [100]. In this reaction, transmetallation of Rh – OR with B – Ph gave Rh – Ph species **167**, which inserted into the alkyne, cyclized to **168**, and finally underwent β-alkoxide elimination to provide $Rh\text{-}OCH_3$. This reaction is limited to the formation of five-membered rings, but it can also undergo cascade type reactions of enediynes to give multicyclic products [100].

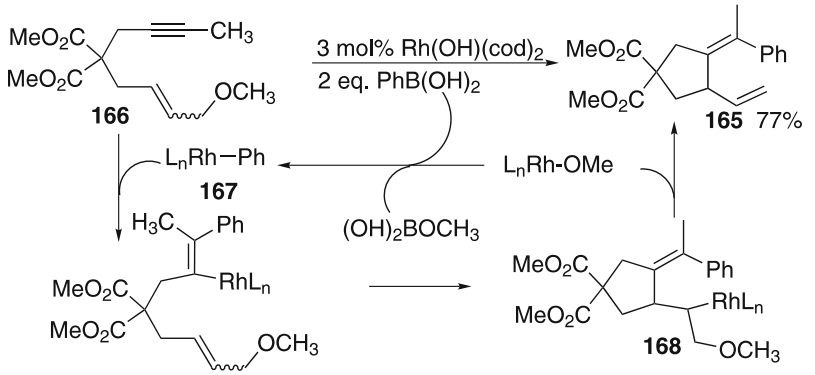

Scheme 35 Mechanism of the arylboronic acid-mediated reductive cyclization

3.4.4
Alkyne–Alkyne Cyclization Reactions

Rhodium complexes facilitate the reductive cyclization of diyne species in good yield, although the product olefin geometry depends on the catalysts used. Moderate yields of *E*-dialkylideneclopentane **169** resulted if a mixture of diyne **146** and trialkylsilane was added to Wilkinson's catalyst $ClRh[PPh_3]_3$ (Eq. 33) [101]. If, however, the diyne followed by silane were added to the catalyst, a Diels–Alder derived indane **170** was produced (Eq. 34). Cationic Rh complex, (*S*-BINAP)Rh(cod) BF_4, provides good yields of the *Z*-dialkylidenecyclopentane derivatives, although in this case, terminal alkynes are not tolerated (Eq. 35) [102].

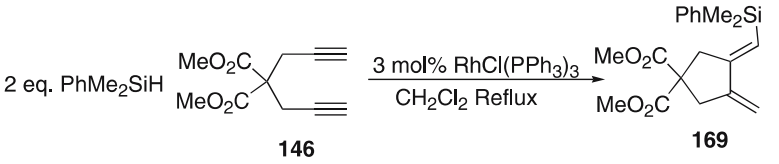

146 **169**

Equation 33

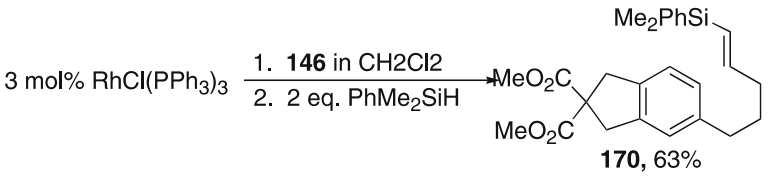

170, 63%

Equation 34

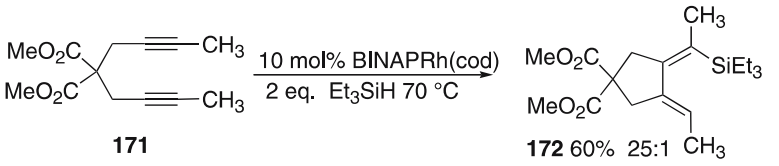

171 **172** 60% 25:1

Equation 35

4
Conclusion

A tremendous amount of progress has been made over the past decade in the understanding of the catalyzed reductive coupling of unactivated alkenes and alkynes. Both early and late transition metal complexes accomplish the reaction with good yields and with low catalyst loadings. Enynes and dienes can

be cyclized with excellent stereo- and regiocontrol. There is still much to be done to make these reactions useful for a broad range of chemists. Most of the cyclization reactions mentioned require or use geminal substitution within the backbone, which generally favors cyclization reactions over completing processes. While this is acceptable in a proof of concept study, it constrains the scope of the reactions. However, many of the reactions have been used to generate complicated natural products with excellent control of stereochemistry and this provides the impetus for continuing research into better and more selective catalysts.

References

1. Beletskaya I, Moberg C (2006) Chem Rev 106:2320
2. Broene RD (1995) In: Hegedus LS (ed) Transition metal organometallics in organic synthesis. Comprehensive organometallic chemistry II, vol 12. Pergamon, Tarrytown, p 323
3. Fujita T, Makio H (2007) In: Hiyama T (ed) Applications II: transition metal compounds in organic synthesis 2. Comprehensive organometallic chemistry III, vol 11. Elsevier, Oxford, p 691
4. Dzhemilev UM, Vostrikova OS (1985) J Organomet Chem 285:43
5. Broene RD, Buchwald SL (1993) Science 261:1696
6. Lewis DP, Muller PM, Whitby RJ, Jones RVH (1991) Tetrahedron Lett 32:6797
7. Morken JP, Didiuk MT, Hoveyda AH (1993) J Am Chem Soc 115:6997
8. Bell L, Whitby RJ, Jones RVH, Standen MCH (1996) Tetrahedron Lett 37:7139
9. Bell L, Brookings DC, Dawson GJ, Whitby RJ, Jones RVH, Standen MCH (1998) Tetrahedron 54:14617
10. Wild FRWP, Zsolani L, Huttner G, Brintzinger HH (1985) J Organomet Chem 232:233
11. Liang B, Novak T, Tan Z, Negishi E (2006) J Am Chem Soc 128:2770
12. Negishi E, Novak T (2007) In: Ojima I (ed) Applications II: transition metal compounds in organic synthesis 1. Comprehensive organometallic chemistry III, vol 10. Elsevier, Oxford, p 251
13. Knight KS, Wang D, Waymouth RM, Ziller J (1994) J Am Chem Soc 116:1845
14. Negishi E, Rousset CJ, Choueiry D, Maye JP, Suzuki N, Takahashi T (1998) Inorg Chem Acta 280:8
15. Knight KS, Waymouth RM (1991) J Am Chem Soc 113:6268
16. Negishi E, Cederbaum FE, Takahashi T (1986) Tetrahedron Lett 27:2829
17. Uesaka N, Mori M, Okamura K, Date T (1994) J Org Chem 59:4542
18. Yamaura Y, Hyakutake M, Mori M (1997) J Am Chem Soc 119:7615
19. Yamaura Y, Mori M (1999) Tetrahedron Lett 40:3221
20. Mori M, Takaki T, Makabe M, Sato Y (2003) Tetrahedron Lett 44:3797
21. Houri AF, Didiuk MT, Xu Z, Horan NR, Hoveyda AH (1993) J Am Chem Soc 115:6614
22. Hoveyda AH, Morken JP (1993) J Org Chem 58:4237
23. de Armas J, Kolis SP, Hoveyda AH (2000) J Am Chem Soc 122:5977
24. Didiuk MT, Johannes CW, Morken JP, Hoveyda AH (1995) J Am Chem Soc 117:7097
25. Visser MS, Heron NM, Didiuk MT, Sagal JF, Hoveyda AH (1996) J Am Chem Soc 118:4291

26. Hoveyda AH, Didiuk MT (1998) Curr Org Chem 2:489
27. Adams JA, Ford JG, Stamatos PJ, Hoveyda AH (1999) J Org Chem 64:9690
28. Knight KS, Waymouth RM (1994) Organometallics 13:2575
29. Millward DB, Sammis G, Waymouth RM (2000) J Org Chem 65:3902
30. Takahashi T, Kondakov DY, Suzuki N (1994) Organometallics 13:3411
31. Barluenga J, Alvarez-Rodrigo L, Rodriguez F, Fananas FJ (2006) Angew Chem, Int Ed 45:6362
32. Molander GA, Corrette CP (1998) Tetrahedron Lett 39:5011
33. Montchamp JL, Negishi E (1998) J Am Chem Soc 120:5345
34. Kondakov DY, Wang S, Negishi E (1996) Tetrahedron Lett 37:3803
35. Okamoto S, Livinghouse T (2000) J Am Chem Soc 122:1223
36. Molander GA, Romero JAC (2002) Chem Rev 102:2161
37. Cotton S (1991) Lanthanides and actinides. Oxford University Press, New York
38. Molander GA, Dowdy ED, Noll BC (1998) Organometallics 17:3754
39. Watson PL, Tebbe FN (1990) DuPont de Nemours and Co., US Patent 4 965 386
40. Onozawa S, Sakakura T, Tanaka M (1994) Tetrahedron Lett 35:8177
41. Fu PF, Brard L, Li YW, Marks TJ (1995) J Am Chem Soc 117:7157
42. Molander GA, Nichols PJ (1995) J Am Chem Soc 117:4415
43. Smitrovich JH, Woerpel KA (1996) J Org Chem 61:6044
44. Molander GA, Nichols PJ, Noll BC (1998) J Org Chem 63:2292
45. Molander GA, Dowdy ED, Schumann H (1998) J Org Chem 63:3386
46. Molander GA, Nichols PJ (1996) J Org Chem 61:6040
47. Molander GA, Romero JAC (2005) Tetrahedron 61:2631
48. Molander GA, Schmitt MH (2000) J Org Chem 65:3767
49. Muci AR, Bercaw JE (2000) Tetrahedron Lett 41:7609
50. Horino Y, Livinghouse T (2004) Organometallics 23:12
51. Molander GA, Pfeiffer D (2001) Org Lett 3:361
52. Gagne MR, Nolan SP, Marks TJ (1990) Organometallics 9:1716
53. Aubert C, Buisine O, Malacria M (2002) Chem Rev 102:813
54. Zhang Z, Zhu G, Tong X, Wang F, Xie X, Wang J, Jiang L (2006) Curr Org Chem 10:1457
55. Molander GA, Retsch WH (1997) J Am Chem Soc 119:8817
56. Molander GA, Corrette CP (1999) J Org Chem 64:9697
57. Molander GA, Retsch WH (1998) J Org Chem 63:5507
58. Rix FC, Brookhart M (1995) J Am Chem Soc 117:1137
59. Rix FC, Brookhart M, White PS (1996) J Am Chem Soc 118:4746
60. LaPointe AM, Rix FC, Brookhart M (1997) J Am Chem Soc 119:906
61. Uozumi Y, Tsuji H, Hayashi T (1998) J Org Chem 63:6137
62. Widenhoefer RA, DeCarli MA (1998) J Am Chem Soc 120:3805
63. Widenhoefer RA (2002) Acc Chem Res 35:905
64. Wang X, Chakrapani H, Stengone CN, Widenhoefer RA (2001) J Org Chem 66:1755
65. Stengone CN, Widenhoefer RA (1999) Tetrahedron Lett 40:1451
66. Pei T, Widenhoefer RA (2001) J Org Chem 66:7639
67. Perch NS, Pei T, Widenhoefer RA (2000) J Org Chem 65:3836
68. Perch NS, Kisanga P, Widenhoefer RA (2000) Organometallics 19:2541
69. Perch NS, Widenhoefer RA (2004) J Am Chem Soc 126:6332
70. Trost BM, Rise F (1987) J Am Chem Soc 109:3161
71. Wakayanagi S, Shimamoto T, Chimori M, Yamamoto K (2005) Chem Lett 34:160
72. Shimamoto T, Hirano T, Nishimoto H, Yamamoto K (2006) Chem Lett 35:846
73. Shimamoto T, Chimori M, Sogawa H, Yamamoto K (2005) J Am Chem Soc 127:16410

74. Lautens M, Mancuso J (2000) Org Lett 2:671
75. Oh CH, Jung HH (1999) Tetrahedron Lett 40:1535
76. Oh CH, Um SY (2001) Bull Korean Chem Soc 22:797
77. Oh CH, Jung HH, Kim JS, Cho SW (2000) Angew Chem, Int Ed 39:752
78. Oh CH, Jung HH, Sung HR, Kim JD (2001) Tetrahedron 57:1723
79. Oh CH, Jung SH, Park DI, Choi JH (2004) Tetrahedron Lett 45:2499
80. Oh CH, Rhim CY, Kim M, Park DI, Gupta AK (2005) Synlett p 2694
81. Yamada H, Aoyagi S, Kibayashi C (1996) Tetrahedron Lett 37:8787
82. Trost BM, Lee DC (1988) J Am Chem Soc 110:7255
83. Kawanami Y, Yamamoto K (1995) Synlett p 1232
84. Uno T, Wakayanagi S, Sonoda Y, Yamamoto K (2003) Synlett p 1997
85. Lautens M, Smith ND, Ostrovsky D (1997) J Org Chem 62:8970
86. Trost BM, Fleitz FJ, Watkins WJ (1996) J Am Chem Soc 118:5146
87. Trost BM, Chung CK, Pinkerton AB (2004) Angew Chem, Int Ed 43:4327
88. Madine JW, Wang X, Widenhoefer RA (2001) Org Lett 3:385
89. Wang X, Chakrapani H, Madine JW, Keyerleber MA, Widenhoefer RA (2002) J Org Chem 67:2778
90. Varchi G, Ojima I (2006) Curr Org Chem 10:1341
91. Ojima I, Donovan RJ, Shay WR (1992) J Am Chem Soc 114:6580
92. Fukuta Y, Matsuda I, Itoh K (1999) Tetrahedron Lett 40:4703
93. Ojima I, Vu AT, Lee SY, McCullagh JV, Moralee AC, Fujiwara M, Hoang TH (2002) J Am Chem Soc 124:9164
94. Park KH, Jung IG, Kim SY, Chung YK (2003) Org Lett 5:4967
95. Park KH, Kim SY, Son SU, Chung YK (2003) Eur J Org Chem 2003(22):4341
96. Shibata T, Kadowaki S, Takagi K (2004) Organometallics 23:4116
97. Chakrapani H, Liu C, Widenhoefer RA (2003) Org Lett 5:157
98. Maerten E, Delerue H, Queste M, Nowicki A, Suisse I, Agbossou-Niedercorn F (2004) Tetrahedron Asymm 15:3019
99. Kinder RE, Widenhoefer RA (2006) Org Lett 8:1967
100. Miura T, Shimada M, Murakami M (2005) J Am Chem Soc 127:1094
101. Muraoka T, Matsuda I, Itoh K (2002) Organometallics 21:3650
102. Liu C, Widenhoefer RA (2002) Organometallics 21:5666

Author Index Volumes 251–279

Author Index Vols. 26–50 see Vol. 50
Author Index Vols. 51–100 see Vol. 100
Author Index Vols. 101–150 see Vol. 150
Author Index Vols. 151–200 see Vol. 200
Author Index Vols. 201–250 see Vol. 250

The volume numbers are printed in italics

Subject Index